TECHNISCHE UNIVERSITÄT WIEN

DISSERTATION

Comparing two simulation tools for severe accident scenarios of the TRIGA MARK II reactor

ausgeführt zum Zwecke der Erlangung des akademischen Grades einer Doktorin der technischen Wissenschaften unter der Leitung von

Ao.Prof.Dipl.Ing.Dr.techn. Helmuth Böck

Atominstitut, Technische Universität Wien

eingereicht an der Technischen Universität Wien

Fakultät für Physik

von

Dipl.Ing. Eileen Langegger

Matrikelnummer 00430729

Wien, am 14.04.2020

Die approbierte gedruckte Originalversion dieser Dissertation ist an der TU Wien Bibliothek verfügbar.
The approved original version of this doctoral thesis is available in print at TU Wien Bibliothek.

TU Bibliothek WIEN Your knowledge hub

Die approbierte gedruckte Originalversion dieser Dissertation ist an der TU Wien Bibliothek verfügbar.
The approved original version of this doctoral thesis is available in print at TU Wien Bibliothek.

Für Flora und Rupert

Die approbierte gedruckte Originalversion dieser Dissertation ist an der TU Wien Bibliothek verfügbar.
The approved original version of this doctoral thesis is available in print at TU Wien Bibliothek.

Abstract

The TRIGA MARK II reactor in Vienna operates as a research and training reactor continuously since 1962. In 2012 the reactor received a new core inventory due to a US regulation. Meeting the regulatory requirements required a conversion of the core from high enriched uranium to low enriched uranium. This made an amendment of the safety analyses report (SAR) necessary.

Looking at historic severe accident scenarios and its analyses this work questions the choice of previous performed analysis.

SAR are a necessary and powerful tool to evaluate risks and develop procedures in case of emergency situations. The IAEA states that SAR need to include dispersion calculations regarding severe accidents.

In order to perform this analyses, this work selected two codes, namely RODOS and LASAIR.

RODOS (Real On time DecisiOn Support Program) was developed after the Chernobyl accident to enable easier communication with the public. This powerful tool can use on time data and perform forecast dispersion calculation with direct input from facilities. Its output data include dose and dose rate forecasts as well as possible countermeasure information. For this work the dispersion model DIPCOT (DIsPersion over COmplex Terrain) was used. DIPCOT is a Lagrangian puff model for dispersion over complex terrain.

LASAIR is a simulation tool designed to simulate explosion of fire scenarios including radionuclides. It is based on the dispersion model LASAT, a Lagrangian particle model. LASAIR is less flexible in its input data compared to RODOS.

For this work the meteorological station of the Atominstitut provided the basic weather data. The data of the years 2012 and 2013 were evaluated and prepared for the simulation. While previous works evaluated only averaged scenarios with respect to the meteorological date, e.g. the dispersion of wind direction, this work selected a novel approach and defined both average and specific scenarios.

This work chose four different averaged scenarios representing the four seasons. The specific scenarios included a thunderstorm, a hot day and a foggy day.

The source term calculations were performed in accordance with previous works. This work evaluated 2 burn-up data. First after 1 year of operation and the second at the end of lifetime of the reactor. The calculation was performed with ORIGEN. This work chose a set of nuclides in accordance with previous data. For the LASAIR simulation this data were further reduced to fit the input. The source term was calculated for four accident scenarios, namely the exposure of one fuel element, the exposure of all fuel elements, a small airplane crash and a large airplane crash.

For the simulation with RODOS the release time was set to 1 h, the prognosis to 24 h. For all four accident scenarios all seven meteorological scenarios were simulated. The evaluated

Die approbierte gedruckte Originalversion dieser Dissertation ist an der TU Wien Bibliothek verfügbar.
The approved original version of this doctoral thesis is available in print at TU Wien Bibliothek.
TU Bibliothek Your knowledge hub WIEN

results included total dose, dose rate and potential dose. For the accident scenarios exposure of one fuel element, exposure of all fuel elements and the small airplane crash the highest dose was 1.92 µSv after 1 year effective dose for the average scenarios. For the specific scenarios it was 1.88 µSv after 1 year effective dose. These results all are well below the limit in the Austrian Radiation Protection Law of 1 mSv in one year.

The results for the large airplane crash show a deposition with the main wind direction for the average scenarios. The highest dose is 3.2 mSv after one year. The dose drops below 1 mSv at the boundaries of the institute and is hence below the limit of the Austrian Radiation Protection Law.

For the specific scenarios the maximum effective dose after one year is 13.8 mSv. It drops below 1 mSv at 900 m distance of the source. The distribution is no longer with the main wind direction. This outcome shows that a necessity of the simulation of specific scenarios. Considering only the average, would not reflect the reality and disregard possible necessary countermeasures for affected regions beyond the main wind direction.
The simulation with LASAIR were only performed for the large airplane crash scenario. The highest dose was 3.15 mSv after 1 year for the average scenario and 0.78 mSv after 1 year for the specific scenarios.
The last part of this work compares the above mentioned simulation tools.
The TRIGA MARK II reactor, as a research reactor, appears as a special case for dispersion simulations.
RODOS is designed for the simulation of severe nuclear power plant accidents, while LASAIR is a simulation tool for explosion scenarios and fires including radionuclides.
This general difference is reflected in the results. RODOS offers the possibility to put time evolving data into the simulation, or online and real time data. LASAIR has limited input data possibility, that allow only averaged data.
The different design purposes of LASAIR and RODOS allow comparison in a narrow scope. RODOS and LASAIR give comparable results regarding the deposition of nuclides in average scenarios. Regarding the specific scenarios, LASAIR underestimates the consequences.

Concluding, this work compared two simulation tools for dispersion calculation after accident scenarios at the TRIGA MARK II reactor in Vienna.
This work did not only look at average scenarios, but also included specific scenarios
The analysis of these scenarios showed that the perspective for countermeasures after accidents needs to be wider. The average scenarios showed dose values of below 1 mSv in the first year, which lies in accordance with the Austrian Radiation Protection Law.

Die approbierte gedruckte Originalversion dieser Dissertation ist an der TU Wien Bibliothek verfügbar.
The approved original version of this doctoral thesis is available in print at TU Wien Bibliothek.
TU Bibliothek Your knowledge hub WIEN

Kurzfassung

Der Wiener TRIGA MARK II Reaktor wird seit 1962 kontinuierlich als Forschungs- und Trainingsreaktor betrieben. Das Kerninventar musste 2012 gewechselt werden, da auf Grund einer US Regulierung kein hoch angereichertes Uran mehr in Forschungsreaktoren verwenden werden darf. Seitdem wird der Reaktor ausschließlich mit niedrig angereichertem Uran betrieben. Wegen diesem Austausch wurde eine Adaptierung der Sicherheitsanalyse notwendig.

Ausgehend von den früheren Unfallszenarien und deren Analyse stellt diese Arbeit die Wahl der Szenarien in früheren Arbeiten in Frage, bzw. adaptiert und erweitert sie vor allem in Hinblick auf die gewählten meteorlogischen Szenarien.

Die Sicherheitsanalysen sind ein notwendiges und mächtiges Hilfsmittel um Risiken zu evaluieren und auf Notfallszenarien vorbereitet zu sein. Die IAEO weist darauf hin, dass Ausbreitungberechnungen in Hinblick auf schwere Unfälle Teil einer Sicherheitsanalyse sein sollen.

Um diese Berechnungen durchführen zu könne, wurden 2 verschiedene Simulationstools für diese Arbeit ausgewählt: RODOS und LASAIR.

RODOS (Real On time DecisiOn Support Program) wurde nach dem Unfall von Tschernobyl entwickelt, um der Bevölkerung schnell und einfach verständliche Informationen zukommen zu lassen. Dieses Tool hat nicht nur die Möglichkeit Daten manuell einzugeben, sondern kann auch direkt von Anlagen „live“ Daten erhalten, und mit Wettervorhersagen „on time“ Berechnungen durchführen. Die Ergebnisse beinhalten neben der Dosis und Dosisleistungsvorhersage auch mögliche notwendige Gegenmaßnahmen. Für diese Arbeit wurde das Ausbreitungsmodel DIPCOT (DIspersion over COmplex Terrain) gewählt. DIPCOT ist ein Lagrangesches Puff Modell um Ausbreitungen über komplexem Gelände zu berechnen.

LASAIR ist ein Simulationstool, das für Feuer mit Radionukliden bzw. Explosionsszenarien gedacht ist. Es basiert auf dem Ausbreitungsmodell LASAT, auch das ist ein Lagrangesches Teilchenmodel. LASAIR ist verglichen zu RODOS deutlich weniger flexibel in Hinblick auf die Eingangsparameter.

Für diese Arbeit wurde die Wetterstation am Dach des Atominstituts herangezogen, um die Grunddaten für die Berechnungen zu erhalten. Die Daten der Jahre 2012 und 2013 wurden herangezogen, evaluiert und bearbeitet. Vorangegangene Arbeiten betrachteten ausschließlich durchschnittliche Wetterszenarien. Diese Arbeit verfolgt einen neuen Ansatz und untersucht sowohl durchschnittliche Wetterszenarien als auch spezielle Wetterszenarien.

Diese Arbeit hat daher vier durchschnittliche Wetterszenarien gewählt, die den Jahreszeiten entsprechen. Die speziellen Szenarien sind ein Gewittertag, ein heißer Tag und ein Nebeltag.

Die approbierte gedruckte Originalversion dieser Dissertation ist an der TU Wien Bibliothek verfügbar.
The approved original version of this doctoral thesis is available in print at TU Wien Bibliothek.
TU Bibliothek Your knowledge hub WIEN

Die Quelltermanalysen wurden in Anlehnung an frühere Arbeiten durchgeführt. Diese Arbeit betrachtet zwei Abbrandszenarien, das erste nach einem Jahr Betrieb, das zweiten betrachtet den Abbrand am Ende der voraussichtlichen Betriebsdauer. Die Berechnungen wurden mit ORIGEN durchgeführt. Diese Arbeit wählte dieselben Nuklide, in Übereinstimmung mit früheren Arbeiten. Für die Simulation mit LASAIR musste die Liste der gewählten Nuklide weiter reduziert werden. Der Quellterm wurde für vier Unfallszenarien berechnet: Die Exposition eines Brennelementes, die Exposition aller Brennelemente, ein Crash eines kleinen Flugzeugs und der Crash eines großen Flugzeuges.

Für die Simulationen mit RODOS wurde eine Freisetzung von 1h und eine Prognose für 24 h gewählt. Alle vier Unfallszenarien wurden mit sieben Wetterszenarien gerechnet. Die analysierten Ergebnisse beinhalteten die Gesamtdosis, die Dosisleistung und die mögliche Dosis ohne getroffene Gegenmaßnahmen. Für die Szenarien Exposition eines Elements, Exposition aller Elemente und Crash eines kleinen Flugzeugs wurde die maximale effektive Dosis zu 1,92 µSv nach einem Jahr bei den Durchschnittsszenarien bestimmt. Für die speziellen Szenarien ergab sie sich zu 1,88 µSv nach einem Jahr. Alle Ergebnisse liegen weit unter den Grenzwerten des österreichischen Strahlenschutzgesetzes von 1 mSv in einem Jahr.

Die Ergebnisse für das Szenario Crash eines großen Flugzeugs zeigen eine Hauptdeposition mit der Hauptwindrichtung. Die höchste Dosis ergab sich zu 3,2 mSv nach einem Jahr. Die Dosis liegt an den Grenzen des Instituts unter 1 mSv, und damit unter den Grenzwerten des österreichischen Strahlenschutzgesetzes.

Für die speziellen Szenarien liegt die maximale effektive Dosis nach einem Jahr bei 13,8 mSv. Sie fällt in einem Abstand von 900 m von der Quelle unter 1 mSv. Die Hauptdeposition liegt nicht mehr in Hauptwindrichtung. Diese Erkenntnis zeigt, dass die Simulation von Durchschnittsszenarien nicht ausreichend ist. Dabei würden mögliche Gegenmaßnahmen außer Acht gelassen.

Die Simulationen mit LASAIR wurden nur für das Szenario Crash eines großen Flugzeugs durchgeführt. Die höchste Dosis lag bei 3,15 mSv nach einem Jahr für Durchschnittszenarien und 0,78 mSv für ein spezielles Szenario.

Der letzte Teil der Arbeit befasst sich mit dem Vergleich der beiden obenstehenden Simulationstools.
Der TRIGA MARK II Reaktor als Forschungsreaktor stellt einen Spezialfall für Ausbreitungsrechnungen dar.
RODOS wurde als Tool für Ausbreitungsrechnungen nach schweren Kernkraftwerksunfällen entwickelt, LASAIR dient als Tool zur Simulation von Explosions- oder Feuerszenarien. Dieser generelle Unterschied zeigt sich auch in den Ergebnissen. RODOS bietet die Möglichkeit Zeitverläufe oder on time Daten als Input zu nutzen. LASAIR hat nur sehr limitierte Eingabeparameter, die nur gemittelte Werte erlauben.

Die approbierte gedruckte Originalversion dieser Dissertation ist an der TU Wien Bibliothek verfügbar.
The approved original version of this doctoral thesis is available in print at TU Wien Bibliothek.
TU Bibliothek Your knowledge hub WIEN

Dieser generelle Unterschied ermöglicht nur einen sehr eingeschränkten Vergleich beider Tools. RODOS und LASAIR Simulation ergeben vergleichbare Ergebnisse in der Deposition bei den Durchschnittsszenarien. Bei den speziellen Szenarien unterschätzt LASAIR die Auswirkungen.

Zusammenfassend vergleicht diese Arbeit zwei Simulationstools für die Ausbreitungsrechnung nach Störfallszenarien des TRIGA MARK II Reaktors in Wien. Diese Arbeit befasste sich nicht nur mit Durchschnittsszenarien, sondern inkludierte auch spezielle Szenarien hinsichtlich der Meteorologie. Die Analyse dieser Auswahl ergab, dass die möglichen Gegenmaßnahmen weiter gesteckt werden sollten. Die Durchschnittszenarien zeigen, dass die Dosiswerte unter 1 mSv nach einem Jahr an den Grenzen des Reaktorinstituts liegen, und sich somit unter den Grenzwerten des österreichischen Strahlenschutzgesetzes befinden. Selbst ein Unfallszenario mit einem Absturz eines großen Flugzeugs beeinträchtigt die Sicherheit der Bevölkerung nicht.

Die approbierte gedruckte Originalversion dieser Dissertation ist an der TU Wien Bibliothek verfügbar.
The approved original version of this doctoral thesis is available in print at TU Wien Bibliothek.
TU Bibliothek Your knowledge hub WIEN

Contents

Die approbierte gedruckte Originalversion dieser Dissertation ist an der TU Wien Bibliothek verfügbar.
The approved original version of this doctoral thesis is available in print at TU Wien Bibliothek.
TU Bibliothek Your knowledge hub WIEN

Die approbierte gedruckte Originalversion dieser Dissertation ist an der TU Wien Bibliothek verfügbar.
The approved original version of this doctoral thesis is available in print at TU Wien Bibliothek.
TU Bibliothek Your knowledge hub WIEN

Die approbierte gedruckte Originalversion dieser Dissertation ist an der TU Wien Bibliothek verfügbar.
The approved original version of this doctoral thesis is available in print at TU Wien Bibliothek.
TU Bibliothek Your knowledge hub WIEN

Die approbierte gedruckte Originalversion dieser Dissertation ist an der TU Wien Bibliothek verfügbar.
The approved original version of this doctoral thesis is available in print at TU Wien Bibliothek.
TU Bibliothek Your knowledge hub WIEN

1 The TRIGA MARK-II Reactor

1.1 The History of the TRIGA

The concept of the TRIGA reactor originates in 1955. F. de Hoffmann persuaded his company General Dynamics Corporation after a conference held in Geneva, Switzerland, to develop nuclear reactors and nuclear energy on a commercial bases. In 1956 General Atomic (GA) was founded with de Hoffmann as president. One of the research groups of GA insisted that the reactor to be build should be as safe as one that "could be given to a bunch of high school children to play with, without any fear that they would get hurt" [1]. Also the reactor fuel itself should have inherent safety features, and not only the reactor itself. The prototype of the reactor, TRIGA Mark I achieved first criticality on May 3^{rd} 1958 in California. The safety of this reactor type was shown during several conferences, and initiated a quick selling process of this reactor [2]. The research reactor of the Technical University Vienna at the Atominstitut is located close to the center of Vienna. The reactor was built by General Atomic (San Diego, California, U.S.A) in the years 1959 - 1962. The first criticality was achieved on March 7^{th} 1962. TRIGA stands for Training, Research, Isotope, General Atomics, and is a pure research reactor of the swimming pool type. It is the most widely used, non-power nuclear reactor in the world. Worldwide, 66 TRIGA reactors were sold, wereby in Europe 10 reactors were installed [1].

The TRIGA in Vienna is operational in average 220 days a year, without any long outages. The maximum continuous power output is 250 kW (thermal). The heat produced is released into a channel of the river Danube via a primary coolant circuit and a secondary coolant circuit. The primary cooling circuit is deionized, distilled water at temperatures between 20°C and 40°C. The secondary circuit is ground water at temperatures between 12°C and 18°C. The two circuits are being

[1] DYSON, F., "The little red schoolhouse", Disturbing the Universe, Basic Books, New York (1979) 94–103.

Die approbierte gedruckte Originalversion dieser Dissertation ist an der TU Wien Bibliothek verfügbar.
The approved original version of this doctoral thesis is available in print at TU Wien Bibliothek.
TU Bibliothek Your knowledge hub WIEN

separated by a heat exchanger. At nominal power of 250 kW_{th} the centre fuel temperature is about 200°C and the thermal flux amounts $1 \times 10^{13} cm^{-2} s^{-1}$ in the core centre. Figure 1.1 shows a schematic drawing of the reactor [1].

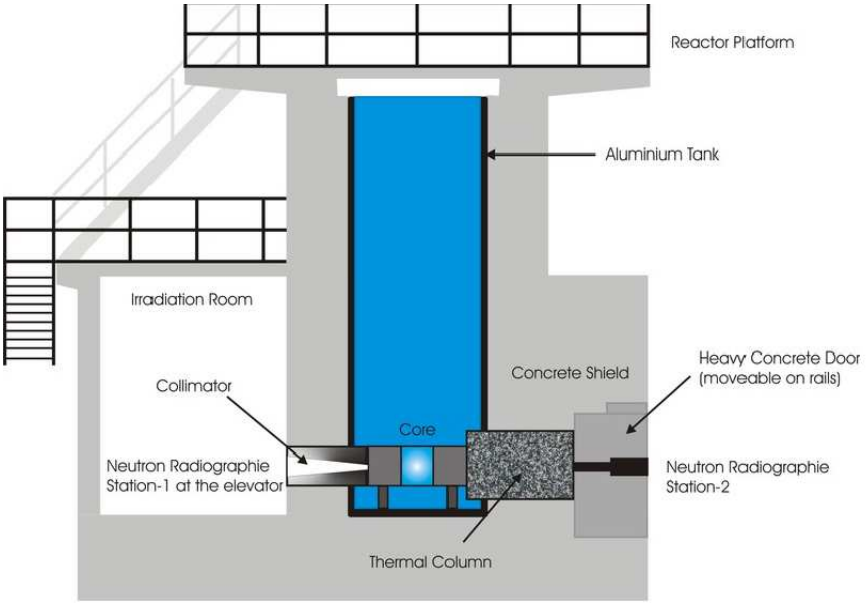

Figure 1.1: Schematic Drawing of Triga MARK II Reactor Vienna, [6]

1.2 TRIGA characteristics

The following paragraph outlines the technical data of the TRIGA reactor in Vienna[2]:

1. Reactor Core
    - The fuel -moderator material consists of 8wt% uranium, 91wt% zirconium and 1wt% hydrogen.
    - The maximum uranium enrichment is 19.75 % uranium 235.
    - The fuel element dimensions are 3.75 cm in diameter and 72.24 cm in length.
    - The cladding consists of 0.51 mm steel

[2][1,p.5-6]

Die approbierte gedruckte Originalversion dieser Dissertation ist an der TU Wien Bibliothek verfügbar.
The approved original version of this doctoral thesis is available in print at TU Wien Bibliothek.
TU Bibliothek Your knowledge hub WIEN

- The active core volume is max. 49.5 cm in diameter and 35.56 cm in height.

2. Reflector
   - The material is graphite with an aluminum cladding.
   - The radial thickness is 30.5 cm.
   - The top and bottom thickness is 10.2 cm.

3. Construction
   The reactor is constructed with a heavy and standard concrete, 6.55 m high, 6.19 m wide, 8.76 m long. The tank is 1.98 m in diameter and 6.4 m in depth.

4. Shielding
   - The radial shielding consists of 30.5 m of graphite, 45.7 cm of water and at least of 206 cm of heavy concrete.
   - The vertical shielding is 4.9 of water above the core and 10.2 cm of graphite underneath the core and additional 61 cm of water followed by minimum 91 cm of standard concrete.

5. Irradiation Devices
   - There are four beam holes, each with 15.2 cm in diameter.
   - The reactor has one central irradiation tube in the middle of core.
   - There are five reflector irradiation tubes.
   - The reactor has one pneumatic transfer system near the core edge
   - A thermal column with cross section 1.22 m × 1.22 m and length 1.68 m
   - An experimental tank with surface area 2.44 m × 2.74 m and depth 3.66 m; connected to the reactor by means of a neutron radiography collimator 0.61 m × 0.61 m in cross section and 1.22 m long.
   - Withe neutron beam, with a thermal neutron flux of up to $10^7/cm^2s$ The accessible experimental site has a size of 3.7 × 3.7 × 2.2m^3, the cross section of the beam is up to 65 × 65 mm^2

Die approbierte gedruckte Originalversion dieser Dissertation ist an der TU Wien Bibliothek verfügbar.
The approved original version of this doctoral thesis is available in print at TU Wien Bibliothek.
TU Bibliothek Your knowledge hub WIEN

6. Control System
   The control system consists of :
   - Two boron carbide control rods with electric motor moved by a rack and pinion drive
   - One pneumative boron carbide transient rod driven by compressed air

   The maximum reactivity insertion rate - time rate of change (excluding pulse operation) is 0.04%δ k/k per second. The total rod worth about 4.8%δ k/k.

1.2.1 TRIGA Safety

The safety features of the reactor are due to its large negative temperature coefficient of reactivity ($10^{-4}\Delta k/k/^{\circ}C$) and negative void coefficient, which are based on the increase of neutron temperature by the crystalline effect of the ZrH material used in the fuel. This negative temperature coefficient limits the power excursion during a sudden increase of reactivity. A large insertion of reactivity can pulse the reactor to a power level of 250 MW. This is directly linked to the homogenous mixture of the fuel (U) with the moderator (Zr, H) in the fuel rods. The prompt negative temperature coefficient as a self limiting property brings down the power immediately (40 ms) after the increase. The reactor is controlled by the three control rods described above, which contain boron carbide as absorber material. When these rods are fully inserted into the reactor core, the neutrons continuously emitted from a start-up source (Sb-Be photo-neutron source) are absorbed by the rods and the reactor remains sub-critical. If the absorber rods are withdrawn from the core, (two of them by an electric motor and one pneumatically) the number of fissions in the core and the power level increases. The start-up process takes roughly five minute for the reactor to reach a power level of 250 kW from the sub-critical state. The reactor can be shut-down either manually or automatically by the safety system. It takes about 1/10 of a second for the control rods to fall into the core [1, 2].

1.2.2 The fuel core

In 2013 the core consisted of 78 fuel elements, currently (2020) there are 82. They are 3.75 cm in diameter and 72.24 cm long as shown in Figure 1.2. They are arranged in an annular lattice as shown in Figure 1.3. Two of the elements have

Die approbierte gedruckte Originalversion dieser Dissertation ist an der TU Wien Bibliothek verfügbar.
The approved original version of this doctoral thesis is available in print at TU Wien Bibliothek.
TU Bibliothek Your knowledge hub WIEN

thermocouples implemented, those allow a temperature measurement of the fuel during reactor operation. The total uranium mass is 2.3 kg of uranium. A TRIGA fuel element consists of a uniform mixture of 8 wt% uranium, 1 wt% hydrogen and 91 wt% zirconium, with zirconium-hydride as main moderator. The cladding of the current core is stainless steel, before the HEU to LEU conversion (see Chapter 1.3) there were also some elements with aluminum cladding[1].

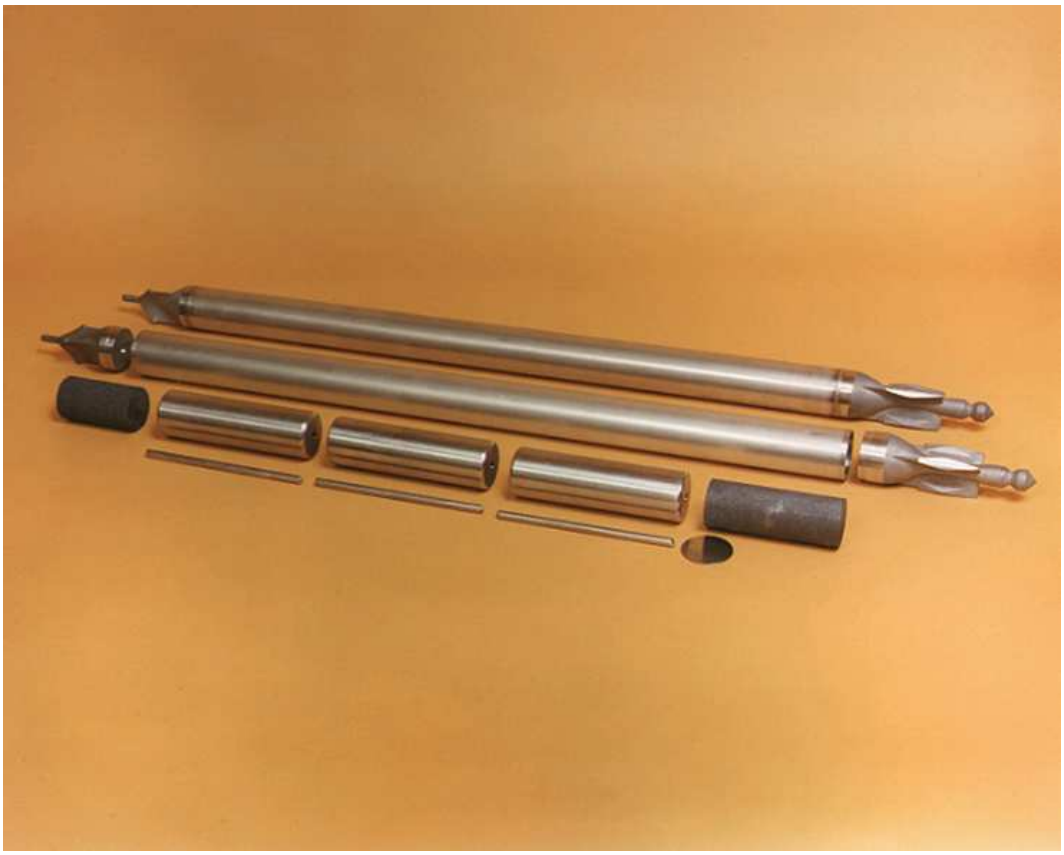

Figure 1.2: Drawings of Fuel Elements of TRIGA Reactor, [1, p.10]

Die approbierte gedruckte Originalversion dieser Dissertation ist an der TU Wien Bibliothek verfügbar.
The approved original version of this doctoral thesis is available in print at TU Wien Bibliothek.

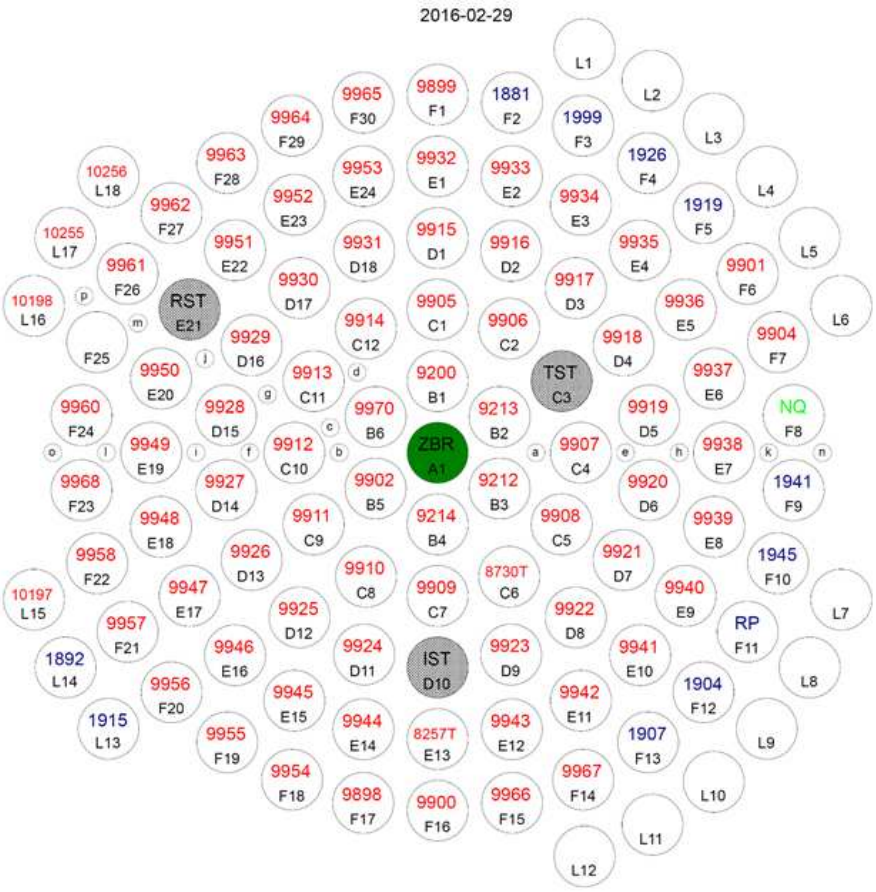

Figure 1.3: The current lattice of the core elements. The neutron source is shown in green label, the graphite elements in blue, and regular elements in red. The central irradiation rod is shown in the middle, [1, p.11]

1.3 HEU to LEU conversion project

According to the CODE 10 CFR 50.64 of the United States Code of Federal Regulations, it is required that non power reactors replace all HEU fuel (fuel with more than 20% enrichment) with LEU (fuel with less then 20% enrichment). Several TRIGA reactors have undergone this change in the US; in 2012 the Austrian TRIGA reactor followed this regulation. This was also necessary as the original fuel elements reached their maximum burn-up. An additional incentive to this requirement is the Austrian position not to store any spent nuclear fuel in the country. In order to keep the reactor at the Atominstitut operational, new fuel

Die approbierte gedruckte Originalversion dieser Dissertation ist an der TU Wien Bibliothek verfügbar.
The approved original version of this doctoral thesis is available in print at TU Wien Bibliothek.
TU Bibliothek Your knowledge hub WIEN

elements were necessary. The negotiations started in April 2011 between the US Department of Energy (DOE), the International Atomic Energy Agency (IAEA) and the Atominstitut. The IAEA had a very high interest in keeping the reactor operational, as it's the closest nuclear facility to its headquarters. In early summer 2011, the Austrian ministries, the IAEA and the DOE reached the following conclusion: Austria returned 91 spent fuel elements to the US (Idaho National Laboratory INL), and received 77 new fuel elements with low burn up, steel cladding and low enrichment. The fuel exchange was carried out in November 2012, through Slovenia and Italy [1, 2, 3].

1.4 Radioactive Core Inventory as of April 2012

Date	**Number of fuel elements**	**Cladding Material**	**Remarks**
05.12.1961	66	Al, 20%	2 instrumented fuel elements
19.02.1965	2	Al, 20%	
02.08.1966	3	SST, 20%	
21.10.1968	3	SST, 20%	1 instrumented fuel element 5284 TCE
19.10.1972	9	SST, 70%	
02.12.1980	1	SST, 20%	1 instrumented fuel element 8257 TCE
09.08.1982	3	SST, 20%	
15.02.1983	2	SST, 20%	2 instrumented fuel elements 8730, 8731 TCE
21.08.1987	3	SST, 20%	
19.10.1988	3	SST, 20%	
01.02.1990	3	SST, 20%	
14.12.2000	8	SST, 20%	
Total	104		

Table 1.1: Number of elements and date of entry into core for reactor core before 2012 [3, p.2]

Of those 104 fuel elements, 6 fresh fuel elements were kept, as well as 5 with the fewest burn-up. 91 were returned.

Die approbierte gedruckte Originalversion dieser Dissertation ist an der TU Wien Bibliothek verfügbar.
The approved original version of this doctoral thesis is available in print at TU Wien Bibliothek.
TU Bibliothek Your knowledge hub WIEN

1.5 Severe accidents analysis for TRIGA MARK II reactor Vienna

1.5.1 Severe accident analysis for TRIGA reactors

Accident scenarios for TRIGA reactors were analysed over the whole operational period of TRIGA reactors. S.C. Hawley, R.L. Kathren et al. [10] describe several accident scenarios :

- excess reactivity insertions
- metal water reactions
- lost, misplaced or inadvertent experiment
- mechanical rearrangement of the core
- loss-of-coolant accident
- changes in fuel morphology and ZrH_x composition
- fuel handling

The above mentioned scenarios showed little impact on the public in previous analyes. The case of mechanical rearrangements due to external events was only mentioned in the analyses. It would lead to a major loss of coolant. The results were found to be "not sufficient to present an offside hazard" [3]. In order to prove this hypotheses and with the development of powerful computer codes, the following accident analyses were possible.

1.5.2 Severe accident analysis for Vienna TRIGA reactor

The first severe accident analyses were done in 1978 with the program STRISK(see [4]). It looked at the destruction of the most activated fuel element, and the destruction of all fuel elements, as well as a plane crash on the reactor. In 2009 it was decided that updates were necessary to those analyses. Computer codes had evolved, and the program PC-Cosyma was chosen as tool. The burn-up of the elements was calculated with ORIGEN. To get better and more realistic weather

[3] [10], page V

Die approbierte gedruckte Originalversion dieser Dissertation ist an der TU Wien Bibliothek verfügbar.
The approved original version of this doctoral thesis is available in print at TU Wien Bibliothek.
TU Bibliothek Your knowledge hub WIEN

data, the weather station of the Atominstitut was installed. The scenarios were updated, and a small plane crash was added as scenario.

1.5.3 Results of severe accident analyses before 2012

Haydn chose for his analysis four scenarios[5, p. 68-96], the outcome of those will be shortly described:

1. Destruction of fuel element with highest activity content
2. Destruction of all fuel elements
3. Case of a small airplane crash
4. Case of a large airplane crash

Scenario 1 - Destruction of fuel element with highest activity content

The effective dose (ICRP-60) is smaller than 1×10^{-10} Sv in a radius outside of 0.31 km after 1 day. The effective dose (ICRP-60) is smaller than 1×10^{-10} Sv in a radius outside of 0.6 km after 50 years. This applies to a wind speed of 1 m/s and no rain. The wind direction was WNW.

Scenario 2 - Destruction of all fuel elements

The effective dose (ICRP-60) is smaller than 1×10^{-8} Sv in a radius outside of 0.21 km after 1 day. The effective dose (ICRP-60) is smaller than 1×10^{-8} Sv in a radius outside of 0.46 km after 50 years. This applies to a wind speed of 1 m/s and no rain. The wind direction was WNW.

Scenario 3 - Case of a small airplane crash

The effective dose (ICRP-60) is smaller than 1×10^{-7} Sv in a radius outside of 0.21 km after 1 day. The effective dose (ICRP-60) is smaller than 1×10^{-7} Sv in a radius outside of 0.53 km after 50 years. This applies to a wind speed of 1 m/s and no rain. The wind direction was WNW.

Die approbierte gedruckte Originalversion dieser Dissertation ist an der TU Wien Bibliothek verfügbar.
The approved original version of this doctoral thesis is available in print at TU Wien Bibliothek.
TU Bibliothek Your knowledge hub WIEN

Scenario 3 - Case of a large airplane crash

The effective dose (ICRP-60) is smaller than 1×10^{-4} Sv in a radius outside of 0.6 km after 1 day. The effective dose (ICRP-60) is smaller than 1×10^{-4} Sv in a radius outside of 0.6 km after 50 years. This applies to a wind speed of 1 m/s and no rain. The wind direction was WNW.

Discussion of the severe accident analyses before 2012

The work of Haydn [5] shows comparable results to previous works. The computational model offered only few variation possibilities regarding the meteorological conditions. So only the average wind and rain distribution over the year was used for the calculations. Especially the rain was neglected in this analysis, and rain during an accident can strongly influence the outcome and the consequences in the surroundings of the reactor.

1.5.4 Severe accident analysis for new core after 2012

After the return of the HEU elements to the US, and the initialization of the new core it was necessary to re-evaluate the severe accident scenarios. The re-simulation with the code PC-Cosyma was one option, the other option was to look for newer or better equipped computational codes. One option was the code RODOS - Real Ontime DesiciOn Support Program. RODOS is described in detail in chapter 4. It is mainly used to calculate the environmental consequences after severe accidents in nuclear power plants, as it is equipped with the necessary data of the European NPPs, but the tool is also able to be used for smaller utilities, such as research reactors. The input parameters are flexible as shown in chapter 4.1.1. The aim of this work was to show that the chosen scenarios are credible, and that the choice of a new computational code was necessary. It will also show that the TRIGA Reactor in Vienna is an ultrasafe reactortype, with extremely little impact on the environment even in case of a severe accident.

Die approbierte gedruckte Originalversion dieser Dissertation ist an der TU Wien Bibliothek verfügbar.
The approved original version of this doctoral thesis is available in print at TU Wien Bibliothek.
TU Bibliothek Your knowledge hub WIEN

2 Safety of Research Reactors and Definitions

The safety and operational principle of a TRIGA reactor is described in chapter 1. In this chapter this work will take a general view on safety requirements of research reactors. The IAEA [7] defines a research reactor as "a nuclear reactor (including critical assemblies and subcritical assemblies) used for nuclear research and for the generation and utilization of radiation for research and other purposes. This definition excludes nuclear reactors used for the production of electricity, naval propulsion, desalination or district heating. The term covers the reactor core, radioactive sources used, experimental devices, all systems needed for their operation, installations managed by the facility that contain nuclear material (irradiated or not), and radioactive waste management facilities and all other facilities relevant to either the reactor or its associated experimental facilities and devices located on the reactor site"[1]. Due to its size, research reactors pose a smaller hazard to the public then power reactors [7, p.12]. The IAEA states three safety objectives[2]:

1. General Nuclear Safety Objective
   To protect individuals, society and the environment from harm by establishing and maintaining in nuclear installations effective defenses against radiological hazards.
   The General Nuclear Safety Objective is supported by two complementary Safety Objectives dealing with radiation protection and technical aspects. They are interdependent: the technical aspects in conjunction with administrative and procedural measures ensure defense against hazards due to ionizing radiation.

[1] Safety of Research Reactors, IAEA Specific Safety Requirements No. SSR-3, ISBN 978–92–0–104816–5, Vienna, 2016, p.3

[2] International Atomic Energy Agency, The Safety of Nuclear Installations, Safety Series No. 110, IAEA, Vienna, 1993, par. 203-206

Die approbierte gedruckte Originalversion dieser Dissertation ist an der TU Wien Bibliothek verfügbar.
The approved original version of this doctoral thesis is available in print at TU Wien Bibliothek.
TU Bibliothek Your knowledge hub WIEN

2. Radiation Protection Objective
   To ensure that in all operational states radiation exposure within the installation or due to any planned release of radioactive material from the installation is kept below prescribed limits and as low as reasonably achievable, and to ensure mitigation of the radiological consequences of any accidents.

3. Technical Safety Objective
   To take all reasonably practicable measures to prevent accidents in nuclear installations and to mitigate their consequences should they occur, to ensure with a high level of confidence that, for all possible accidents taken into account in the design of the consequences would be minor and below prescribed limits, and to ensure that the likelihood of accidents with serious radiological consequences is extremely low.

2.1 Safety Analysis Report (SAR)

The IAEA states [7] that the main goal of the safety of a research reactor has to be the limitation of any radiological consequences in the case of an accident. Further, measures to limit radiation exposure for workers during normal operation, and the minimization of the likelihood of an accident. To reach those goals, the following measures can be taken: engineered safety features, on and off site procedures prepared in case of accidents to mitigate consequences in case of accidents. The competent authority has to verify all the above described measures or has to implement them, if not present. This can happen through the licensing process, which includes a detailed SAR. The report is prepared by the operating personnel, it includes the design specifications, and protection design for on and off site people. This document needs to be updated regularly, especially in case of changes to the core inventory or on the basis of requests by the competent authority. It has to include a safety analysis of accident sequences, and the measures taken to limit consequences for operational personnel or the public.

This work will describe several possible accident scenarios and calculate the radiological consequences for public off site. The scenarios were chosen in the first safety report of the TRIGA reactor, only the calculation methods and the data acquisition for those calculation changed. The following paragraphs will explain the choice of the scenarios in a general manner.

Die approbierte gedruckte Originalversion dieser Dissertation ist an der TU Wien Bibliothek verfügbar.
The approved original version of this doctoral thesis is available in print at TU Wien Bibliothek.
TU Bibliothek Your knowledge hub WIEN

The IAEA states further the importance of the site evaluation. In the SAR the safety of the site is shown, and effects that can influence this safety are taken into account[3]:

- The effects of natural and human induced external events (e.g. seismic events, fire or flooding) that may occur in the region of the site;
- The characteristics of the site and its environment that could influence the transfer of released radioactive material to humans
- The population density and population distribution and other characteristics in the vicinity of the site having relevance to emergency arrangements, and the need to evaluate the risks to individuals and the population
- Other collocated site facilities such as other research reactors, radioisotope plants, fuel cycle related facilities, post-irradiation examination or non-nuclear facilities (e.g. chemical facilities)
- The capability for an ultimate heat sink at the site, as appropriate
- The on-site and off-site emergency plans aimed at mitigating the consequences for the public and the environment in the event of a substantial release of radioactive material to the environment

For the TRIGA reactor in Vienna, especially the first point is of uttermost importance. The proximity of the airport enhances the probability of an airplane accident, hence the radiological consequences need to be calculated beforehand to prove the safety of the reactor. The IAEA stated in an earlier publication [8, p. 36] explicitly the calculation of atmospheric dispersion of radioactive material: "A meteorological description of the region, including the basic meteorological parameters and phenomena shall be prepared. Data for at least one representative year should be presented, together with any other data that may be available from other sources. Data should be collected that adequately represent local meteorological conditions. [...] On this basis of the data obtained from the investigations of the region, the possible atmospheric dispersion of any radioactive material released shall be assessed."

[3]Safety of Research Reactors, IAEA Specific Safety Requirements No. SSR-3, ISBN 978–92–0–104816–5, Vienna, 2016, page 26 -27

Die approbierte gedruckte Originalversion dieser Dissertation ist an der TU Wien Bibliothek verfügbar.
The approved original version of this doctoral thesis is available in print at TU Wien Bibliothek.
TU Bibliothek Your knowledge hub WIEN

2.2 General Safety Requirements

The general design of a reactor implements three basic safety functions: shut down of a reactor, cooling the reactor and its core and confining the radioactive material. These functions shall be met by the design of the reactor in principle. For those function the single failure criteria has to be applied, regular inspections, testing and maintenance must be possible to have high reliability of the system. Within the design process all challenges of the reactor during its lifetime have to be taken into account. This includes accident conditions, site characteristics, design and the limits of parameters, modes of operation etc. There are several general requirements that do not only apply to research reactors. The IAEA [8] states the following:

1. Redundancy and single failure criterion
   No single failure shall lead to a loss of system capability.

2. Diversity
   Redundant systems shall be diverse - attributes are:
   - different operational principles
   - different operating conditions
   - different manufacturer

3. Independence
   This can be physical separation, functional isolation or barriers for safety relevant systems

4. Fail Safe design
   In case of an accident systems shall pass into safe states.

5. Ease of testing and maintenance

Especially safety relevant systems are designed regarding the above criteria. The IAEA has summarized the most important safety functions for research reactors in a Table [4]:

[4] Safety of Research Reactors, IAEA Specific Safety Requirements No. SSR-3, ISBN 978–92–0–104816–5, Vienna, 2016 page 119-120

Die approbierte gedruckte Originalversion dieser Dissertation ist an der TU Wien Bibliothek verfügbar.
The approved original version of this doctoral thesis is available in print at TU Wien Bibliothek.
TU Bibliothek Your knowledge hub WIEN

Items important to safety	**Safety function**
Buildings and structures	barrier for uncontrolled release of radioactive materials protection against external or internal events for safety systems shielding against radiation
Reactor core	maintain fuel geometry and coolant flow to ensure shutdown and heat removal negative reactivity feedback moderation and control of neutron flux
Fuel matrix and cladding	barrier for release of fission products or material from fuel constant configuration
Reactivity control system	control reactivity, shut down possibility, no limits exceeded
Reactor coolant primary circuit	adequate cooling and ensure no limits exceeded
Emergency core cooling system	transfer heat to prevent damage from fuel
Reactor protection system	shut down reactor, coll and contain material, mitigation of accident consequences, control interlocks against operational errors
Other safety I&C	keep reactor parameters within limits give information about reactor status to operator
Electrical power supply	provide enough power to ensure safety
Fuel handling and storage system	minimize radiation exposure prevent inadvertent criticality limit any rise in fuel temperature store fresh and irradiated fuel prevent damage to fuel
Radiation monitoring system	measure and warn operational and research personal

Table 2.1: Selected Safety functions for research reactors

Die approbierte gedruckte Originalversion dieser Dissertation ist an der TU Wien Bibliothek verfügbar.
The approved original version of this doctoral thesis is available in print at TU Wien Bibliothek.
TU Bibliothek Your knowledge hub WIEN

2.3 Definitions

This section will define terms used in the following chapters.

Bateman equations

The production of radionuclides and the variation in their inventory during and after reactor irradiation are governed by the Bateman equations [5] . This method sets up differential equations for decay chains, that describe the chain of interest based on known properties. A general forumla can be described as follows[6]:

$$N_n(t) = \sum_{i=1}^{n} \left[N_i(0) \times \left(\prod_{j=i}^{n-1} \right) \times \left(\sum_{j=i}^{n} \left(\frac{e^{-\lambda_j t}}{\prod_{p=i,p\neq j}^{n} (\lambda_p - \lambda_j)} \right) \right) \right] \tag{2.1}$$

2.3.1 Radiation protection terms

Effective Dose

According to the International Committee on Radiation Protection the effective dose is defined as: "The tissue-weighted sum of the equivalent doses in all specified tissues and organs of the body, given by the expression

$$E = \sum_{T} w_T \sum_{R} w_R D_{T,R} \tag{2.2}$$

or

$$E = \sum_{T} w_T H_T \tag{2.3}$$

where H_T or $w_R D_{T,R}$ is the equivalent dose in a tissue or organ,T, and w_T is the tissue weighting factor. The unit for the effective dose is Jkg^{-1} and its special name is sievert (Sv)"[7]

[5] Nuclear Safety in Light Water Reactors, 2012,page 425

[6] https://en.wikipedia.org/wiki/Bateman_equation, 12.03.2020

[7] Annals of the ICRP, Publication 103, The 2007 Recommendation of the International Commission on Radiological Protection, Editor J.Valentin, Elsevier, 2007

Die approbierte gedruckte Originalversion dieser Dissertation ist an der TU Wien Bibliothek verfügbar.
The approved original version of this doctoral thesis is available in print at TU Wien Bibliothek.
TU Bibliothek Your knowledge hub WIEN

2.3.2 Terms used by RODOS

The dose conversion factors for external gamma exposure from radionuclides in the cloud were calculated for RODOS in 2015 [33]. The dose rate factors do not include any contributions from radionuclides emerging via radioactive decay chains during cloud travel. For radionuclides that are members of a radioactive decay chain, there is a physical built-up of radionuclides via mother - daughter decays during plume travel. For the simulation of this work only one pair is interesting - the Kr-88 to Rb-88 mother daughter pair. Terms used by RODOS are:

- Potential dose
  Dose calculated under the assumption of open air exposure without consideration of dose-or exposure reducing actions, resulting from the summed-up exposure by all radionuclides considered in the LSMC calculation. Those doses apply to adults.

- Projected dose
  Dose that would be expected if no countermeasure were to be taken.

- Total effective gamma dose rate
  Is used for the total effective gamma dose rate in mSv/h for a height of 1 m above ground. This is the so called local dose rate resulting from the gamma radiation of all nuclides in the cloud and on the ground.

Die approbierte gedruckte Originalversion dieser Dissertation ist an der TU Wien Bibliothek verfügbar.
The approved original version of this doctoral thesis is available in print at TU Wien Bibliothek.
TU Bibliothek Your knowledge hub WIEN

3 Atmospheric Dispersion Physics

Emissions of chemical materials into the atmosphere have different origins. In the case of this work, a point source is the origin. Dispersion physics has deeper routes, such as weather forecasts or nowadays dispersion modeling for various events, such as volcano eruptions or oil disasters in oceans.

3.1 Basic Physics

3.1.1 Buoyancy

The pressure is defined by the force F applied perpendicular to the surface A of an object:

$$p = \frac{F}{A} \tag{3.1}$$

In a fluid there are two forces applied to an object, one from below and one from above. The difference is defined as buoyancy:

$$F_A = g\rho V \tag{3.2}$$

with V the volume of the object.

3.1.2 Flow

A flow Φ of a fluid is described by a vector field $\mathbf{v}(r)$, with $\mathbf{v}$ being the flow velocity. If the field is independent of the time, the flow is stationary. The flow though a surface is given by

$$\Phi = \int \rho\mathbf{v} \cdot d\mathbf{A} = \int \mathbf{j} \cdot d\mathbf{A} \tag{3.3}$$

with $\mathbf{j}$ being the flow density. The *div* $\mathbf{j}$ is defined as source density. The Gauss theorem claims that if the flow Φ through a surface A of a volume V is not zero,

Die approbierte gedruckte Originalversion dieser Dissertation ist an der TU Wien Bibliothek verfügbar.
The approved original version of this doctoral thesis is available in print at TU Wien Bibliothek.
TU Bibliothek Your knowledge hub WIEN

the change of mass can be seen as a sum over the change in density:

$$\Phi = \oiint \rho \, \mathbf{v} dA = - \iiint_V \dot{\rho} \, dV = \iiint_V \rho \, div \, \mathbf{v} dV$$

The rotation of a fluid is defined through:

$$rot \, \mathbf{v} = \nabla \times \mathbf{v} \tag{3.4}$$

A force field $\mathbf{F(r)}$ has a potential $U(\mathbf{r})$ if the $rot \, F$ is zero everywhere. This is also defined through the Stokes theorem:

$$\oint_C \mathbf{v} \, d\mathbf{s} = \iint_A rot \, \mathbf{v} \, d\mathbf{A} \tag{3.5}$$

If a flow is determined only by its inner friction, it is called a laminar flow. Otherwise it's a turbulent flow. The Reynold number Re is defined by:

$$Re = \rho \, v \, l/\eta \tag{3.6}$$

with l the measurements of the object dimensions. If the Reynolds number gets bigger (>1000) the flow gets turbulent.

3.1.3 Navier - Stokes Equation

Acceleration is the sum of all applied forces. The motion equation of a fluid has two parts of acceleration: the a_1 is the change in velocity at the place of the object, and the part a_2 the movement of the object to a place with a different velocity. Together with the Newtons motion equation one gets the Navier Stokes equation:

$$\rho(\mathbf{a}_1 + \mathbf{a}_2) = -grad \, p + \eta \, \partial \mathbf{v} \tag{3.7}$$

with η the viscosity of the fluid. One has to look at three cases:

- ideal fluids - all friction forces can be neglected
- laminar flows - the part a_2 can be neglected, friction forces are essential
- turbulent flows - the part a_2 is the most important part, more important

Die approbierte gedruckte Originalversion dieser Dissertation ist an der TU Wien Bibliothek verfügbar.
The approved original version of this doctoral thesis is available in print at TU Wien Bibliothek.
TU Bibliothek Your knowledge hub WIEN

then friction forces.

3.1.4 Prandtl Layer

This layer defines the near surface boundary layer from the earth surface up to 100 m in the atmosphere. It is the lower part of the atmospheric boundary layer (peplosphere). The atmospheric boundary layer defines the atmosphere up to 500 m to 2000 m. The main characteristic of this layer are the strong spatial and temporal changes of the meteorological fields. The atmospheric boundary layer consists of the already mentioned Prandtl layer and the Ekman layer. All turbulent fluxes are constant with the change of height. This leads to the possibility to classify wind and temperature profiles from the Monin-Obukhov-Theory (see chapter 3.1.5).

3.1.5 Monin-Obukhov theory

It describes the rules for the wind and temperature profiles in the Prandtl-layer. It claims that the gradients of wind and temperature are a universal function of the height z/L. L is the so called Monin-Obukhov-Length. It is defined as:

$$L = -\frac{(-\overline{u'w'})^{\frac{3}{2}}}{\kappa \frac{g}{T} \overline{T'w'}} \tag{3.8}$$

With T',u' and w' as the temperature, horizontal and vertical wind turbulent fluctuations. T is the temperature and κ is the Karman constant which equals 0.4 [20]. During the day the Monin Obukhov length is negative, and is defined as the height at which the buoyant production of turbulence kinetic energy is equal to the energy produced by the shearing action of the wind [17,18].

3.2 Atmospheric Modeling

The above described theories are the basis for the now following explanations. Atmospheric dispersion is a complex area of research, especially if turbulence become part of the problem. Computational models have eased out the issue, as numerical approaches were found.Leelössy, Molnàr et al [13] describe basic concepts of atmospheric modeling, which are shown below.

Die approbierte gedruckte Originalversion dieser Dissertation ist an der TU Wien Bibliothek verfügbar.
The approved original version of this doctoral thesis is available in print at TU Wien Bibliothek.
TU Bibliothek Your knowledge hub WIEN

3.2.1 Transport Equation

The spatial - temporal change of air pollutants concentrations is described by the atmospheric transport equation:

$$\frac{\partial c}{\partial t} = -\nabla \cdot (c\ \vec{v}) + S_c + \nabla \cdot (D_c \nabla c) \tag{3.9}$$

were $\vec{v}$ is the wind vector, S_c the source term, and D_c the diffusion coefficient. Equation 3.9 describes the change of concentration at a point as a sum of the advective flux, the source term and the diffusion flux. The source term includes the dry and wet deposition, and more importantly the radioactive decay. The atmospheric transport equation does not include any turbulences. Reynolds theory splits the wind and the concentration field into a time averaged and a turbulent perturbation part:

$$\vec{v} = \overline{\vec{v}} + \vec{v}' \tag{3.10}$$

$$c = \overline{c} + c' \tag{3.11}$$

With equations 3.10 and 3.11 equation 3.9 forms to:

$$\frac{\partial c}{\partial t} = -\nabla \cdot (\overline{\vec{v}}\overline{c}) + S_c + D_c \nabla^2 \overline{c} - \frac{\partial \overline{(u'c')}}{\partial x} - \frac{\partial \overline{(v'c')}}{\partial y} - \frac{\partial \overline{(w'c')}}{\partial z} \tag{3.12}$$

The terms on the right side of equation 3.12 are the advection, the source term, the molecular diffusion and the horizontal and vertical turbulent fluxes. The molecular diffusion component can be neglected, as the turbulent mixing is several orders of magnitude higher. The only exception arises in laminar ground layers.

3.2.2 Turbulence

Mechanical and thermal effects can cause near surface turbulence. Mechanical turbulence is caused by friction forces in a viscous flow driven by wind shear. To calculate the intensity of this turbulence, a 3D wind field data is required [13, p.4]. Buoyancy drives thermal turbulence, they can be easily described by stability measures. Turbulence intensity can be described in various ways, one way is the Reynolds-averaged approach (RANS). Here the turbulent kinetic energy (TKE)

Die approbierte gedruckte Originalversion dieser Dissertation ist an der TU Wien Bibliothek verfügbar.
The approved original version of this doctoral thesis is available in print at TU Wien Bibliothek.
TU Bibliothek Your knowledge hub WIEN

represents the average kinetic energy of the subgrid scale wind fluctuations [1]:

$$TKE = \frac{1}{2}(\overline{u'^2} + \overline{v'^2} + \overline{w'^2}) \tag{3.13}$$

with u',v' and w' the wind component fluctuations with respect to the time averaged wind.

3.2.3 Stability Classes

Wind shear and buoyancy drive the turbulent mixing in the atmosphere. To ease this problem, there are categories defined that include radiation parameters, wind speed, surface roughness and cloud cover. These so called categories are called Pasquill stability classes, ranging from class A very unstable to class F moderately stable [14,15]. Basic meteorological measurements can then be estimated from those classes. It must be said, that those classes show very low accuracy compared to direct calculations.

3.2.4 Richardson Number

The gradient Richardson Number defines the ratio between the thermal and the mechanical turbulence[16]:

$$R_i = \frac{-\frac{g}{\rho_0}\frac{\partial p}{\partial z}}{(\frac{\partial u}{\partial z})^2 + (\frac{\partial v}{\partial z})^2} \tag{3.14}$$

with ρ_0 the reference density. The numerator of equation 3.14 is the thermal turbulence (buoyancy), the denominator is the wind shear term. The generator of the turbulence is always the positive wind shear term. Buoyancy can be negative or positive. A negative Richardson number stands therefore for an unstable stratification that can develop thermal turbulence, while a positive Richardson number stands for a stable stratified atmosphere.

[1] R.B.Stull, An introduction to Boundary Layer Metreology, Kluwer Academic Publishers, 1988

Die approbierte gedruckte Originalversion dieser Dissertation ist an der TU Wien Bibliothek verfügbar.
The approved original version of this doctoral thesis is available in print at TU Wien Bibliothek.
TU Bibliothek Your knowledge hub WIEN

3.2.5 Summary

Taking the three mentioned theories together (Pasquill stability classes, Richardson number and the Monin Obukhov theory) it is possible to compare them in the following way:

Stability Class	Richardson Number	Monin-Obhukhov Length (m)
A	$R_i < -0.86$	-2 to -3
B	$-0.86 \leq R_i \geq -0.37$	-4 to -5
C	$-0.37 \leq R_i \geq -0.10$	-12 to -15
D	$-0.10 \leq R_i \geq 0.053$	infinite
E	$0.053 \leq R_i \geq 0.134$	35 to 75
F	$0.134 \leq R_i$	8 to 35

Table 3.1: Values for Richardson Number and Monin-Obukhov length for each stability class [21]

The Pasquill stability classes have several weaknesses and can only give a basic guidance. The Monin-Obukhov theory was the one validated against several computational models and measurements. It showed the most reliable basis for atmospheric modeling.

3.3 Computational Models

There are three main modeling possibilities for atmospheric dispersion: The Gaussian dispersion model, the Eulerian dispersion model and the Lagrangian dispersion model. In the next paragraphs each will be discussed shortly. The model used for this work, the Lagrangian model, is discussed in more details in chapter 4.2. The basis for all three models is the solution of the transport equation, equation 3.9.

3.3.1 The Gaussian dispersion model

The equation 3.9 can be analytically integrated, if a homogenous, steady state flow and a steady state point source at (0,0,h) is assumed. This leads to the Gaussian

Die approbierte gedruckte Originalversion dieser Dissertation ist an der TU Wien Bibliothek verfügbar.
The approved original version of this doctoral thesis is available in print at TU Wien Bibliothek.
TU Bibliothek Your knowledge hub WIEN

plume distribution (see derivation in [22][2]:

$$\overline{c}(x,y,z) = \frac{Q}{2\pi\sigma_y\sigma_z\overline{u}} exp\left(\frac{-y^2}{2\sigma_y^2}\right)\left(exp\left(\frac{-(z-h)^2}{2\sigma_z^2}\right) + exp\left(\frac{-(z+h)^2}{2\sigma_z^2}\right)\right) \tag{3.15}$$

with $\overline{c}$ the time averaged concentration at a given position, Q the source term, x the downwind, y the crosswind and z the vertical direction and $\overline{u}$ the time averaged wind speed at the release height h. σ_z and σ_y are the crosswind and vertical mixing of the pollutant. The equation 3.15 describes a mixing process, resulting in a Gaussian distribution in vertical and crosswind direction. The distribution is centred at the downwind line from the source. The total reflection from the ground is the last term in the equation. As in the Gaussian model there is only one equation to solve, the models are quickly calculated. So if a fast response time is needed and the model is robust, the Gauss model can be chosen. The Gauss model fails however in situations with low wind speed or where a three dimensional diffusion is necessary. Gauss models can handle only close range applications, up to 100 km [23].

3.3.2 Lagrangian Dispersion Models

In contrast to the Gaussian models, for the Lagrangian models the trajectory of each particle is calculated. The trajectories are influenced by the wind field and the buoyancy (which are deterministic terms) and turbulence effects(which is a stochastic term). To avoid spatial truncation errors and numerical diffusion ordinary differential equations are used to calculate the trajectories. In the end, the distribution of a large number of particles in the field gives the concentration. The Lagrangian model is mainly used for short range simulations, due to the fact that the computational capacities have to increase with the range of the calculated model. This leads to the fact, that several models use a Lagrangian approach in the close range, and change to an Euler Model in the long range [13, 24, 25]. The trajectory of a particle can be described by:

$$\frac{d\vec{r}}{dt} = \vec{v} + \vec{v_1} \tag{3.16}$$

[2][13, p.8]

Die approbierte gedruckte Originalversion dieser Dissertation ist an der TU Wien Bibliothek verfügbar.
The approved original version of this doctoral thesis is available in print at TU Wien Bibliothek.
TU Bibliothek Your knowledge hub WIEN

with $\vec{r}$ the position of the particle, $\vec{v}$ the velocity of the particle and $\vec{v_1}$ the turbulent wind fluctuation vector. Using the Langevin equation, the turbulent wind fluctuation can be described [26]:

$$dw_t = -\frac{W_t}{T_L}dt + \sqrt{\frac{2\sigma_W^2}{T_L}}dW \tag{3.17}$$

with w_t the vertical turbulent fluctuation, T_L the integration time step , σ_W the vertical turbulent velocity fluctuation and dW a white noise process. There are 2 models that need to be discussed here:

- Puff Models
  Puff Models have its basis in Gaussian and Lagrangian models. "Puffs" are a superposition of several pollution clouds. The trajectories of these puffs are calculated. The way of calculation depends on the size of the puffs, below puff size the Gaussian model is taken, above puff size, the Lagrangian model is applied. Gaussian models gave a distribution along the centerline, puff models give a Gaussian plum along the wind driven trajectory. The concentration is then given by the overlap of all puffs. This leads to a computational effective model that can also handle spatial and temporal changes of the wind direction. To include turbulence there is either a stochastic random walk in the trajectories of the puffs, or a deviation of a normal distribution inside each puff [13].

- Trajectory Models
  These model types use a fraction of the released pollution and simulates the trajectory as a stochastic process for single point particles. These are influenced by advection, buoyancy and turbulence. The result is a good estimation of turbulence mixing, without solving differential equations, but with the disadvantage of high computational efforts. This method can also be used to calculate the origin of a pollution[13].

3.3.3 Euler Dispersion Models

The transport equation (Eq. 3.9) can be solved numerically in a fixed coordinate system, meaning that at each point in the system the atmospheric properties such as temperature, pressure, concentrations of pollutants are monitored over

Die approbierte gedruckte Originalversion dieser Dissertation ist an der TU Wien Bibliothek verfügbar.
The approved original version of this doctoral thesis is available in print at TU Wien Bibliothek.
TU Bibliothek Your knowledge hub WIEN

time. This leads to a second order partial differential equation, with its solution providing a spatio-temporal evolution of the concentration. The model is usually applied for large scale models, starting at 10 km of dispersion[13].

Die approbierte gedruckte Originalversion dieser Dissertation ist an der TU Wien Bibliothek verfügbar.
The approved original version of this doctoral thesis is available in print at TU Wien Bibliothek.
TU Bibliothek Your knowledge hub WIEN

4 RODOS - Description and Features

The simulation tool RODOS was developed by the Forschungszentrum Karlsruhe [12]. The accidents of Chernobyl, Fukushima and the attacks in September 2001 in the US showed the need of a quick, reliable and easy to communicate tool to limit fears of the public. Especially the Chernobyl accident showed that the trust of people in governments can be profoundly damaged, if the communication with them is not open and understandable. Since then a lot of improvements have been made, nevertheless continuous research and improvement is necessary. The nuclear security threat demands governments to act quickly in case of threat scenarios. In summary there are numerous requirements, including[1]:

- the need for a more coherent and harmonized response in Europe and in the different stages of an accident (in particular, to limit the loss of public confidence in the measures taken by the authorities for their protection);
- exchange of information and data in an emergency to enable neighboring countries to take more timely and effective actions; and
- the necessity to make better use of limited technical resources and avoid duplication.

The research group was founded in 1989, it gathers 40 institutions from over 20 countries in Europe. The system is designed to support decision makers before, during or after releases of radioactivity into the environment. It can help determining countermeasures such as evacuation, sheltering, iodine tablet distribution or food restrictions. A special feature is the part "on time", meaning that there is a connection possibility with local meteorological stations or weather forecasts to

[1] The RODOS System, Version PV6.0, page 6 [12]

Die approbierte gedruckte Originalversion dieser Dissertation ist an der TU Wien Bibliothek verfügbar.
The approved original version of this doctoral thesis is available in print at TU Wien Bibliothek.
TU Bibliothek Your knowledge hub WIEN

feed the current data into the system and have on time and local calculations. In Figure 4.1 the principle input possibilities of RODOS are shown.

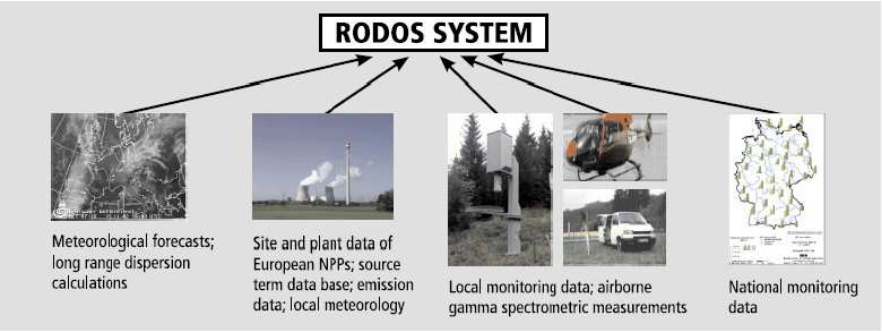

Figure 4.1: Principle input parameters and options for RODOS [12, p.10]

4.1 Design and features of RODOS

The RODOS architecture is depending on three subsystems, that are fed by databases: The Analysing Susbsystem, the Countermeasure Subsystem and the Evaluating Subsystem. In Figure 4.2 the communication of the different databases and the enduser is shown.

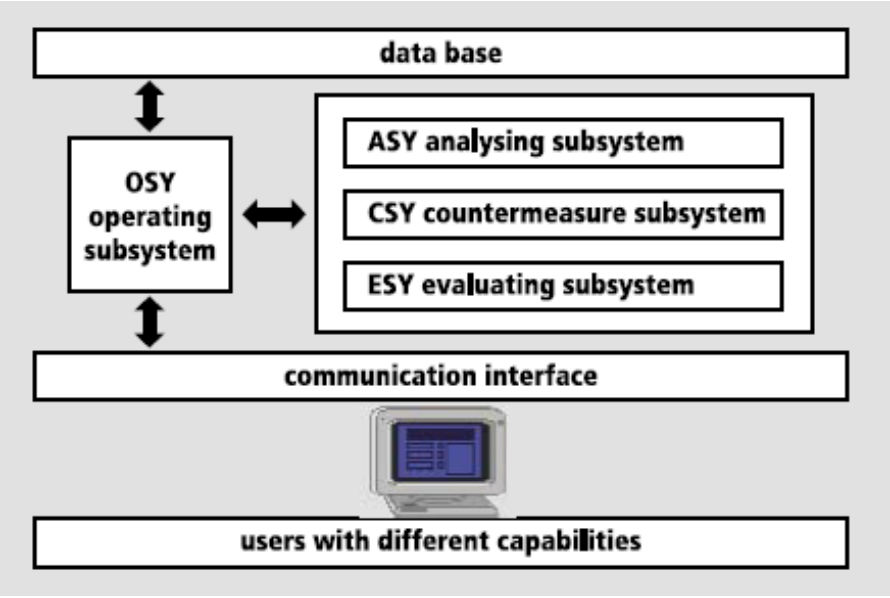

Figure 4.2: Database structure of RODOS System[12, p.9]

Die approbierte gedruckte Originalversion dieser Dissertation ist an der TU Wien Bibliothek verfügbar.
The approved original version of this doctoral thesis is available in print at TU Wien Bibliothek.
TU Bibliothek Your knowledge hub WIEN

The enduser is flexible in its operational mode. The RODOS designer developed two different modes of usage, the interactive and the automatic mode. The automatic mode is used if the end-user enters all known information to predict the possible consequences at a later stage. This option is limited to the closer surrounding of a nuclear installation (up to 160 by 160 km area). This mode was also chosen for this work, as there are no stable conditions, and predictions are needed. The interactive mode covers all consequences in wider areas, and also is applied after a certain time scale after the accident. In Figure 4.3 the comparison of the two modes are shown.

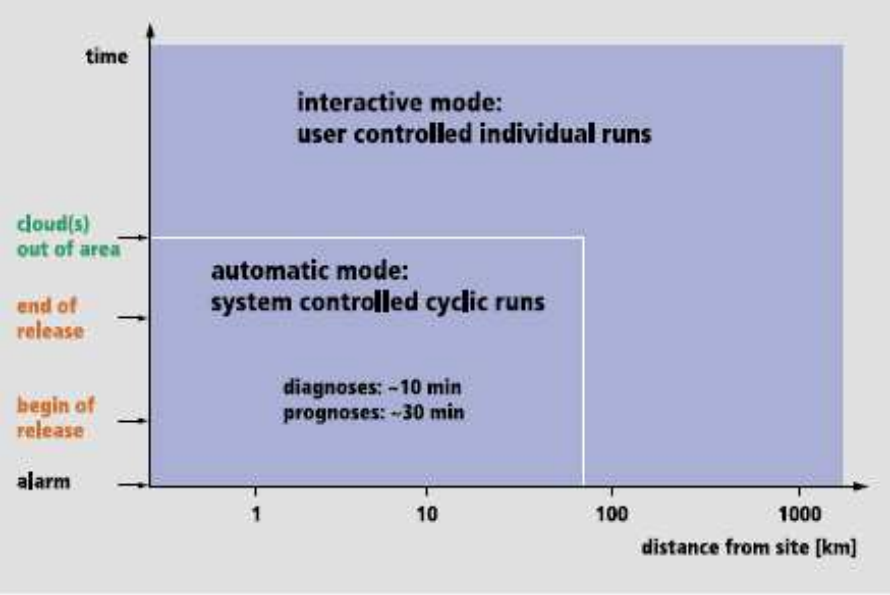

Figure 4.3: Operational modes of RODOS depending on time and distance to event position [12, p.9]

RODOS offers 4 near range models to choose from:

- ATSTEP: this model, a Gauß-puff model was the standard model developed by KIT in Karlsruhe. It is no longer supported by the developers.
- RIMPUFF: this model is also a Gauß-puff model
- DIPCOT: this model can be used for a more complex terrain, it is a particle model (see chapter 4.2)
- LASAT: it is a Lagrangian particle model, it needs strong servers and can only be operated with a license (see chapter 5).

Die approbierte gedruckte Originalversion dieser Dissertation ist an der TU Wien Bibliothek verfügbar.
The approved original version of this doctoral thesis is available in print at TU Wien Bibliothek.
TU Bibliothek Your knowledge hub WIEN

The choice for this work fell to DIPCOT, as it showed the most detailed possibilities to simulate and the computational possibilities were high enough to perform simulations within a realistic time. Also it was possible to simulate the surroundings of the reactor in details, to further precise the outcomes. In all simulations the Emergency Lite mode was used. This model chain is a simpler version of the Emergency model chain, that is designed to assess the radiological situation up to 1000 km, including countermeasures. The Emergency Lite mode uses the same model chains but has some reduced input parameters and uses less computational storage and time. The main difference is that the user has no possibilities to influence the countermeasure and food chain settings. In addition the models EmerSim (a model for simulating early emergency measures and resulting doses with and without actions) and FDMT (RODOS Food chain and Dose Models Terrestrial) run with default settings. For the scenarios chosen for this work and the dispersion calculations that were performed, the emergency measures and food chain restrictions are not considered, and can therefore be neglected. This lead to the choice of the Emergency Lite model.

4.1.1 Input Parameters

For the dispersion scenario calculations the following input parameters had to be included:

- General Selections
  For this work the model chain Emergency Lite was chosen. Further the dispersion model was set to DIPCOT.

- Site Information
  The first entry information are the site information. The user chooses the scenario option (Nuclear Power Plant accident, or other accident), and chooses the country where the accident happens. The second information entered is the location of the site, in a geographic coordinate system. Also the country for the countermeasures is chosen.

- Source Term Information
  RODOS has several possibilities to enter a source term. This can either be done manually by adding the different nuclides including the activity at the time of the release or using a given library source term for training

Die approbierte gedruckte Originalversion dieser Dissertation ist an der TU Wien Bibliothek verfügbar.
The approved original version of this doctoral thesis is available in print at TU Wien Bibliothek.
TU Bibliothek Your knowledge hub WIEN

calculations. RODOS has also stored source terms of several NPPs, to enable quick calculations in case of accidents. The time and duration of the release are set. It is possible to release all nuclides at the same time, or at different times. The thermal power of the nuclear power plant as the operation history before the accident is added as well. If the nuclides are added manually, the duration and height of the release are input parameters. The iodine fraction of organic-, aerosol- and elementary- bound iodine has to be set. The default value is 100 % elementary bound iodine. The additional parameters are the thermal power released, the vertically released volume flux and the vent area of the release to atmosphere.

- Weather Information
  As mentioned above, it is possible to feed RODOS with on-time information from a weather station. Otherwise the user has to input the data manually. The information needed are:
  - the begin and end of the weather interval
  - the wind direction in degree
  - the wind velocity in m/s or km/h
  - the rain intensity in mm/h
  - the diffusion category

  The diffusion category is equivalent to the Pasquill stability classes, with a range from A to F. There is an automated check in RODOS if the given conditions are plausible for the class. For this work the category D was chosen. It describes neutral weather, clouded sky at any windspeed (see also chapter 3.2.3). The measurement height of the weather data has also to be selected. At this point the user is able to choose the landuse around the site, with maximum width and height of buildings. The most important part is the choice of the prognoses interval, which was chosen to be 24 h for this work.

- Run and Summary Information
  The last input parameter is the radius of the calculation area, including the grid size. The user is able to choose between a 20 km up to 800 km radius for the calculations. For this work the value was set to 20 km with a grid

Die approbierte gedruckte Originalversion dieser Dissertation ist an der TU Wien Bibliothek verfügbar.
The approved original version of this doctoral thesis is available in print at TU Wien Bibliothek.
TU Bibliothek Your knowledge hub WIEN

cell size of 50 m. Before starting the simulation the user can verify all input parameters in a summary created by RODOS.

4.2 Dispersion Model DIPCOT

DIPCOT (DIsPersion over COmplex Terrain) is a computational model based on the Lagrangian Dispersion Model (see chapter 3.3.2) and the puff model for the dispersion of pollutants over complex terrain [28] . This model can simulate both in homogeneous and inhomogeneous conditions. The pollutants are distributed to fictitious puffs. The puffs are placed in the grid depending on the wind velocity and a random component is added for the turbulence. The spacious and temporal distribution of the particles can be calculated, with this the air concentration of the pollutants at specific times and places is known. The particle trajectories are calculated with

$$x_i^{n+1} = x_i^n + (\overline{u_i} + u_i')\Delta t \tag{4.1}$$

with n the time step index, i the Cartesian coordinates and $\overline{u_i}$ the mean wind velocity component in direction i and u_i' the turbulent velocity fluctuations. The one dimensional Langevin equation is used to estimate the parameter u_i':

$$du_i' = a_i dt + b_i dW_i(t) \tag{4.2}$$

The parameters a_i represents the drift term, b_i the diffusion term. The parameter a_i is determined through the consistency between Eulerian and Lagrangian statistics:

$$a_i = \left[\frac{\partial}{\partial u_i'}\left(\frac{1}{2}b_i^2 P_a\right) + \Phi_i\right]/P_a \tag{4.3}$$

with P_a is the Eulerian velocity probability density function, Φ_i the . The diffusion term b_i is calculated through the consistency with the Kolmogorov's similarity theory through comparing it with eq. 4.2.

$$b_i = (2\sigma_{ui}^2/T_{Lui})^{1/2} \tag{4.4}$$

with σ_{ui} the standard deviation of the wind fluctuations and T_{Lui} the Lagrangian time scale.

Die approbierte gedruckte Originalversion dieser Dissertation ist an der TU Wien Bibliothek verfügbar.
The approved original version of this doctoral thesis is available in print at TU Wien Bibliothek.
TU Bibliothek Your knowledge hub WIEN

4.2.1 Concentration Calculation

DIPCOT implements two methods to calculate the concentration of particles: The box counting method and the density kernel estimation method. The user of RODOS is able to chose the preferred method, the standard is set to the kernel distribution method, which will be described here. This method was proposed by Yamada and Bunker in 1988, it describes that each particle represents the centre of a puff. The concentration is then distributed in a Gaussian manner in three directions. To calculate the concentration at a point (x,y,z) the contributions from all particle puffs are summed:

$$c(x,y,z) \tag{4.5}$$
$$= \frac{1}{(2\pi)^{2/3}} \sum_{i=1}^{N} \frac{Q_i}{\sigma_{xi}\sigma_{yi}\sigma_{zi}} exp\left[-\frac{1}{2}\frac{(x_i-x)^2}{\sigma_{xi}^2}\right] exp\left[-\frac{1}{2}\frac{(y_i-y)^2}{\sigma_{yi}^2}\right] \left\{exp\left[-\frac{1}{2}\frac{(z_i-z)^2}{\sigma_{zi}^2}\right] + exp\left[-\frac{1}{2}\frac{(z_i+z-2z_g)^2}{\sigma_{zi}^2}\right]\right\}$$

with (x,y,z) the point coordinates of the concentration, (x_i, y_i, z_i) the puff i coordinates, and $(\sigma_{hi}, \sigma_{zi})$ the standard deviations of the i-particle position in horizontal and vertical directions. Q_i is the load - meaning the radioactivity or the mass of the puff, z_g is the ground height at (x,y).

Die approbierte gedruckte Originalversion dieser Dissertation ist an der TU Wien Bibliothek verfügbar.
The approved original version of this doctoral thesis is available in print at TU Wien Bibliothek.
TU Bibliothek Your knowledge hub WIEN

5 LASAIR

To achieve a validation of the data, a second tool for comparisons, the simulation tool LASAIR was chosen. The acronym stands for Lagrangsche Simulation der Ausbreitung und Inhalation von Radionukliden (Lagrangian Simulations of dispersion and inhalation of radionuclides). It was developed as a graphical tool for the modeling chain LASAT (see chapter 3.3.2). It is mainly used to calculate the consequences after explosion scenarios or fires. The biggest difference to RODOS is the smaller possible grid size, but the lesser variation possibility in terms of source term and meteorology. LASAIR was developed in 2001 on behalf of the German Federal Office for Radiation Protection.

5.1 Features of LASAIR

The aim of the model LASAIR is to easily and rapidly simulate the atmospheric dispersion of radioactive substances with a diagnostic windfield model in combination with a Lagrangian particle model (see [35]). The exposure and potential doses are calculated in a second step. The input data contain meteorological data as

- the wind speed
- the wind direction and
- the stability class

Additionally it gives information on the release (short term or continuous release) and the program provides the topography, such as the individual roughness length. The LASAIR output gives

- Radionuclide information
  up to 5 nuclides, the activity in the base layer, the deposition on the surface

Die approbierte gedruckte Originalversion dieser Dissertation ist an der TU Wien Bibliothek verfügbar.
The approved original version of this doctoral thesis is available in print at TU Wien Bibliothek.
TU Bibliothek Your knowledge hub WIEN

(this is the only parameter to include rain rates - and only an average term) and the cloud arrival time.

- Exposition
  here information are given such as inhalation, ground-shine and the cloud-shine

Overall, this model gives a quick overview of the potential areas that have to be informed or evacuated, but due to the lack of detailed meteorological input data (such as rain rate), it can't be used for all weather scenarios.

5.2 Dispersion Model LASAT

The model calculates the dispersion of particles in the atmosphere. LASAT (LAgrange-Simulation von Aerosol-Transport - Lagrangian Simulation of Aerosol Transport) is a Lagrangian simulation model (see 3.3.2) that calculates for a group of representative particles their dispersion in the atmosphere. A random process initiates this simulation. The model was developed in the 1980s, since 1990 its an open software tool. It can simulate the dispersion up to 2000 m into the atmosphere, in local and regional areas, up to 200 km[34]. LASAT is based on the Lagrangian particle model described in VDI 3945, sheet 3. Depending on the time, it simulates the following procedures:

- transport through average wind
- dispersion in atmosphere
- sedimentation of heavy aerosols
- deposition on soil (dry deposition)
- washing out of particles through rain and wet deposition
- chemical change of first order

5.3 Summary

The fundamental difference between both simulation tools is the original intent. RODOS can be used on-time with live data to simulate complex scenarios, as NPP

Die approbierte gedruckte Originalversion dieser Dissertation ist an der TU Wien Bibliothek verfügbar.
The approved original version of this doctoral thesis is available in print at TU Wien Bibliothek.
TU Bibliothek Your knowledge hub WIEN

accidents. LASAIR is intended to simulate smaller events. The TRIGA reactor scenarios can be classified as small events (looking at the source term and the outcome), hence the comparison between the tools is valid. Nevertheless, LASAIR offers a smaller range of parameters that can be modified by the user. Comparing the meteorological input parameters, RODOS has more possibilities to simulate the weather conditions, especially with regards to the precipitation. LASAIR does not take precipitation into account for its meteorological simulation. Precipitation is only taken into account for a deposition of activity on the ground, but not for dose calculations. As this work compares gamma life time doses, the results will vary due to this feature. RODOS does take precipitation into account, all results (also gamma life time dose) include the deposition data (not averaged). In addition LASAIR only take the meteorological data during the release into account. RODOS takes the data during and after the release for the prediction time into account. The source term data also show big differences: RODOS is able to include as many nuclides as needed, LASAIR only allows five nuclides. RODOS allows nuclides to be emitted at different time steps, this is not possible with LASAIR. The simulation area is more detailed for LASAIR, starting at a grid size of 5 m, 10 m or 20 m, while RODOS starts at 50 m grid size.

Die approbierte gedruckte Originalversion dieser Dissertation ist an der TU Wien Bibliothek verfügbar.
The approved original version of this doctoral thesis is available in print at TU Wien Bibliothek.
TU Bibliothek Your knowledge hub WIEN

6 Meteorological Data

The Atominstitut possesses its own weather station. It was therefore feasible to use meteorological data from this station to perform the described work. The weather station is in operation since 2009. The station is also used inside the reactor hall for the sampling of data like temperature and humidity inside.

6.1 Characteristics of the station

The station collects 33 parameters every 10 minutes. Besides the parameters that are measured inside the hall, all other parameters are collected on the rooftop of the institute. A photovoltaic cell is used to power the station. This can lead to sample failures during longer periods without sun. In Figure 6.1 the weather station is shown.

Figure 6.1: Weather station on the roof of the Institute

In Table 6.1 the parameters measured by the station are shown.

Die approbierte gedruckte Originalversion dieser Dissertation ist an der TU Wien Bibliothek verfügbar.
The approved original version of this doctoral thesis is available in print at TU Wien Bibliothek.
TU Bibliothek Your knowledge hub WIEN

Paramete Name	Explanation
Date	Measurement Date
Time	Measurement Time
Temp out	The temperature returned
Hi Temp	highest measured temperature
low Temp	lowest measured temperature
Out Hum	relative Humidity returned
Dew pt	
Wind speed	Wind speed
Wind Dir	Wind direction
Wind Run	
Hi Speed	highest measured wind speed
hi Dir	highest measured direction
Wind Chill	
Heat Index	
THW Index	
THSW Index	
Wind speed	
Rain	Rain in mm
Rain Rate	
Solar Rad	Solar Radiation
Solar Energy	
Hi Solar Rad	
Heat D-D	
Cool D-D	
In Temp	Temperature inside
In Hum	Humidity inside
In Dew	
In Heat	
ET	
Wind Samp	
Wind Tx	
ISS Recept	
Arc. Int	

Table 6.1: Metereological Data points from the ATI weather station and its explanations

The data for this work were taken from the years 2010 till 2013 and evaluated. RODOS and LASAIR need only a small set of data for performing the simulations,

Die approbierte gedruckte Originalversion dieser Dissertation ist an der TU Wien Bibliothek verfügbar.
The approved original version of this doctoral thesis is available in print at TU Wien Bibliothek.
TU Bibliothek Your knowledge hub WIEN

which are the following:

- Wind direction in degrees
- Wind speed in m/s
- Rain per hour in mm
- Stability class

6.2 Weather scenarios

In the subsequent work, Haydn (see [5]) looked only at an average weather scenario. This work has now a fundamental different approach - it looks at specific weather scenarios that occur during a year. In the following sections those scenarios are described, these are the average scenarios:

1. Spring day
2. Summer day
3. Autumn day
4. Winter day

and the specific scenarios:

1. Hot day
2. Foggy day
3. Thunderstorm day

All scenarios were taken for a 24 h simulation period with RODOS and for 1 h with LASAIR. The average scenarios use mean values for the calculation input in RODOS, see Berger [9]. For the specific scenarios Berger [9] chose data from three individual days without averaging the data. For simulation with LASAIR these data had to be further adapted (see chapter 6.2.9).

Die approbierte gedruckte Originalversion dieser Dissertation ist an der TU Wien Bibliothek verfügbar.
The approved original version of this doctoral thesis is available in print at TU Wien Bibliothek.
TU Bibliothek Your knowledge hub WIEN

6.2.1 Preparation of weather data

In order to be able to use the weather data provided by the weather station, it was necessary to perform corrections. In previous works (see [9]) this was started, but while looking at the output it was found out that the calculations were not thoroughly performed. The wind speed data and the wind direction data were incorrect, and hence re-evaluated for this work. So the raw data were taken and analyzed. Berger [9] describes the malfunctions of the system. Berger did a research on the specific dates for the scenarios, which was later on the bases for the calculations. The station delivers a value for each measurement point every ten minutes. To gain average data over specific time periods, the following calculations had to be made: For the wind direction and the wind speed the mean value over the specific time period was taken. For the rain rate, over one 1 hour the values were summed up. Then the average was calculated for each hour, as for the wind speed and wind direction values. To show the main wind direction is slightly variating between the seasons, windroses were drawn for each season for the years 2012 and 2013. They are shown below.

6.2.2 Spring day

For the spring calculations the work from Berger (see [9]) was taken. The average spring day he calculated was corrected and used for the calculations. The corrections included the wind direction and the wind speed. Figures 6.2 and 6.3 show the wind directions over spring time during 2012 and 2013. The calculations were performed with the raw data of the weather station data. Table 6.2 shows the averaged data for the spring season. These were the data used for the later analysis.

Time	Windspeed [km/h]	Winddirection	Rain [mm]
00:00	6.45	323	0.03
01:00	6.35	324	0.02
02:00	6.30	325	0.01
03:00	6.31	325	0.02
04:00	6.21	326	0.04
05:00	6.36	332	0.04
06:00	6.93	337	0.03

Continued on next page

Die approbierte gedruckte Originalversion dieser Dissertation ist an der TU Wien Bibliothek verfügbar.
The approved original version of this doctoral thesis is available in print at TU Wien Bibliothek.
TU Bibliothek Your knowledge hub WIEN

Table 6.2 – *Continued from previous page*

Time	Windspeed [km/h]	Winddirection	Rain [mm]
07:00	7.93	346	0.04
08:00	9.12	354	0.03
09:00	9.96	0	0.03
10:00	10.56	360	0.05
11:00	11.04	8	0.06
12:00	11.41	14	0.07
13:00	11.55	15	0.08
14:00	11.35	20	0.05
15:00	11.41	18	0.05
16:00	10.90	21	0.14
17:00	9.83	29	0.07
18:00	8.32	26	0.08
19:00	7.40	5	0.08
20:00	6.92	336	0.06
21:00	6.81	325	0.06
22:00	6.66	322	0.03
23:00	6.62	323	0.04

Table 6.2: Metereological data for an average spring day

Die approbierte gedruckte Originalversion dieser Dissertation ist an der TU Wien Bibliothek verfügbar.
The approved original version of this doctoral thesis is available in print at TU Wien Bibliothek.

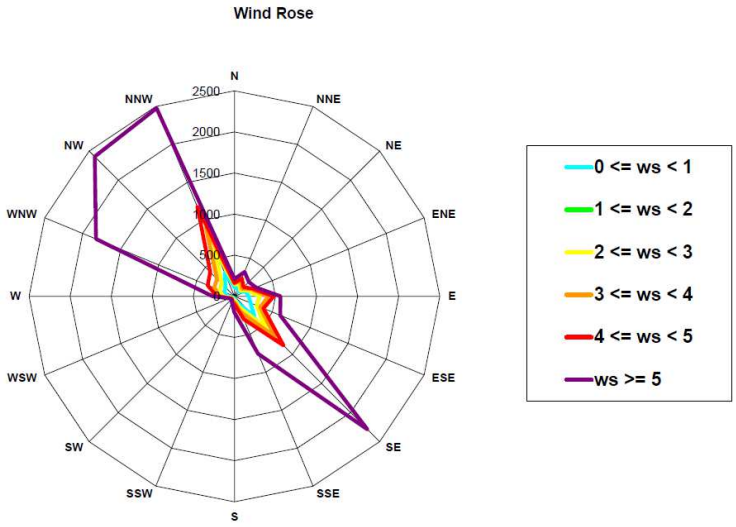

Figure 6.2: Wind Rose for Spring data of 2012, ws is the wind speed in m/s

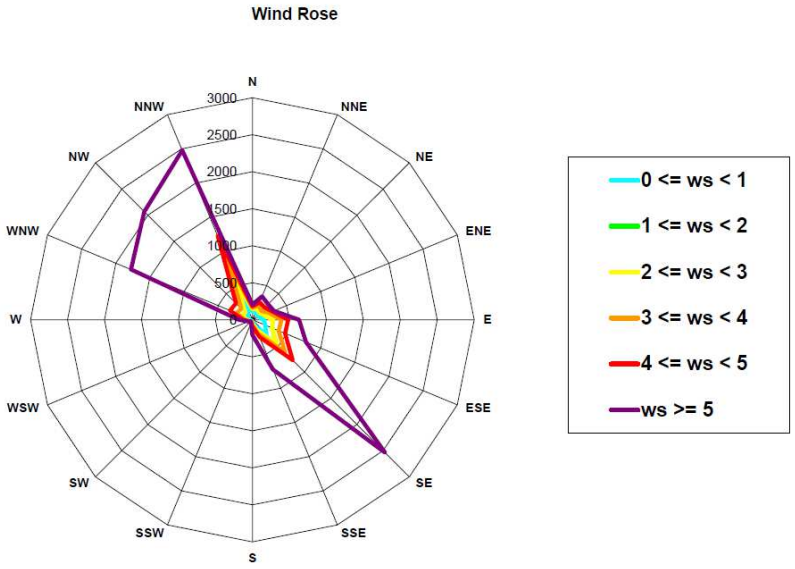

Figure 6.3: Wind Rose for Spring data of 2013, ws is the wind speed in m/s

Die approbierte gedruckte Originalversion dieser Dissertation ist an der TU Wien Bibliothek verfügbar.
The approved original version of this doctoral thesis is available in print at TU Wien Bibliothek.
TU Bibliothek Your knowledge hub WIEN

6.2.3 Summer day

For the summer calculations the work from Berger (see [9]) was taken. The average summer day he calculated was corrected and used for the calculations. The corrections included the wind direction and the wind speed. Figures 6.4 and 6.5 show the wind directions over summer time during 2012 and 2013. The calculations were performed with the raw data of the weather station data. Table 6.2 shows the averaged data for the summer season. These were the data used for the later analysis.

Time	Windspeed [km/h]	Winddirection	Rain [mm]
00:00	5.39	313	0.13
01:00	5.39	316.	0.11
02:00	5.47	319	0.06
03:00	5.33	318	0.08
04:00	5.37	317	0.07
05:00	5.61	322	0.05
06:00	6.66	331	0.08
07:00	7.55	338	0.07
08:00	8.15	347	0.08
09:00	8.58	353	0.06
10:00	8.83	352	0.06
11:00	9.14	354	0.05
12:00	9.41	1	0.10
13:00	9.62	2	0.20
14:00	9.86	2	0.07
15:00	9.64	358	0.05
16:00	9.51	357	0.11
17:00	9.03	359	0.19
18:00	7.79	354	0.10
19:00	6.37	340	0.15
20:00	6.01	327	0.11
21:00	5.88	316	0.21
22:00	5.96	313	0.10
23:00	5.70	315	0.07

Table 6.3: Metereological data for an average summer day

Die approbierte gedruckte Originalversion dieser Dissertation ist an der TU Wien Bibliothek verfügbar.
The approved original version of this doctoral thesis is available in print at TU Wien Bibliothek.
TU Bibliothek Your knowledge hub WIEN

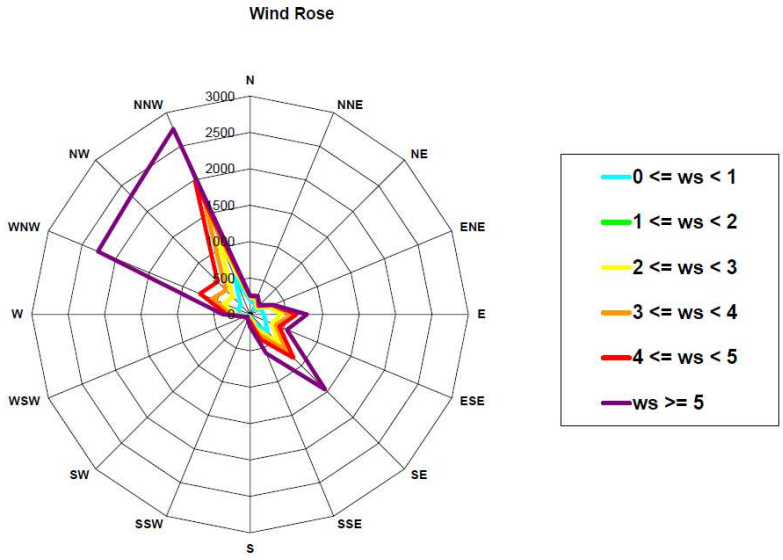

Figure 6.4: Wind Rose for Summer data of 2012, ws is the wind speed in m/s

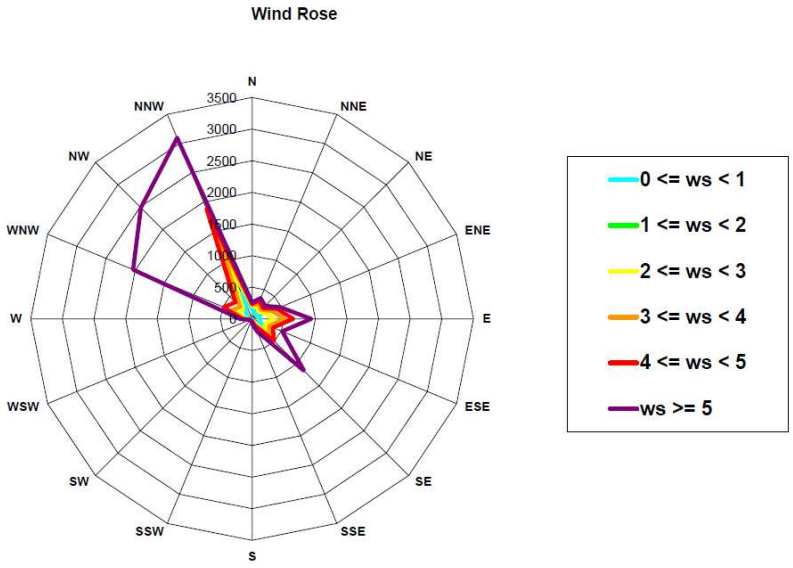

Figure 6.5: Wind Rose for Summer data of 2013, ws is the wind speed in m/s

Die approbierte gedruckte Originalversion dieser Dissertation ist an der TU Wien Bibliothek verfügbar.
The approved original version of this doctoral thesis is available in print at TU Wien Bibliothek.
TU Bibliothek Your knowledge hub WIEN

6.2.4 Autumn day

For the autumn calculations the work from Berger (see [9]) was taken. The average autumn day he calculated was corrected and used for the calculations. The corrections included the wind direction and the wind speed. Figures 6.6 and 6.7 show the wind directions over autumn time during 2012 and 2013. The calculations were performed with the raw data of the weather station data. Table 6.2 show the averaged data for the autumn season. These were the data used for the later analysis.

Time	Windspeed [km/h]	Winddirection	Rain [mm]
00:00	1.54	322	0.06
01:00	1.53	336	0.08
02:00	1.52	334	0.05
03:00	1.53	335	0.06
04:00	1.53	340	0.05
05:00	1.51	349	0.05
06:00	1.61	7	0.04
07:00	1.80	37	0.04
08:00	2.13	48	0.03
09:00	2.41	68	0.02
10:00	2.57	62	0.03
11:00	2.73	77	0.04
12:00	2.72	87	0.03
13:00	2.79	88	0.03
14:00	2.76	83	0.03
15:00	2.55	83	0.04
16:00	2.28	83	0.04
17:00	1.96	77	0.04
18:00	1.84	57	0.05
19:00	1.76	338	0.06
20:00	1.72	332	0.07
21:00	1.60	335	0.08
22:00	1.53	343	0.05
23:00	1.51	330	0.05

Table 6.4: Metereological data for an average autumn day

Die approbierte gedruckte Originalversion dieser Dissertation ist an der TU Wien Bibliothek verfügbar.
The approved original version of this doctoral thesis is available in print at TU Wien Bibliothek.
TU Bibliothek Your knowledge hub WIEN

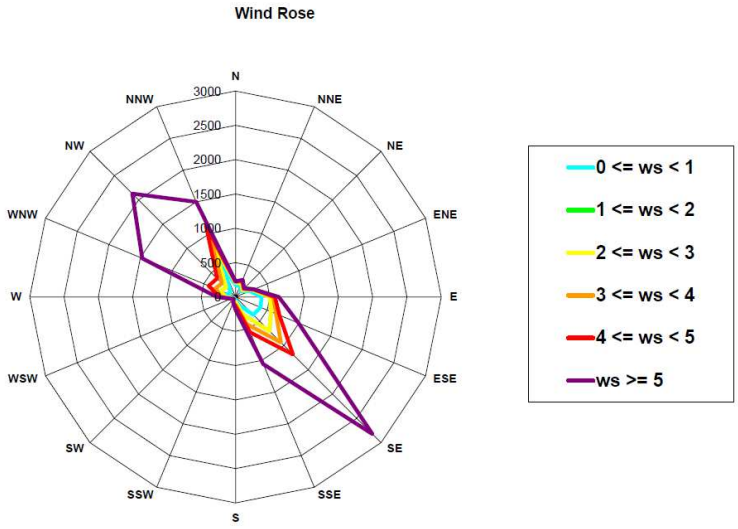

Figure 6.6: Wind Rose for Autumn data of 2012, ws is the wind speed in m/s

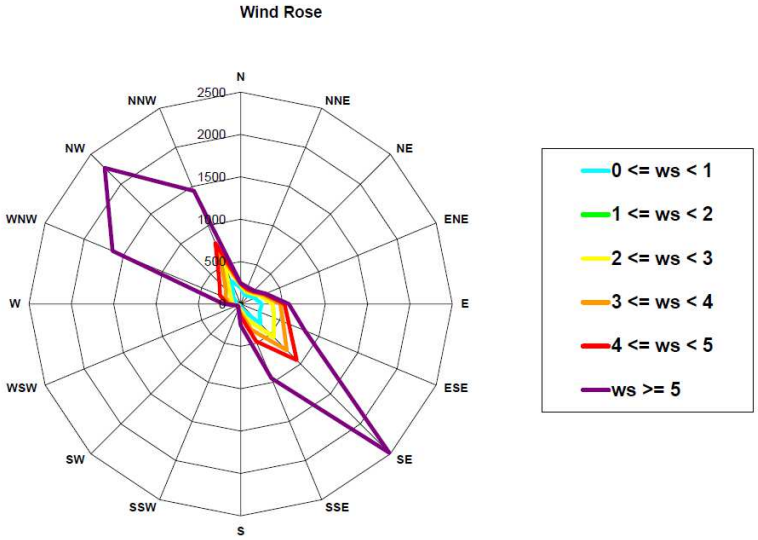

Figure 6.7: Wind Rose for Autumn data of 2013, ws is the wind speed in m/s

Die approbierte gedruckte Originalversion dieser Dissertation ist an der TU Wien Bibliothek verfügbar.
The approved original version of this doctoral thesis is available in print at TU Wien Bibliothek.
TU Bibliothek Your knowledge hub WIEN

6.2.5 Winter day

For the winter calculations the work from Berger (see [9]) was taken. The average winter day he calculated was corrected and used for the calculations. The corrections included the wind direction and the wind speed. Figures 6.8 and 6.9 show the wind directions over winter time during 2012 and 2013. The calculations were performed with the raw data of the weather station data. Table 6.2 show the averaged data for the winter season. These were the data used for the later on analysis.

Time	Windspeed [km/h]	Winddirection	Rain [mm]
00:00	9.01	328	0.03
01:00	9.08	325	0.03
02:00	8.88	326	0.05
03:00	8.73	329	0.03
04:00	8.64	332	0.02
05:00	8.75	330	0.01
06:00	8.98	327	0.02
07:00	9.11	329	0.02
08:00	9.38	332	0.03
09:00	10.03	340	0.02
10:00	10.44	342	0.03
11:00	10.95	340	0.05
12:00	11.41	334	0.05
13:00	11.18	336	0.06
14:00	10.85	340	0.04
15:00	10.22	349	0.04
16:00	9.78	348	0.03
17:00	9.13	341	0.04
18:00	9.05	334	0.03
19:00	9.17	328	0.03
20:00	8.90	333	0.03
21:00	8.63	333	0.03
22:00	8.82	332	0.03
23:00	8.98	326	0.04

Table 6.5: Metereological data for an average winter day

Die approbierte gedruckte Originalversion dieser Dissertation ist an der TU Wien Bibliothek verfügbar.
The approved original version of this doctoral thesis is available in print at TU Wien Bibliothek.
TU Bibliothek Your knowledge hub WIEN

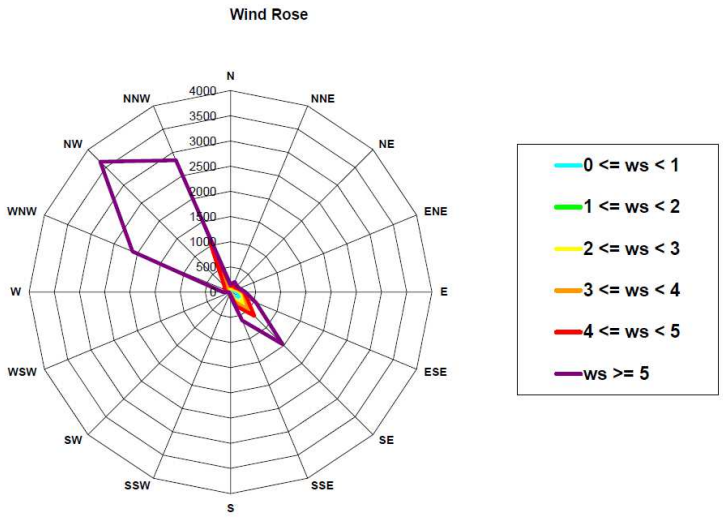

Figure 6.8: Wind Rose for Spring data of 2012, ws is the wind speed in m/s

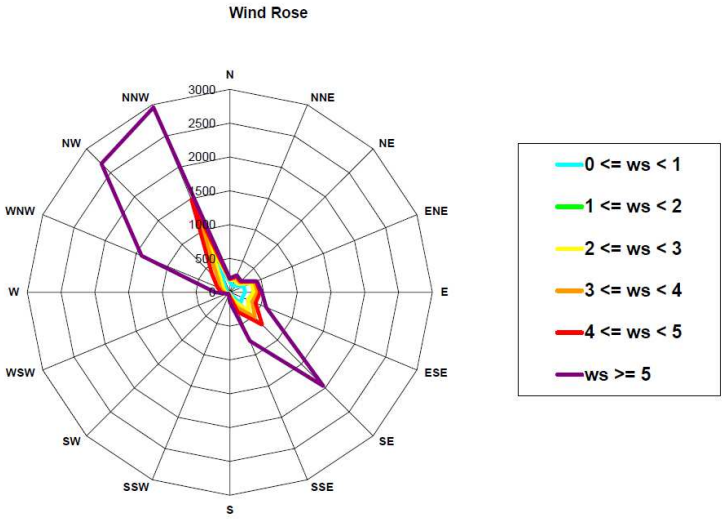

Figure 6.9: Wind Rose for Spring data of 2013, ws is the wind speed in m/s

Die approbierte gedruckte Originalversion dieser Dissertation ist an der TU Wien Bibliothek verfügbar.
The approved original version of this doctoral thesis is available in print at TU Wien Bibliothek.
TU Bibliothek Your knowledge hub WIEN

6.2.6 Hot day

For the hot day calculations the work from Berger (see [9]) were taken. The hot day he calculated was corrected and used for the calculations. The corrections included the wind direction and the wind speed. The calculations were performed with the data from Table 6.6.

Time	Windspeed [km/h]	Winddirection	Rain [mm]
00:00	6.13	135	0.00
01:00	3.47	135	0.00
02:00	1.33	105	0.00
03:00	0.27	128	0.00
04:00	0.27	112	0.00
05:00	5.35	135	0.00
06:00	2.40	135	0.00
07:00	2.13	153	0.00
08:00	2.40	109	0.00
09:00	2.40	79	0.00
10:00	3.73	90	0.00
11:00	4.27	97	0.00
12:00	8.30	113	0.00
13:00	11.30	120	0.00
14:00	13.17	131	0.00
15:00	12.37	112	0.00
16:00	12.10	131	0.00
17:00	14.77	135	0.00
18:00	10.22	135	0.00
19:00	6.67	146	0.00
20:00	11.27	289	0.00
21:00	14.77	293	0.00
22:00	14.50	293	0.00
23:00	16.63	296	0.00

Table 6.6: Metereological data for a hot day

Die approbierte gedruckte Originalversion dieser Dissertation ist an der TU Wien Bibliothek verfügbar.
The approved original version of this doctoral thesis is available in print at TU Wien Bibliothek.

6.2.7 Foggy day

For the foggy day calculations the work from Berger (see [9]) were taken. The foggy day he calculated was corrected and used for the calculations. The corrections included the wind direction and the wind speed. The calculations were performed with the data from Table 6.7.

Time	Windspeed [km/h]	Winddirection	Rain [mm]
00:00	0.00	135	0.00
01:00	0.00	135	0.20
02:00	0.00	357	0.00
03:00	0.00	90	0.00
04:00	0.00	135	0.00
05:00	0.27	68	0.00
06:00	0.80	86	0.00
07:00	2.13	101	0.00
08:00	2.67	97	0.00
09:00	2.67	105	0.00
10:00	4.00	120	0.00
11:00	3.47	109	0.00
12:00	1.07	131	0.00
13:00	0.00	84	0.00
14:00	0.00	354	0.00
15:00	0.00	360	0.00
16:00	0.27	346	0.00
17:00	0.00	359	0.00
18:00	0.00	45	0.00
19:00	0.00	345	0.00
20:00	1.33	296	0.00
21:00	0.00	351	0.00
22:00	0.00	336	0.00
23:00	0.00	315	0.00

Table 6.7: Metereological data for a foggy day

Die approbierte gedruckte Originalversion dieser Dissertation ist an der TU Wien Bibliothek verfügbar.
The approved original version of this doctoral thesis is available in print at TU Wien Bibliothek.
TU Bibliothek Your knowledge hub WIEN

6.2.8 Thunderstorm day

For the thunderstorm day calculations the work from Berger (see [9]) were taken. The Thunderstorm day he calculated was corrected and used for the calculations. The corrections included the wind direction and the wind speed. The calculations were performed with the data from Table 6.8.

Time	Windspeed [km/h]	Winddirection	Rain [mm]
00:00	1.07	246	0.00
01:00	0.00	270	0.00
02:00	0.00	263	0.00
03:00	0.00	171	0.00
04:00	0.27	36	0.00
05:00	1.07	303	0.00
06:00	0.80	135	0.00
07:00	4.27	154	0.00
08:00	0.80	155	0.00
09:00	2.40	110	0.00
10:00	1.07	131	0.00
11:00	5.08	116	0.00
12:00	6.68	153	0.00
13:00	7.77	131	0.00
14:00	7.47	124	0.00
15:00	8.03	62	0.00
16:00	5.35	64	3.00
17:00	7.23	257	17.60
18:00	1.07	6	0.20
19:00	1.60	292	0.00
20:00	3.47	281	0.00
21:00	4.53	293	0.00
22:00	8.30	293	0.00
23:00	12.63	304	0.00

Table 6.8: Metereological data for a thunderstorm day

Die approbierte gedruckte Originalversion dieser Dissertation ist an der TU Wien Bibliothek verfügbar.
The approved original version of this doctoral thesis is available in print at TU Wien Bibliothek.
TU Bibliothek Your knowledge hub WIEN

6.2.9 Data for LASAIR

Lasair is designed for simulating consequences of explosion or fire scenarios. Those have only a near range (< 10 km) impact, and require data only for short time frames. Hence the input data flexibility is smaller than for RODOS. LASAIR requires:

- Wind direction
- Wind speed
- Pasquill stability class

Rain data can only be added in a second calculation step, but they are not included in the dispersion calculation. To fulfill the LASAIR requirements, the above data (see Table 6.2 to 6.8) had to be adapted. The mean wind direction was calculated using the following equation [29]:

$$\overline{\alpha} = atan(\frac{\sum sin\alpha}{\sum cos\alpha}) \tag{6.1}$$

with α being the wind direction in degree, and $\overline{\alpha}$ the mean wind direction. In dependence of the outcome of the sum of sine and sum of cosine, the angle $\overline{\alpha}$ has to be amended: if the sum of the sine and cosine is positive, not correction is necessary. If the sum of sine is positive and the sum of cosine is negative, the correct mean angle is $180 - \overline{\alpha}$. If the sum of the sine is negative and the sum of the cosine as well, the correct mean angle is $180 + \overline{\alpha}$. If the sum of the sine is negative and the sum of the cosine is positive, the correct mean angle is $360 - \overline{\alpha}$ [29]. This calculation was performed for all the above mentioned scenarios except the Thunderstorm scenario. Here, the wind direction, the wind speed and rain rate at the time of the thunderstorm were taken, and not the average values. The minimum wind speed in LASAIR is 0.5 m/s, hence a no-wind-scenario is not possible. This caused issues with the Foggy Day scenario. The original value of 0.22 m/s for the Foggy Day scenario had to be changed to 0.5 m/s. Otherwise a calculation would not have been possible. Table 6.9 shows the input parameters for the LASAIR calculations.

Die approbierte gedruckte Originalversion dieser Dissertation ist an der TU Wien Bibliothek verfügbar.
The approved original version of this doctoral thesis is available in print at TU Wien Bibliothek.
TU Bibliothek Your knowledge hub WIEN

	Wind direction	Windspeed $[m/s]$	Rainrate $[mm/h]$
Spring Day	351	2.35	0.05
Summer Day	338	2.04	0.10
Autumn Day	24	0.57	0.05
Winter Day	334	2.64	0.03
Thunderstorm	257	7.23	17.60
Foggy Day	57	0.5*	0.01
Hot Day	305	2.09	0.00

Table 6.9: Meteorological input data for LASAIR simulations, * this value was changed from 0.22 to 0.5

6.2.10 Summary of Weather data

The weather data show a consistent wind direction. The only visible deviation appears in spring time. The rain rates differ strongly depending on the season, this strongly influences the outcomes of the different scenarios.

Since the meteorological conditions can strongly differ from the average scenarios, it is important to investigate the three specific scenarios (Hot day, Foggy day and Thunderstorm day) individually.

Comparing the RODOS and LASAIR input data shows several differences. LASAIR allows less flexibility with the meteorological input data, hence all three specific scenarios can not be reflected with LASAIR as accurately as with RODOS. Furthermore the fact that LASAIR requires a wind speed > 0.5 m/s will falsify the Foggy Day scenario. A comparison of scenarios is therefore only possible for the average scenarios.

Die approbierte gedruckte Originalversion dieser Dissertation ist an der TU Wien Bibliothek verfügbar.
The approved original version of this doctoral thesis is available in print at TU Wien Bibliothek.
TU Bibliothek Your knowledge hub WIEN

7 Source Term Calculations

Next to the meteorological data, the source term is the most important input for the simulation. Previous simulations used calculation data for the old core (see [5]). As the Triga reactor received a new core in 2012, it was necessary to update the core data. This was done with the program ORIGEN, as described by Stummer et al. [31], [32]. At the end of 2014 the calculations were repeated, with the correct data of operation from 2012 till 2014. The reactor operated for 1718,96 h in this time. The second simulation was done for the end of life-time of the reactor in 2025, assuming a continuous operation from 2014 till 2025 for 24 h 7 days a week, this leads to 50875 h of operation. This calculation overestimates the burnup as the reactor is usually 2000 h per year in operation, which would lead to a maximum operation time of 24000 h till 2025.

7.1 Simulation data

The core consisted in 2013 of 78 fuel elements, split in 5 rings, as shown in chapter 1.2.2 and Figure 1.3. For the severe accident simulations some assumptions were made as described below. The core configuration did not change in the first two years of operation. This made an average calculation per ring possible: For each ring an averaged burnup was calculated for one fuel element with averaged activity values, representative of each ring. The ORIGEN simulation revealed the nuclides present in the element. The full simulation output can be found in appendix B.2, Tables B.1 to B.10.The burnup assumed that the reactor was driven at maximum power over the two years (2012 - 2014). This leads to an overestimation of the burnup. Taking the averaged power over the two years would lead to an underestimation of the burnup. In regard to conservativeness the first option with the maximum power was chosen. After two years of operation the main activity input comes from short lived nuclides, which are in equilibrium already.

Die approbierte gedruckte Originalversion dieser Dissertation ist an der TU Wien Bibliothek verfügbar.
The approved original version of this doctoral thesis is available in print at TU Wien Bibliothek.
TU Bibliothek Your knowledge hub WIEN

7.1.1 Nuclides for Simulation

The next step was to choose the representative nuclides for the severe accident simulations. Haydn (see [5]) used krypton, xenon and iodine nuclides for the simulation.

These elements are the representative ones for dose calculation. Two points are important to be considered: Shall non-gaseous fission elements be included in the source term data, and are short lived isotopes relevant for the simulation. Regarding the first point, Foushee and Peters showed in their publication that the "release of non-gaseous fission products is typically one or more orders of magnitude lower, and thus, exposure from the source is secondary to exposure from gaseous radionuclides."[1]. They state further that even the release fractions from non-gaseous fission products from damaged irradiated TRIGA fuel elements are not well characterized. The fraction can be considered negligible. A factor of 1×10^{-6} could be applied, which would lead to an activity of several kBq in this works simulation. Therefore non-gaseous fission elements were not considered in calculations for this work. This was also driven by the fact that previous simulations did not take non-gaseous fission elements into account. Regarding the discussion about short lived isotopes, this work continuous with the choice of previous works and included only nuclides with half-lives > 14 min. Several nuclides were excluded from the new simulations, as they are not yet present in the ORIGEN calculations (He, Ne, Ar, Ra, Fl, Cl, As, Br).

This brought the list of nuclides to the following list, which are included in all simulations with RODOS, including their half-lives:

Isotope	**Half-Live**
Kr-83m	1.83 h
Kr-85m	4.48 h
Kr-85	10.76 a
I-130	12.36 h
I-131	8.02 d
I-132	2.3 h
I-134	52 min

Continued on next page

[1] F.C.Foushee, R.H.Peters, Summary of TRIGA Fuel Fission Product Release Experiments, Gulf-EES-A10801, TRIGA Reactors, Gulf Energy and Environmental Systems, Inc San Diego, California, US, 1971

Die approbierte gedruckte Originalversion dieser Dissertation ist an der TU Wien Bibliothek verfügbar.
The approved original version of this doctoral thesis is available in print at TU Wien Bibliothek.
TU Bibliothek Your knowledge hub WIEN

Table 7.1 – *Continued from previous page*

Isotope	**Half-Live**
I-135	6.61 h
Xe-131m	11.9 d
Xe-133m	2.19 d
Xe-133	5.25 d
Xe-135m	15.3 min
Xe-135	9.1 h
Xe-138	14.1 min

Table 7.1: Isotopes for simulation including their half-lives

7.2 Source Terms for Accident Scenarios for RODOS simulation

Nuclide data in 7.1 were taken to create the source terms. As the ORIGEN data (see B.1 to B.10) calculation gave values for an average fuel element per ring, the values had to be multiplied by the number of elements per ring (see Figure 1.3) and summed up in order to achieve a full source term for the core. For the 1 element scenario, this was not necessary. Depending on the Accident Scenario, the source term had to be adapted as shown by Baldwin [30]. Haydn [5] used the same approach. Only a fraction of the fission products is released. This fraction is defined for halogens and noble gasses by Foushee and Peters [11] the following way:

$$w_i = e_i \cdot f_i \cdot g_i \tag{7.1}$$

Here e_i describes the fraction of fission products migrating into the gap between fuel and fuel element, f_i describes the fraction of fission products migrating from the gap between fuel and fuel element into the water and g_i describes the fraction of fission products migrating from the water tank into the reactor hall respectively the atmosphere. As shown in 30 the value of e_i was experimentally found out to be $1,5 \times 10^{-5}$. All other values were taken in consistency with Haydn [5] and Villa et al. [4]. In Table 7.2 these factors of GA are shown, which were multiplied with the activity of the nuclides. The fraction for the organic halogens was 92% to 8% of other halogens (see [1]), hence the iodine activities where fractured into 92:8.

Die approbierte gedruckte Originalversion dieser Dissertation ist an der TU Wien Bibliothek verfügbar.
The approved original version of this doctoral thesis is available in print at TU Wien Bibliothek.
TU Bibliothek Your knowledge hub WIEN

Factor GA	Nobel Gases	Organic Halogens	Other Halogens
Fuel Element Damage			
e_i	1.50E-05	1.50E-05	1.50E-05
f_i	1	0.5	0.5
g_i	1	0.1	0.009
w_i	1.50E-05	7.50E-07	6.75E-08
Small Airplane Crash			
e_i	1.50E-05	1.50E-05	1.50E-05
f_i	1	0.5	0.5
g_i	1	0.1	0.9
w_i	1.50E-05	7.50E-07	6.75E-06
Large Airplane Crash			
e_i	1	1.50E-05	1.50E-05
f_i	1	1	1
g_i	1	0.1	0.9
w_i	1	1.50E-06	1.35E-05

Table 7.2: GA calculated factors for all accident scenarios, e_i defines the leakage from the fuel element into the gap, f_i from the gap into the water and g_i from the water into the atmosphere. w_i is the product of all the above factors.

7.2.1 Source Term for accident with 1 fuel element exposed

The scenario is the burst of a fuel element (see also [5] and [4]). The source term for RODOS simulation was calculated to the values in Table 7.3 for the burnup in 2014 and 2025.

Nuclides	**Burnup 2014 [Bq]**	**Burnup 2025 [Bq]**
Kr-83m	1.24E+07	1.19E+07
Kr-85m	2.92E+07	2.80E+07
Kr-85	1.23E+05	5.99E+05
I-130	1.47E+03	7.05E+03
I-131	3.10E+06	3.01E+06
I-132	4.62E+06	4.47E+06
I-134	8.10E+06	7.81E+06
I-135	6.67E+06	6.44E+06

Continued on next page

Die approbierte gedruckte Originalversion dieser Dissertation ist an der TU Wien Bibliothek verfügbar.
The approved original version of this doctoral thesis is available in print at TU Wien Bibliothek.
TU Bibliothek Your knowledge hub WIEN

Table 7.3 – *Continued from previous page*

Nuclides	Burnup 2014 [Bq]	Burnup 2025 [Bq]
Xe-131m	6.66E+05	7.19E+05
Xe-133m	4.56E+06	4.41E+06
Xe-133	1.56E+08	1.50E+08
Xe-135m	2.55E+07	2.47E+07
Xe-135	1.08E+08	1.04E+08
Xe-138	1.12E+08	1.07E+08

Table 7.3: Source term for accidents with 1 fuel element exposed, burnup after 1 year and after 11 years

7.2.2 Source Term for accident with whole core exposed

Nuclides	Burnup 2014 [Bq]	Burnup 2025 [Bq]
Kr-83m	6.13E+08	5.96E+08
Kr-85m	1.44E+09	1.40E+09
Kr-85	7.16E+06	3.06E+07
I-130	6.13E+04	2.53E+05
I-131	1.53E+08	1.50E+08
I-132	2.28E+08	2.23E+08
I-134	3.99E+08	3.89E+08
I-135	3.29E+08	3.21E+08
Xe-131m	3.54E+07	3.58E+07
Xe-133m	2.25E+08	2.19E+08
Xe-133	7.68E+09	7.50E+09
Xe-135m	1.25E+09	1.23E+09
Xe-135	5.84E+09	5.68E+09
Xe-138	5.51E+09	5.36E+09

Table 7.4: Source term for accidents with all fuel element exposed, burnup after 1 year and after 11 years

Die approbierte gedruckte Originalversion dieser Dissertation ist an der TU Wien Bibliothek verfügbar.
The approved original version of this doctoral thesis is available in print at TU Wien Bibliothek.
TU Bibliothek Your knowledge hub WIEN

7.2.3 Source Term for Small airplane crash

Nuclides	Burnup 2014 [Bq]	Burnup 2025 [Bq]
Kr-83m	6.13E+08	5.96E+08
Kr-85m	1.44E+09	1.40E+09
Kr-85	7.16E+06	3.06E+07
I-130	1.08E+05	4.47E+05
I-131	2.70E+08	2.65E+08
I-132	4.03E+08	3.94E+08
I-134	7.06E+08	6.88E+08
I-135	5.82E+08	5.67E+08
Xe-131m	3.54E+07	3.58E+07
Xe-133m	2.25E+08	2.19E+08
Xe-133	7.68E+09	7.50E+09
Xe-135m	1.25E+09	1.23E+09
Xe-135	5.84E+09	5.68E+09
Xe-138	5.51E+09	5.36E+09

Table 7.5: Source term for a small airplane crash accident, burnup after 1 year and after 11 years

7.2.4 Source Term for Large airplane crash

Nuclides	Burnup 2014 [Bq]	Burnup 2025 [Bq]
Kr-83m	4.08E+13	3.97E+13
Kr-85m	9.58E+13	9.31E+13
Kr-85	4.77E+11	2.04E+12
I-130	2.17E+05	8.94E+05
I-131	5.41E+08	5.29E+08
I-132	8.06E+08	7.88E+08
I-134	1.41E+09	1.38E+09
I-135	1.16E+09	1.13E+09
Xe-131m	2.36E+12	2.39E+12
Xe-133m	1.50E+13	1.46E+13

Continued on next page

Die approbierte gedruckte Originalversion dieser Dissertation ist an der TU Wien Bibliothek verfügbar.
The approved original version of this doctoral thesis is available in print at TU Wien Bibliothek.
TU Bibliothek Your knowledge hub WIEN

Table 7.6 – *Continued from previous page*

Nuclides	Burnup 2014 [Bq]	Burnup 2025 [Bq]
Xe-133	5.12E+14	5.00E+14
Xe-135m	8.36E+13	8.18E+13
Xe-135	3.90E+14	3.79E+14
Xe-138	3.67E+14	3.57E+14

Table 7.6: Source term for a large airplane crash accident, burnup after 1 year and after 11 years

7.2.5 Summary of RODOS Source term

Comparing each of the source terms between the different burnups, the activity of the chosen nuclides is slightly lower after 11 years. Comparing the complete data (see appendix B.2), the total activity is higher after 11 years of burnup, with respect to the groups of activation products, fission products and actinides. The total activity is driven by short lived elements, and is in an equal state after 2 years, as the reactor power is assumed constant. The lower activity in the second set of data can only be explained through the simulation itself: the Bateman equation is solved for this simulation with discrete time steps, and leads to fluctuations around the estimated value. Isotopes with high cross sections (Xe and Sm for example) will show higher fluctuations. This effect will lead to the lower burnup activity after 11 years. A second effect that could play a role are small rounding errors[2].

[2]Personal information from Thomas Stummer

Die approbierte gedruckte Originalversion dieser Dissertation ist an der TU Wien Bibliothek verfügbar.
The approved original version of this doctoral thesis is available in print at TU Wien Bibliothek.
TU Bibliothek Your knowledge hub WIEN

7.3 Source term for LASAIR

Starting with the source term for the RODOS simulation, small amendments had to be made for the LASAIR simulations. LASAIR can only include five nuclides in the calculation. For the LASAIR simulation only the scenario with the large airplane crash was calculated. This work used the 5 isotopes containing the highest activity from the scenario "large airplane crash" (see 7.2.4) with the data after 1 year of burnup.

Nuclide	**Activity[Bq]**
Kr-85m	9.58E+13
Xe-133	5.12E+14
Xe-135m	8.36E+13
Xe-135	3.90E+14
Xe-138	3.67E+14

Table 7.7: Source term for LASAIR simulation data

Die approbierte gedruckte Originalversion dieser Dissertation ist an der TU Wien Bibliothek verfügbar.
The approved original version of this doctoral thesis is available in print at TU Wien Bibliothek.

8 Calculations with RODOS

This chapter describes the simulations with RODOS. RODOS is described in chapter 4. The following chapter displays the simulation results. Four accident scenarios were simulated. These scenarios are described in chapter 1.5. This work discusses the following accident scenarios, as done in previous works by Haydn (see [5]):

- Accident Scenario with 1 fuel element exposed
- Accident Scenario with all fuel elements exposed
- Accident Scenario with small airplane crash
- Accident Scenario with large airplane crash

These 4 accident scenarios were each simulated with 7 different weather scenarios. The weather scenarios are described in detail in chapter 6. The first four scenarios are average scenarios representing an averaged day of the season. The later three are specific scenarios representing a specific day of the described weather scenario.

1. Average spring day
2. Average summer day
3. Average autumn day
4. Average winter day
5. Hot day
6. Foggy day
7. Thunderstorm day

Die approbierte gedruckte Originalversion dieser Dissertation ist an der TU Wien Bibliothek verfügbar.
The approved original version of this doctoral thesis is available in print at TU Wien Bibliothek.
TU Bibliothek Your knowledge hub WIEN

The input parameters varied in the meteorological parameters (see chapter 6) and in the source term (see chapter 7). The Rodos input (see chapter 4.1.1) was the following:

- Geographic coordinates: 16.413; 48.197
- Grid size: 20 km radius, 50 m cell size
- Calculation time step: 60 minutes
- Activity release: For consistency reasons with Haydn [5] the release interval was set to 1 h. All nuclides were released at the same time.
- Calculation time: the prognostic model was calculated for a 24 h time interval. RODOS offers the feature of estimating a 1 year and a lifetime dose. This feature is used for comparison reasons with Haydn [5].

All scenarios were simulated with 2 different burnups. The first set of simulations was performed with a burnup of 1 year, the second set with a burnup of 11 years, which describes the current end of life for the reactor. The source term is described in detail in chapter 7.

8.1 Accident Scenario with 1 fuel element exposed

8.1.1 Results with 1 year burnup

The first accident scenario was the exposure of one fuel element (see 7.2.1) the calculation was performed for a burnup of one year. Table 8.1 shows the results of the RODOS simulation for the average days. Three representative values are analysed: The total dose after one year (except ingestion), the total effective dose rate and the total potential effective dose. The values given are the maximum values of the simulation. Table 8.2 shows the results of the specific scenarios for one year of burnup and the exposure of 1 fuel element.

Die approbierte gedruckte Originalversion dieser Dissertation ist an der TU Wien Bibliothek verfügbar.
The approved original version of this doctoral thesis is available in print at TU Wien Bibliothek.
TU Bibliothek Your knowledge hub WIEN

	Spring day	Summer day	Autumn day	Winter day
total dose except ingestion 1 year [mSv]	3.35E-06	4.07E-06	3.74E-06	1.49E-06
total effective gamma dose rate [mSv/h]	1.34E-06	1.76E-06	1.74E-06	8.50E-07
total potential dose effective [mSv]	6.66E-06	7.30E-06	6.84E-06	2.25E-06

Table 8.1: RODOS results for exposure of 1 fuel element after 1 year of burnup, average scenarios

	Thunderstorm day	Foggy day	Hot day
total dose except ingestion 1 year [mSv]	1.29E-05	2.38E-05	2.45E-06
total effective gamma dose rate [mSv/h]	6.18E-06	1.26E-05	1.99E-06
total potential dose effective [mSv]	1.47E-05	2.12E-05	4.37E-06

Table 8.2: RODOS results for exposure of 1 fuel element after 1 year of burnup, specific scenarios

In the two tables above it is evident that especially the scenarios with lesser wind (foggy day and hot day) show a higher total potential dose and higher dose rates. The foggy day scenario has a maximum wind speed of 1,11 m/s which is not sufficient to effectively disperse nuclides (see below in detail for the large airplane crash scenario, chapter 8.4). As for the results of the thunderstorm day, here the precipitation has the largest effect (17,6 mm maximum) compared to 0,2 mm maximum of rain during an average summer day. The dispersion of the nuclides are shown in Figure 8.1, comparing two scenarios - the foggy day and the summer day.

Die approbierte gedruckte Originalversion dieser Dissertation ist an der TU Wien Bibliothek verfügbar.
The approved original version of this doctoral thesis is available in print at TU Wien Bibliothek.
TU Bibliothek Your knowledge hub WIEN

Figure 8.1: Comparison of the summer (top) and foggy day scenario (bottom), effective dose after 1 year, exposure of 1 fuel element, 1 year of burnup

Die approbierte gedruckte Originalversion dieser Dissertation ist an der TU Wien Bibliothek verfügbar.
The approved original version of this doctoral thesis is available in print at TU Wien Bibliothek.
TU Bibliothek Your knowledge hub WIEN

8.1.2 Results with 11 years burnup

For the accident scenario "exposure of one fuel element" (see 7.2.1) the calculation was performed for a burnup of 11 years. Table 8.3 shows the results of the RODOS simulation for the average days. Three representative values are analysed: The total dose after one year (except ingestion), the total effective dose rate and the total potential effective dose. The values given are the maximum values of the simulation. Table 8.4 shows the results of the specific scenarios for 11 years of burnup and the exposure of 1 fuel element.

	Spring day	**Summer day**	**Autumn day**	**Winter day**
total dose except ingestion 1 year [mSv]	3.24E-06	3.93E-06	4.07E-06	1.44E-06
total effective gamma dose rate all nuclides[mSv/h]	1.29E-06	1.70E-06	1.71E-06	8.20E-07
total potential dose effective[mSv]	6.28E-06	7.06E-06	4.81E-06	2.18E-06

Table 8.3: RODOS results for exposure of 1 fuel element after 11 years of burnup, average scenarios

	Thunderstorm day	**Foggy day**	**Hot day**
total dose except ingestion 1 year [mSv]	1.25E-05	2.30E-05	2.37E-06
total effective gamma dose rate [mSv/h]	5.96E-06	1.21E-05	1.92E-06
total potential dose effective [mSv]	1.43E-05	2.05E-05	4.23E-06

Table 8.4: RODOS results for exposure of 1 fuel element after 11 years of burnup, specific scenarios

Comparing the results for 1 and 11 years of burnup (see tables 8.3 to 8.4, the differences are minimal. The 11 year results show lower doses (up to 8%, only the total potential dose of the autumn day scenario differs more), which can be explained through the source term calculation (see section 7.2). Comparing the average with the specific scenarios - it shows clearly that the dose distribution differs strongly from the upper to the lower picture. This depends on the wind and precipitation influence. Looking at the upper pictures, the dose is distributed

Die approbierte gedruckte Originalversion dieser Dissertation ist an der TU Wien Bibliothek verfügbar.
The approved original version of this doctoral thesis is available in print at TU Wien Bibliothek.
TU Bibliothek Your knowledge hub WIEN

with the main wind direction. The foggy day scenario in the lower picture shows how this can differ if the wind is not blowing.

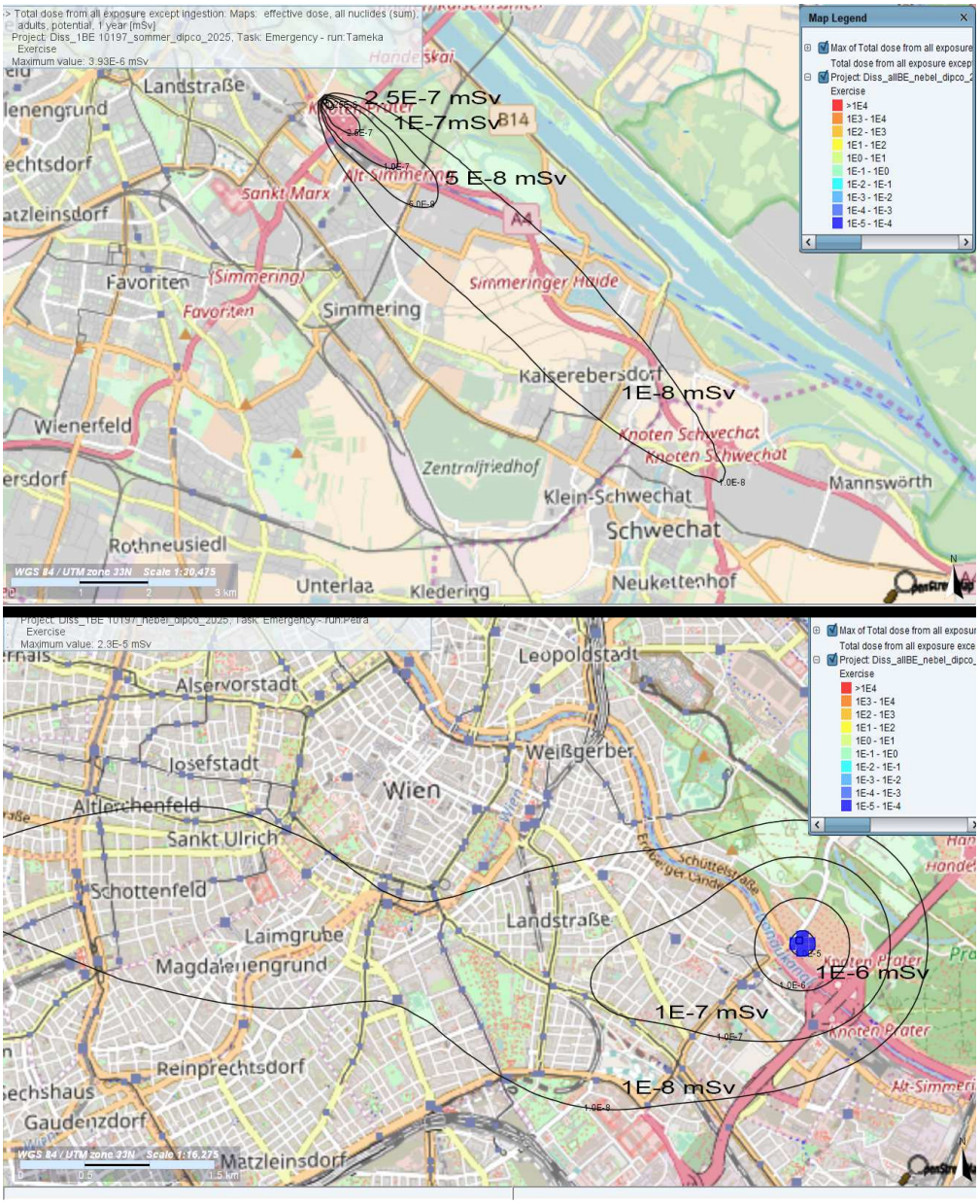

Figure 8.2: Comparison of the summer (top) and foggy day scenario (bottom), effective dose after 1 year, exposure of 1 fuel element, 11 years of burnup

Die approbierte gedruckte Originalversion dieser Dissertation ist an der TU Wien Bibliothek verfügbar.
The approved original version of this doctoral thesis is available in print at TU Wien Bibliothek.
TU Bibliothek Your knowledge hub WIEN

8.2 Accident Scenario with all fuel elements exposed

8.2.1 Results with 1 year burnup

The second accident scenario was the exposure of all fuel elements (see 7.2.2). The calculation was performed for a burnup of one year. Table 8.5 shows the results of the RODOS simulation for the average days. Three representative values are analysed: The total dose after one year (except ingestion), the total effective dose rate and the total potential effective dose. The values given are the maximum values of the simulation. Table 8.6 shows the results of the specific scenarios for one year of burnup and the exposure of all fuel elements.

	Spring day	**Summer day**	**Autumn day**	**Winter day**
total dose except ingestion 1 year [mSv]	1.66E-04	2.01E-04	1.85E-04	7.39E-05
total effective gamma dose rate all nuclides [mSv/h]	6.69E-05	8.78E-05	8.67E-05	4.24E-05
total potential dose effective [mSv]	3.21E-04	3.62E-04	3.39E-04	1.11E-04

Table 8.5: RODOS results for exposure of all fuel elements after 1 year of burnup, average scenarios

	Thunderstorm day	**Foggy day**	**Hot day**
total dose exept ingestion 1 year [mSv]	6.40E-04	1.21E-04	1.18E-03
total effective gamma dose rate all nuclides [mSv/h]	3.08E-04	9.92E-05	6.29E-04
total potential dose effective [mSv]	7.33E-04	2.16E-04	1.06E-03

Table 8.6: RODOS results for exposure of all fuel elements after 1 year of burnup, specific scenarios

The trend from the exposure of 1 fuel element continues. The doses after 1 year are still below 1 μSv, except again for the foggy day scenario, that shows a

Die approbierte gedruckte Originalversion dieser Dissertation ist an der TU Wien Bibliothek verfügbar.
The approved original version of this doctoral thesis is available in print at TU Wien Bibliothek.
TU Bibliothek Your knowledge hub WIEN

maximum total effective dose of 1.18 μSv after 1 year of exposure. Comparing the average scenario with the special day scenario, it shows again that the lack of wind leads to a higher dose distribution around the source.

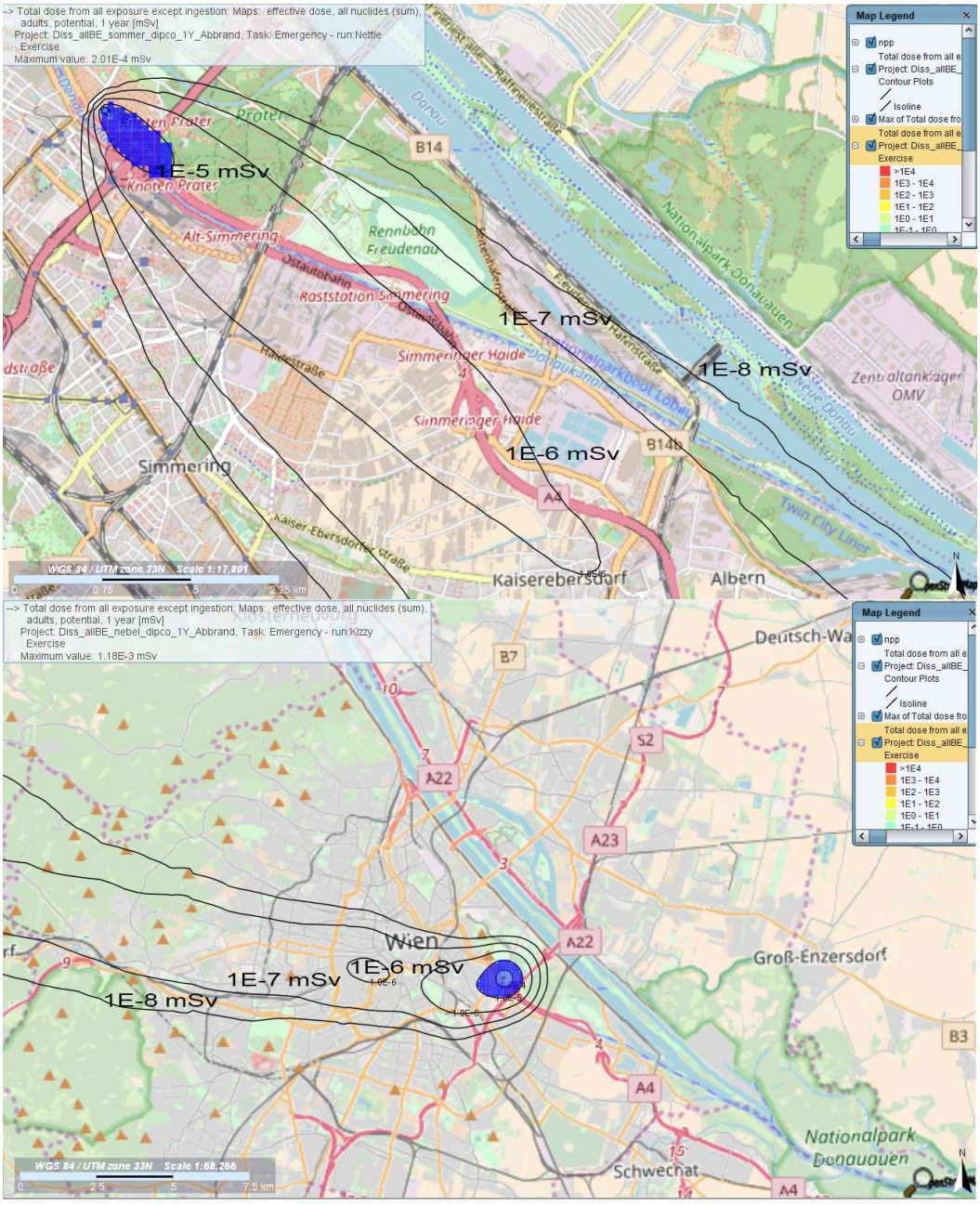

Figure 8.3: Comparison of the summer (top) and foggy day scenario (bottom), exposure of all fuel elements, 1 year of burnup

Die approbierte gedruckte Originalversion dieser Dissertation ist an der TU Wien Bibliothek verfügbar.
The approved original version of this doctoral thesis is available in print at TU Wien Bibliothek.

8.2.2 Results with 11 years burnup

For the accident scenario "exposure of all fuel elements" (see 7.2.2) the calculation was performed for a burnup of 11 years. Table 8.7 shows the results of the RODOS simulation for the average days. Three representative values are analysed: The total dose after one year (except ingestion), the total effective dose rate and the total potential effective dose. The values given are the maximum values of the simulation. Table 8.8 shows the results of the specific scenarios for 11 years of burnup and the exposure of all fuel elements.

	Spring day	**Summer day**	**Autumn day**	**Winter day**
total dose exept ingestion 1 year [mSv]	1.62E-04	1.96E-04	1.81E-04	1.78E-04
total effective gamma dose rate all nuclides [mSv/h]	6.51E-05	8.55E-05	8.45E-05	4.63E-05
total potential dose effective [mSv]	3.14E-04	3.54E-04	3.31E-04	2.32E-04

Table 8.7: RODOS results for exposure of all fuel elements after 11 years of burnup, average scenarios

	Thunderstorm day	**Foggy day**	**Hot day**
total dose exept ingestion 1 year [mSv]	9.19E-04	1.18E-04	1.15E-03
total effective gamma dose rate all nuclides [mSv/h]	3.27E-04	9.66E-05	6.13E-04
total potential dose effective [mSv]	7.88E-04	2.11E-04	1.03E-03

Table 8.8: RODOS results for exposure of all fuel elements after 11 years of burnup, specific scenarios

The comparison to the shorter burnup time shows differences in the order of 3%. The slightly lower dose results can be explained through the source term calculation (see 7.2). In the comparison of the 11 years burnup scenarios (see 8.4) the foggy day scenario was looked at in detail. Here the lack of wind leads to the higher dose around the source, but also shows that the dose values quickly drop in the vicinity of the source. One grid cell is 20 m long, so the dose has dropped

Die approbierte gedruckte Originalversion dieser Dissertation ist an der TU Wien Bibliothek verfügbar.
The approved original version of this doctoral thesis is available in print at TU Wien Bibliothek.
TU Bibliothek Your knowledge hub WIEN

by one order of magnitude outside of a 40 m times 40 m square, which equals the building of the institute.

Die approbierte gedruckte Originalversion dieser Dissertation ist an der TU Wien Bibliothek verfügbar.
The approved original version of this doctoral thesis is available in print at TU Wien Bibliothek.

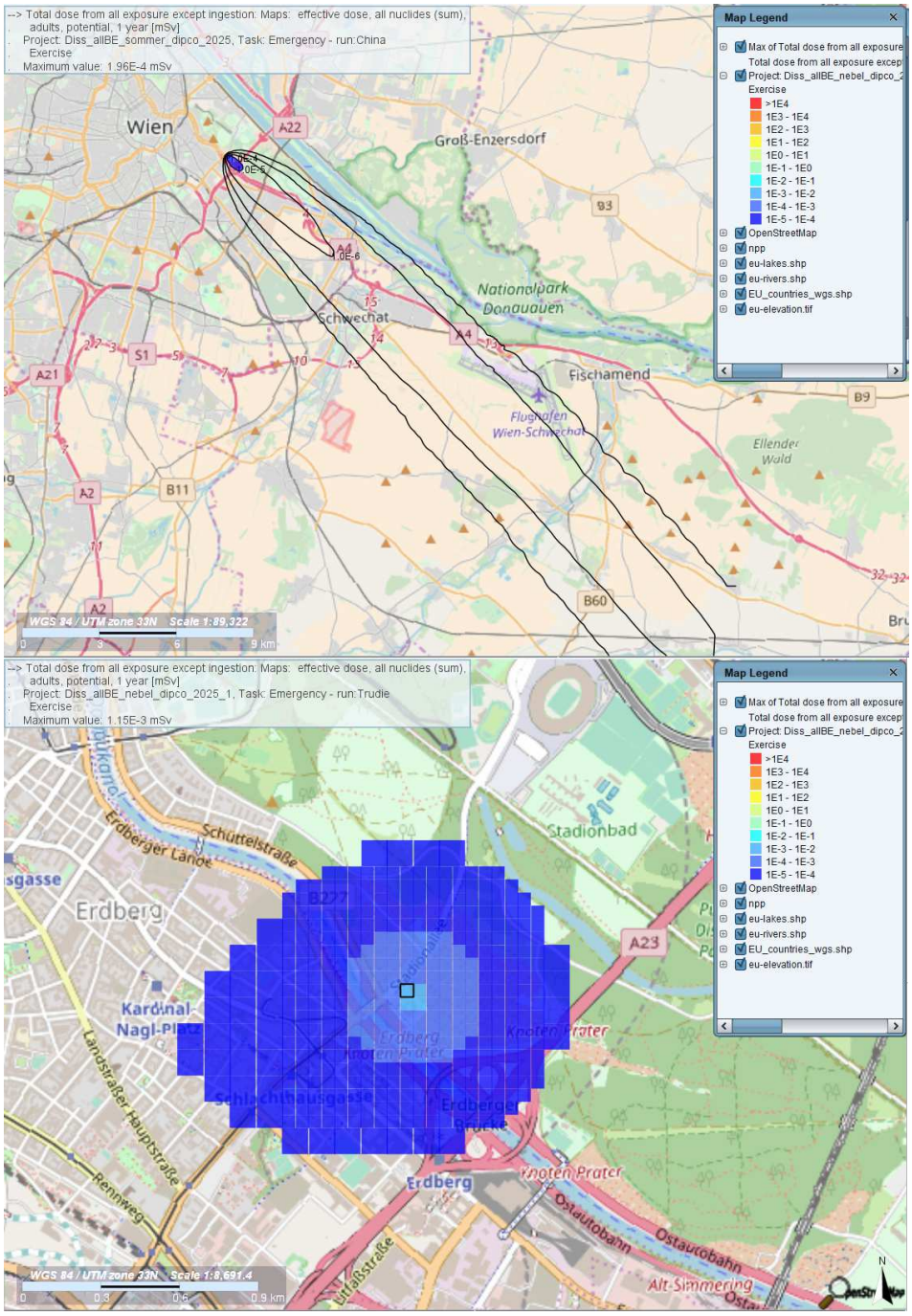

Figure 8.4: Comparison of the summer day (top) and the foggy day scenario (bottom), all fuel elements exposed, 11 years of burnup

Die approbierte gedruckte Originalversion dieser Dissertation ist an der TU Wien Bibliothek verfügbar.
The approved original version of this doctoral thesis is available in print at TU Wien Bibliothek.
TU Bibliothek Your knowledge hub WIEN

8.3 Accident Scenario with small airplane crash

8.3.1 Results with 1 year burnup

The third accident scenario was a small airplane crash (see 7.2.3). The calculation was performed for a burnup of one year. Table 8.9 shows the results of the RODOS simulation for the average days. Three representative values are analysed: The total dose after one year (except ingestion), the total effective dose rate and the total potential effective dose. The values given are the maximum values of the simulation. Table 8.10 shows the results of the specific scenarios for one year of burnup and the small airplane crash.

	Spring day	**Summer day**	**Autumn day**	**Winter day**
total dose exept ingestion 1 year [mSv]	2.62E-04	3.19E-04	2.91E-04	1.10E-04
total effective gamma dose rate all nuclides [mSv/h]	8.43E-05	1.11E-04	1.10E-04	5.34E-05
total potential dose effective [mSv]	5.38E-04	6.04E-04	5.63E-04	1.76E-04

Table 8.9: RODOS results after small airplane crash, 1 year of burnup, average scenarios

	Thunderstorm day	**Foggy day**	**Hot day**
total dose exept ingestion 1 year [mSv]	9.97E-04	1.84E-04	1.92E-03
total effective gamma dose rate all nuclides [mSv/h]	3.90E-04	1.25E-04	8.24E-04
total potential dose effective [mSv]	1.20E-03	3.52E-04	1.73E-03

Table 8.10: RODOS results after small airplane crash, 1 year of burnup, specific scenarios

The doses are in average below 1 μSv except for the special scenarios of the thunderstorm and the foggy day, where they reach a maximum of 1.93 μSv. The maximum dose rate is 0.82 μSv. The trend that scenarios with lesser wind speed show higher doses continues as expected. In Figure 8.5 the doses are higher than

Die approbierte gedruckte Originalversion dieser Dissertation ist an der TU Wien Bibliothek verfügbar.
The approved original version of this doctoral thesis is available in print at TU Wien Bibliothek.
TU Bibliothek Your knowledge hub WIEN

for the scenarios with 1 fuel element or all fuel elements exposed, still the doses drop in the near vicinity of the source by one order of magnitude.

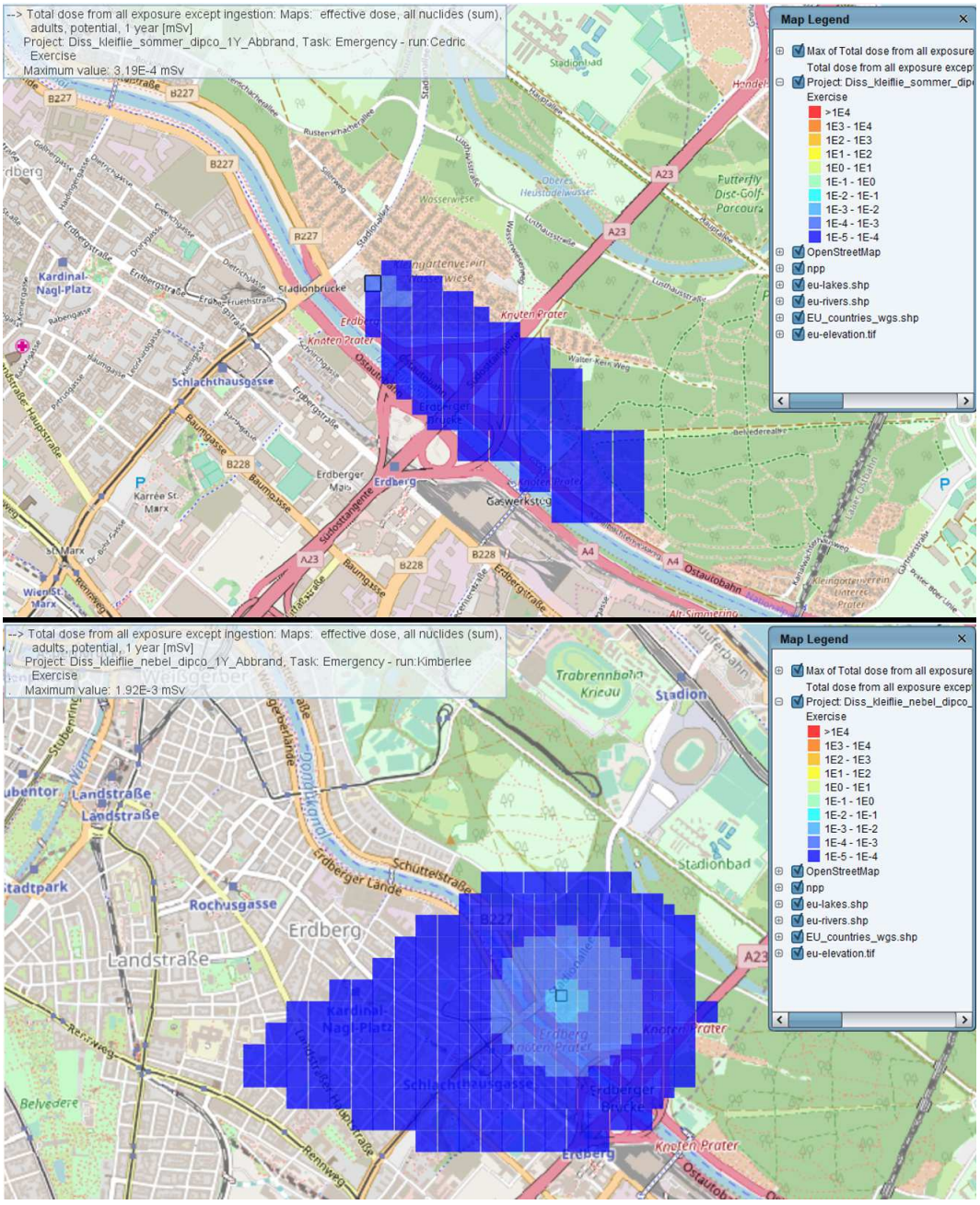

Figure 8.5: Comparison of the summer day (top) and foggy day scenario (bottom) with a small airplane crash, 1 year of burnup

Die approbierte gedruckte Originalversion dieser Dissertation ist an der TU Wien Bibliothek verfügbar.
The approved original version of this doctoral thesis is available in print at TU Wien Bibliothek.
TU Bibliothek Your knowledge hub WIEN

8.3.2 Results with 11 years burnup

For the accident scenario "small airplane crash" (see 7.2.3) the calculation was performed for a burnup of 11 years. Table 8.11 shows the results of the RODOS simulation for the average days. Three representative values are analysed: The total dose after one year (except ingestion), the total effective dose rate and the total potential effective dose. The values given are the maximum values of the simulation. Table 8.12 shows the results of the specific scenarios for 11 years of burnup and the exposure of all fuel elements.

	Spring day	**Summer day**	**Autumn day**	**Winter day**
total dose except ingestion 1 year [mSv]	2.56E-04	3.12E-04	2.84E-04	7.21E-05
total effective gamma dose rate all nuclides [mSv/h]	8.22E-05	1.08E-04	1.07E-04	4.13E-05
total potential dose effective [mSv]	5.26E-04	5.91E-04	5.54E-04	1.09E-04

Table 8.11: RODOS results after small airplane crash, 11 years of burnup, average scenarios

	Thunderstorm day	**Foggy day**	**Hot day**
total dose except ingestion 1 year [mSv]	9.74E-04	1.80E-04	1.88E-03
total effective gamma dose rate all nuclides [mSv/h]	3.80E-04	1.22E-04	8.03E-04
total potential dose effective [mSv]	1.18E-03	3.44E-04	1.69E-03

Table 8.12: RODOS results after small airplane crash, 11 years of burnup, specific scenarios

Comparing the results of the 2 different burnup times, the 11 years of burnup simulation shows again similar, but by 3% lower results. The maximum dose is 1.88 μSv, the maximum dose rate is 0.803 μSv/h. The trend that scenarios with lesser wind speed show higher doses continues as expected. In Figure 8.6 the doses are higher than for the scenarios with 1 fuel element or all fuel elements exposed, still the doses drop in the near vicinity of the source by one order of magnitude.

Die approbierte gedruckte Originalversion dieser Dissertation ist an der TU Wien Bibliothek verfügbar.
The approved original version of this doctoral thesis is available in print at TU Wien Bibliothek.
TU Bibliothek Your knowledge hub WIEN

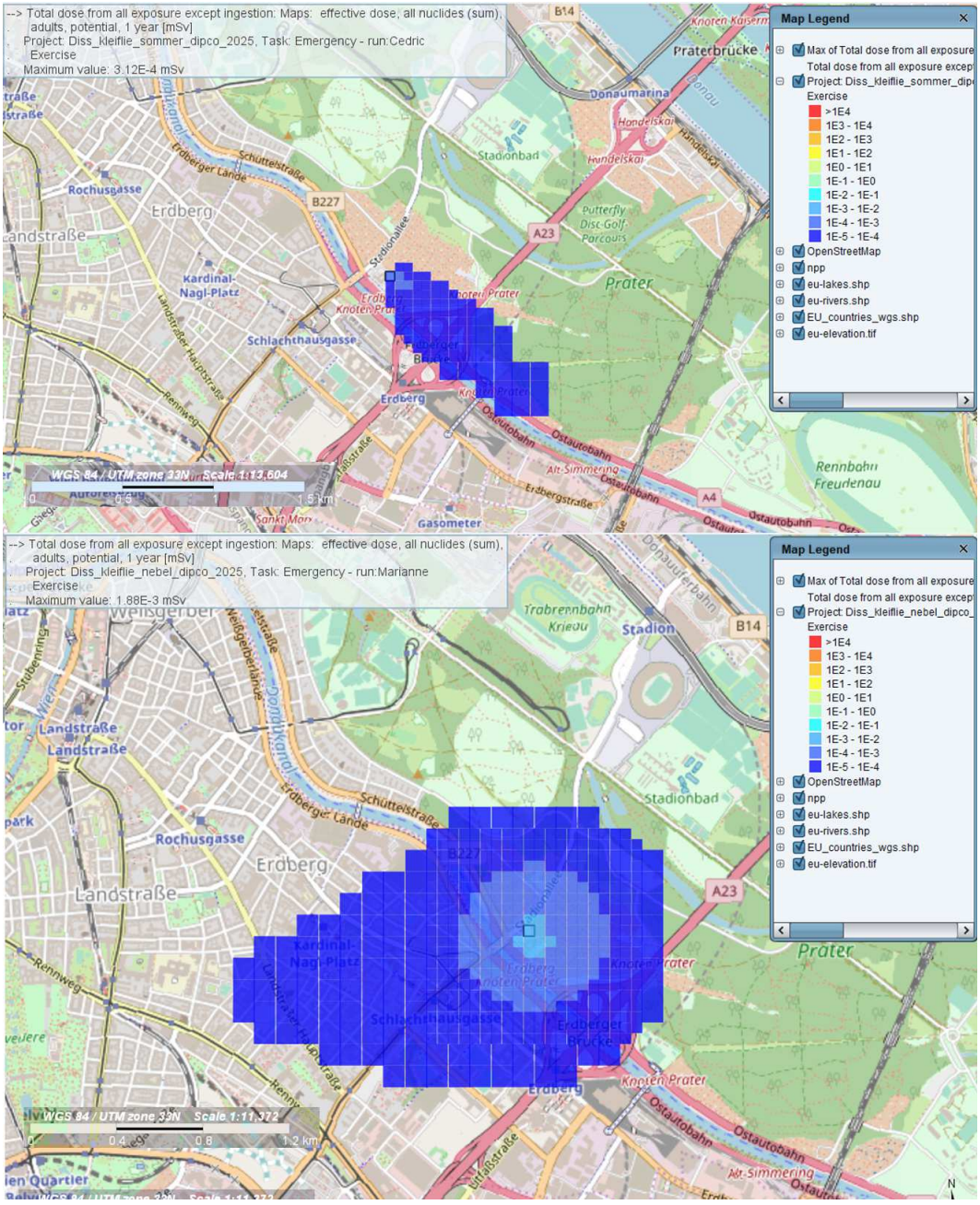

Figure 8.6: Comparison of summer day (top) and foggy day (bottom), small airplane crash, 11 years of burnup

The scenarios in chapters 8.1 to 8.3 all show maximum dose values around the order of 1 - 2 μSv. This lies well below the dose limit given in the Austrian radiation protection law of 1 mSv per year for the public. Therefore in the chapters 8.1 to 8.3

Die approbierte gedruckte Originalversion dieser Dissertation ist an der TU Wien Bibliothek verfügbar.
The approved original version of this doctoral thesis is available in print at TU Wien Bibliothek.
TU Bibliothek Your knowledge hub WIEN

only the comparison of the most relevant scenarios was analysed. The graphical output of all scenarios described in the chapters 8.1 to 8.3 can be found in Annex B.1.

8.4 Accident Scenario with large airplane crash

8.4.1 Results with 1 year burnup

The fourth accident scenario was a large airplane crash (see 7.2.4). The calculation was performed for a burnup of one year. Table 8.13 shows the results of the RODOS simulation for the average days. Three representative values are analysed: The total dose after one year (except ingestion), the total effective dose rate and the total potential effective dose. The values given are the maximum values of the simulation. Table 8.14 shows the results of the specific scenarios for one year of burnup and the large airplane crash.

	Spring day	**Summer day**	**Autumn day**	**Winter day**
total dose except ingestion 1 year [mSv]	2.7	3.18	3.2	1.83
total effective gamma dose rate all nuclides [mSv/h]	2.94	3.82	3.8	1.87
total potential dose effective [mSv]	2.69	3.17	3.19	1.83

Table 8.13: RODOS results after large airplane crash, 1 year of burnup, average scenarios

	Thunderstorm day	**Foggy day**	**Hot day**
total dose exept ingestion 1 year [mSv]	11.9	2.66	13.8
total effective gamma dose rate all nuclides [mSv/h]	13.5	4.4	25.1
total potential dose effective [mSv]	11.5	2.65	12.5

Table 8.14: RODOS results after large airplane crash, 1 year of burnup, specific scenarios

Die approbierte gedruckte Originalversion dieser Dissertation ist an der TU Wien Bibliothek verfügbar.
The approved original version of this doctoral thesis is available in print at TU Wien Bibliothek.
TU Bibliothek Your knowledge hub WIEN

For the scenarios with a large airplane crash, the whole core is exposed, and the building is destroyed. (see chapter 7 for the source description). Nuclides can spread, and this is reflected in the dose and dose rate scenarios. Compared to previous results (see tables 8.1 to 8.12 the results are now 3 orders of magnitude higher. This lies in accordance with previous works (see [5], chapter 4.16-4.19). Again, the specific scenarios show a higher dose and dose rate result. The maximum is 13.8 mSv for the foggy day scenario. In order to analyse all results more deeply, the graphical output of the average large airplane crash scenarios is shown below.

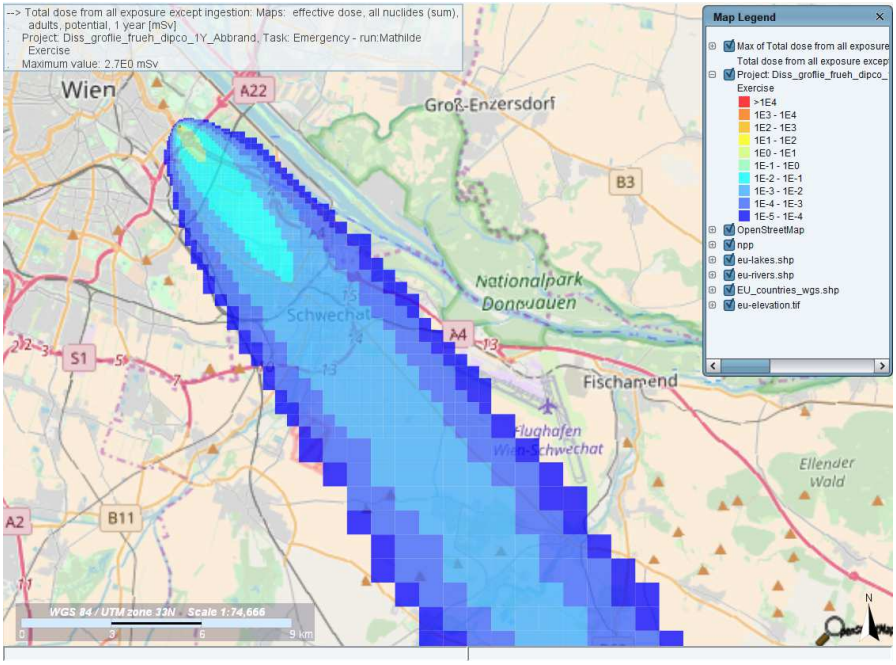

Figure 8.7: Large airplane crash scenario, average spring day, 1 year of burnup

Die approbierte gedruckte Originalversion dieser Dissertation ist an der TU Wien Bibliothek verfügbar.
The approved original version of this doctoral thesis is available in print at TU Wien Bibliothek.

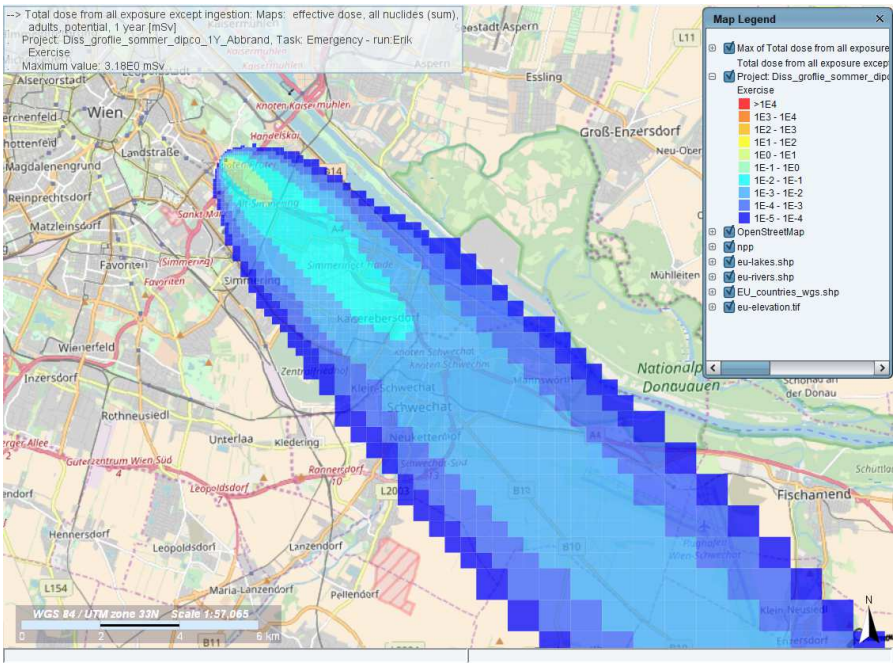

Figure 8.8: Large airplane crash scenario, average summer day, 1 year of burnup

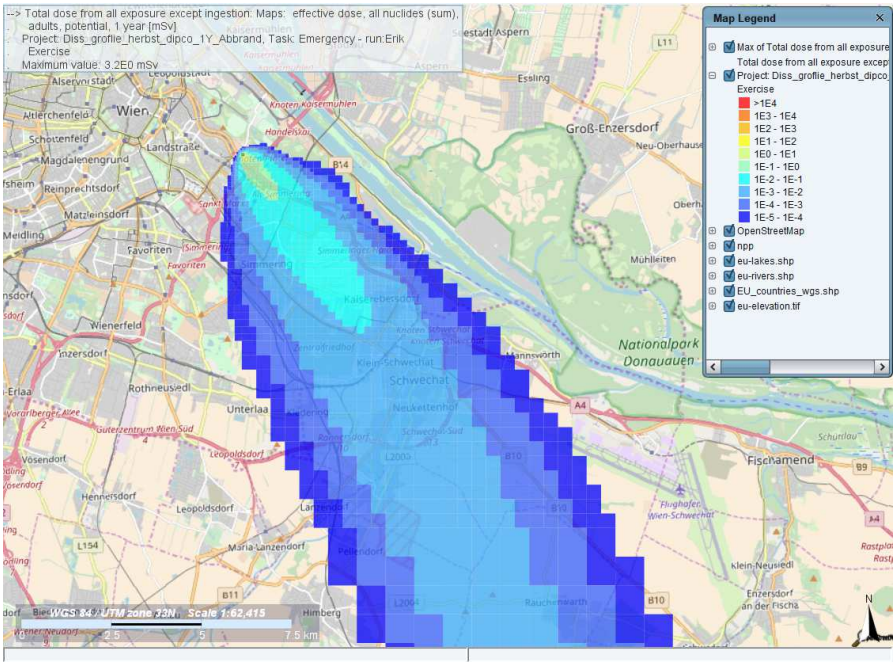

Figure 8.9: Autumn day scenario, large airplane crash, 1 year of burnup

Die approbierte gedruckte Originalversion dieser Dissertation ist an der TU Wien Bibliothek verfügbar.
The approved original version of this doctoral thesis is available in print at TU Wien Bibliothek.
TU Bibliothek Your knowledge hub WIEN

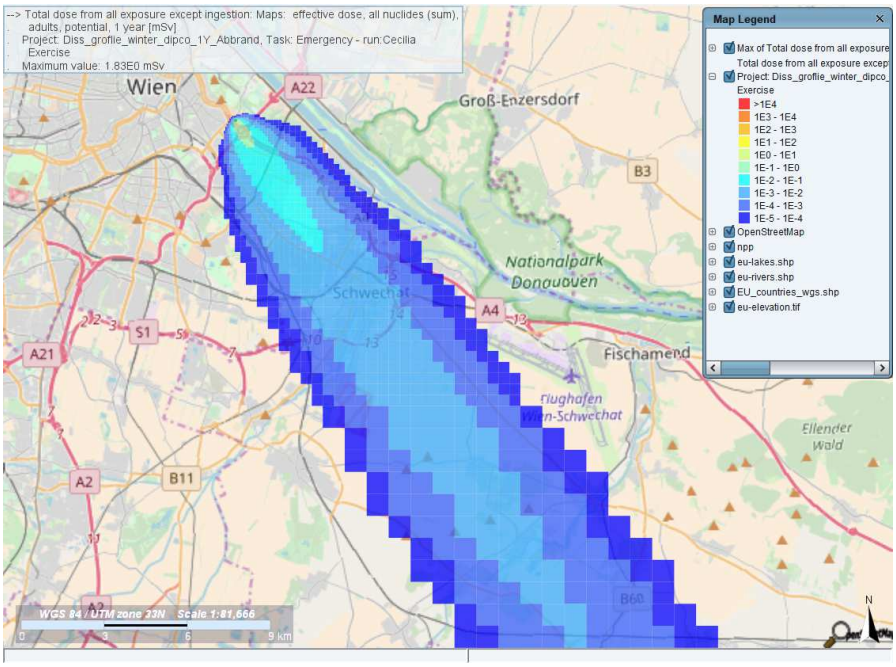

Figure 8.10: Winter day scenario, large airplane crash, 1 year of burnup

The Figures 8.7 to 8.10 show all the deposition of the released nuclides with the main wind direction. Comparing these to the results of Haydn [5] the main contaminated areas are comparable. Haydns work [5] shows a start of the contamination south of the source, in this work, the contamination is also seen around the source, and spreads to the south. It's impossible that contamination is spread only south of the source, this result is due to the simulation tool. This work shows a more realistic approach and outcome. To analyze the outcome more in detail, a closer look at the result is necessary. In Figure 8.11 a closer look at the winter scenario is done.

Die approbierte gedruckte Originalversion dieser Dissertation ist an der TU Wien Bibliothek verfügbar.
The approved original version of this doctoral thesis is available in print at TU Wien Bibliothek.
TU Bibliothek Your knowledge hub WIEN

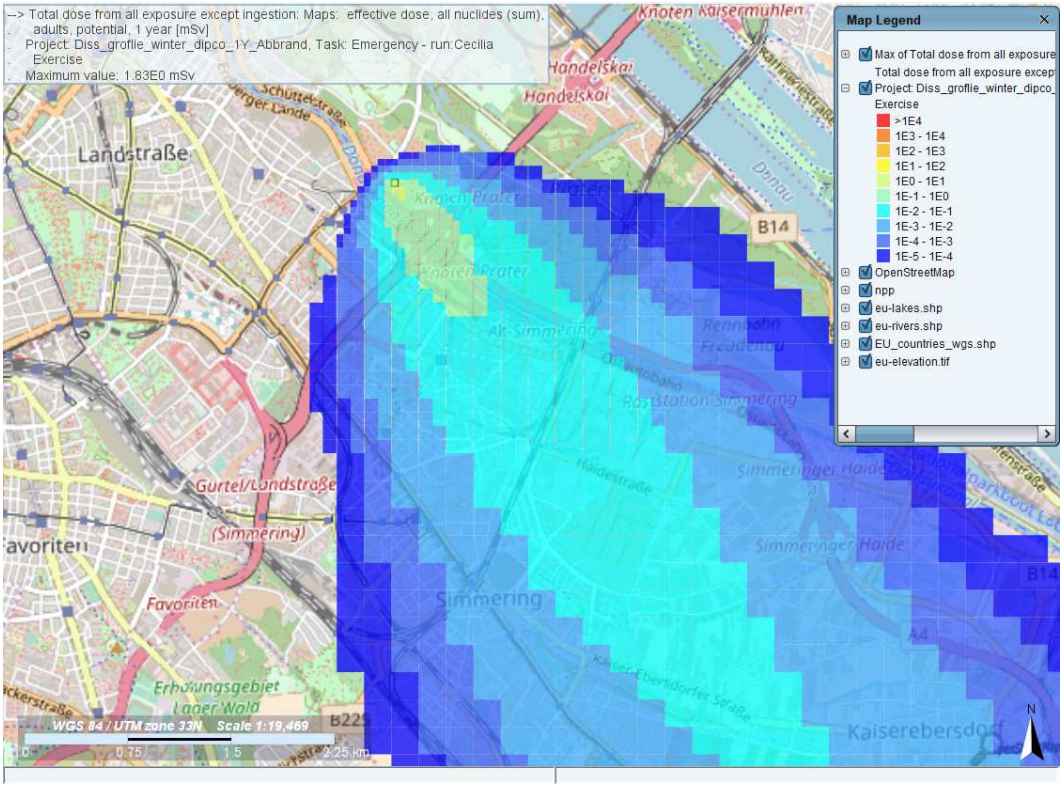

Figure 8.11: Close up look at the winter scenario, 1 year burnup, large airplane crash

The Austrian radiation protection law limits the dose for public to 1 mSv/year, in Figure 8.11 the areas exceeding 1 mSv in the first year are within the boundary areas of the institute (dark yellow area). This is shown also more in detail in the next section with the analyses of the specific scenario outcomes. Throughout the seasons, the results have a standard deviation of 0.64 for the total dose, for the dose rate 0.92 and for the total potential effective dose 0.64, as shown in Table 8.13. The autumn and summer results are the highest, due to the fact that the rain rate is high, combined with a low wind speed (see section 6). This is a typical Viennese phenomenon, the wind is always blowing, except above 30°C where it stops completely and leaves the Viennese sweating. The combination of a low precipitation and an average wind speed leads to the winter results, which are lower than throughout the rest of the year. The influence of snow needs to be looked at separately, but there is still no good simulation possibility for snow. Looking at the specific scenarios, the results differ from the above described

Die approbierte gedruckte Originalversion dieser Dissertation ist an der TU Wien Bibliothek verfügbar.
The approved original version of this doctoral thesis is available in print at TU Wien Bibliothek.
TU Bibliothek Your knowledge hub WIEN

average scenarios. Also, a more detailed look at each scenario is necessary to further analyse this outcome.

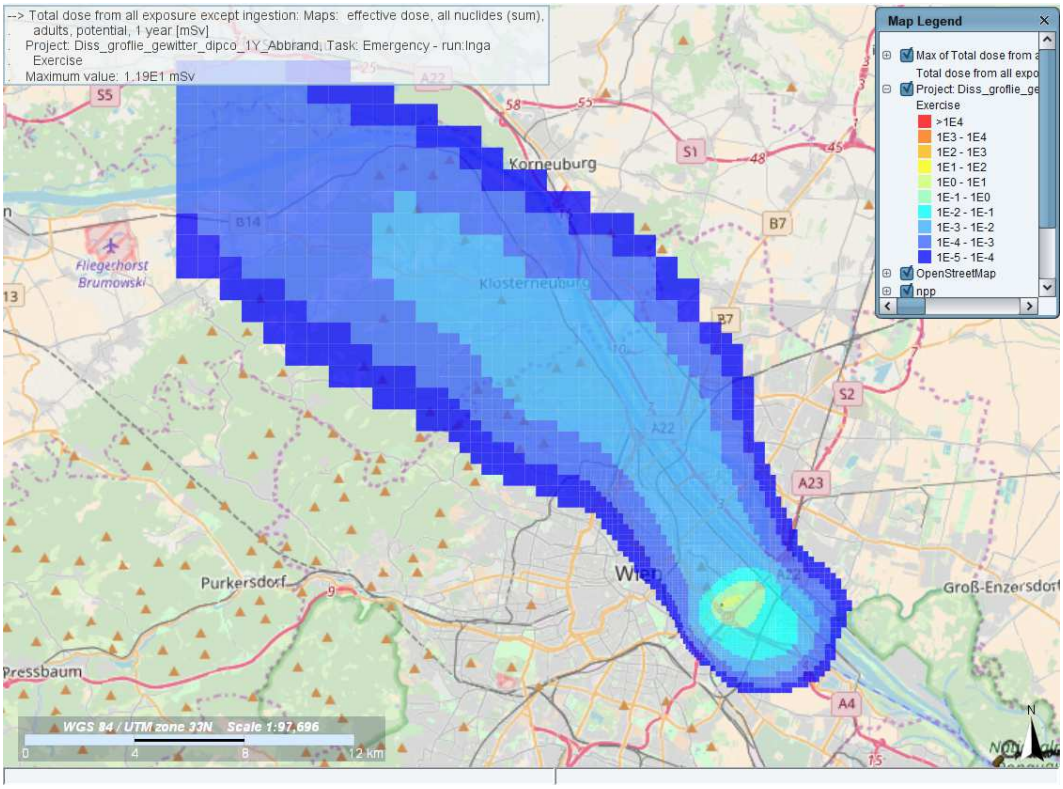

Figure 8.12: Thunderstorm scenario, large airplane crash, 1 year burnup

Figure 8.12 shows the simulated dispersion results for an specific scenario with a thunderstorm day. Compared to Figures 8.7 to 8.10 the affected areas don't match. This can be explained by the nature of the meteorology. The thunderstorm day was chosen randomly, the average scenarios reflect the average of the wind speed and direction, of which the thunderstorm day is part. Still, this simulation of the thunderstorm day demonstrates the necessity of the simulation of specific scenarios. Considering only the average, it would not reflect the reality and disregard possible necessary countermeasures for affected regions. In this scenario the area subjected to doses above 1 mSv in the first year is bigger than in the average scenarios. At the boundaries of the institute, the dose reaches 6.34 mSv in the first year. It is below 1 mSv at 900 m in the north east direction, showing a elliptical form of dispersion. The radius of the ellipse is 175 m. The dose dispersion shows a rapid drop, at 500 m from the source it is below 2 mSv.

Die approbierte gedruckte Originalversion dieser Dissertation ist an der TU Wien Bibliothek verfügbar.
The approved original version of this doctoral thesis is available in print at TU Wien Bibliothek.
TU Bibliothek Your knowledge hub WIEN

This reflects also the other two specific scenarios and their dispersion.

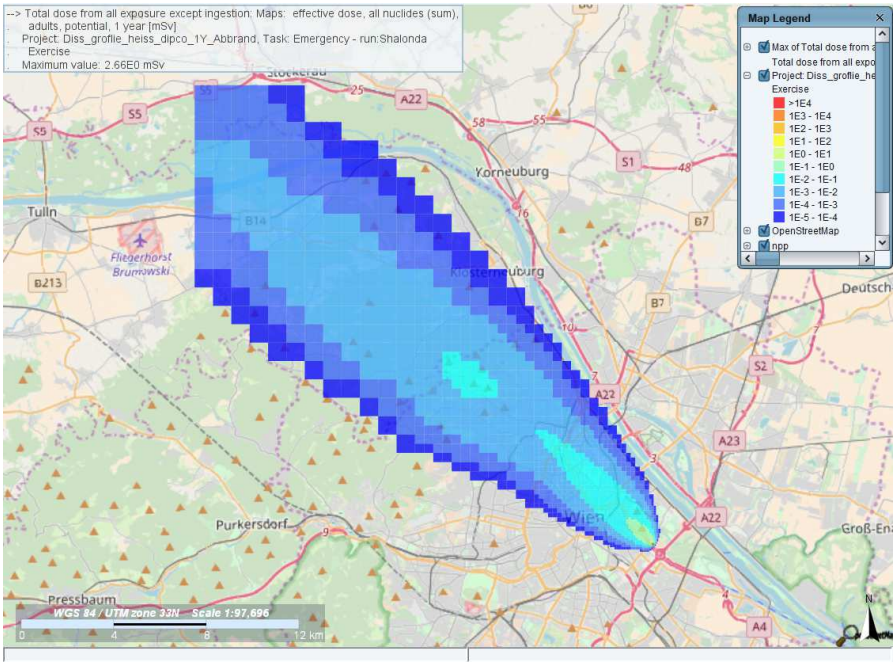

Figure 8.13: Hot day scenario, large airplane crash, 1 year burnup

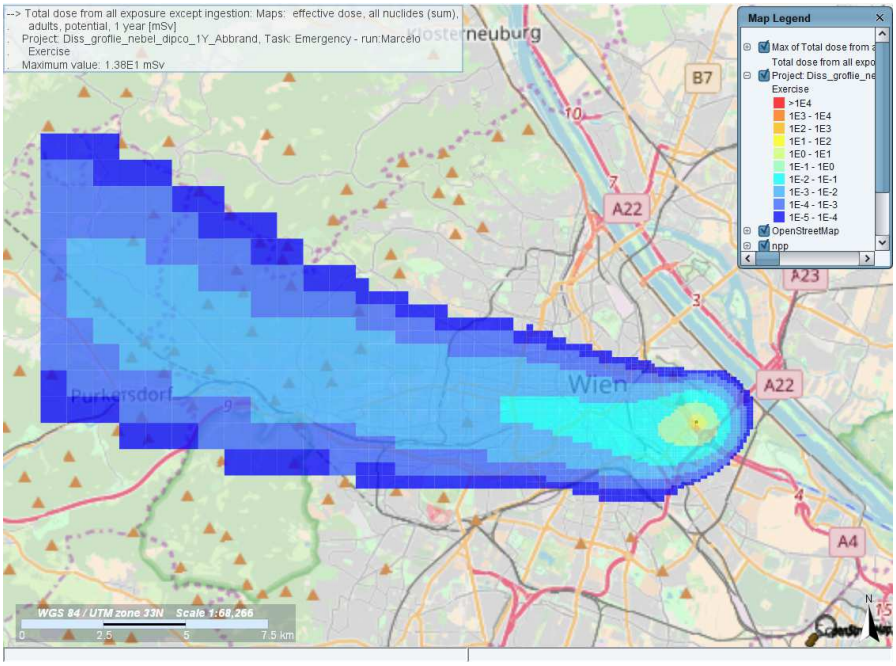

Figure 8.14: Foggy day scenario, large airplane crash, 1 year burnup

Die approbierte gedruckte Originalversion dieser Dissertation ist an der TU Wien Bibliothek verfügbar.
The approved original version of this doctoral thesis is available in print at TU Wien Bibliothek.
TU Bibliothek Your knowledge hub WIEN

In the hot day scenario (Figure 8.13) the regions affected by doses above 1 mSv are located close to the source origin, same as in the average scenarios. Again as randomly a day with hot weather was chosen, the area affected by the dispersion does not cover the same regions as in the average scenarios. The same argumentation applies to the foggy day scenario, see Figure 8.14. Here the effect with the localized high dose area is even stronger, due to the fact that the wind speed and the precipitation in this scenario are very low. So the dose distribution is circular around the source location, and is only distributed to a very small extend with the wind. Again the above described phenomenon of the randomly chosen day shows how important it is to look at individual scenarios for a safety analysis, and not only consider the average. The dose drops here below 10 mSv in the first year inside of the institute's boundaries, reaches 2 mSv at 200 m in all directions from the source location, and is below 1 mSv at 260 m from the source location.

8.4.2 Results with 11 years burnup

For the accident scenario "large airplane crash" (see 7.2.4) the calculation was performed for a burnup of 11 years. Table 8.15 shows the results of the RODOS simulation for the average days. Three representative values are analysed: The total dose after one year (except ingestion), the total effective dose rate and the total potential effective dose. The values given are the maximum values of the simulation. Table 8.16 shows the results of the specific scenarios for 11 years of burnup and the exposure of all fuel elements.

	Spring day	**Summer day**	**Autumn day**	**Winter day**
total dose exept ingestion 1 year [mSv]	2.63	3.09	3.11	1.78
total effective gamma dose rate all nuclides [mSv/h]	2.86	3.72	3.7	1.82
total potential dose effective [mSv]	2.62	3.08	3.11	1.78

Table 8.15: RODOS results after large airplane crash, 11 years of burnup, average scenarios

Throughout the seasons, the results have a standard deviation of 0.54 for the total dose, for the dose rate 0.78 and for the total potential effective dose 0.54, as

Die approbierte gedruckte Originalversion dieser Dissertation ist an der TU Wien Bibliothek verfügbar.
The approved original version of this doctoral thesis is available in print at TU Wien Bibliothek.
TU Bibliothek Your knowledge hub WIEN

shown in Table 8.15. The autumn and summer results are the highest, due to the fact that the rain rate is high, combined with a low wind speed (see section 6). The combination of a low precipitation and an average wind speed leads to the winter results, which are lower than throughout the rest of the year. The influence of snow needs to be looked at separately, but there is still no good simulation possibility for snow. Comparing the results of the 11 years burnup to those of 1 year burnup, they show again similar, but slightly lower results. The maximum dose is 3.11 mSv, the maximum dose rate is 3.72 mSv/h. Figures 8.15 to 8.18 show the graphical results of the dispersion simulation.

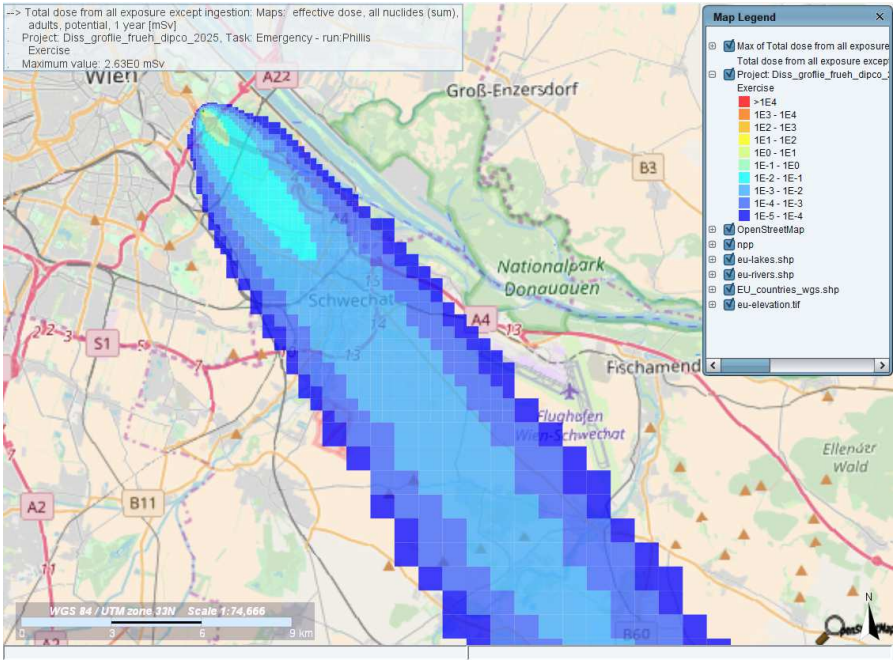

Figure 8.15: Large airplane crash scenario, average spring day, 11 years of burnup

Die approbierte gedruckte Originalversion dieser Dissertation ist an der TU Wien Bibliothek verfügbar.
The approved original version of this doctoral thesis is available in print at TU Wien Bibliothek.
TU Bibliothek Your knowledge hub WIEN

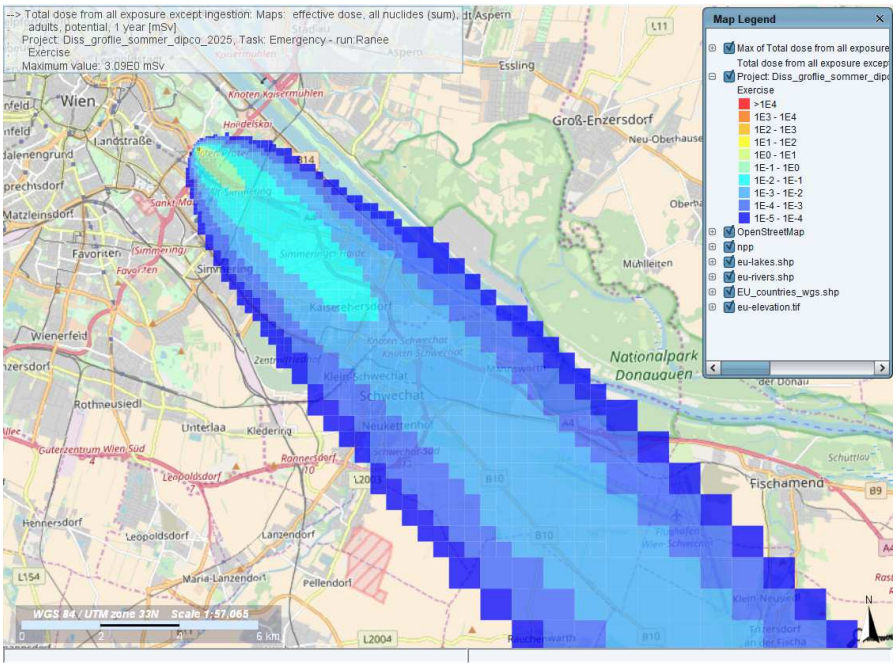

Figure 8.16: Large airplane crash scenario, average summer day, 11 years of burnup

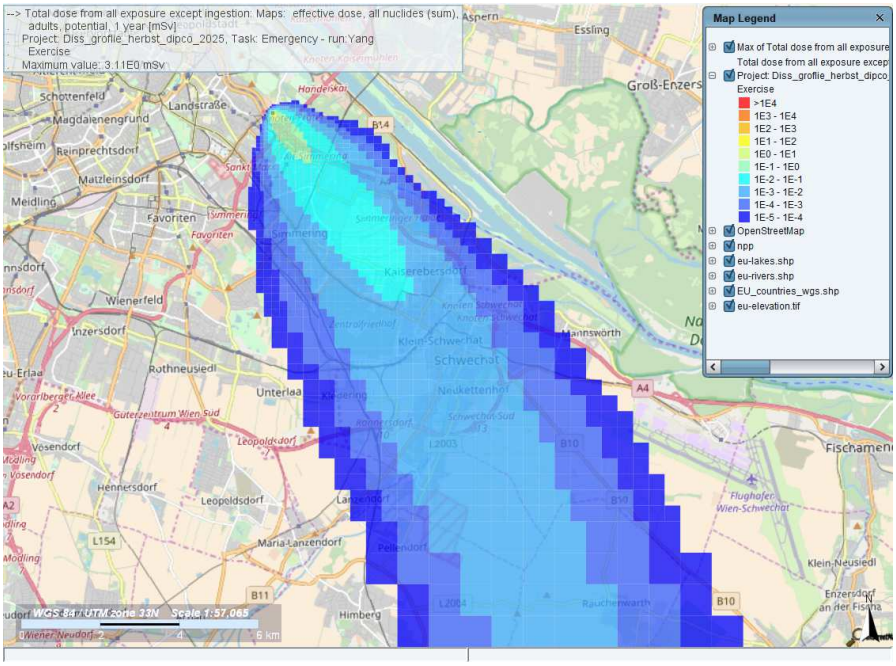

Figure 8.17: Autumn day scenario, large airplane crash, 11 years of burnup

Die approbierte gedruckte Originalversion dieser Dissertation ist an der TU Wien Bibliothek verfügbar.
The approved original version of this doctoral thesis is available in print at TU Wien Bibliothek.
TU Bibliothek Your knowledge hub WIEN

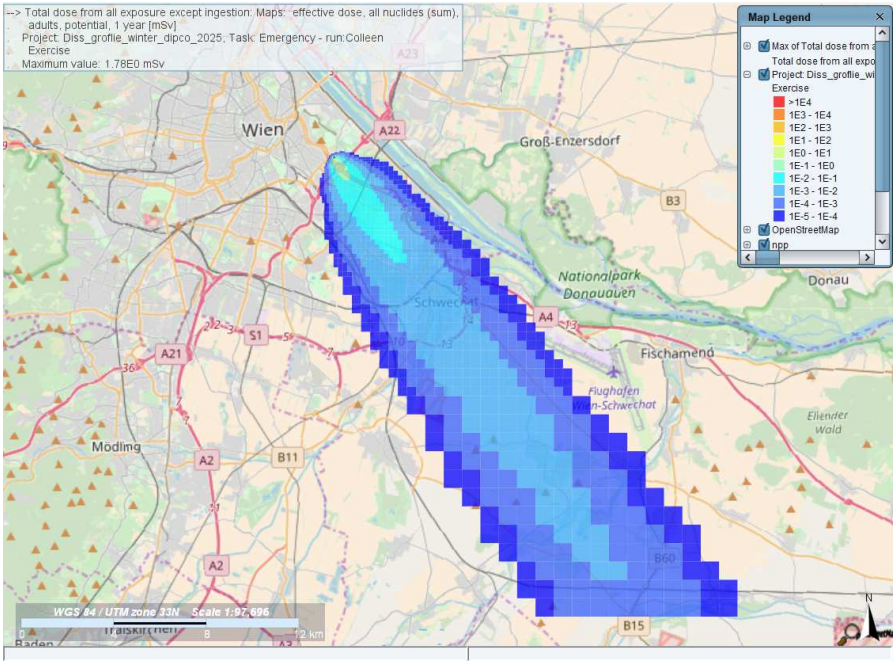

Figure 8.18: Winter day scenario, large airplane crash, 11 years of burnup

As described in 8.4.1 the average scenarios showed a distribution into the main wind direction. The Austrian radiation protection law limits the dose for public to 1 mSv/year, in Figure 8.19 the areas exceeding 1 mSv in the first year are within the boundary areas of the institute (dark yellow area). This is shown also more in detail in the next section with the analyses of the specific scenario outcomes.

Die approbierte gedruckte Originalversion dieser Dissertation ist an der TU Wien Bibliothek verfügbar.
The approved original version of this doctoral thesis is available in print at TU Wien Bibliothek.
TU Bibliothek Your knowledge hub WIEN

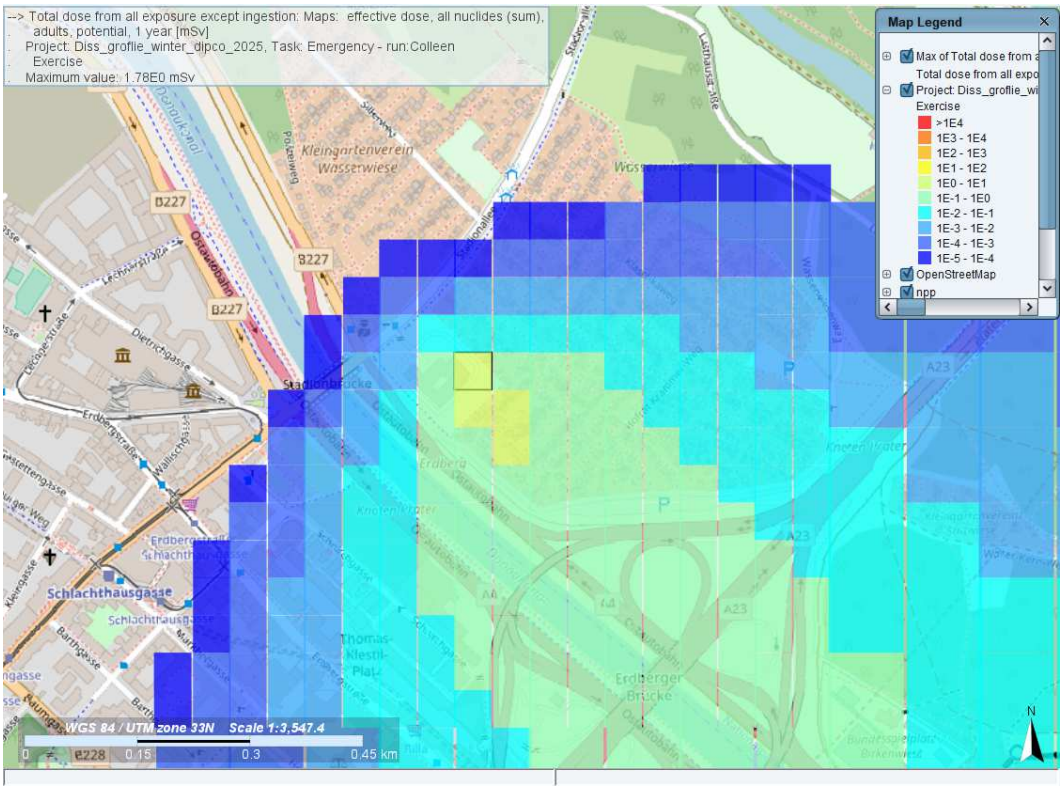

Figure 8.19: Close up look at the winter scenario, 11 years burnup, large airplane crash

Looking at the specific scenarios, the results differ from the above described average scenarios. Also, a more detailed look at each scenario is necessary to further analyse this outcome.

	Thunderstorm day	**Foggy day**	**Hot day**
total dose exept ingestion 1 year [mSv]	11.6	2.59	13.5
total effective gamma dose rate all nuclides [mSv/h]	13.1	4.28	24.4
total potential dose effective [mSv]	11.2	2.58	12.2

Table 8.16: RODOS results after large airplane crash, 11 years of burnup, specific scenarios

Die approbierte gedruckte Originalversion dieser Dissertation ist an der TU Wien Bibliothek verfügbar.
The approved original version of this doctoral thesis is available in print at TU Wien Bibliothek.
TU Bibliothek Your knowledge hub WIEN

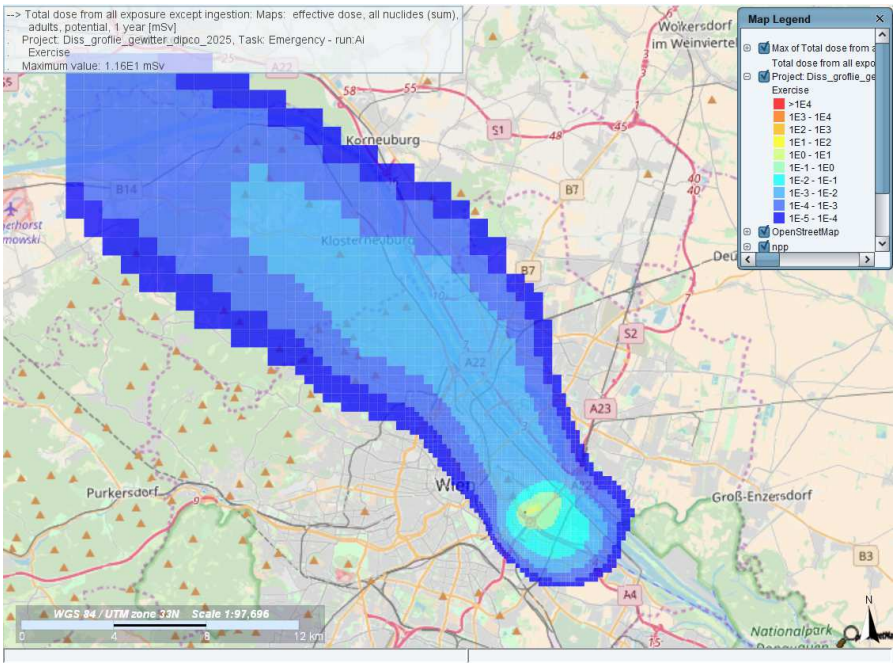

Figure 8.20: Thunderstorm scenario, large airplane crash, 11 years burnup

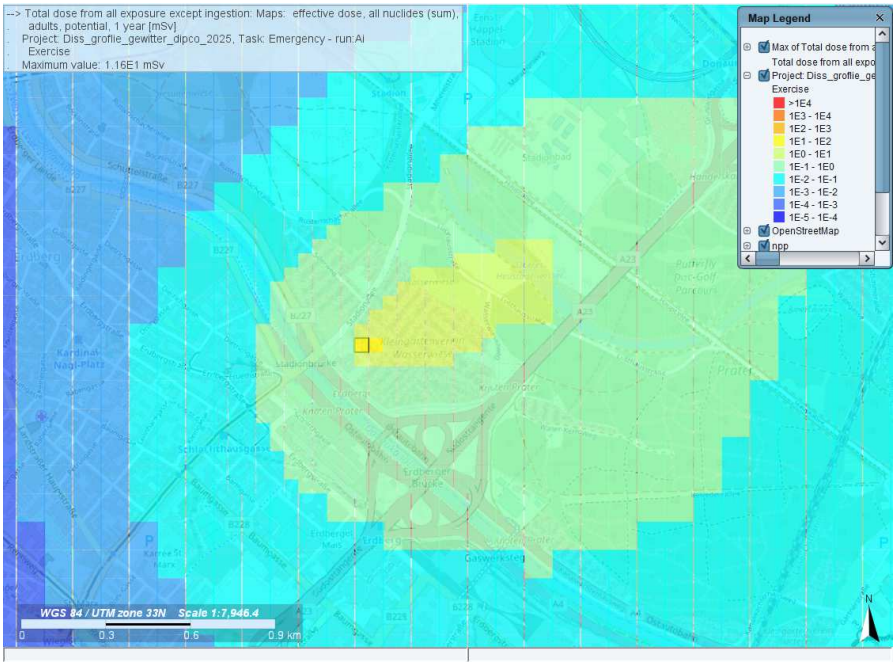

Figure 8.21: Close up look at the thunderstorm scenario, large airplane crash, 11 years burnup

Die approbierte gedruckte Originalversion dieser Dissertation ist an der TU Wien Bibliothek verfügbar.
The approved original version of this doctoral thesis is available in print at TU Wien Bibliothek.
TU Bibliothek Your knowledge hub WIEN

Figure 8.20 shows the simulated dispersion results for an specific scenario with a thunderstorm day. Compared to Figures 8.15 to 8.18 the affected areas don't match. This can be explained by the nature of the meteorology. The thunderstorm day was chosen randomly, the average scenarios reflect the average of the wind speed and direction, of which the thunderstorm day is part. Still, this simulation of the thunderstorm day demonstrates the necessity of the simulation of specific scenarios. Considering only the average, it would not reflect the reality and disregard possible necessary countermeasures for affected regions. In this scenario the area subjected to doses above 1 mSv in the first year is bigger than in the average scenarios. At the boundaries of the institute, the dose reaches 6.34 mSv in the first year (see 8.21). It is below 1 mSv at 900 m in the north east direction, showing a elliptical form of dispersion. The radius of the ellipse is 175 m. The dose dispersion shows a rapid drop, at 500 m from the source it is below 2 mSv.

This reflects also the other two specific scenarios and their dispersion.

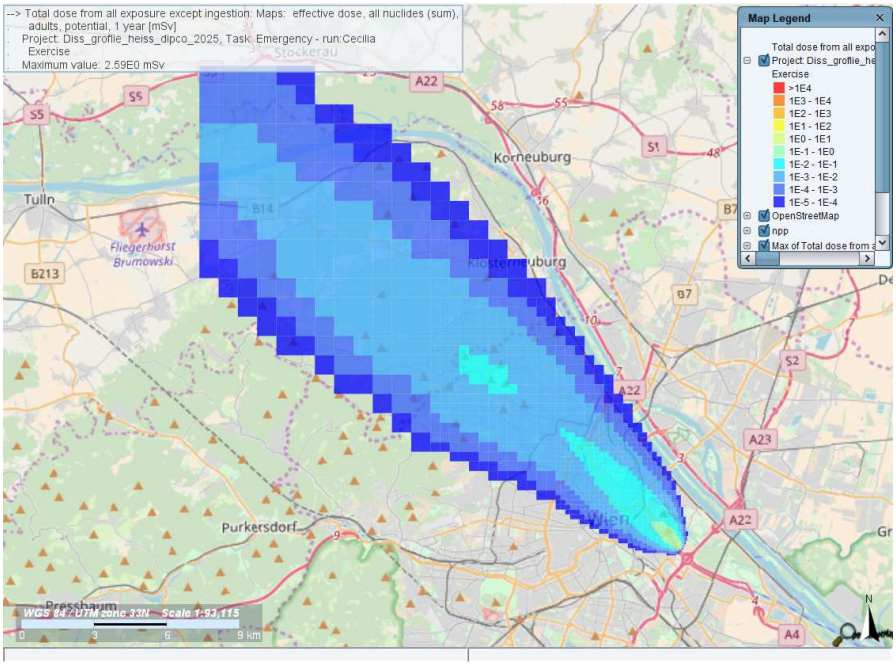

Figure 8.22: Hot day scenario, large airplane crash, 11 years burnup

Die approbierte gedruckte Originalversion dieser Dissertation ist an der TU Wien Bibliothek verfügbar.
The approved original version of this doctoral thesis is available in print at TU Wien Bibliothek.
TU Bibliothek Your knowledge hub WIEN

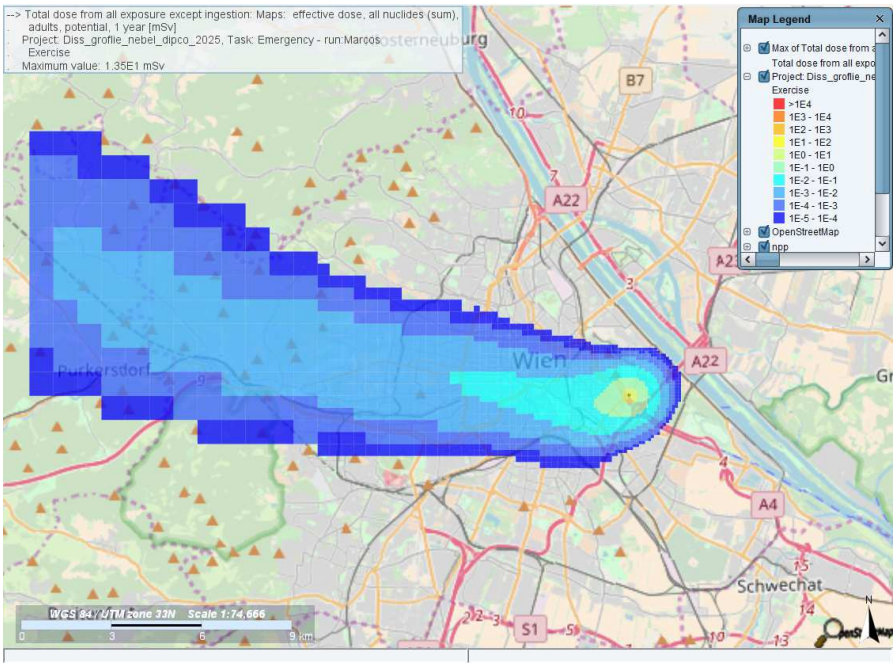

Figure 8.23: Foggy day scenario, large airplane crash, 11 years burnup

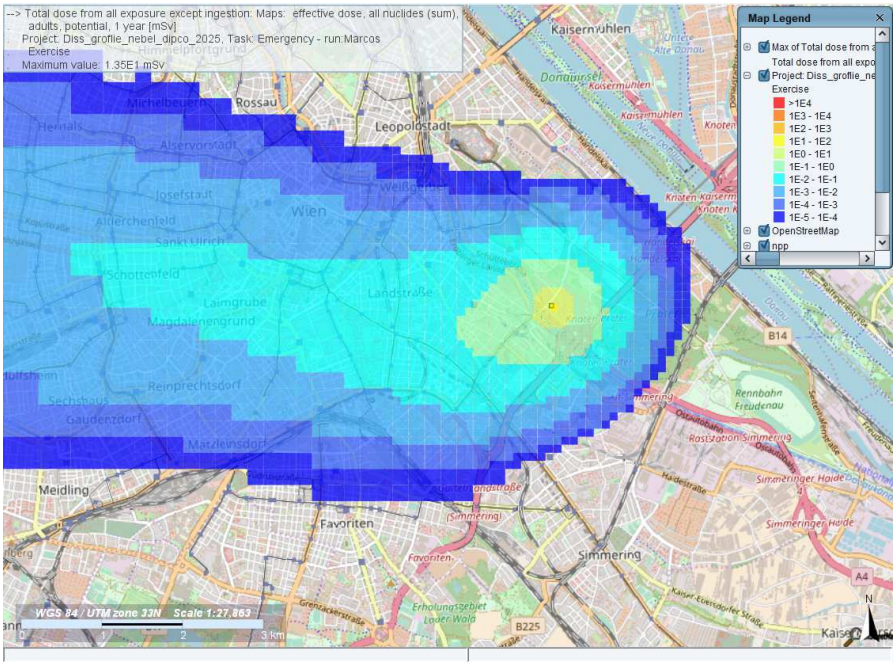

Figure 8.24: Close up look at the foggy day scenario, large airplane crash, 11 years burnup

Die approbierte gedruckte Originalversion dieser Dissertation ist an der TU Wien Bibliothek verfügbar.
The approved original version of this doctoral thesis is available in print at TU Wien Bibliothek.
TU Bibliothek Your knowledge hub WIEN

In the hot day scenario (Figure 8.22) the regions affected by doses above 1 mSv are located close to the source origin, same as in the average scenarios. Again as randomly a day with hot weather was chosen, the area affected by the dispersion does not cover the same regions as in the average scenarios. The same argumentation applies to the foggy day scenario, see Figure 8.23. Here the effect with the localized high dose area is even stronger (see 8.24), due to the fact that the wind speed and the precipitation in this scenario are very low. So the dose distribution is circular around the source location, and is only distributed to a very small extend with the wind. Again the above described phenomenon of the randomly chosen day shows how important it is to look at individual scenarios for a safety analysis, and not only consider the average. The dose drops here below 10 mSv in the first year inside of the institute's boundaries, reaches 2 mSv at 200 m in all directions from the source location, and is below 1 mSv at 260 m from the source location.

8.4.3 Summary

Tables 8.1, 8.2, 8.3 and 8.4 show the RODOS simulation results for the exposure of 1 fuel element with 1 year and 11 years burnup. The highest effective dose after 1 year results from the foggy day scenario with 2.38 E-5 mSv for 1 year burnup and the highest effective dose after 1 year for 11 years burnup results also from the foggy day scenario with 2.3 E-5 mSv. Figures 8.1 to 8.2 show the graphical results of the simulation.

Tables 8.5, 8.6, 8.7 and 8.8 show the RODOS simulation results for the exposure of all fuel elements with 1 year and 11 years burnup. The highest effective dose after 1 year results from the hot day scenario with 1.18 μSv for 1 year burnup and the highest effective dose after 1 year for 11 years burnup results also from the hot day scenario with 1.15 μSv. Figures 8.3 to 8.4 show the graphical results of the simulation.

Tables 8.9, 8.10, 8.11 and 8.12 show the RODOS simulation results for the exposure after a small airplane crash with 1 year and 11 years burnup. The highest effective dose after 1 year results from the hot day scenario with 1.92 μSv for 1 year burnup and the highest effective dose after 1 year for 11 years burnup results also from the hot day scenario with 1.88 μSv. Figures 8.5 to 8.6 show the graphical results of the simulation. In Annex [B.1] are all graphical results of the simulations described above.

Die approbierte gedruckte Originalversion dieser Dissertation ist an der TU Wien Bibliothek verfügbar.
The approved original version of this doctoral thesis is available in print at TU Wien Bibliothek.
TU Bibliothek Your knowledge hub WIEN

Tables 8.13, 8.14, 8.15 and 8.16 show the RODOS simulation results for the exposure after a large airplane crash with 1 and 11 years burnup. The highest effective dose after 1 year results from the hot day scenario with 13.8 mSv for 1 year burnup, the highest effective dose after 1 year results also from the hot day scenario after 11 years burnup with 13.5 mSv. Figures 8.7 to 8.10 show the graphical results of the simulation for the average day scenarios. Figures 8.12 to 8.14 show the graphical results of the simulation for the specific day scenarios. The affected areas for the average day scenarios are within the main wind-direction in the south-eastern region from the source, while for the specific days-scenarios they lie close to the source (foggy day) or in the north-western direction. (thunderstorm day).

The results of the accident scenarios with 1 fuel element exposed, all fuel elements exposed and the small airplane crash show that the exposure for the public is well below 1 mSv/year. The highest value for the average scenario was 0.3 μSv in the first year after the accident, for the specific scenario it was 1.92 μSv in the first year after the accident. The accident scenario Large airplane crash showed a maximum dose in the first year after the accident of 3.2 mSv for the average scenarios, and a maximum dose of 13.8 mSv in the first year for the specific scenarios. For the specific scenarios the dose dropped below 1 mSv at 900 m from the source. The chosen weather scenarios showed the necessity of the evaluation of specific scenarios. Simulation of scenarios that represent only the average weather conditions will lead to wrongly planned and hence ineffective countermeasures. If countermeasures are to be prepared by the authorities, they need to look at the specific scenarios, which represent the worst cases. Nevertheless even in case of the unlikely event of a large airplane crash, the average scenarios show that it is unlikely that paragraph 14 of the Austrian Radiation Protection Law will be met, which is set to 5 mSv in 5 years in average.

Die approbierte gedruckte Originalversion dieser Dissertation ist an der TU Wien Bibliothek verfügbar.
The approved original version of this doctoral thesis is available in print at TU Wien Bibliothek.
TU Bibliothek Your knowledge hub WIEN

9 Calculations with LASAIR

The second part of the simulation was performed with the program LASAIR. LASAIR is described in chapter 5. The LASAIR input parameters are less flexible compared to RODOS, hence the calculation scenarios had to be adapted. Since the RODOS calculation showed only a significant dose for the big airplane crash scenario, the LASAIR simulation was only performed for the big airplane crash scenario. The following meteorological scenarios were calculated:

- Average spring day
- Average summer day
- Average autumn day
- Average winter day
- Hot day
- Foggy day
- Thunderstorm day

As described in 6.2.9 the weather data for the thunderstorm scenario and the foggy day scenario had to be adapted for the LASAIR simulations. The scenarios were only calculated with the burnup data after 1 year of reactor operation. The source term is described in chapter 7.3. The input data varied only for the meteorological and source term data. All other parameters were taken as follows: The chimney is assumed to be 20 m high and has a diameter of 1.5 m. The release takes 600 s, and all released particles are smaller then 2.5 μm. The prediction is simulated for 1 hour.

Die approbierte gedruckte Originalversion dieser Dissertation ist an der TU Wien Bibliothek verfügbar.
The approved original version of this doctoral thesis is available in print at TU Wien Bibliothek.
TU Bibliothek Your knowledge hub WIEN

9.1 Results

9.1.1 Spring day results

The maximum γ - ground dose in 1 year for the spring day scenario is 3.15 mSv. Adding a precipitation of 0.05 mm of rain for the time of simulation, the maximum contamination is 1.51×10^9 Bq/m^2. In Figure 9.1 the dose distribution is shown on the left side, on the right side the deposition is shown. The line on the dose distribution figure equals 1 mSv.

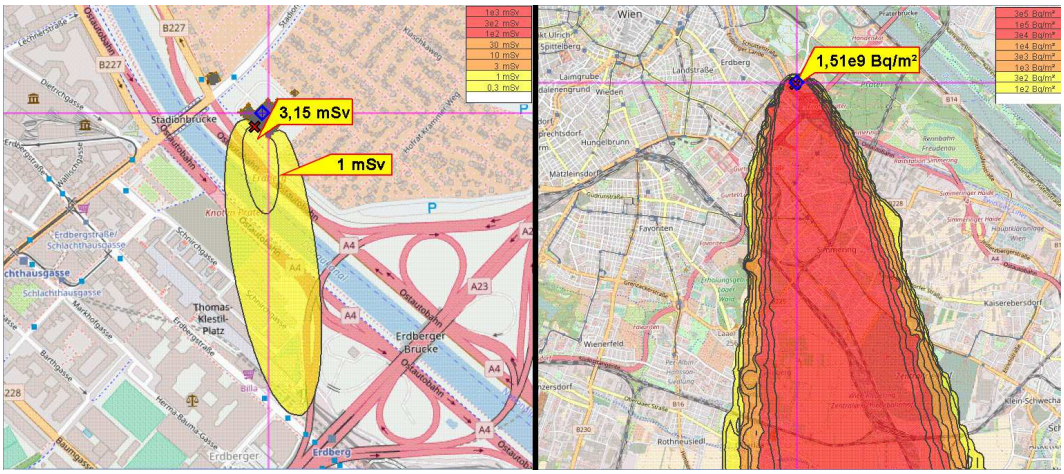

Figure 9.1: Left: The γ-ground dose after 1 year, right: deposition of activity after 1 year in case of a large airplane crash on an average spring day

9.1.2 Summer day results

The maximum γ - ground dose in 1 year for the summer day scenario is 0.746 mSv. Adding a precipitation of 0.1 mm of rain for the time of simulation, the maximum contamination is 2.98×10^8 Bq/m^2. In Figure 9.2 the dose distribution is shown on the left side, on the right side the deposition is shown.

Die approbierte gedruckte Originalversion dieser Dissertation ist an der TU Wien Bibliothek verfügbar.
The approved original version of this doctoral thesis is available in print at TU Wien Bibliothek.
TU Bibliothek Your knowledge hub WIEN

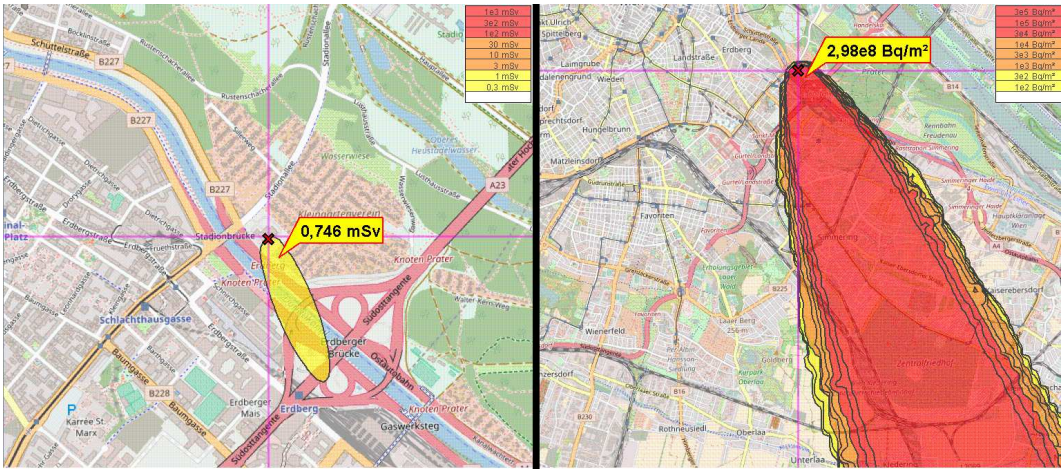

Figure 9.2: Left: The γ-ground dose after 1 year, right: deposition of activity after 1 year in case of a large airplane crash on an average summer day

9.1.3 Autumn day results

The maximum γ - ground dose in 1 year for the autumn day scenario is 2.61 mSv. Adding a precipitation of 0,05 mm of rain for the time of simulation, the maximum contamination is 4.4×10^8 Bq/m^2. In Figure 9.3 the dose distribution is shown on the left side, on the right side the deposition is shown. The line on the dose distribution figure equals 1 mSv.

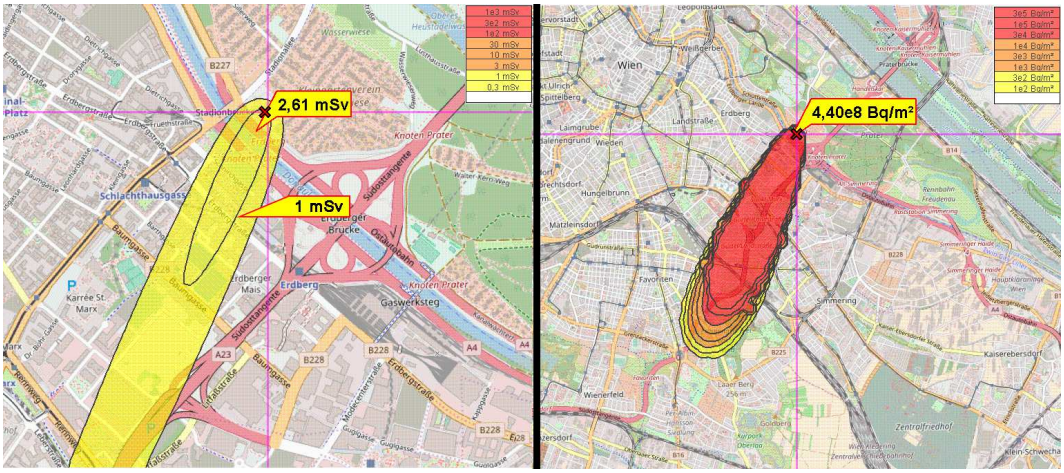

Figure 9.3: Left: The γ-ground dose after 1 year, right: deposition of activity after 1 year in case of a large airplane crash on an average autumn day

Die approbierte gedruckte Originalversion dieser Dissertation ist an der TU Wien Bibliothek verfügbar.
The approved original version of this doctoral thesis is available in print at TU Wien Bibliothek.

9.1.4 Winter day results

The maximum γ - ground dose in 1 year for the summer day scenario is 1.85 mSv. Adding a precipitation of 0,034 mm of rain for the time of simulation, the maximum contamination is 2.25×10^9 Bq/m^2. In Figure 9.4 the dose distribution is shown on the left side, on the right side the deposition is shown. The line on the dose distribution figure equals 1 mSv.

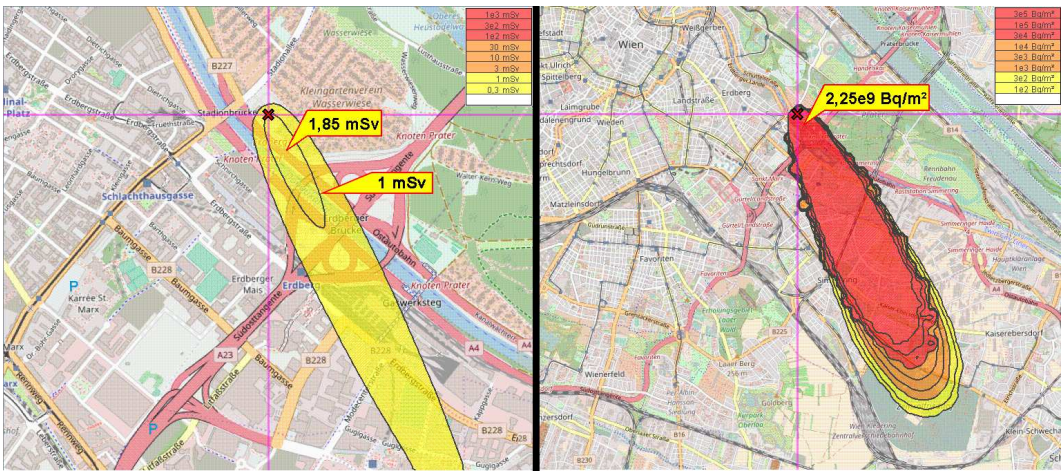

Figure 9.4: Left: The γ-ground dose after 1 year, right: deposition of activity after 1 year in case of a large airplane crash on an average winter day

9.1.5 Hot day results

The maximum γ - ground dose in 1 year for the hot day scenario is 0.777 mSv. The maximum contamination is 8.79×10^8 Bq/m^2. In Figure 9.5 the dose distribution is shown on the left side, on the right side the deposition is shown.

Die approbierte gedruckte Originalversion dieser Dissertation ist an der TU Wien Bibliothek verfügbar.
The approved original version of this doctoral thesis is available in print at TU Wien Bibliothek.
TU Bibliothek Your knowledge hub WIEN

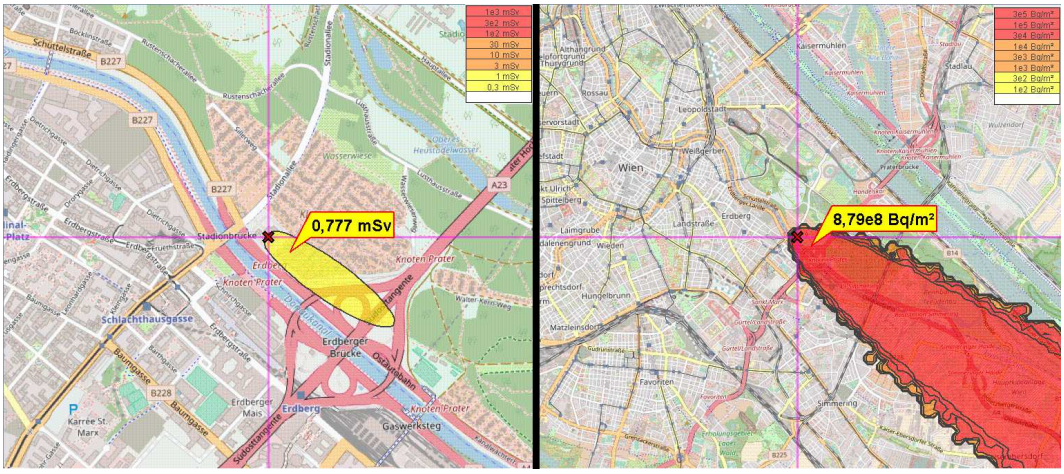

Figure 9.5: Left: The γ-ground dose after 1 year, right: deposition of activity after 1 year in case of a large airplane crash on a hot day

9.1.6 Foggy day results

The maximum γ - ground dose in 1 year for the foggy day scenario is 3.12 mSv. LASAIR does not allow a no wind situation, hence the smallest possible wind speed was taken of 0.5 m/s. Adding a precipitation of 0.01 mm of rain for the time of simulation, the maximum contamination is 2.89×10^9 Bq/m^2. In Figure 9.6 the dose distribution is shown on the left side, on the right side the deposition is shown. The line on the dose distribution figure equals 1 mSv.

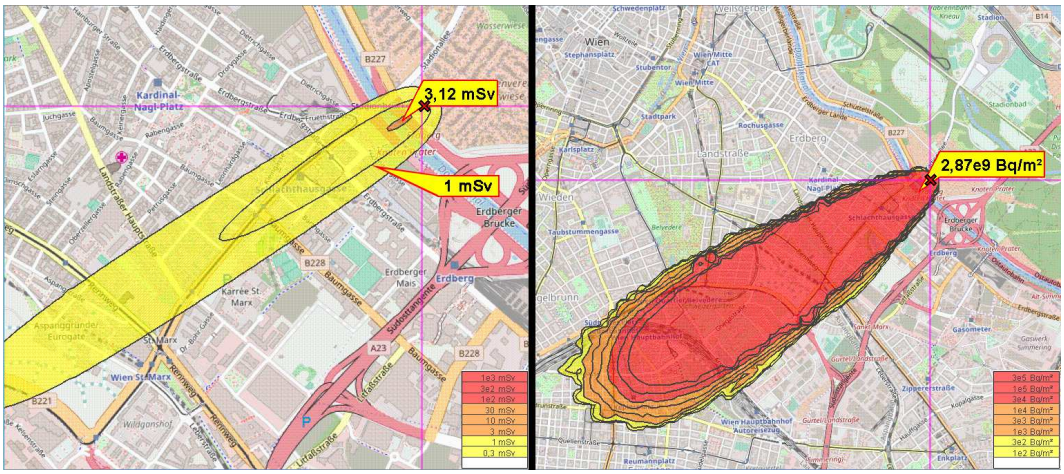

Figure 9.6: Left: The γ-ground dose after 1 year, right: deposition of activity after 1 year in case of a large airplane crash on a foggy day

Die approbierte gedruckte Originalversion dieser Dissertation ist an der TU Wien Bibliothek verfügbar.
The approved original version of this doctoral thesis is available in print at TU Wien Bibliothek.
TU Bibliothek Your knowledge hub WIEN

9.1.7 Thunderstorm day results

In contrast to the other scenarios, only the hour of the thunderstorm was simulated. The maximum γ - ground dose in 1 year for the foggy day scenario is 0.124 mSv. Adding a precipitation of 17.6 mm of rain for the time of simulation, the maximum contamination is 9.7×10^8 Bq/m^2. In Figure 9.7 the dose distribution is shown on the left side, on the right side the deposition is shown.

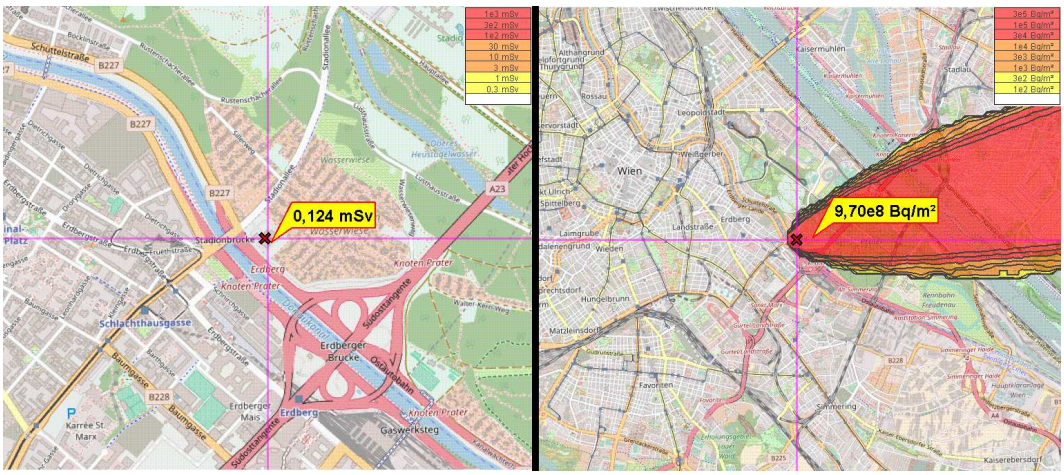

Figure 9.7: Left: The γ-ground dose after 1 year, right: deposition of activity after 1 year in case of a large airplane crash during a thunderstorm

9.1.8 Summary

In Table 9.1 the results of the LASAIR simulations are shown.

Scenario	**Dose [mSv]**	**Deposition**[Bq/m^2]
Spring day	3.15	1.51E+09
Summer day	0.746	2.98E+08
Autumn day	2.61	4.40E+08
Winter day	1.85	2.25E+09
Hot day	0.777	8.79E+08
Foggy day	3.12	2.89E+09
Thunderstorm day	0.124	9.70E+08

Table 9.1: Summary of simulation results with LASAIR, dose and deposition are accumulated values after 1 year

Die approbierte gedruckte Originalversion dieser Dissertation ist an der TU Wien Bibliothek verfügbar.
The approved original version of this doctoral thesis is available in print at TU Wien Bibliothek.
TU Bibliothek Your knowledge hub WIEN

10 Comparison of RODOS and LASAIR

10.1 General comparison of RODOS and LASAIR as simulation tools

The simulation tool RODOS was developed after the Chernobyl accident. It provides a quick estimation of consequences and possible countermeasures after a nuclear accident. RODOS offers 4 different computational models:

- ATSTEP: a Gaussian model
- RIMPUFF: a Gaussian model
- DIPCOT: a particle model
- LASAT: a Lagrangian particle model

The simulation tool LASAIR was developed to simulate consequences of nuclear explosions or fires in nuclear facilities. It is based on the computational model LASAT.

10.2 Comparison of input data

RODOS general input data are site information, source information and weather data. The source information data are flexible with nuclides (all nuclides possible) and timing (release of all nuclides at once or at different time steps). The source data is added before the simulation is performed. Weather data contains wind speed and direction, rain rate and the stability class for a chosen time interval. The meteorological information is added for a chosen time interval (minutes, hours

Die approbierte gedruckte Originalversion dieser Dissertation ist an der TU Wien Bibliothek verfügbar.
The approved original version of this doctoral thesis is available in print at TU Wien Bibliothek.
TU Bibliothek Your knowledge hub WIEN

or days). As RODOS provides countermeasure information, it is possible to add weather data until the end of the countermeasures. LASAIR input data are location, wind speed and direction as well as the stability class. It is not possible to simulate without wind. The minimum wind speed is 0.5 m/s. The source information is added after the simulation. The source term contains 5 nuclides. The precipitation is also added after the simulation with an average over the simulated time. Comparing the input data, it shows that LASAIR is optimized for quick calculations after explosion scenarios, not for longer term prognostic information after bigger events as RODOS. RODOS offers a wider variety of input parameters, they can be adapted for small time steps. There are no limitations on weather conditions. RODOS can simulate precise weather scenarios. In RODOS the source term is not limited, in LASAIR only 5 nuclides are included. A choice of nuclides for comparison reasons is difficult.

10.3 Comparison of output data

RODOS output data contain:

- activity concentrations
- acute dose/dose without early emergency actions
- acute dose with early emergency actions
- areas affected by
- cloud arrival time
- day of exceeding the intervention level
- dose rates
- frequency spectra of organ doses with early emergency actions
- frequency spectra of organ doses without early emergency actions
- intervention doses
- longterm doses

Die approbierte gedruckte Originalversion dieser Dissertation ist an der TU Wien Bibliothek verfügbar.
The approved original version of this doctoral thesis is available in print at TU Wien Bibliothek.
TU Bibliothek Your knowledge hub WIEN

- meteorological information
- potential doses

Each of the above listed items contains subfolders, for specific nuclides, or parts of the food chain. Details for specific output data can be found in [33]. For this work only the points dose rates, long term doses and potential doses were used. The dose rate point contains

- From ground (deposition on ideal lawn; nuclide specific, contributions of noble gases are zero)
- From cloud (nuclide sum)
- From ground (deposition on ideal lawn; nuclide sum)
- Total dose rate (sum of cloud and ground contribution; nuclide sum).

For calculations in this work, the last point, total dose rate was used.
The point long term doses contains:

- ground dose
- ingestion dose
- inhalation dose (normal breath)
- total dose from all exposure except ingestion

For calculations in this work, the last point, total dose from all exposure except ingestion was used.
The point potential doses contains:

- cloud gamma dose
- ground gamma dose
- inhalation dose
- total potential dose
  - bone marrow

Die approbierte gedruckte Originalversion dieser Dissertation ist an der TU Wien Bibliothek verfügbar.
The approved original version of this doctoral thesis is available in print at TU Wien Bibliothek.
TU Bibliothek Your knowledge hub WIEN

  - effective
  - lung
  - thyroid
  - uterus
- local skin dose

For calculations in this work, the point total potential dose - effective was used. RODOS has huge capacities regarding output data. Only a reduced set of parameters was used for this work. They were sufficient for the data preparation of the safety analysis. All output data are automatically calculated and stored and can be extracted if needed.

LASAIR needs, as described above, only the meteorological data for its simulation. The output data are calculated in a second step after the nuclide input. The output data are:

- Inhalation dose for adults, children or infants, can be specified for organs
- Activity - this is the mean value of activity over the calculation time
- Deposition - this is the complete activity per square meter of deposed activity, wet or dry
- Gamma Dose with or without ground radiation, it's calculated with the German incident calculation data.
- Gamma activity - the mean value of the gamma nuclides over the calculation time

For this work, the gamma dose with ground radiation and the deposition after precipitation was used. LASAIR is optimized for calculations of 5 nuclides, due to the fact it is designed for explosion or fire incident scenarios. The output data contain necessary information regarding dose and activity. RODOS is designed for accident scenario calculations in NPPs, its output data contain not only information on dose and activity but also on possible countermeasures (food chain, agriculture, long term effects).

Die approbierte gedruckte Originalversion dieser Dissertation ist an der TU Wien Bibliothek verfügbar.
The approved original version of this doctoral thesis is available in print at TU Wien Bibliothek.
TU Bibliothek Your knowledge hub WIEN

10.4 Comparison of Results

The aim of this work was to calculate the dispersion of radionuclides after four accident scenarios for the TRIGA MARK II Reactor Vienna. Two different simulation tools were used for this calculation, RODOS and LASAIR. The simulations were first performed with RODOS and in a second step with LASAIR. RODOS results showed only significant doses for the big airplane crash scenario, hence the calculations with LASAIR were only performed for this scenario. In the next paragraphs a comparison of the results has been evaluated. A quantitative comparison is not feasible due to the following points: The release times used in RODOS and LASAIR differ. For RODOS simulation a 1h release time was chosen to stay consistent with previous works. This was not possible in LASAIR, hence 10 min release time were used. The prediction times altered, RODOS offers a 24 h prediction, LASAIR only 1 h. RODOS has the possibility to put time evolving weather data into the simulation. As described in chapter 6.2.9 LASAIR does not offer this possibility, only a mean value for wind speed and the wind direction can be put into the simulation. Also LASAIR does not allow a scenario without wind. Due to the above mentioned points, a comparison of the dose results is not possible. The input parameters were altered for LASAIR, and do not reflect the same meteorological scenario any more. The nuclide input for LASAIR had to be reduced to five nuclides. Is a comparison completely impossible? There are several points in the simulation results that show similarities: The average scenario results show with both simulation tools a dispersion release with the main wind direction. This needs to be carefully evaluated for LASAIR, as the wind direction was averaged. LASAIR does only allow the input of the wind speed, wind direction and the rain rate at the time of release. There is no possibility of a change over the release time. For its designed purpose (explosion or fire scenario) this works out if there is no change in the meteorological conditions during the time of release. It is only a snap shot. RODOS allows changes of meteorological conditions. Looking at the specific scenarios a comparison of the tools becomes impossible. The input data for LASAIR were adapted too much (see chapter 6.2.9) to reflect the original meteorological condition. The exclusion of "no wind scenarios" alters the input data in a way that the don't reflect the input.

Die approbierte gedruckte Originalversion dieser Dissertation ist an der TU Wien Bibliothek verfügbar.
The approved original version of this doctoral thesis is available in print at TU Wien Bibliothek.
TU Bibliothek Your knowledge hub WIEN

10.5 Summary

RODOS was developed after the Chernobyl accident as a communication tool. With its fast calculation times and its graphical output it is an ideal tool to simulate consequences after major NPP accidents. It offers the choice of several model chains for its simulation (ATSTEP, RIMPUFF, DIPCOT and LASAT). LASAIR was developed as a tool for consequence simulation after nuclear explosions or fires. It is based on the LASAT model.

LASAIR shows a strong dependence on one set of input data (only one value for wind speed, direction and rain rate) and has only the capacity to simulate the spread of 5 nuclides.

RODOS offers the possibility to put time evolving data into the simulation, or online and real time data. The output data are constraint to inhalation dose, activity, gamma dose and activity and deposition for LASAIR, while RODOS offers not only dose and activity data, but also countermeasure information. The different design purposes of LASAIR and RODOS allow comparison in a narrow scope.

Die approbierte gedruckte Originalversion dieser Dissertation ist an der TU Wien Bibliothek verfügbar.
The approved original version of this doctoral thesis is available in print at TU Wien Bibliothek.
TU Bibliothek Your knowledge hub WIEN

11 Conclusion

The purpose of this work was to re-evaluate the consequences of four accident scenarios for the TRIGA MARK II in Vienna. The reactor had a core replacement and received new fuel elements without HEU elements in 2012 (see chapter1.3). This made the re-evaluation necessary. This work used two different simulation tools LASAIR and RODOS. The former is described in chapter 4 and the latter in chapter 5. The Atominstitut possesses a weather station, which collects weather data at the rooftop of the main building. Berger [9] evaluated the 2012 and 2013 data of this station. The evaluated data are the input data for this thesis. The detailed description of the meteorological data and its preparation for the simulation data is found in chapter 6. The source term for this thesis was simulated with ORIGEN. The source term was calculated for two burnup times, the initial burnup after one year, and the burnup after 11 years. The detailed description of the source term data and its preparation for the simulation is found in chapter 7.

This thesis analysed four different accident scenarios:

- Destruction of fuel element with highest activity content
- Destruction of all fuel elements
- Case of a small airplane crash
- Case of a large airplane crash

This is in accordance with previous works (see Villa, [4]). A detailed description of those scenarios is found in chapters 7.2.1 to 7.2.4. For these four accident scenarios seven weather scenarios were chosen:

- Spring day scenario
- Summer day scenario
- Autumn day scenario

Die approbierte gedruckte Originalversion dieser Dissertation ist an der TU Wien Bibliothek verfügbar.
The approved original version of this doctoral thesis is available in print at TU Wien Bibliothek.
TU Bibliothek Your knowledge hub WIEN

- Winter day scenario
- Thunderstorm day scenario
- Foggy day scenario
- Hot day scenario

The first four scenarios represent averaged data, the later three represent specific days. A detailed description of those weather scenarios is found in chapter 6.2. RODOS performed simulations for all four accident scenarios. The results for the destruction of one fuel element can be found in chapter 8.1. The highest effective dose after one year results from the foggy day scenario with 2.38 E-5 mSv for one year burnup. The results for the destruction of all fuel elements can be found in chapter 8.2. The highest effective dose after one year results from the hot day scenario with 1.18 μSv for one year burnup. The results for the small airplane crash scenario can be found in chapter 8.3. The highest effective dose after one year results from the hot day scenario with 1.92 μSv for one year burnup. The results for the large airplane crash scenario can be found in chapter 8.4. The highest effective dose after 1 year results from the hot day scenario with 13.8 mSv for 1 year burnup. The average case scenarios for the large airplane crash show a maximum dose of 3.82 mSv in the first year for the summer scenario. The dose declines to values below 1 mSv at the boundaries of the institute (see Figure 8.11). This does not apply for the specific scenarios.

The Austrian Radiation protection law allows an additional dose of 1 mSv / year for the public. Looking at the results above, only the large airplane crash scenario shows a relevant dose. LASAIR simulations were hence only performed for this case. As described in chapter 5 the input data for the LASAIR simulation had to be adopted in order to perform the calculations. The maximum dose in the LASAIR simulation for the average scenario were 3.15 mSv after one year, for the autumn day scenario. The maximum dose in the LASAIR simulation for the specific scenario were 0.777 mSv after one year, for the hot day scenario. The detailed results of all LASAIR simulations are in chapter 9.

The TRIGA MARK II reactor, as a research reactor, appears as a special case for dispersion simulations. The simulation programs are either designed for radiological explosions or fire (e.g. LASAIR) or for releases in NPP accidents (e.g. RODOS). Looking at the results, LASAIR results underestimate the release. This

Die approbierte gedruckte Originalversion dieser Dissertation ist an der TU Wien Bibliothek verfügbar.
The approved original version of this doctoral thesis is available in print at TU Wien Bibliothek.
TU Bibliothek Your knowledge hub WIEN

is not only due to the fact that the weather data were averaged, but also due to the fact that it can only simulate 5 nuclides. RODOS data lie in accordance with previous works. Nevertheless, RODOS delivers far more output then needed for the evaluation of accident scenarios for a research reactor.

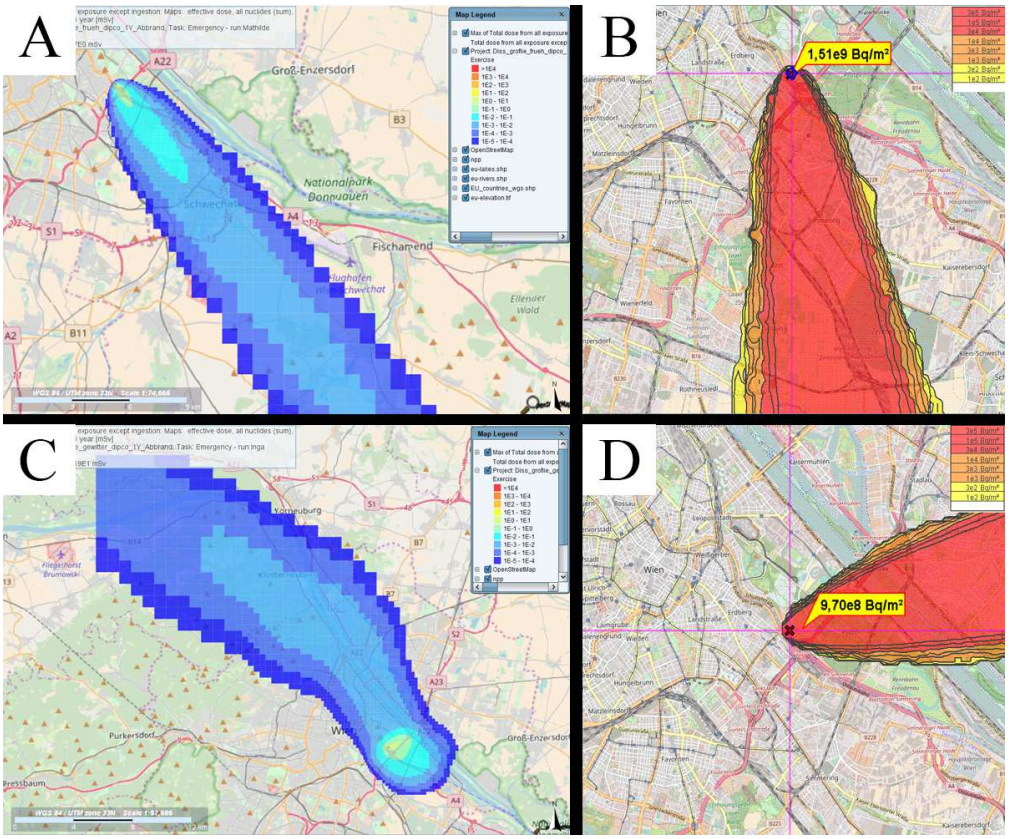

Figure 11.1: Comparison of results upper part RODOS (A) and LASAIR (B) results for the spring day scenario, lower part RODOS (C) and LASAIR (D) results for a thunderstorm day scenario

Figure 11.1 shows the graphical results for a big airplane crash with the spring day scenario after one year burnup with RODOS (A) and LASAIR (B) in the upper part. In the lower part it shows the graphical results of the thunderstorm day scenario with RODOS (C) and LASAIR (D). The average scenarios show, as described above, a release and deposition with the main wind direction. The specific scenario simulated with LASAIR does only deliver a dispersion with the precipitation. The limited input parameters of LASAIR lead to this result, which make a comparison of the specific scenarios impossible. Looking at the average

Die approbierte gedruckte Originalversion dieser Dissertation ist an der TU Wien Bibliothek verfügbar.
The approved original version of this doctoral thesis is available in print at TU Wien Bibliothek.
TU Bibliothek Your knowledge hub WIEN

versus the specific day scenarios, the specific day poses a special case within the average. Taking only the average scenarios for countermeasure preparation would be misleading. Countermeasure preparation needs to be looked at for numerous weather scenarios and not only the average scenarios. Nevertheless looking at the calculated values show that an overstatement is not necessary. Even with the specific scenarios, the dose development shows a rapid drop off. It falls below 7 mSv at the boundaries of the institute in the first year.

The new core composition of the TRIGA MARK II reactor in Vienna made a reevaluation of the dispersion calculations after possible accidents necessary. This work used two different simulation tools, RODOS and LASAIR. LASAIR, a tool for dispersion calculations after explosions or fires, is not powerful enough to simulate accidents in research reactors. Hence, the focus was put on RODOS simulations. The overall results of RODOS are in accordance with previous works. This work did not only look at average scenarios, but also included specific scenarios (thunderstorm, fog and scenarios with little wind - hot days). The analysis of these scenarios showed that the perspective for countermeasures after accidents needs to be wider. The average scenarios showed dose values of below 1 mSv in the first year, which lies in accordance with the Austrian Radiation Protection Law.

Die approbierte gedruckte Originalversion dieser Dissertation ist an der TU Wien Bibliothek verfügbar.
The approved original version of this doctoral thesis is available in print at TU Wien Bibliothek.
TU Bibliothek Your knowledge hub WIEN

List of Figures

Die approbierte gedruckte Originalversion dieser Dissertation ist an der TU Wien Bibliothek verfügbar.
The approved original version of this doctoral thesis is available in print at TU Wien Bibliothek.
TU Bibliothek Your knowledge hub WIEN

Die approbierte gedruckte Originalversion dieser Dissertation ist an der TU Wien Bibliothek verfügbar.
The approved original version of this doctoral thesis is available in print at TU Wien Bibliothek.
TU Bibliothek Your knowledge hub WIEN

Die approbierte gedruckte Originalversion dieser Dissertation ist an der TU Wien Bibliothek verfügbar.
The approved original version of this doctoral thesis is available in print at TU Wien Bibliothek.
TU Bibliothek Your knowledge hub WIEN

Die approbierte gedruckte Originalversion dieser Dissertation ist an der TU Wien Bibliothek verfügbar.
The approved original version of this doctoral thesis is available in print at TU Wien Bibliothek.
TU Bibliothek Your knowledge hub WIEN

List of Tables

Die approbierte gedruckte Originalversion dieser Dissertation ist an der TU Wien Bibliothek verfügbar.
The approved original version of this doctoral thesis is available in print at TU Wien Bibliothek.
TU Bibliothek Your knowledge hub WIEN

Die approbierte gedruckte Originalversion dieser Dissertation ist an der TU Wien Bibliothek verfügbar.
The approved original version of this doctoral thesis is available in print at TU Wien Bibliothek.
TU Bibliothek Your knowledge hub WIEN

Die approbierte gedruckte Originalversion dieser Dissertation ist an der TU Wien Bibliothek verfügbar.
The approved original version of this doctoral thesis is available in print at TU Wien Bibliothek.
TU Bibliothek Your knowledge hub WIEN

A References

1. H.Böck, M.Villa, Practical Course on Reactor Physics and Reactor Kinetics, AIAU 27309, Vienna, 2017

2. IAEA, History, Development and Future of TRIGA Research Reactors, Vienna, 2016

3. M. Villa, R.Bergmann et al, Tätigkeitsbericht, Progress Report, 2011- 2013, Vienna, 2013

4. M.Villa, H.Boeck, M.Haydn, Accident Scenarios of the TRIGA Mark II reactor in Vienna, Atominstitut, Vienna, 2010

5. M.Haydn, Accident Scenario with Environmental Impact of the TRIGA Mark II reactor Vienna, Master theses, Vienna, 2009

6. https://ati.tuwien.ac.at/reaktor/querschnitt/, 08.03.2020

7. Safety of Research Reactors, IAEA Specific Safety Requirements No. SSR-3, ISBN 978–92–0–104816–5, Vienna, 2016

8. Safety of Research Reactors, IAEA Safety Requirements No. NS-R-4, Vienna, 2005

9. M.Berger, Analyse der Wetterdaten des Standortes Atominstitut, Zeitraum 2010 bis 2013, Projektarbeit Reaktorphysik, ATIR 1405. Vienna, 2015

10. S.C.Hawley, R.L.Kathren, Credible Accident Analyses for TRIGA and TRIGA-fueled Reactors, Pacific Northwest Laboratory, NUREG/CR-2387, PNL-4028, Richland, USA, 1982

11. F.C.Foushee, R.H.Peters, Summary of TRIGA fuel fission product release experiments. GULF-EES-A10801, Sept. 1971

Die approbierte gedruckte Originalversion dieser Dissertation ist an der TU Wien Bibliothek verfügbar.
The approved original version of this doctoral thesis is available in print at TU Wien Bibliothek.
TU Bibliothek Your knowledge hub WIEN

12. Forschungszentrum Karlsruhe GmbH, The RODOS System, Version PV6.0, Karlruhe, Germany, 2005

13. A.Leelossy, F.Molnar, F.Izsak, A.Havasi, I.Lagzi, R.Meszaros, Dispersion Modeling of air pollutants in the atmosphere:a review, Central Eurpean Journal of Geosciences, 6(3), 2014, p 257 - 278

14. G. Sriram, N. Krishna Mohan, V.Gopalasamy, Sensitivity study of Gaussian dispersion models, Journal of Scientific and Industrial Research, 65, 2006, p 321–324

15. D. B. Turner, The long lifetime of the dispersion methods of Pasquill in U.S. regulatory air modeling, J. Appl. Meteorol., 36, 1997, p 1016–1020

16. B. Galperin, S. Sukoriansky, P.S. Anderson, On the critical Richardson number in stably stratified turbulence, Atmos. Sci. Lett., 8, 2007,p 65–69

17. A. J. Cimorelli,S.G. Perry et al.,AERMOD: A dispersion model for industrial source applications. Part I: General model formulation and boundary layer characterization, J. Appl. Meteorol., 44(5), 2005, p. 682–693

18. S. G. Perry, CTDMPLUS: A dispersion model for sources near complex topography. Part I: Technical Formulations, J. Appl. Meteorol., 31, 1992, p.633–645

19. T. Foken, 50 years of the Monin–Obukhov similarity theory. Bound-Lay. Meteorol., 2006, 119, p. 431–447

20. R. B. Stull, An Introduction to Boundary Layer Meteorology. Kluwer Academic Publishers, 1988

21. J. L. Woodward , Estimating the Flammable Mass of a Vapor Cloud: A CCPS Concept Book Appendix A, doi: 10.1002/9780470935361, 1999

22. J.M.Stockie, Mathematics of atmospheric dispersion modelling, SIAM Rev., 53, 2011,p.349–372

23. A. Namdeo,G. Mitchell, et al. TEMMS: an integrated package for modelling and mapping urban traffic emissions and air quality, Environ. Model. Softw., 17, 2002, p. 177–188

Die approbierte gedruckte Originalversion dieser Dissertation ist an der TU Wien Bibliothek verfügbar.
The approved original version of this doctoral thesis is available in print at TU Wien Bibliothek.
TU Bibliothek Your knowledge hub WIEN

24. J. Brandt,T. Mikkelsen, et al., Using a combination of two models in tracer simulations, Math. Comput. Model., 23, 1996,p. 99– 115

25. D. Oettl,U. Uhmer, Development and evaluation of GRAL-C dispersion model, a hybrid Eulerian- Lagrangian approach capturing NO-NO2-O3 chemistry, Atmos. Environ., 45, 2011, p. 839–847

26. J. Pozorski,J-P. Minier, On the Lagrangian turbulent dispersion models based on the Langevin equation, Int. J. Multiphas. Flow, 24, 1998, p.913–945

27. D.Meschede, Gerthsen Physik, 22. Auflage, Springer Verlag, ISBN 3-540-02622-3, Germany, 2004

28. S.Andronopoulos, E.Davakis, J.G.Bartzis, RODOS-DIPCOT Model Description and Evaluation, RODOS(RA2)-TN(09)-01, Greece, 2001

29. http://webspace.ship.edu/pgmarr/Geo441/Lectures/Lec 16 - 20Directional Statistics.pdf, 09.03.2020

30. N.L.Baldwin, F.C.Foushee, J.S.Greenwood, Fission Product Release from TRIGA-LEU Reactor Fuels, GA-A6287,General Atomic Company, USA, 1980

31. T.Stummer, R.Khan, H.Boeck, M.Villa, Monte Carlo Core calculations for a mixed TRIGA HEU/LEU Core, Research Reactor Fuel Management, ISBN: 978-92-95064-04-1, Hamburg, Germany, 2008

32. T.Stummer, M. Villa, H.Boeck, R.Khan, MCNP Calculations Supporting The Start-up Of The New Core At The TRIGA VIENNA, 22nd International Conference Nuclear Energy for New Europe (NENE2013), ISBN: 978.961-6207-36-2, Ljubljana, Slovenia, 2013

33. I.Ievdin, C. Landman, D. Trybushnyi, I.Hasemann, J.Paelser-Sauer, Results Guide for the models in the JRodos Emergency Model Chain, Version 2.1., Karlsruhe, Germany, 2017

34. LASAT, 3.4, Ingenieurbüro Janicke, Gesellschaft für Umweltphysik, Überlingen, Germany, 2017

Die approbierte gedruckte Originalversion dieser Dissertation ist an der TU Wien Bibliothek verfügbar.
The approved original version of this doctoral thesis is available in print at TU Wien Bibliothek.
TU Bibliothek Your knowledge hub WIEN

35. Vergleich aktuell eingesetzter Modelle zur Beschreibung der atmosphärischen Ausbreitung radioaktiver Stoffe, BfS-SCHR-58/16, urn:nbn:de:0221-2016022414011, Salzgitter, Germany, 2016

Die approbierte gedruckte Originalversion dieser Dissertation ist an der TU Wien Bibliothek verfügbar.
The approved original version of this doctoral thesis is available in print at TU Wien Bibliothek.
TU Bibliothek Your knowledge hub WIEN

B Appendix

B.1 Figures

B.1.1 1 Fuel element exposure graphical results

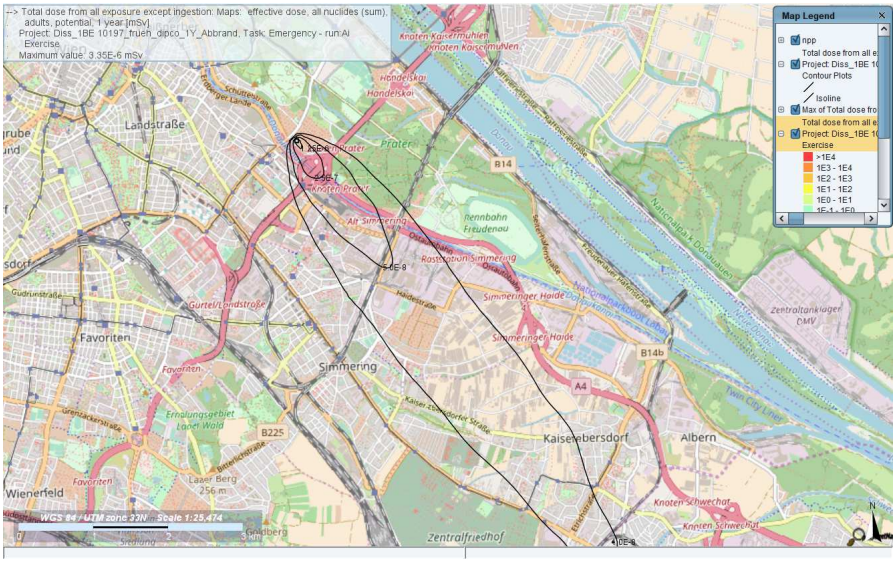

Figure B.1: 1 fuel element exposed, average spring day scenario, 1 year burnup

Die approbierte gedruckte Originalversion dieser Dissertation ist an der TU Wien Bibliothek verfügbar.
The approved original version of this doctoral thesis is available in print at TU Wien Bibliothek.
TU Bibliothek Your knowledge hub WIEN

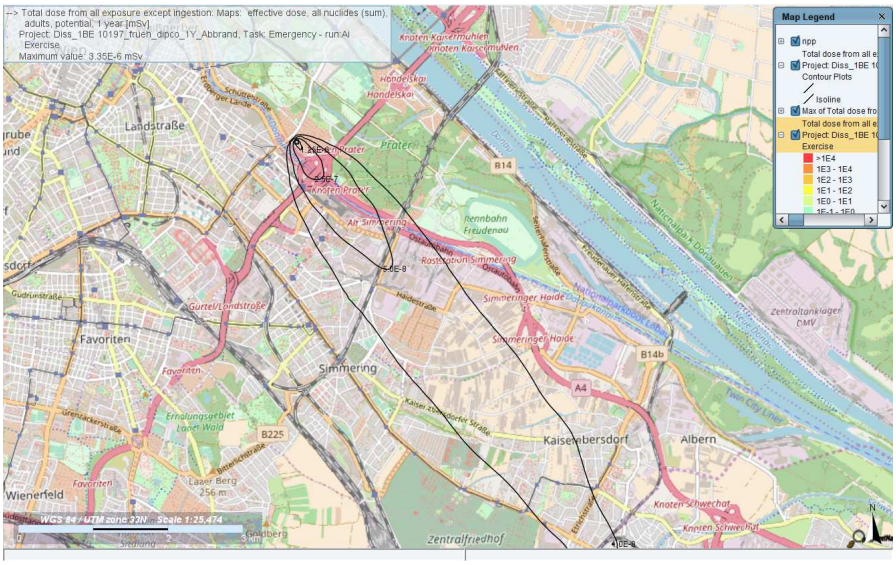

Figure B.2: 1 fuel element exposed, average summer day scenario, 1 year burnup

Figure B.3: 1 fuel element exposed, average autumn day scenario, 1 year burnup

Die approbierte gedruckte Originalversion dieser Dissertation ist an der TU Wien Bibliothek verfügbar.
The approved original version of this doctoral thesis is available in print at TU Wien Bibliothek.
TU Bibliothek Your knowledge hub WIEN

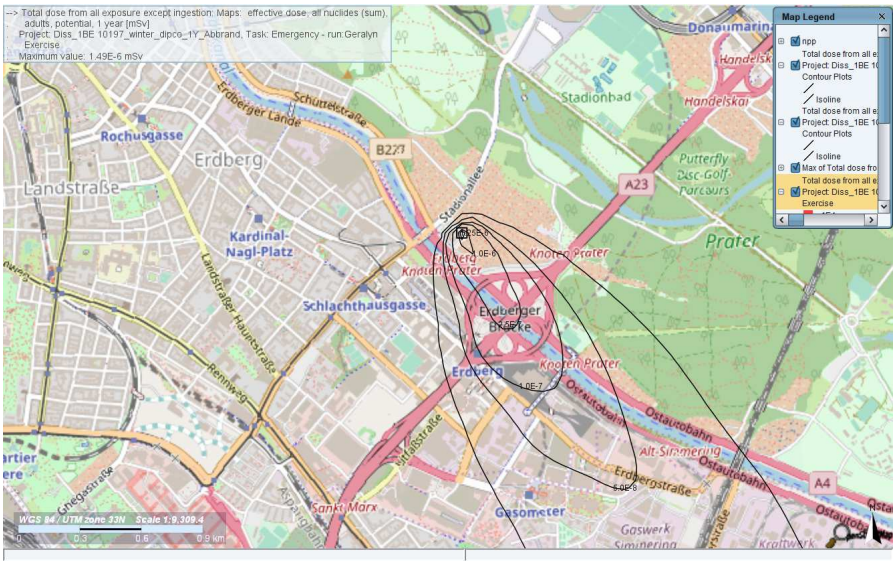

Figure B.4: 1 fuel element exposed, average winter day scenario, 1 year burnup

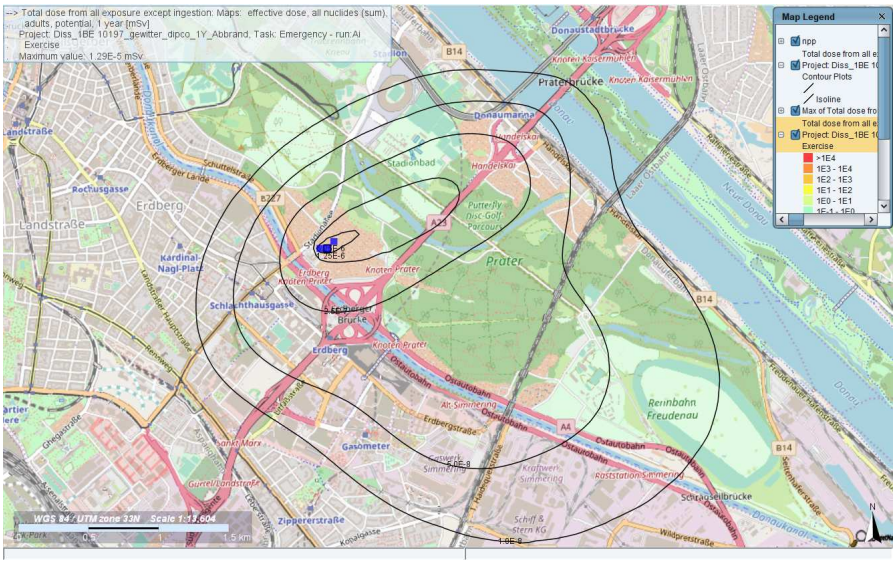

Figure B.5: 1 fuel element exposed, thunderstorm day scenario, 1 year burnup

Die approbierte gedruckte Originalversion dieser Dissertation ist an der TU Wien Bibliothek verfügbar.
The approved original version of this doctoral thesis is available in print at TU Wien Bibliothek.
TU Bibliothek Your knowledge hub WIEN

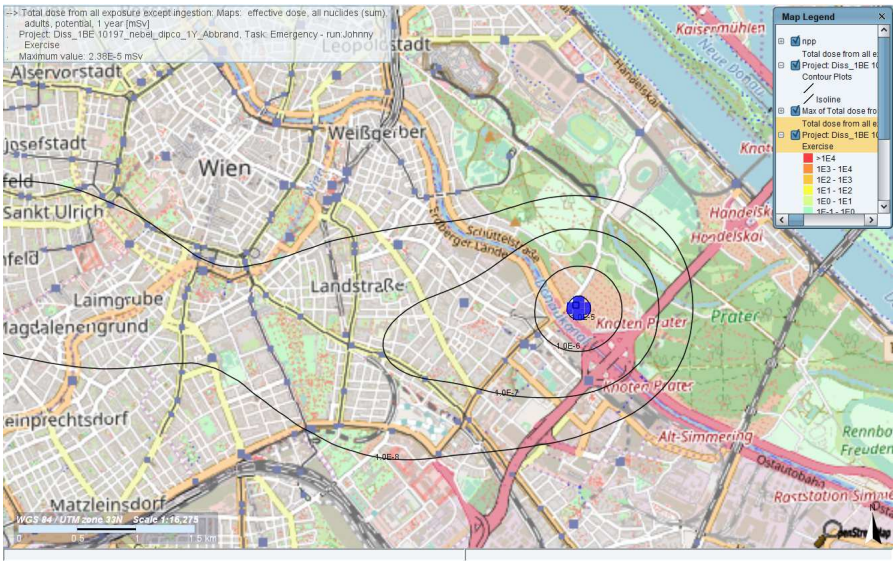

Figure B.6: 1 fuel element exposed, foggy day scenario, 1 year burnup

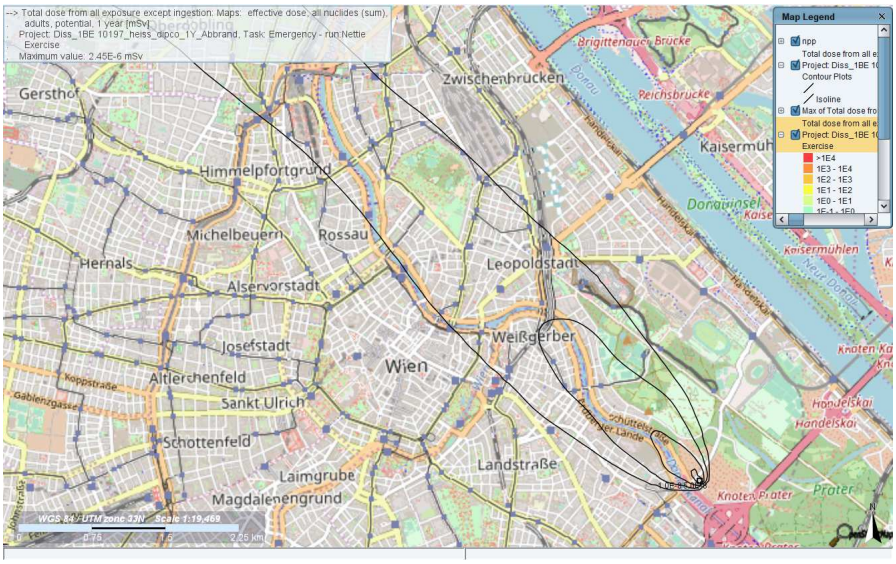

Figure B.7: 1 fuel element exposed, hot day scenario, 1 year burnup

Die approbierte gedruckte Originalversion dieser Dissertation ist an der TU Wien Bibliothek verfügbar.
The approved original version of this doctoral thesis is available in print at TU Wien Bibliothek.
TU Bibliothek Your knowledge hub WIEN

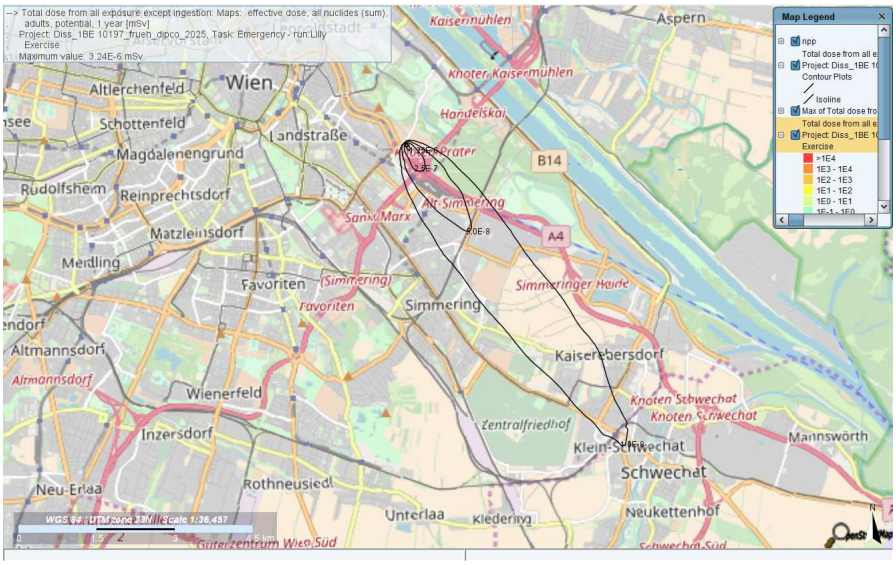

Figure B.8: 1 fuel element exposed, average spring day scenario, 11 years burnup

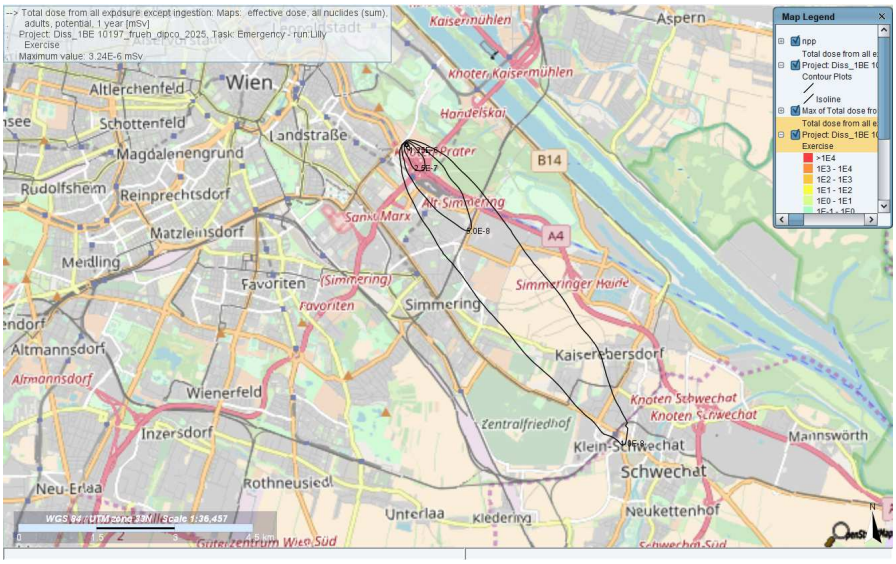

Figure B.9: 1 fuel element exposed, average summer day scenario, 11 years burnup

Die approbierte gedruckte Originalversion dieser Dissertation ist an der TU Wien Bibliothek verfügbar.
The approved original version of this doctoral thesis is available in print at TU Wien Bibliothek.
TU Bibliothek Your knowledge hub WIEN

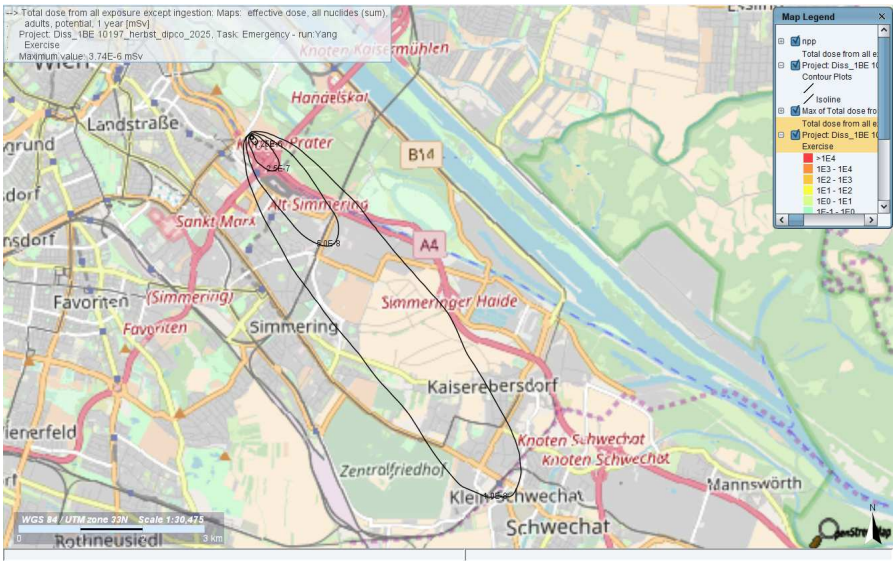

Figure B.10: 1 fuel element exposed, average autumn day scenario, 11 years burnup

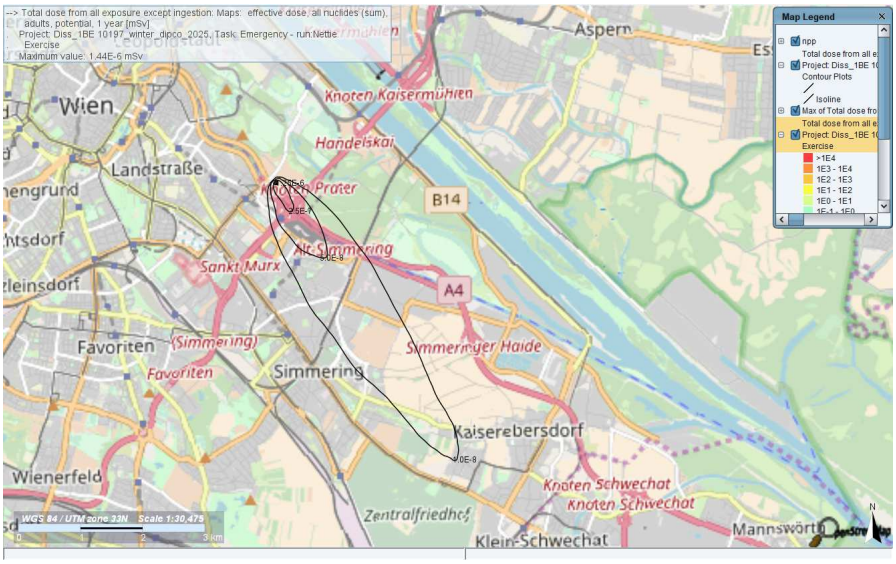

Figure B.11: 1 fuel element exposed, average winter day scenario, 11 years burnup

Die approbierte gedruckte Originalversion dieser Dissertation ist an der TU Wien Bibliothek verfügbar.
The approved original version of this doctoral thesis is available in print at TU Wien Bibliothek.

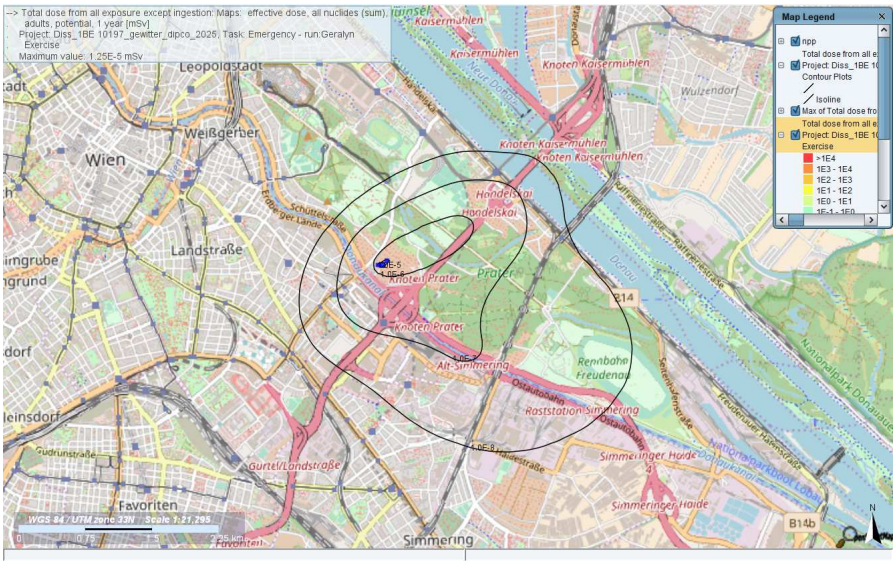

Figure B.12: 1 fuel element exposed, thunderstorm day scenario, 11 years burnup

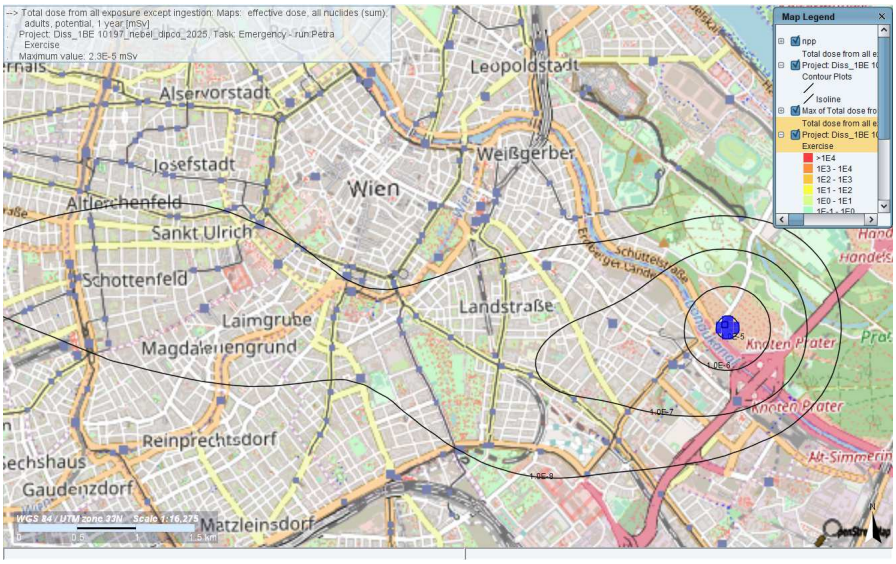

Figure B.13: 1 fuel element exposed, foggy day scenario, 11 years burnup

Die approbierte gedruckte Originalversion dieser Dissertation ist an der TU Wien Bibliothek verfügbar.
The approved original version of this doctoral thesis is available in print at TU Wien Bibliothek.

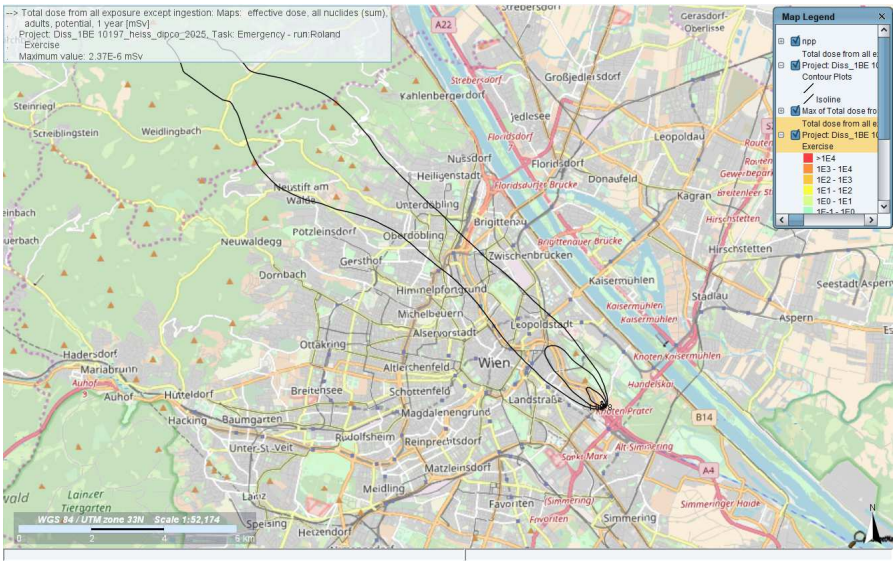

Figure B.14: 1 fuel element exposed, hot day scenario, 11 years burnup

B.1.2 All fuel elements exposed, graphical results

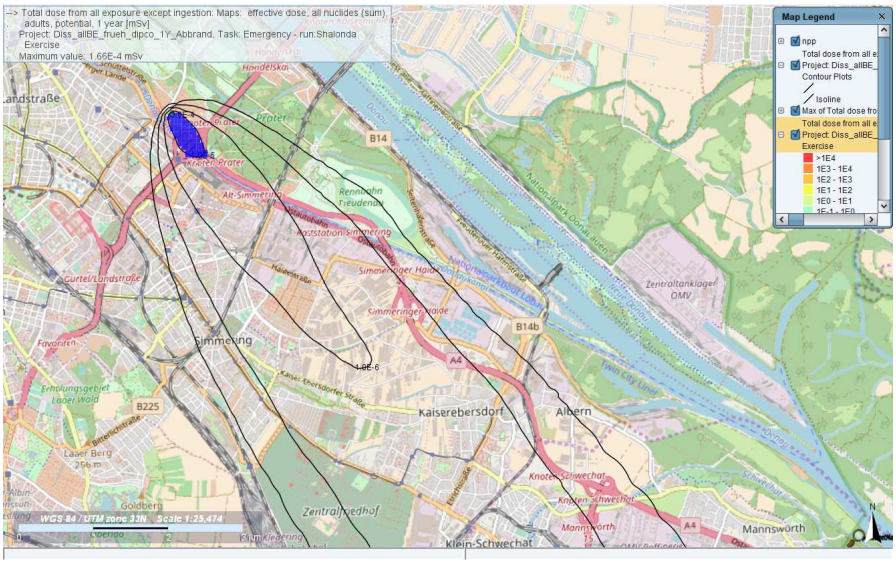

Figure B.15: All fuel elements exposed, average spring day scenario, 1 year burnup

Die approbierte gedruckte Originalversion dieser Dissertation ist an der TU Wien Bibliothek verfügbar.
The approved original version of this doctoral thesis is available in print at TU Wien Bibliothek.
TU Bibliothek Your knowledge hub WIEN

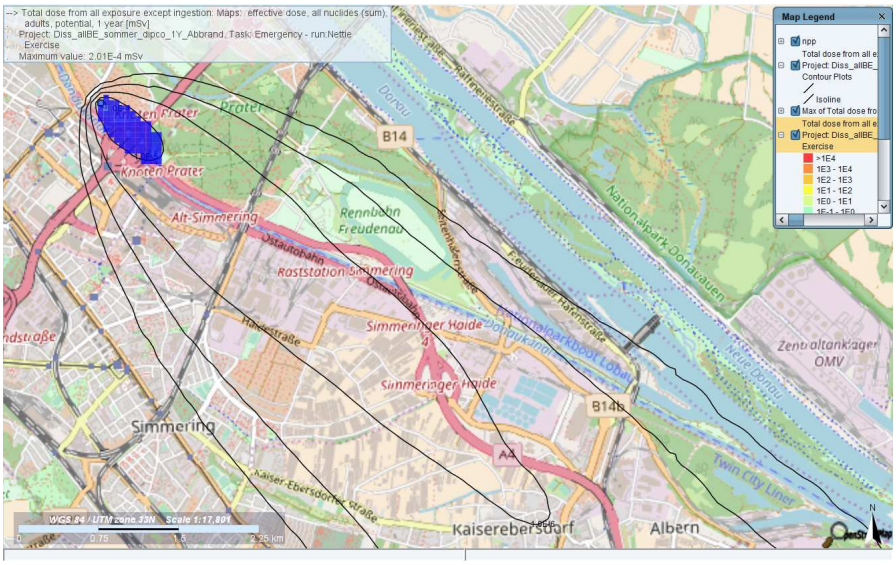

Figure B.16: All fuel elements exposed, average summer day scenario, 1 year burnup

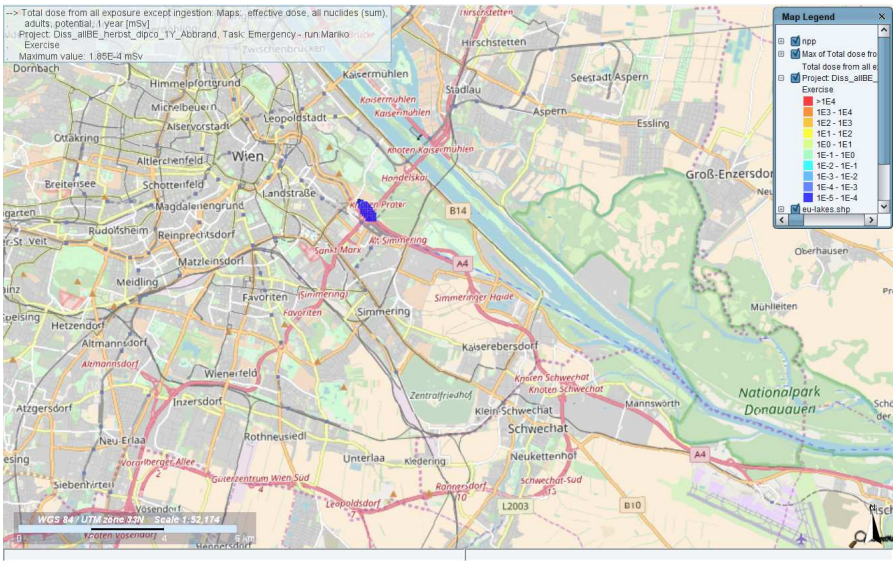

Figure B.17: All fuel elements exposed, average autumn day scenario, 1 year burnup

Die approbierte gedruckte Originalversion dieser Dissertation ist an der TU Wien Bibliothek verfügbar.
The approved original version of this doctoral thesis is available in print at TU Wien Bibliothek.
TU Bibliothek Your knowledge hub WIEN

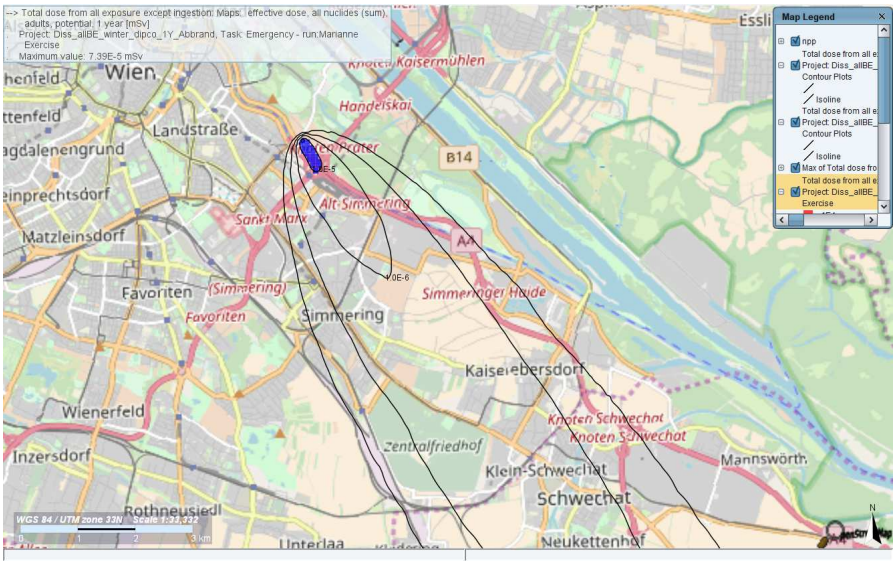

Figure B.18: All fuel elements exposed, average winter day scenario, 1 year burnup

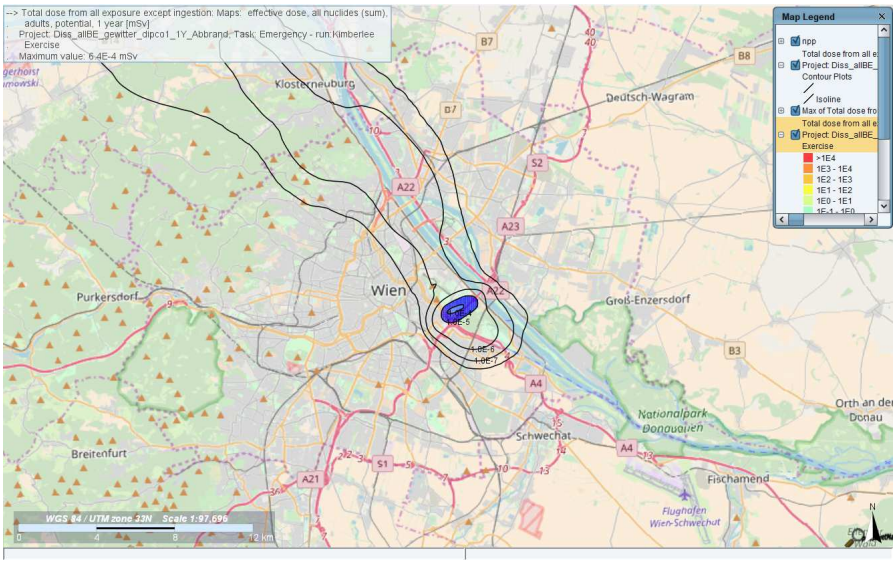

Figure B.19: All fuel elements exposed, thunderstorm day scenario, 1 year burnup

Die approbierte gedruckte Originalversion dieser Dissertation ist an der TU Wien Bibliothek verfügbar.
The approved original version of this doctoral thesis is available in print at TU Wien Bibliothek.
TU Bibliothek Your knowledge hub WIEN

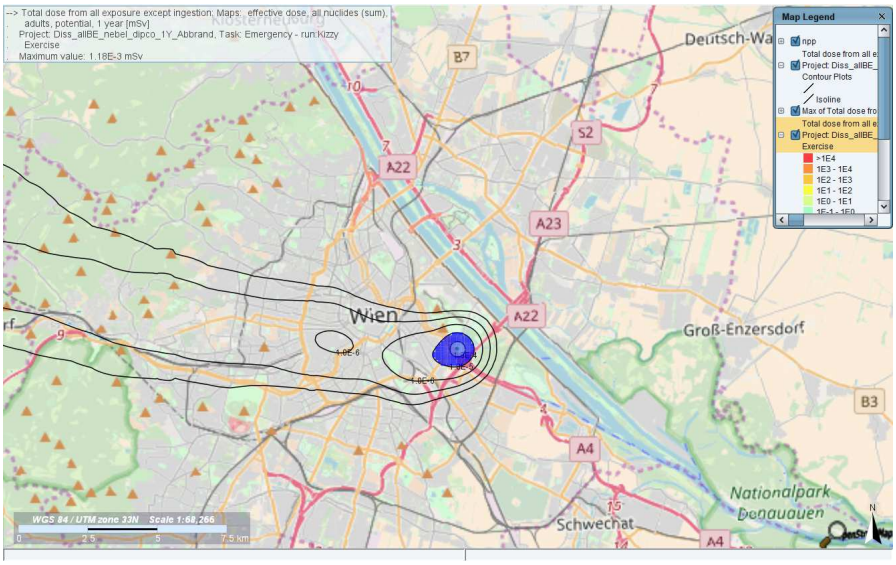

Figure B.20: All fuel elements exposed, foggy day scenario, 1 year burnup

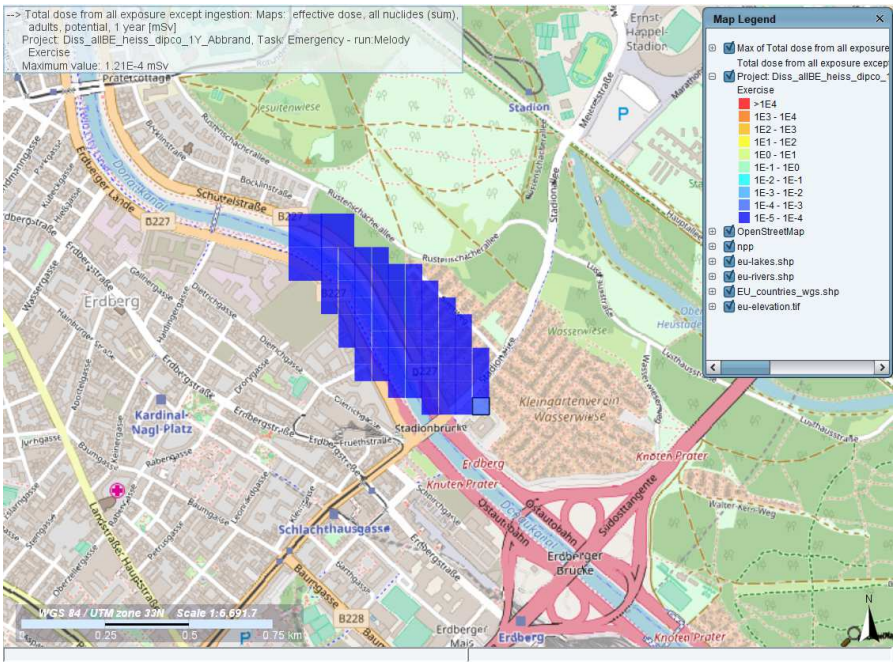

Figure B.21: All fuel elements exposed, hot day scenario, 1 year burnup

Die approbierte gedruckte Originalversion dieser Dissertation ist an der TU Wien Bibliothek verfügbar.
The approved original version of this doctoral thesis is available in print at TU Wien Bibliothek.
TU Bibliothek Your knowledge hub WIEN

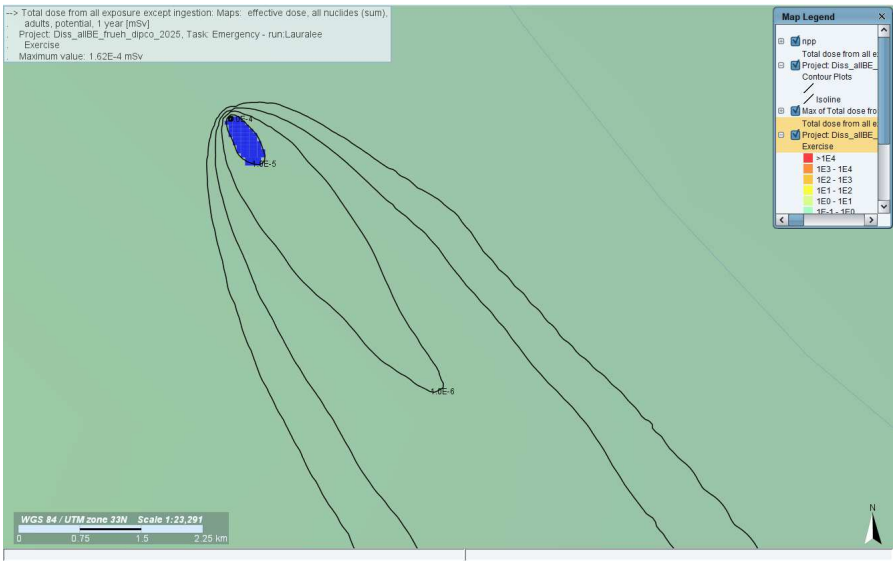

Figure B.22: All fuel elements exposed, average spring day scenario, 11 years burnup

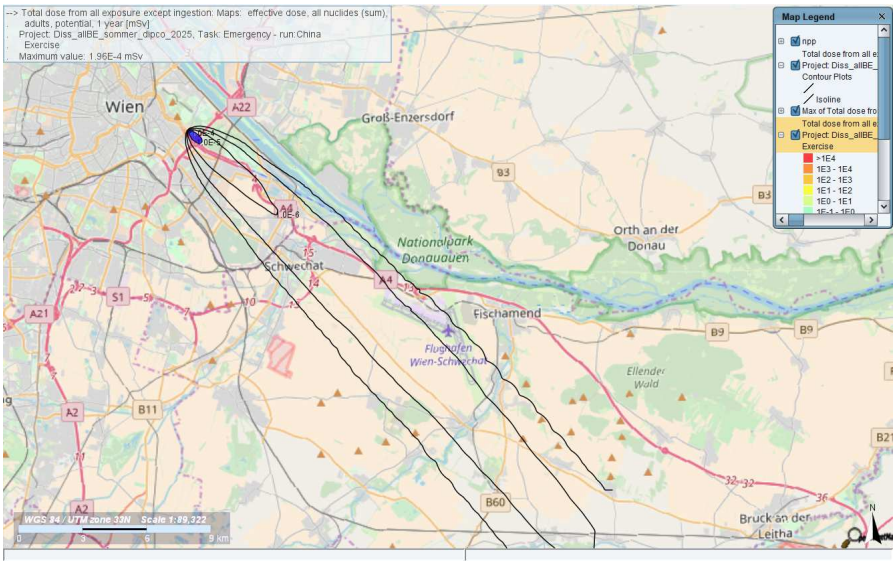

Figure B.23: All fuel elements exposed, average summer day scenario, 11 years burnup

Die approbierte gedruckte Originalversion dieser Dissertation ist an der TU Wien Bibliothek verfügbar.
The approved original version of this doctoral thesis is available in print at TU Wien Bibliothek.
TU Bibliothek Your knowledge hub WIEN

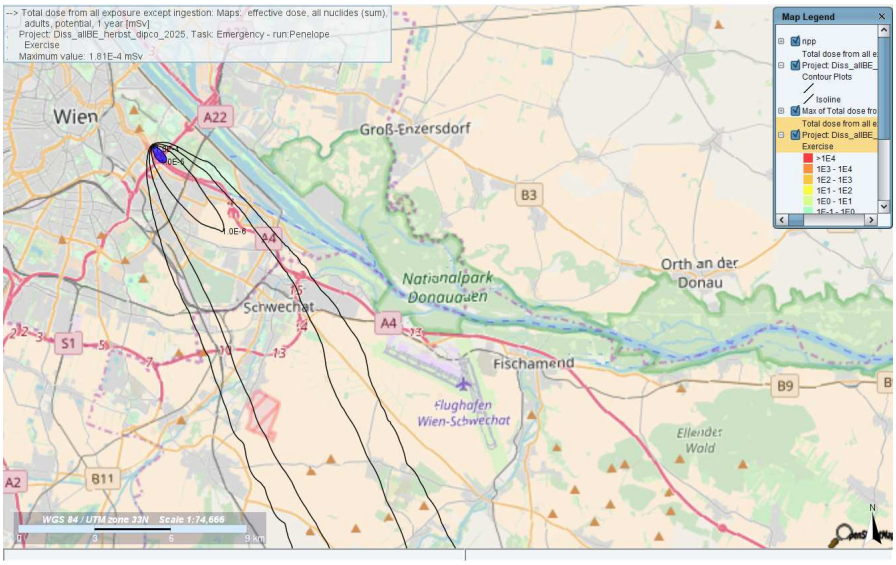

Figure B.24: All fuel elements exposed, average autumn day scenario, 11 years burnup

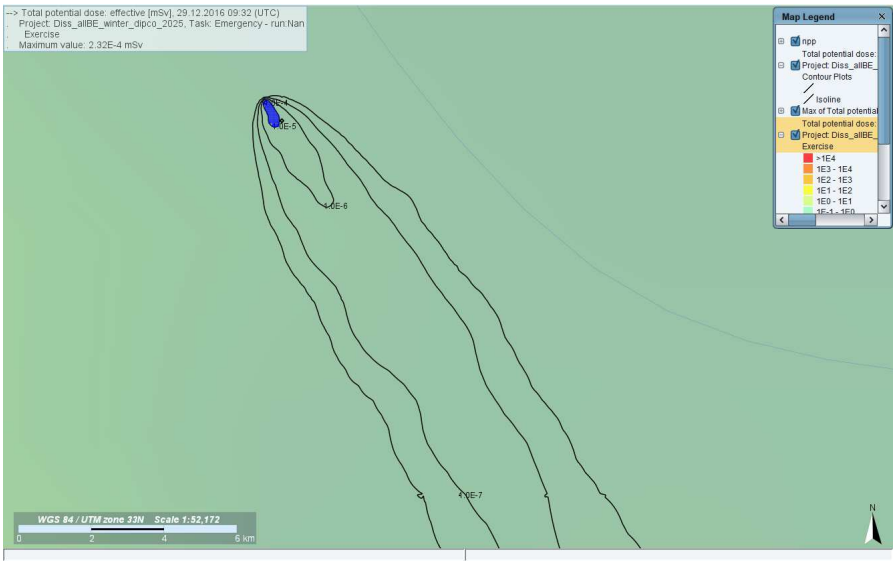

Figure B.25: All fuel elements exposed, average winter day scenario, 11 years burnup

Die approbierte gedruckte Originalversion dieser Dissertation ist an der TU Wien Bibliothek verfügbar.
The approved original version of this doctoral thesis is available in print at TU Wien Bibliothek.
TU Bibliothek Your knowledge hub WIEN

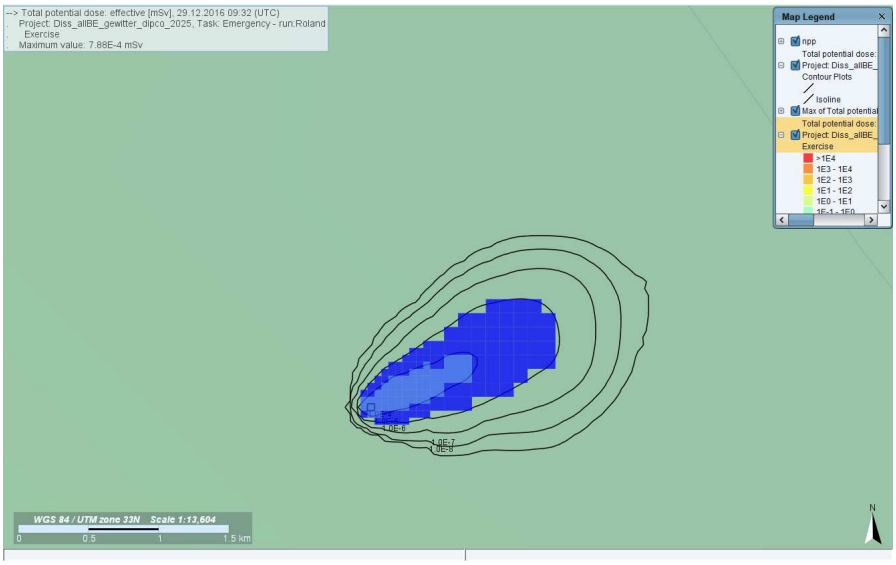

Figure B.26: All fuel elements exposed, thunderstorm day scenario, 11 years burnup

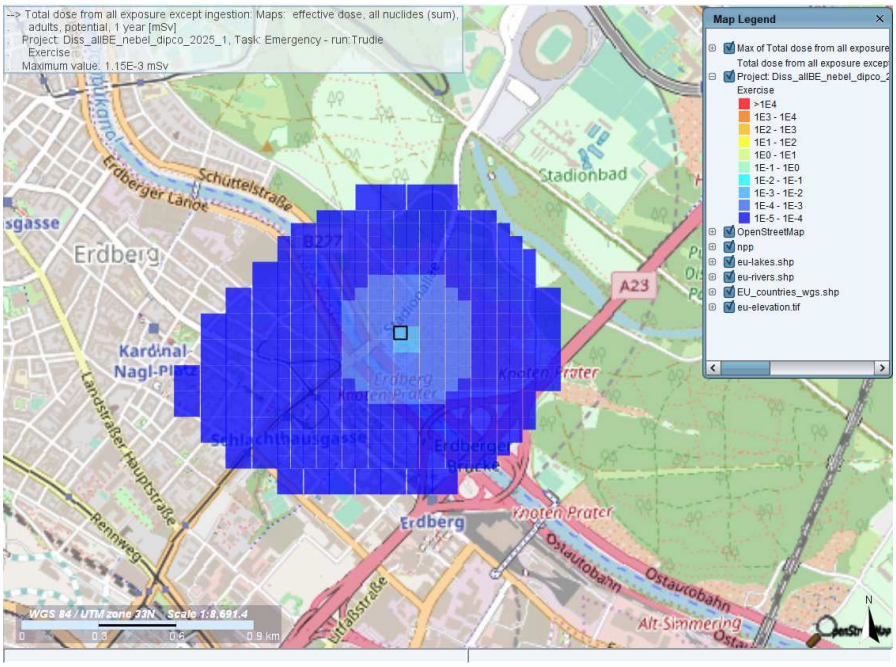

Figure B.27: All fuel elements exposed, foggy day scenario, 11 years burnup

Die approbierte gedruckte Originalversion dieser Dissertation ist an der TU Wien Bibliothek verfügbar.
The approved original version of this doctoral thesis is available in print at TU Wien Bibliothek.
TU Bibliothek Your knowledge hub WIEN

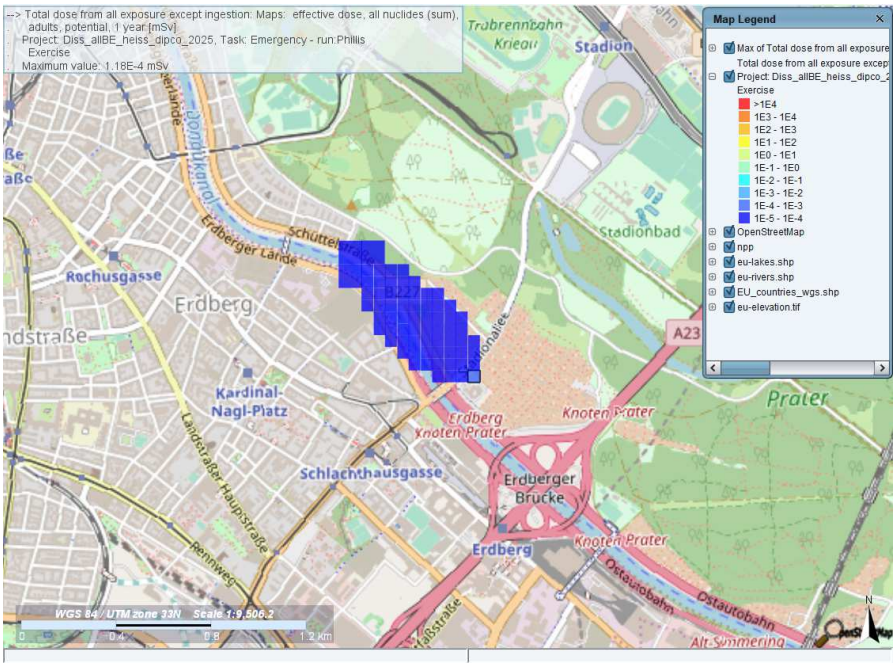

Figure B.28: All fuel elements exposed, hot day scenario, 11 years burnup

Die approbierte gedruckte Originalversion dieser Dissertation ist an der TU Wien Bibliothek verfügbar.
The approved original version of this doctoral thesis is available in print at TU Wien Bibliothek.
TU Bibliothek Your knowledge hub WIEN

B.1.3 Small airplane crash, graphical results

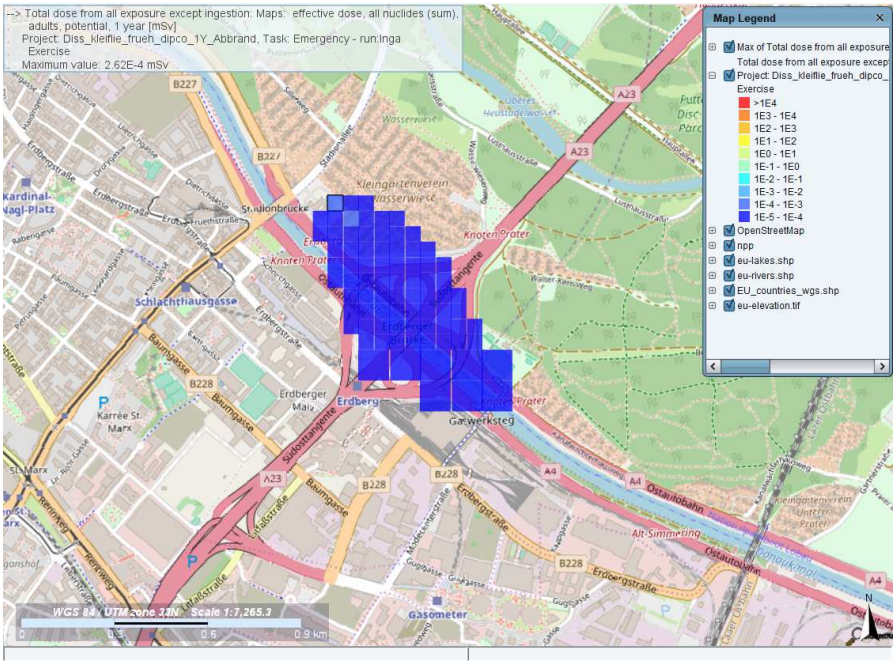

Figure B.29: Small airplane crash, average spring day scenario, 1 year burnup

Die approbierte gedruckte Originalversion dieser Dissertation ist an der TU Wien Bibliothek verfügbar.
The approved original version of this doctoral thesis is available in print at TU Wien Bibliothek.
TU Bibliothek Your knowledge hub WIEN

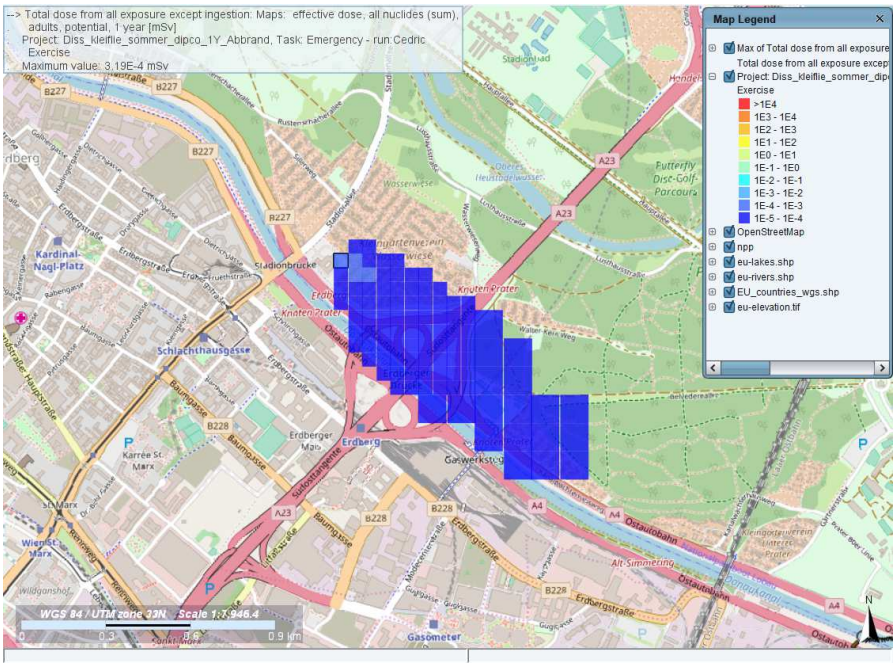

Figure B.30: Small airplane crash, average summer day scenario, 1 year burnup

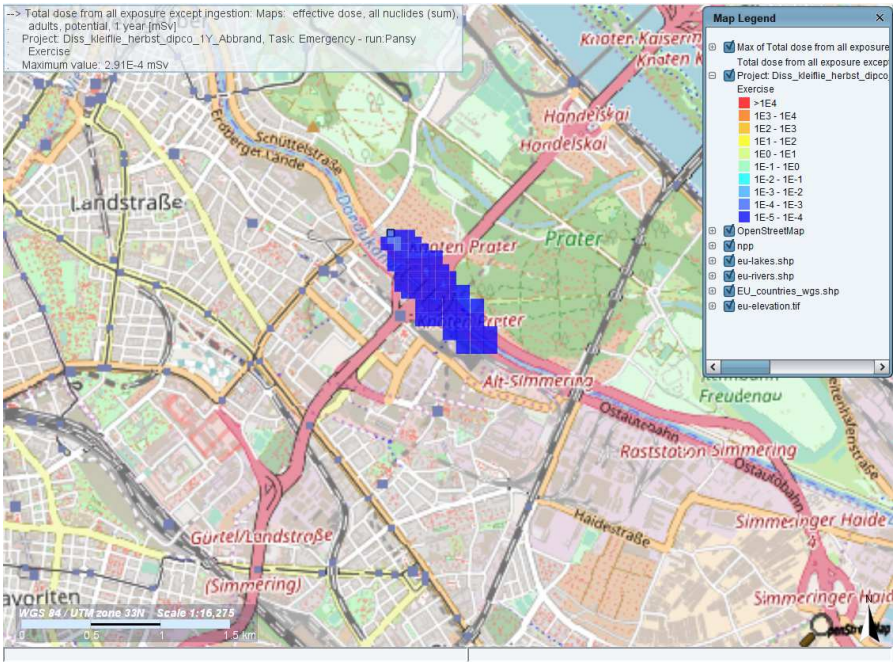

Figure B.31: Small airplane crash, average autumn day scenario, 1 year burnup

Die approbierte gedruckte Originalversion dieser Dissertation ist an der TU Wien Bibliothek verfügbar.
The approved original version of this doctoral thesis is available in print at TU Wien Bibliothek.
TU Bibliothek Your knowledge hub WIEN

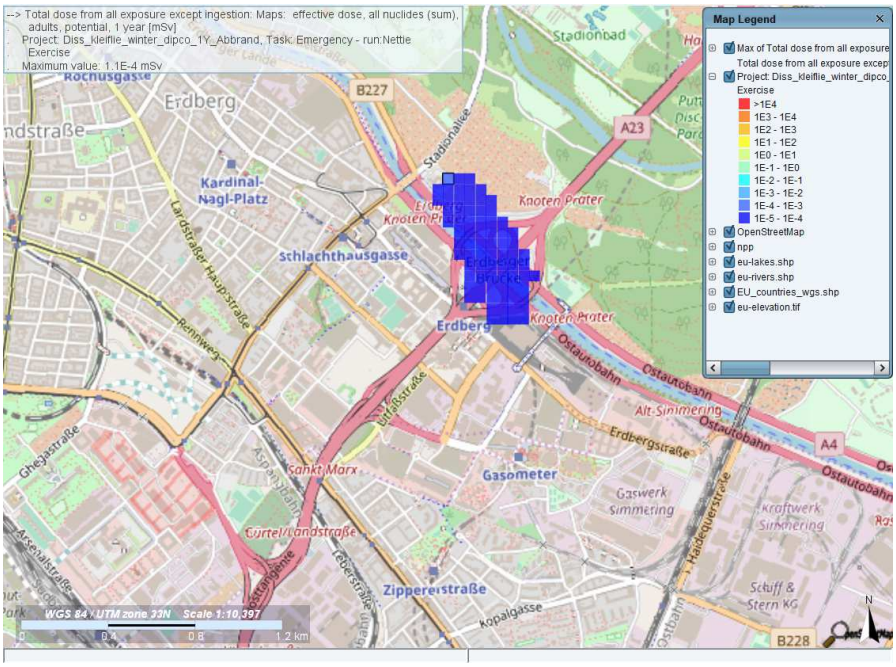

Figure B.32: Small airplane crash, average winter day scenario, 1 year burnup

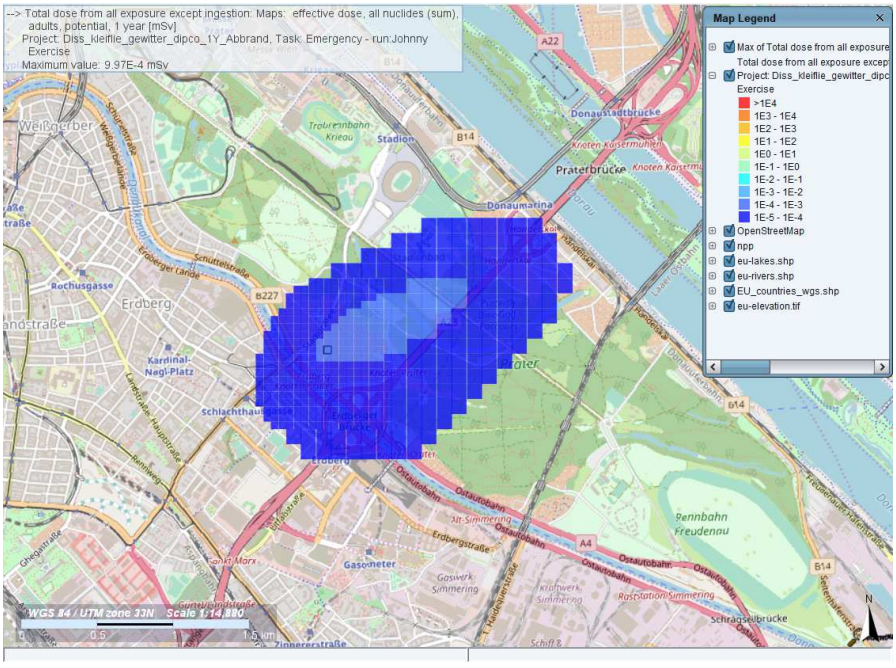

Figure B.33: Small airplane crash, thunderstorm day scenario, 1 year burnup

Die approbierte gedruckte Originalversion dieser Dissertation ist an der TU Wien Bibliothek verfügbar.
The approved original version of this doctoral thesis is available in print at TU Wien Bibliothek.
TU Bibliothek Your knowledge hub WIEN

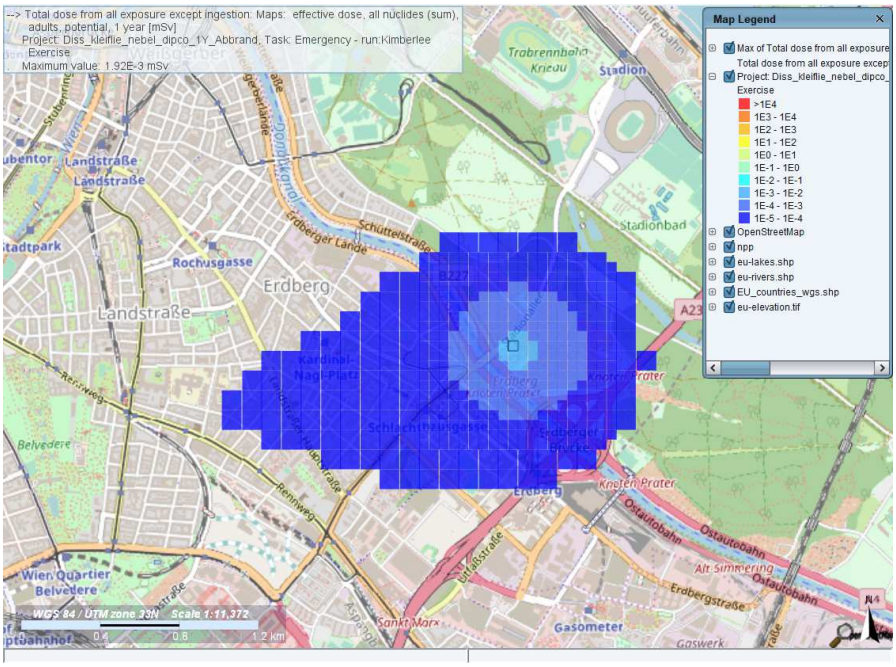

Figure B.34: Small airplane crash, foggy day scenario, 1 year burnup

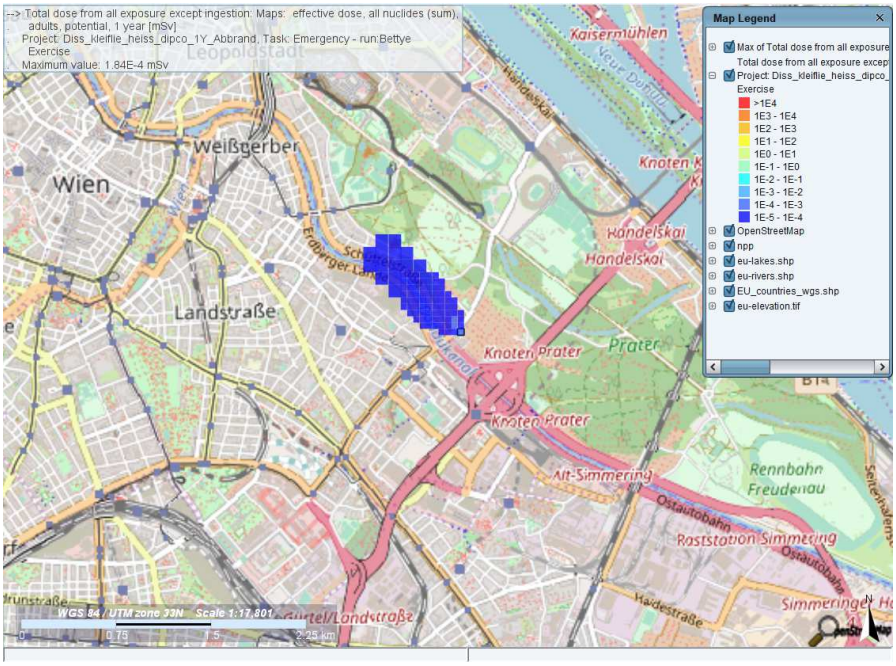

Figure B.35: Small airplane crash, hot day scenario, 1 year burnup

Die approbierte gedruckte Originalversion dieser Dissertation ist an der TU Wien Bibliothek verfügbar.
The approved original version of this doctoral thesis is available in print at TU Wien Bibliothek.
TU Bibliothek Your knowledge hub WIEN

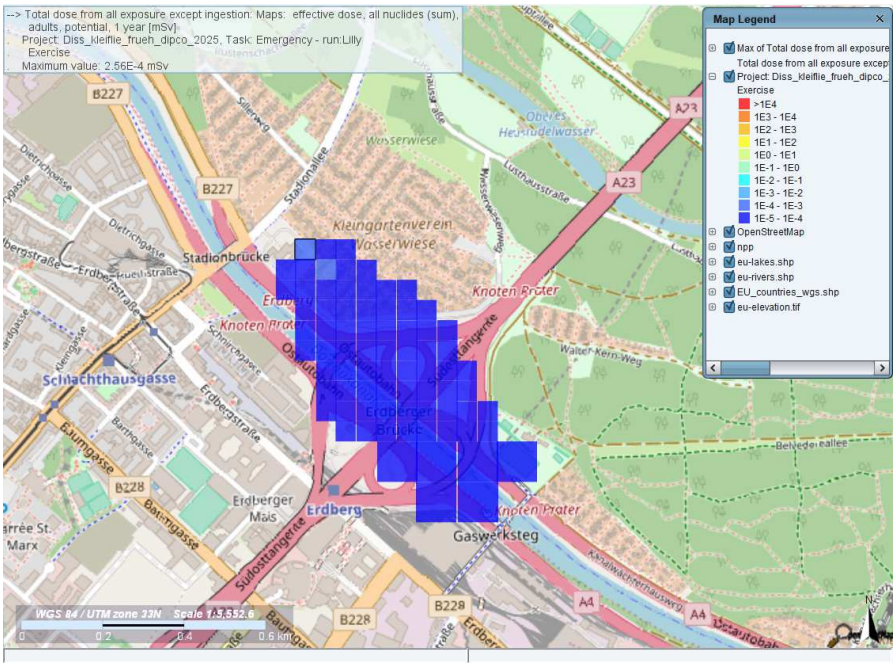

Figure B.36: Small airplane crash, average spring day scenario, 11 years burnup

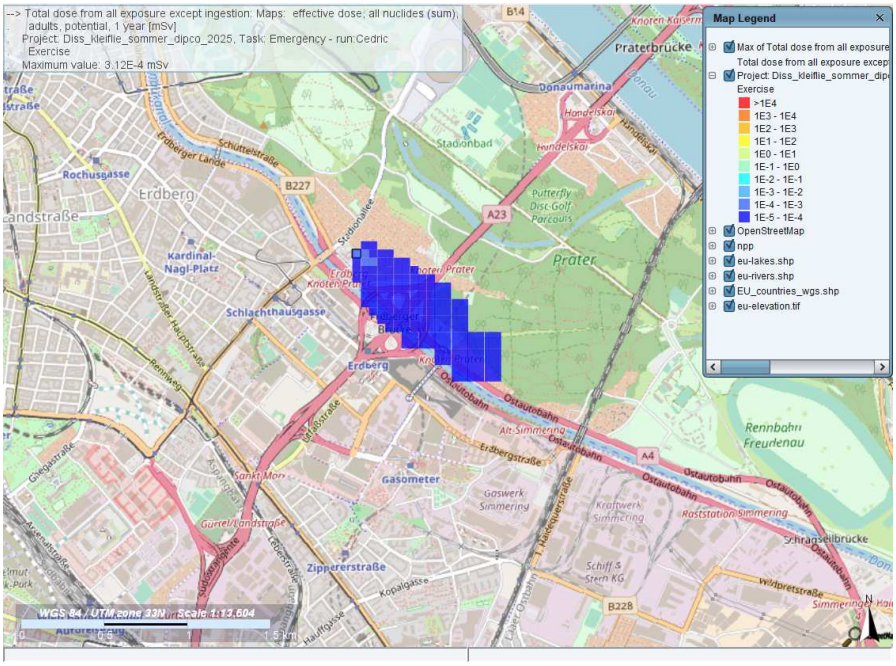

Figure B.37: Small airplane crash, average summer day scenario, 11 years burnup

Die approbierte gedruckte Originalversion dieser Dissertation ist an der TU Wien Bibliothek verfügbar.
The approved original version of this doctoral thesis is available in print at TU Wien Bibliothek.
TU Bibliothek Your knowledge hub WIEN

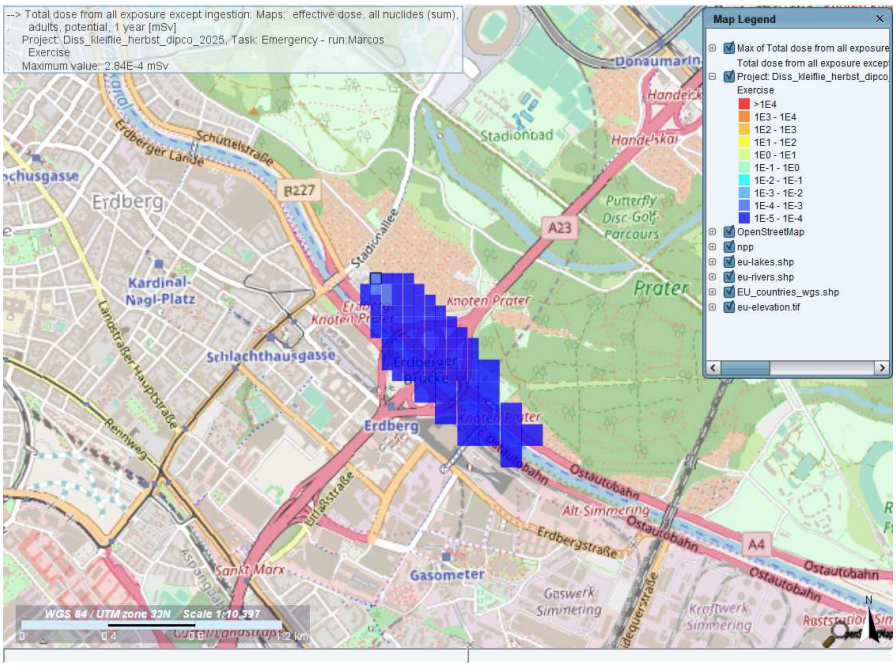

Figure B.38: Small airplane crash, average autumn day scenario, 11 years burnup

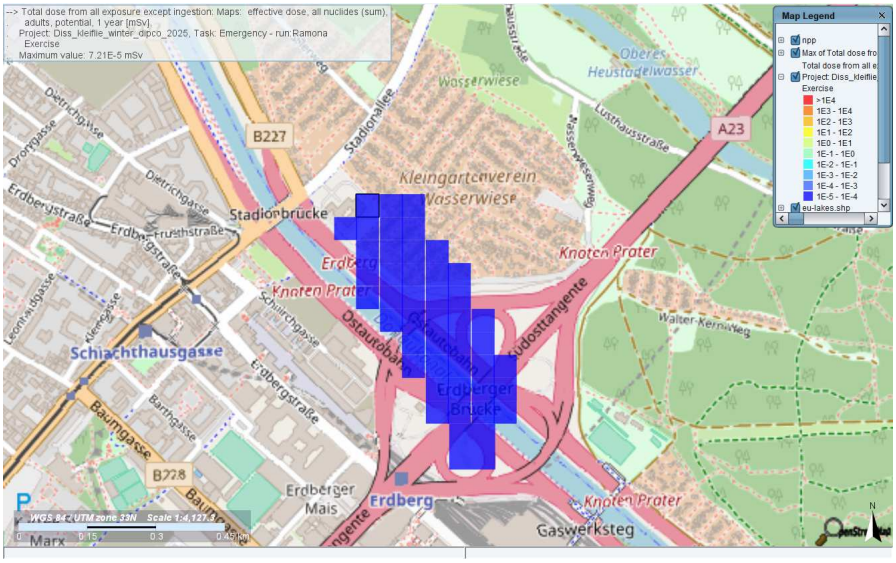

Figure B.39: Small airplane crash, average winter day scenario, 11 years burnup

Die approbierte gedruckte Originalversion dieser Dissertation ist an der TU Wien Bibliothek verfügbar.
The approved original version of this doctoral thesis is available in print at TU Wien Bibliothek.
TU Bibliothek Your knowledge hub WIEN

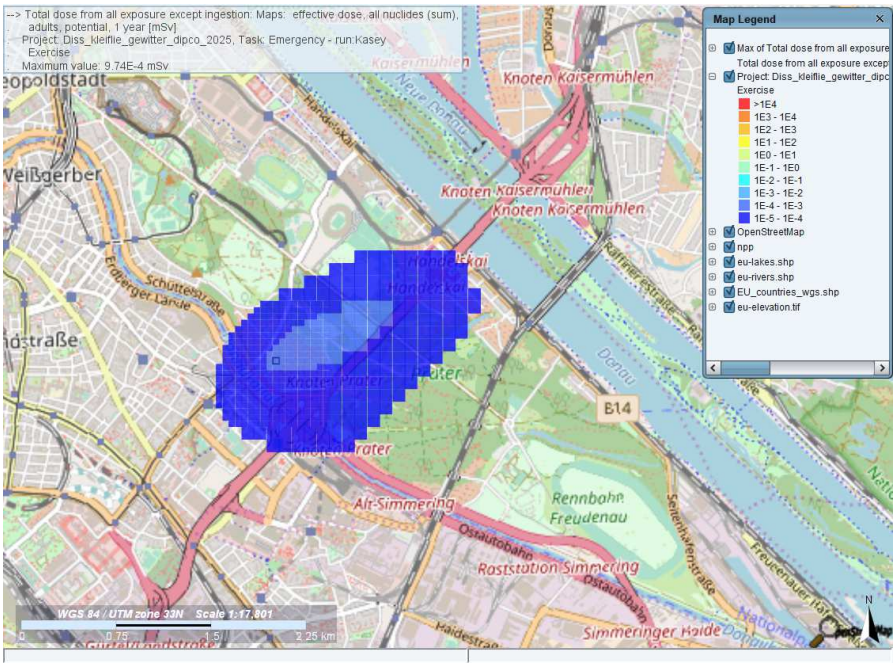

Figure B.40: Small airplane crash, thunderstorm day scenario, 11 years burnup

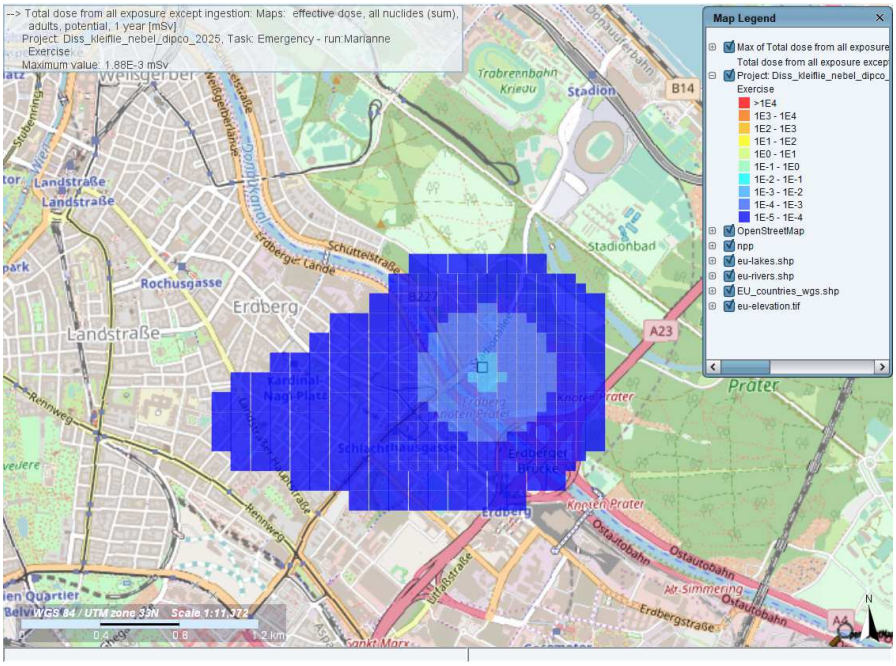

Figure B.41: Small airplane crash, foggy day scenario, 11 years burnup

Die approbierte gedruckte Originalversion dieser Dissertation ist an der TU Wien Bibliothek verfügbar.
The approved original version of this doctoral thesis is available in print at TU Wien Bibliothek.
TU Bibliothek Your knowledge hub WIEN

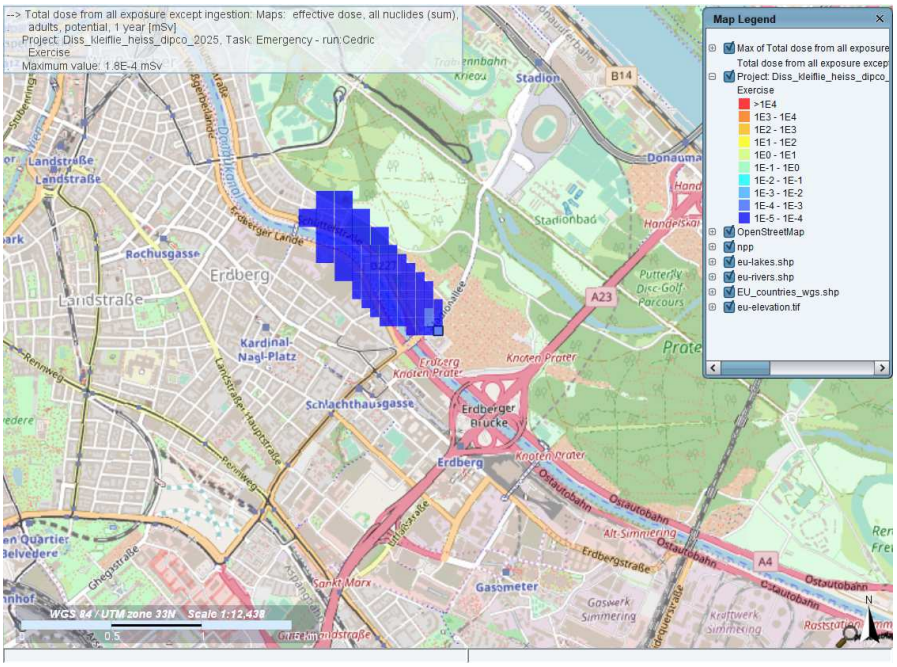

Figure B.42: Small airplane crash, hot day scenario, 11 years burnup

B.2 Tables

10198	Activity[Bq]	10198	Activity[Bq]
C-14	4.42E+05	H-3	3.86E+08
P-32	1.31E+04	Se-79	4.29E+05
P-33	1.81E+01	Kr-85	1.05E+10
S-35	2.58E+05	Rb-86	2.86E+04
Sc-47	5.13E-15	Sr-89	2.62E+10
Cr-51	5.44E+08	Sr-90	9.40E+10
Mn-54	1.74E+09	Y9-0	9.41E+10
Fe-55	2.63E+10	Y9-1	4.18E+10
Fe-59	4.05E+07	Zr-93	2.20E+06
Co-58	6.35E+08	Nb-93M	3.48E+05
Co-60	4.65E+07	Zr-95	5.29E+10
Ni-59	9.87E+06	Nb-95	9.96E+10
Ni-63	1.19E+09	Nb-95M	3.92E+08

Continued on next page

Die approbierte gedruckte Originalversion dieser Dissertation ist an der TU Wien Bibliothek verfügbar.
The approved original version of this doctoral thesis is available in print at TU Wien Bibliothek.
TU Bibliothek Your knowledge hub WIEN

Table B.1 – *Continued from previous page*

10198	**Activity[Bq]**	**10198**	**Activity[Bq]**
Tl-207	1.93E+01	Tc-99	1.47E+07
Tl-208	1.84E+02	Rh-102	1.39E+04
Pb-211	1.93E+01	Ru-103	9.94E+09
Pb-212	5.11E+02	Rh-103M	8.96E+09
Bi-211	1.93E+01	Ru-106	2.88E+10
Bi-212	5.11E+02	Rh-106	2.88E+10
Po-211	5.41E-02	Pd-107	1.70E+04
Po-212	3.28E+02	Ag-109M	3.97E-02
Po-215	1.93E+01	Ag-110	3.06E+04
Po-216	5.11E+02	Ag-110M	2.30E+06
Rn-219	1.93E+01	Ag-111	1.04E+02
Rn-220	5.11E+02	Cd-113M	1.31E+07
Fr-223	2.66E-01	In-114	8.21E+02
Ra-223	1.93E+01	In-114M	8.58E+02
Ra-224	5.11E+02	Cd-115M	7.68E+06
Ac-227	1.93E+01	In-115M	5.40E+02
Th-227	1.90E+01	Sn-119M	1.34E+07
Th-228	5.10E+02	Sn-121M	8.81E+04
Th-230	4.02E-01	Sn-123	1.38E+08
Th-231	2.93E+06	Te-123M	2.66E+02
Th-234	1.89E+06	Sb-124	4.58E+05
Pa-231	2.80E+02	Sn-125	3.26E+03
Pa-233	2.33E+04	Sb-125	3.59E+09
Pa-234M	1.89E+06	Te-125M	8.72E+08
Pa-234	2.46E+03	Sn-126	4.05E+05
U-232	9.81E+02	Sb-126	6.09E+04
U-233	8.47E+00	Sb-126M	4.05E+05
U-234	1.25E+04	Sb-127	1.94E-05
U-235	2.93E+06	Te-127	4.15E+08
U-236	4.95E+05	Te-127M	4.24E+08
U-237	3.40E+03	Te-129	1.33E+08

Continued on next page

Die approbierte gedruckte Originalversion dieser Dissertation ist an der TU Wien Bibliothek verfügbar.
The approved original version of this doctoral thesis is available in print at TU Wien Bibliothek.
TU Bibliothek Your knowledge hub WIEN

Table B.1 – *Continued from previous page*

10198	**Activity[Bq]**	**10198**	**Activity[Bq]**
U-238	1.89E+06	Te-129M	2.05E+08
U-240	5.12E-09	I-129	2.41E+04
Np-235	6.19E+00	I-131	3.57E+04
Np-237	2.33E+04	Xe-131M	2.50E+05
Np-238	6.97E+00	Te-132	7.27E-07
Np-239	5.89E+00	I-132	7.50E-07
Np-240M	5.12E-09	Cs-132	4.63E-03
Pu-236	7.41E+02	Xe-133	1.26E+01
Pu-237	1.56E+01	Cs-134	2.10E+09
Pu-238	3.97E+06	Cs-135	1.19E+06
Pu-239	1.61E+08	Cs-136	9.85E+04
Pu-240	1.02E+07	Ba-136M	1.62E+04
Pu-241	1.36E+08	Cs-137	9.82E+10
Pu-242	3.07E+01	Ba-137M	9.29E+10
Pu-243	4.37E-15	Ba-140	3.30E+07
Am-241	6.06E+05	La-140	3.80E+07
Am-242M	1.40E+03	Ce-141	1.04E+10
Am-242	1.39E+03	Pr-143	6.21E+07
Am-243	5.89E+00	Ce-144	2.82E+11
Cm-242	4.09E+05	Pr-144	2.82E+11
Cm-243	1.31E+01	Pr-144M	3.39E+09
Cm-244	1.00E+01	Pm-146	8.58E+04
		Nd-147	2.47E+06
		Pm-147	1.83E+11
		Pm-148	3.51E+06
		Pm-148M	6.22E+07
		Sm-151	2.01E+09
		Eu-152	2.02E+07
		Gd-153	3.70E+05
		Eu-154	1.55E+08
		Eu-155	2.23E+09

Continued on next page

Die approbierte gedruckte Originalversion dieser Dissertation ist an der TU Wien Bibliothek verfügbar.
The approved original version of this doctoral thesis is available in print at TU Wien Bibliothek.
TU Bibliothek Your knowledge hub WIEN

Table B.1 – *Continued from previous page*

10198	**Activity[Bq]**	**10198**	**Activity[Bq]**
		Eu-156	5.41E+05
		Tb-160	1.21E+05
		Tb-161	1.72E-01
		Dy-166	5.42E-12
		Ho-166	8.08E-12

Table B.1: Inventory of Fuel element 10198, left side fuel element activation, actinides and daughters, right side fission products

9212	**Activity[Bq]**	**9212**	**Activity[Bq]**
C-14	1.49E+05	H-3	1.38E+08
P-32	1.16E+04	Se-79	1.46E+05
P-33	1.60E+01	Kr-85	3.79E+09
S-35	1.84E+05	Rb-86	1.41E+04
Cr-51	4.80E+08	Sr-89	2.32E+10
Mn-54	8.95E+08	Sr-90	3.28E+10
Fe-55	1.11E+10	Y9-0	3.28E+10
Fe-59	3.54E+07	Y9-1	3.61E+10
Co-58	5.07E+08	Zr-93	7.50E+05
Co-60	1.74E+07	Nb-93M	8.83E+04
Ni-59	3.34E+06	Zr-95	4.45E+10
Ni-63	4.05E+08	Nb-95	8.29E+10
Tl-207	7.98E+00	Nb-95M	3.30E+08
Tl-208	1.29E+01	Tc-99	5.01E+06
Pb-211	8.00E+00	Rh-102	1.11E+03
Pb-212	3.59E+01	Ru-103	8.88E+09
Bi-211	8.00E+00	Rh-103M	8.01E+09
Bi-212	3.59E+01	Ru-106	1.44E+10
Po-211	2.24E-02	Rh-106	1.44E+10
Po-212	2.30E+01	Pd-107	5.66E+03
Po-215	8.00E+00	Ag-109M	1.70E-03
Po-216	3.59E+01	Ag-110	4.28E+03

Continued on next page

Die approbierte gedruckte Originalversion dieser Dissertation ist an der TU Wien Bibliothek verfügbar.
The approved original version of this doctoral thesis is available in print at TU Wien Bibliothek.
TU Bibliothek Your knowledge hub WIEN

Table B.2 – *Continued from previous page*

9212	**Activity[Bq]**	**9212**	**Activity[Bq]**
Rn-219	8.00E+00	Ag-110M	3.22E+05
Rn-220	3.59E+01	Ag-111	9.09E+01
Fr-223	1.10E-01	Cd-113M	4.64E+06
Ra-223	8.00E+00	In-114	1.68E+02
Ra-224	3.59E+01	In-114M	1.76E+02
Ac-227	7.98E+00	Cd-115M	6.80E+06
Th-227	7.88E+00	In-115M	4.78E+02
Th-228	3.58E+01	Sn-119M	7.03E+06
Th-230	9.94E-02	Sn-121M	3.02E+04
Th-231	2.98E+06	Sn-123	7.98E+07
Th-234	1.88E+06	Sb-124	1.81E+05
Pa-231	1.81E+02	Sn-125	2.91E+03
Pa-233	5.37E+03	Sb-125	1.51E+09
Pa-234M	1.88E+06	Te-125M	3.64E+08
Pa-234	2.45E+03	Sn-126	1.37E+05
U-232	9.37E+01	Sb-126	2.29E+04
U-233	2.86E+00	Sb-126M	1.37E+05
U-234	4.26E+03	Sb-127	1.73E-05
U-235	2.98E+06	Te-127	2.63E+08
U-236	1.69E+05	Te-127M	2.69E+08
U-237	1.70E+02	Te-129	1.19E+08
U-238	1.88E+06	Te-129M	1.83E+08
U-240	1.87E-11	I-129	8.20E+03
Np-235	5.80E-01	I-131	3.21E+04
Np-237	5.37E+03	Xe-131M	2.25E+05
Np-238	4.18E-02	Te-132	6.55E-07
Np-239	2.65E-02	I-132	6.75E-07
Np-240M	1.87E-11	Cs-132	1.34E-03
Pu-236	6.55E+01	Xe-133	1.13E+01
Pu-237	4.50E+00	Cs-134	2.64E+08
Pu-238	3.25E+05	Cs-135	4.07E+05

Continued on next page

Die approbierte gedruckte Originalversion dieser Dissertation ist an der TU Wien Bibliothek verfügbar.
The approved original version of this doctoral thesis is available in print at TU Wien Bibliothek.
TU Bibliothek Your knowledge hub WIEN

Table B.2 – *Continued from previous page*

9212	Activity[Bq]	9212	Activity[Bq]
Pu-239	5.58E+07	Cs-136	5.91E+04
Pu-240	1.20E+06	Ba-136M	9.74E+03
Pu-241	5.51E+06	Cs-137	3.42E+10
Pu-242	4.21E-01	Ba-137M	3.23E+10
Am-241	2.13E+04	Ba-140	2.97E+07
Am-242M	8.35E+00	La-140	3.42E+07
Am-242	8.31E+00	Ce-141	9.39E+09
Am-243	2.65E-02	Pr-143	5.60E+07
Cm-242	7.39E+03	Ce-144	1.48E+11
Cm-243	9.80E-03	Pr-144	1.48E+11
Cm-244	1.53E-02	Pr-144M	1.78E+09
		Pm-146	1.03E+04
		Nd-147	2.23E+06
		Pm-147	7.92E+10
		Pm-148	1.26E+06
		Pm-148M	2.24E+07
		Sm-151	7.74E+08
		Eu-152	8.76E+05
		Gd-153	4.16E+03
		Eu-154	1.83E+07
		Eu-155	9.02E+08
		Eu-156	4.14E+05
		Tb-160	3.23E+04
		Tb-161	1.42E-01
		Dy-166	4.47E-12
		Ho-166	6.66E-12

Table B.2: Inventory of Fuel element 9212, left side fuel element activation, actinides and daughters, right side fission products

9200	Activity[Bq]	9200	Activity[Bq]
C-14	4.53E+05	H-3	3.90E+08

Continued on next page

Die approbierte gedruckte Originalversion dieser Dissertation ist an der TU Wien Bibliothek verfügbar.
The approved original version of this doctoral thesis is available in print at TU Wien Bibliothek.
TU Bibliothek Your knowledge hub WIEN

Table B.3 – *Continued from previous page*

9200	**Activity[Bq]**	**9200**	**Activity[Bq]**
P-32	1.28E+04	Se-79	4.50E+05
P-33	1.77E+01	Kr-85	1.05E+10
S-35	2.52E+05	Rb-86	2.92E+04
Sc-47	5.12E-15	Sr-89	2.62E+10
Cr-51	5.30E+08	Sr-90	9.69E+10
Mn-54	1.56E+09	Y9-0	9.70E+10
Fe-55	2.36E+10	Y9-1	4.18E+10
Fe-59	3.95E+07	Zr-93	2.31E+06
Co-58	6.19E+08	Nb-93M	4.29E+05
Co-60	4.40E+07	Zr-95	5.29E+10
Ni-59	1.01E+07	Nb-95	9.96E+10
Ni-63	1.21E+09	Nb-95M	3.92E+08
Tl-207	4.19E+01	Tc-99	1.54E+07
Tl-208	5.52E+02	Rh-102	1.56E+04
Pb-211	4.20E+01	Ru-103	9.94E+09
Pb-212	1.54E+03	Rh-103M	8.96E+09
Bi-211	4.20E+01	Ru-106	2.61E+10
Bi-212	1.54E+03	Rh-106	2.61E+10
Po-211	1.18E-01	Pd-107	1.79E+04
Po-212	9.85E+02	Ag-109M	4.24E-02
Po-215	4.20E+01	Ag-110	3.12E+04
Po-216	1.54E+03	Ag-110M	2.35E+06
Rn-219	4.20E+01	Ag-111	1.04E+02
Rn-220	1.54E+03	Cd-113M	1.33E+07
Fr-223	5.78E-01	In-114	1.02E+03
Ra-223	4.20E+01	In-114M	1.07E+03
Ra-224	1.54E+03	Cd-115M	7.68E+06
Ac-227	4.19E+01	In-115M	5.40E+02
Th-227	4.14E+01	Sn-119M	1.27E+07
Th-228	1.53E+03	Sn-121M	9.15E+04
Th-230	5.10E-01	Sn-123	1.37E+08

Continued on next page

Die approbierte gedruckte Originalversion dieser Dissertation ist an der TU Wien Bibliothek verfügbar.
The approved original version of this doctoral thesis is available in print at TU Wien Bibliothek.
TU Bibliothek Your knowledge hub WIEN

Table B.3 – *Continued from previous page*

9200	Activity[Bq]	9200	Activity[Bq]
Th-231	3.00E+06	Te-123M	2.81E+02
Th-234	1.94E+06	Sb-124	4.67E+05
Pa-231	4.23E+02	Sn-125	3.26E+03
Pa-233	2.47E+04	Sb-125	3.32E+09
Pa-234M	1.94E+06	Te-125M	8.05E+08
Pa-234	2.52E+03	Sn-126	4.25E+05
U-232	2.49E+03	Sb-126	6.36E+04
U-233	8.97E+00	Sb-126M	4.25E+05
U-234	1.31E+04	Sb-127	1.94E-05
U-235	3.00E+06	Te-127	4.14E+08
U-236	5.19E+05	Te-127M	4.23E+08
U-237	3.68E+03	Te-129	1.33E+08
U-238	1.94E+06	Te-129M	2.05E+08
U-240	5.83E-09	I-129	2.53E+04
Np-235	6.41E+00	I-131	3.57E+04
Np-237	2.47E+04	Xe-131M	2.50E+05
Np-238	9.14E+00	Te-132	7.27E-07
Np-239	6.72E+00	I-132	7.49E-07
Np-240M	5.83E-09	Cs-132	4.74E-03
Pu-236	7.76E+02	Xe-133	1.26E+01
Pu-237	1.60E+01	Cs-134	2.14E+09
Pu-238	4.29E+06	Cs-135	1.22E+06
Pu-239	1.68E+08	Cs-136	9.89E+04
Pu-240	1.09E+07	Ba-136M	1.63E+04
Pu-241	1.47E+08	Cs-137	1.01E+11
Pu-242	3.40E+01	Ba-137M	9.58E+10
Pu-243	5.42E-15	Ba-140	3.30E+07
Am-241	6.90E+05	La-140	3.80E+07
Am-242M	1.83E+03	Ce-141	1.04E+10
Am-242	1.82E+03	Pr-143	6.21E+07
Am-243	6.72E+00	Ce-144	2.62E+11

Continued on next page

Die approbierte gedruckte Originalversion dieser Dissertation ist an der TU Wien Bibliothek verfügbar.
The approved original version of this doctoral thesis is available in print at TU Wien Bibliothek.
TU Bibliothek Your knowledge hub WIEN

Table B.3 – *Continued from previous page*

9200	Activity[Bq]	9200	Activity[Bq]
Cm-242	4.72E+05	Pr-144	2.62E+11
Cm-243	1.82E+01	Pr-144M	3.15E+09
Cm-244	1.17E+01	Pm-146	6.91E+04
		Nd-147	2.47E+06
		Pm-147	1.69E+11
		Pm-148	3.14E+06
		Pm-148M	5.58E+07
		Sm-151	2.09E+09
		Eu-152	3.69E+07
		Gd-153	8.55E+05
		Eu-154	1.63E+08
		Eu-155	2.15E+09
		Eu-156	5.34E+05
		Tb-160	1.24E+05
		Tb-161	1.72E-01
		Dy-166	5.43E-12
		Ho-166	8.09E-12

Table B.3: Inventory of Fuel element 9200. left side fuel element activation. actinides and daughters. right side fission products

10197	Activity[Bq]	10197	Activity[Bq]
C-14	7.52E+06	H-3	5.70E+08
P-32	1.62E+05	C-14	1.99E+02
P-33	2.24E+02	Se-79	7.20E+05
S-35	2.55E+06	Kr-85	1.52E+10
Sc-47	1.09E-13	Rb-86	5.21E+04
Cr-51	6.69E+09	Sr-89	3.08E+10
Mn-54	1.49E+10	Sr-90	1.49E+11
Fe-55	2.92E+11	Y9-0	1.49E+11
Fe-59	4.95E+08	Y9-1	4.80E+10
Co-58	7.05E+09	Zr-93	3.70E+06

Continued on next page

Die approbierte gedruckte Originalversion dieser Dissertation ist an der TU Wien Bibliothek verfügbar.
The approved original version of this doctoral thesis is available in print at TU Wien Bibliothek.
TU Bibliothek Your knowledge hub WIEN

Table B.4 – *Continued from previous page*

10197	**Activity[Bq]**	**10197**	**Activity[Bq]**
Co-60	6.19E+08	Nb-93M	9.09E+05
Ni-59	1.68E+08	Zr-95	5.93E+10
Ni-63	1.99E+10	Nb-95	1.10E+11
Tl-207	7.87E+02	Nb-95M	4.40E+08
Tl-208	1.46E+04	Tc-99	2.47E+07
Pb-211	7.89E+02	Rh-102	3.53E+04
Pb-212	4.07E+04	Ru-103	1.19E+10
Bi-211	7.89E+02	Rh-103M	1.08E+10
Bi-212	4.07E+04	Ru-106	2.58E+10
Po-211	2.21E+00	Rh-106	2.58E+10
Po-212	2.61E+04	Pd-107	2.92E+04
Po-215	7.89E+02	Ag-109M	1.32E-01
Po-216	4.07E+04	Ag-110	4.56E+04
Rn-219	7.89E+02	Ag-110M	3.43E+06
Rn-220	4.07E+04	Ag-111	1.28E+02
Fr-223	1.08E+01	Cd-113M	1.99E+07
Ra-223	7.89E+02	In-114	2.84E+03
Ra-224	4.07E+04	In-114M	2.97E+03
Ac-227	7.86E+02	Cd-115M	9.24E+06
Th-227	7.77E+02	In-115M	6.50E+02
Th-228	4.05E+04	Sn-117M	5.59E+00
Th-230	1.14E+01	Sn-119M	1.06E+07
Th-231	2.86E+07	Sn-121M	1.44E+05
Th-234	1.89E+07	Sn-123	1.06E+08
Pa-231	5.73E+03	Te-123M	6.69E+02
Pa-233	5.26E+05	Sb-124	8.36E+05
Pa-234M	1.89E+07	Sn-125	3.95E+03
Pa-234	2.45E+04	Sb-125	3.99E+09
U-232	5.83E+04	Te-125M	9.69E+08
U-233	1.47E+02	Sn-126	6.82E+05
U-234	2.10E+05	Sb-126	1.01E+05

Continued on next page

Die approbierte gedruckte Originalversion dieser Dissertation ist an der TU Wien Bibliothek verfügbar.
The approved original version of this doctoral thesis is available in print at TU Wien Bibliothek.
TU Bibliothek Your knowledge hub WIEN

Table B.4 – *Continued from previous page*

10197	**Activity[Bq]**	**10197**	**Activity[Bq]**
U-235	2.86E+07	Sb-126M	6.82E+05
U-236	8.29E+06	Sb-127	2.35E-05
U-237	1.48E+05	Te-127	3.53E+08
U-238	1.89E+07	Te-127M	3.60E+08
U-240	9.26E-07	Te-129	1.60E+08
Np-235	1.45E+02	Te-129M	2.47E+08
Np-237	5.26E+05	I-129	4.06E+04
Np-238	7.80E+02	I-131	4.29E+04
Np-239	8.15E+02	Xe-131M	3.01E+05
Np-240M	9.26E-07	Te-132	8.75E-07
Pu-236	2.23E+04	I-132	9.01E-07
Pu-237	3.26E+02	Cs-132	9.63E-03
Pu-238	1.46E+08	Xe-133	1.51E+01
Pu-239	2.64E+09	Cs-134	4.42E+09
Pu-240	2.81E+08	Cs-135	1.90E+06
Pu-241	6.00E+09	Cs-136	1.57E+05
Pu-242	2.39E+03	Ba-136M	2.59E+04
Pu-243	5.17E-12	Cs-137	1.56E+11
Am-241	3.73E+07	Ba-137M	1.47E+11
Am-242M	1.56E+05	Ba-140	3.96E+07
Am-242	1.55E+05	La-140	4.56E+07
Am-243	8.15E+02	Ce-141	1.25E+10
Cm-242	2.31E+07	Pr-143	7.46E+07
Cm-243	2.89E+03	Ce-144	2.30E+11
Cm-244	2.31E+03	Pr-144	2.30E+11
		Pr-144M	2.76E+09
		Pm-146	1.36E+05
		Nd-147	2.97E+06
		Pm-147	1.99E+11
		Pm-148	4.62E+06
		Pm-148M	8.21E+07

Continued on next page

Die approbierte gedruckte Originalversion dieser Dissertation ist an der TU Wien Bibliothek verfügbar.
The approved original version of this doctoral thesis is available in print at TU Wien Bibliothek.
TU Bibliothek Your knowledge hub WIEN

Table B.4 – *Continued from previous page*

10197	**Activity[Bq]**	**10197**	**Activity[Bq]**
		Sm-151	2.95E+09
		Eu-152	1.26E+08
		Gd-153	2.96E+06
		Eu-154	4.03E+08
		Eu-155	2.75E+09
		Eu-156	6.98E+05
		Tb-160	2.31E+05
		Tb-161	2.24E-01
		Dy-166	7.08E-12
		Ho-166	1.05E-11

Table B.4: Inventory of Fuel element 10197, left side fuel element activation, actinides and daughters, right side fission products

8257	**Activity[Bq]**	**8257**	**Activity[Bq]**
H-3	1.36E+01	H-3	6.57E+08
C-14	1.78E+06	C-14	4.63E+02
P-32	1.06E+04	Se-79	1.68E+06
P-33	1.47E+01	Kr-85	1.59E+10
S-35	1.63E+05	Rb-86	7.54E+04
Sc-47	1.72E-14	Sr-89	1.94E+10
Cr-51	4.37E+08	Sr-90	2.48E+11
Mn-54	6.10E+08	Y-90	2.48E+11
Fe-55	1.48E+10	Y-91	3.02E+10
Fe-59	3.24E+07	Zr-93	8.59E+06
Co-58	4.59E+08	Nb-93M	5.02E+06
Co-60	4.64E+07	Zr-95	3.73E+10
Ni-59	3.94E+07	Nb-95	6.95E+10
Ni-63	4.21E+09	Nb-95M	2.77E+08
Zn-65	8.73E+00	Tc-99	5.71E+07
Tl-207	6.80E+02	Rh-102	6.09E+04
Tl-208	1.32E+04	Ru-103	7.64E+09

Continued on next page

Die approbierte gedruckte Originalversion dieser Dissertation ist an der TU Wien Bibliothek verfügbar.
The approved original version of this doctoral thesis is available in print at TU Wien Bibliothek.
TU Bibliothek Your knowledge hub WIEN

Table B.5 – *Continued from previous page*

8257	**Activity[Bq]**	**8257**	**Activity[Bq]**
Pb-211	6.82E+02	Rh-103M	6.89E+09
Pb-212	3.67E+04	Ru-106	1.14E+10
Bi-211	6.82E+02	Rh-106	1.14E+10
Bi-212	3.67E+04	Pd-107	7.27E+04
Po-211	1.91E+00	Ag-108	4.06E-01
Po-212	2.35E+04	Ag-109M	4.95E-01
Po-215	6.82E+02	Ag-110	5.32E+04
Po-216	3.67E+04	Ag-110M	4.00E+06
Rn-219	6.82E+02	Ag-111	8.75E+01
Rn-220	3.67E+04	Cd-113M	2.60E+07
Fr-223	9.38E+00	In-114	1.15E+04
Ra-223	6.82E+02	In-114M	1.20E+04
Ra-224	3.67E+04	Cd-115M	5.98E+06
Ac-227	6.80E+02	In-115M	4.20E+02
Th-227	6.72E+02	Sn-117M	1.96E+01
Th-228	3.66E+04	Sn-119M	4.29E+06
Th-230	9.42E+00	Sn-121M	2.81E+05
Th-231	2.69E+06	Sn-123	5.86E+07
Th-234	1.90E+06	Te-123M	2.28E+03
Pa-231	1.81E+03	Sb-124	1.19E+06
Pa-233	2.22E+05	Sn-125	2.56E+03
Pa-234M	1.90E+06	Sb-125	2.03E+09
Pa-234	2.47E+03	Te-125M	4.91E+08
U-232	3.97E+04	Sn-126	1.60E+06
U-233	4.63E+01	Sb-126	2.28E+05
U-234	5.30E+04	Sb-126M	1.60E+06
U-235	2.69E+06	Sb-127	1.51E-05
U-236	1.91E+06	Te-127	2.12E+08
U-237	8.83E+04	Te-127M	2.16E+08
U-238	1.90E+06	Te-129	1.03E+08
U-240	6.17E-06	Te-129M	1.58E+08

Continued on next page

Die approbierte gedruckte Originalversion dieser Dissertation ist an der TU Wien Bibliothek verfügbar.
The approved original version of this doctoral thesis is available in print at TU Wien Bibliothek.
TU Bibliothek Your knowledge hub WIEN

Table B.5 – *Continued from previous page*

8257	**Activity[Bq]**	**8257**	**Activity[Bq]**
Np-235	3.36E+01	I-129	9.48E+04
Np-236	8.02E-01	I-131	2.72E+04
Np-237	2.22E+05	Xe-131M	1.91E+05
Np-238	5.81E+03	Te-132	5.54E-07
Np-239	5.07E+03	I-132	5.71E-07
Np-240M	6.17E-06	Cs-132	1.47E-02
Pu-236	7.31E+03	Xe-133	9.55E+00
Pu-237	5.31E+01	Cs-134	6.45E+09
Pu-238	1.43E+08	Cs-135	4.67E+06
Pu-239	5.70E+08	Cs-136	1.93E+05
Pu-240	1.37E+08	Ba-136M	3.19E+04
Pu-241	3.59E+09	Cs-137	2.63E+11
Pu-242	5.11E+03	Ba-137M	2.49E+11
Pu-243	1.02E-09	Ba-140	2.50E+07
Am-241	9.48E+07	La-140	2.88E+07
Am-242M	1.16E+06	Ce-141	7.92E+09
Am-242	1.16E+06	Pr-143	4.71E+07
Am-243	5.07E+03	Ce-144	8.94E+10
Cm-242	4.05E+07	Pr-144	8.95E+10
Cm-243	2.69E+04	Pr-144M	1.07E+09
Cm-244	2.95E+04	Pm-146	8.81E+04
		Nd-147	1.88E+06
		Pm-147	9.74E+10
		Pm-148	1.47E+06
		Pm-148M	2.61E+07
		Eu-150	8.17E+02
		Sm-151	4.49E+09
		Eu-152	9.20E+08
		Gd-153	1.92E+07
		Eu-154	1.18E+09
		Eu-155	1.86E+09

Continued on next page

Die approbierte gedruckte Originalversion dieser Dissertation ist an der TU Wien Bibliothek verfügbar.
The approved original version of this doctoral thesis is available in print at TU Wien Bibliothek.
TU Bibliothek Your knowledge hub WIEN

Table B.5 – *Continued from previous page*

8257	Activity[Bq]	8257	Activity[Bq]
		Eu-156	4.28E+05
		Tb-160	3.76E+05
		Tb-161	1.74E-01
		Dy-166	5.45E-12
		Ho-166	8.12E-12

Table B.5: Inventory of Fuel element 8257, left side fuel element activation, actinides and daughters, right side fission products

Isotope	Activity[Bq]	Isotope	Activity[Bq]	Isotope	Activity[Bq]
C-14	1.45E+06	Y-94	8.08E+12	Sb-130	3.02E+11
N-16	2.75E-09	Nb-94M	4.60E+05	Sb-130M	1.44E+12
O-19	4.00E-01	Sr-95	1.77E+09	I-130	1.01E+10
Mg-27	8.13E+05	Y-95	6.92E+12	I-130M	2.79E+09
Al-28	2.82E+08	Zr-95	9.61E+12	Sn-131	4.55E+10
Al-29	2.78E+07	Nb-95	9.61E+12	Sb-131	3.34E+12
Si-31	8.53E+08	Nb-95M	6.75E+10	Te-131	3.83E+12
P-32	1.33E+09	Y-96	1.85E+12	Te-131M	5.49E+11
P-33	4.60E+04	Nb-96	2.23E+09	I-131	4.32E+12
P-34	5.72E-03	Zr-97	8.68E+12	Xe-131M	4.80E+10
S-35	3.04E+07	Nb-97	8.74E+12	Sn-132	3.73E+09
S-37	3.77E+04	Nb-97M	8.22E+12	Sb-132	7.52E+11
Sc-47	1.40E+03	Zr-98	7.40E+09	Sb-132M	6.68E+11
Sc-48	1.55E+03	Nb-98	8.14E+09	Te-132	6.40E+12
Sc-49	3.58E+02	Nb-98M	3.89E+10	I-132	6.43E+12
Ti-51	2.47E+06	Nb-99	2.37E+06	Cs-132	1.11E+08
V-52	2.29E+09	Nb-99M	5.52E+10	Sb-133	7.30E+11
V-53	4.07E+06	Mo-99	8.91E+12	Te-133	4.88E+12
V-54	7.41E+03	Tc-99	4.65E+07	Te-133M	4.05E+12
Cr-51	8.70E+11	Tc-99M	7.81E+12	I-133	1.00E+13
Cr-55	4.06E+09	Zr-100	3.23E-01	I-133M	5.27E+00
Mn-54	3.46E+10	Nb-100	2.44E-01	Xe-133	1.00E+13

Continued on next page

Die approbierte gedruckte Originalversion dieser Dissertation ist an der TU Wien Bibliothek verfügbar.
The approved original version of this doctoral thesis is available in print at TU Wien Bibliothek.
TU Bibliothek Your knowledge hub WIEN

Table B.6 – *Continued from previous page*

Isotope	Activity[Bq]	Isotope	Activity[Bq]	Isotope	Activity[Bq]
Mn-56	1.97E+12	Nb-100M	2.45E-01	Xe-133M	2.94E+11
Mn-57	1.15E+07	Tc-100	1.42E+05	Sb-134	9.28E+02
Mn-58	1.28E+04	Nb-101	3.13E-01	Sb-134M	5.03E+02
Fe-55	1.74E+11	Mo-101	5.98E+12	Te-134	9.11E+12
Fe-59	1.46E+10	Tc-101	7.41E+12	I-134	1.12E+13
Co-58	9.35E+10	Zr-102	1.27E+09	I-134M	2.55E+11
Co-60	2.30E+08	Nb-102	1.42E+09	Cs-134	4.75E+10
Co-60M	6.84E+07	Mo-102	4.69E+12	Cs-134M	1.92E+10
Co-61	4.19E+07	Tc-102	4.73E+12	Te-135	5.45E+07
Co-62	6.95E+05	Tc-102M	9.35E+08	I-135	9.26E+12
Ni-59	3.21E+07	Rh-102	2.90E+05	Xe-135	6.91E+12
Ni-63	3.97E+09	Nb-103	2.93E+06	Xe-135M	1.64E+12
Ni-65	9.46E+09	Mo-103	1.56E+11	Cs-135	3.37E+06
Ni-66	1.02E+04	Tc-103	5.44E+11	Cs-135M	1.85E+09
Cu-64	1.71E+06	Ru-103	4.80E+12	Ba-135M	2.21E+06
Cu-66	1.98E+06	Rh-103M	4.33E+12	Te-136	8.24E+07
Actinides &	Daugthers	Mo-104	2.93E+11	I-136	3.93E+11
Th-231	2.75E+06	Tc-104	2.61E+12	I-136M	2.47E+10
Th-233	3.66E+03	Rh-104	1.29E+10	Cs-136	4.35E+10
Th-234	1.90E+06	Rh-104M	9.52E+09	Ba-136M	7.17E+09
Pa-232	3.23E+05	Mo-105	2.61E+10	I-137	6.72E+08
Pa-233	1.56E+05	Tc-105	1.17E+12	Xe-137	3.65E+12
Pa-234M	1.90E+06	Ru-105	1.67E+12	Cs-137	3.36E+11
Pa-234	2.70E+03	Rh-105	1.66E+12	Ba-137M	3.18E+11
U-232	2.57E+03	Rh-105M	4.68E+11	I-138	3.44E-03
U-234	3.92E+04	Mo-106	1.64E+01	Xe-138	7.16E+12
U-235	2.75E+06	Tc-106	2.45E+09	Cs-138	9.80E+12
U-236	1.57E+06	Ru-106	4.77E+11	Cs-138M	1.05E+11
U-237	5.39E+11	Rh-106	4.77E+11	Xe-139	2.96E+10
U-238	1.90E+06	Rh-106M	5.30E+09	Cs-139	6.81E+12
U-239	1.06E+13	Mo-107	2.88E-04	Ba-139	9.52E+12

Continued on next page

Die approbierte gedruckte Originalversion dieser Dissertation ist an der TU Wien Bibliothek verfügbar.
The approved original version of this doctoral thesis is available in print at TU Wien Bibliothek.
TU Bibliothek Your knowledge hub WIEN

Table B.6 – *Continued from previous page*

Isotope	Activity[Bq]	Isotope	Activity[Bq]	Isotope	Activity[Bq]
U-240	3.35E+06	Tc-107	2.06E+08	Xe-140	5.33E+05
Np-236M	4.18E+05	Ru-107	1.76E+11	Cs-140	3.23E+11
Np-237	1.52E+05	Rh-107	3.57E+11	Ba-140	9.21E+12
Np-238	1.74E+10	Pd-107	5.86E+04	La-140	9.24E+12
Np-239	1.23E+13	Pd-107M	1.41E+02	Pr-140	2.95E+06
Np-240M	2.30E+08	Tc-108	8.98E-08	Cs-141	1.05E+09
Np-240	1.40E+09	Ru-108	8.77E+10	Ba-141	7.27E+12
Pu-236	2.56E+04	Rh-108	9.35E+10	La-141	8.74E+12
Pu-237	1.86E+04	Rh-108M	3.56E+08	Ce-141	8.75E+12
Pu-238	7.98E+07	Tc-109	7.91E+08	Ba-142	6.10E+12
Pu-239	4.72E+08	Ru-109	2.37E+09	La-142	8.66E+12
Pu-240	9.57E+07	Rh-109	3.10E+10	Pr-142	2.84E+10
Pu-241	4.58E+09	Rh-109M	4.97E+09	Pr-142M	4.74E+09
Pu-242	3.19E+03	Pd-109	1.09E+11	Ba-143	8.24E+05
Pu-243	6.35E+07	Pd-109M	4.25E+10	La-143	6.81E+12
Am-241	2.88E+06	Ag-109M	1.09E+11	Ce-143	8.75E+12
Am-242M	3.70E+04	Ru-110	7.47E+04	Pr-143	8.74E+12
Am-242	2.36E+08	Rh-110	7.74E+07	Ba-144	1.42E+04
Am-244M	9.74E+05	Ag-110	3.06E+06	La-144	4.32E+10
Am-244	5.86E+04	Ag-110M	1.65E+08	Ce-144	6.22E+12
Cm-242	6.87E+07	Ru-111	2.87E+04	Pr-144	6.23E+12
Cm-244	1.19E+04	Rh-111	2.03E+09	Pr-144M	7.47E+10
Su-Mtot	2.35E+13	Pd-111	4.70E+10	Ba-145	1.35E-03
Fission	Products	Pd-111M	4.75E+08	La-145	3.28E+09
H-3	1.45E+09	Ag-111	5.24E+10	Ce-145	2.06E+12
Cu-72	2.17E-08	Ag-111M	4.87E+10	Pr-145	5.78E+12
Zn-72	1.27E+08	Cd-111M	8.79E+04	La-146	1.31E+01
Ga-72	1.27E+08	Rh-112	2.29E-10	Ce-146	3.44E+12
Zn-73	3.90E+04	Pd-112	3.71E+10	Pr-146	4.35E+12
Ga-73	4.01E+08	Ag-112	3.74E+10	Pm-146	1.45E+06
Ge-73M	4.01E+08	Pd-113	3.16E+09	La-147	5.07E+02

Continued on next page

Die approbierte gedruckte Originalversion dieser Dissertation ist an der TU Wien Bibliothek verfügbar.
The approved original version of this doctoral thesis is available in print at TU Wien Bibliothek.
TU Bibliothek Your knowledge hub WIEN

Table B.6 – *Continued from previous page*

Isotope	Activity[Bq]	Isotope	Activity[Bq]	Isotope	Activity[Bq]
Zn-74	9.67E+07	Ag-113	3.16E+10	Ce-147	1.57E+11
Ga-74	7.65E+08	Ag-113M	8.25E+08	Pr-147	2.77E+12
Zn-75	5.80E-02	Cd-113M	4.94E+07	Nd-147	3.39E+12
Ga-75	3.76E+08	Ru-114	8.54E-10	Pm-147	1.07E+12
Ge-75	2.34E+09	Rh-114	1.29E-09	Ba-148	1.88E-06
Ge-75M	2.54E+07	Pd-114	6.96E+09	La-148	2.41E-06
Zn-76	1.18E-08	Ag-114	7.19E+09	Ce-148	1.41E+10
Ga-76	2.46E+06	In-114	2.32E+05	Pr-148	7.21E+11
As-76	9.77E+06	In-114M	2.28E+05	Pm-148	2.82E+11
Ga-77	6.83E+02	Rh-115	2.19E-06	Pm-148M	9.62E+10
Ge-77	5.28E+09	Pd-115	1.00E+08	Pr-149	3.30E+11
Ge-77M	2.93E+08	Ag-115	1.91E+10	Nd-149	1.60E+12
As-77	1.53E+10	Ag-115M	4.91E+07	Pm-149	1.69E+12
Se-77M	3.79E+07	Cd-115	2.81E+10	Pr-150	2.01E+04
Ga-78	1.30E-09	Cd-115M	2.76E+09	Pm-150	2.92E+09
Ge-78	2.94E+10	In-115M	2.82E+10	Nd-151	4.78E+11
As-78	3.09E+10	Pd-116	4.37E+03	Pm-151	6.41E+11
Ge-79	4.12E+08	Ag-116	4.21E+09	Sm-151	4.60E+09
As-79	5.66E+10	Ag-116M	8.47E+03	Ce-152	3.63E+03
Se-79	1.38E+06	In-116	7.92E+02	Pr-152	8.92E+03
Se-79M	7.17E+10	In-116M	3.26E+09	Nd-152	2.99E+11
Ge-80	1.81E+07	Pd-117	2.92E-09	Pm-152	3.72E+11
As-80	5.72E+07	Ag-117	8.07E+08	Pm-152M	3.50E+09
Br-80	9.86E+05	Ag-117M	2.83E-07	Eu-152	6.41E+07
Br-80M	4.98E+05	Cd-117	1.91E+10	Eu-152M	8.33E+08
Ge-81	8.22E+01	Cd-117M	1.03E+10	Pr-153	2.69E-02
As-81	4.30E+08	In-117	1.79E+10	Nd-153	9.22E+09
Se-81	2.72E+11	In-117M	2.27E+10	Pm-153	1.59E+11
Se-81M	9.44E+09	Sn-117M	2.01E+06	Sm-153	3.48E+11
Ge-82	4.18E-10	Cd-118	3.00E+10	Gd-153	2.46E+07
As-82	1.11E+07	In-118	3.00E+10	Nd-154	3.73E+08

Continued on next page

Die approbierte gedruckte Originalversion dieser Dissertation ist an der TU Wien Bibliothek verfügbar.
The approved original version of this doctoral thesis is available in print at TU Wien Bibliothek.
TU Bibliothek Your knowledge hub WIEN

Table B.6 – *Continued from previous page*

Isotope	Activity[Bq]	Isotope	Activity[Bq]	Isotope	Activity[Bq]
As-82M	5.79E+03	In-118M	3.12E+06	Pm-154	3.64E+10
Br-82	2.07E+09	Ag-119	3.81E-06	Pm-154M	1.96E+09
Br-82M	4.96E+08	Cd-119	1.05E+10	Eu-154	2.00E+09
As-83	5.80E+04	Cd-119M	5.05E+09	Nd-155	6.48E+06
Se-83	2.54E+11	In-119	6.09E+09	Pm-155	2.99E+08
Se-83M	2.59E+10	In-119M	2.21E+10	Sm-155	5.26E+10
Br-83	7.87E+11	Sn-119M	3.69E+08	Eu-155	8.88E+09
Kr-83M	7.95E+11	Cd-120	4.28E+08	Nd-156	1.49E+08
As-84	1.89E-05	In-120	9.02E+08	Pm-156	1.93E+08
Se-84	4.90E+11	In-120M	2.28E+08	Sm-156	2.54E+10
Br-84	1.43E+12	Cd-121	1.27E+03	Eu-156	5.18E+10
Br-84M	1.55E+10	In-121	1.99E+07	Pm-157	3.00E+08
Se-85	3.42E+09	In-121M	2.46E+09	Sm-157	9.34E+09
Se-85M	6.65E+06	Sn-121	3.33E+10	Eu-157	1.41E+10
Br-85	6.18E+11	Sn-121M	3.00E+05	Nd-158	1.42E-04
Kr-85	4.00E+10	Cd-122	1.52E-07	Pm-158	2.73E-04
Kr-85M	1.86E+12	In-122	2.12E+01	Sm-158	6.11E+09
Se-86	3.62E+06	Sb-122	3.31E+08	Eu-158	7.04E+09
Br-86	3.40E+10	Sb-122M	1.25E+06	Sm-159	5.58E+08
Br-86M	2.48E+06	Cd-123	1.35E-01	Eu-159	2.38E+09
Rb-86	8.95E+08	In-123	3.60E-01	Gd-159	2.74E+09
Rb-86M	4.35E+06	In-123M	1.34E+08	Sm-160	4.44E+08
Se-87	1.49E-05	Sn-123	9.20E+09	Eu-160	5.22E+08
Br-87	6.60E+10	Sn-123M	2.90E+10	Tb-160	5.32E+07
Kr-87	3.64E+12	Te-123M	1.43E+05	Sm-161	5.65E+00
Sr-87M	1.86E+06	Cd-124	7.70E+04	Eu-161	2.19E+06
Br-88	5.43E+06	In-124	9.46E+04	Gd-161	1.85E+08
Kr-88	5.24E+12	Sb-124	2.15E+08	Tb-161	4.06E+08
Rb-88	5.37E+12	Sb-124M	1.09E+06	Sm-162	3.56E+02
Br-89	2.02E-09	In-125M	2.23E+02	Eu-162	5.59E+07
Kr-89	2.16E+12	Sn-125	2.65E+10	Gd-162	1.70E+08

Continued on next page

Die approbierte gedruckte Originalversion dieser Dissertation ist an der TU Wien Bibliothek verfügbar.
The approved original version of this doctoral thesis is available in print at TU Wien Bibliothek.
TU Bibliothek Your knowledge hub WIEN

Table B.6 – *Continued from previous page*

Isotope	Activity[Bq]	Isotope	Activity[Bq]	Isotope	Activity[Bq]
Rb-89	6.38E+12	Sn-125M	2.87E+10	Tb-162	1.97E+08
Sr-89	7.03E+12	Sb-125	2.24E+10	Tb-162M	5.71E+06
Y-89M	5.91E-01	Te-125M	4.51E+09	Eu-163	1.12E+01
Kr-90	7.81E+09	Sn-126	1.31E+06	Gd-163	7.86E+06
Rb-90	2.08E+12	Sb-126	1.71E+09	Tb-163	7.41E+07
Rb-90M	6.73E+11	Sb-126M	6.71E+08	Gd-164	2.75E+07
Sr-90	3.21E+11	Sn-127	1.59E+11	Tb-164	3.22E+07
Y-90	3.23E+11	Sn-127M	3.29E+10	Gd-165	1.37E+06
Y-90M	2.10E+07	Sb-127	2.55E+11	Tb-165	2.04E+06
Kr-91	5.85E+01	Te-127	2.54E+11	Dy-165	3.58E+07
Rb-91	2.12E+11	Te-127M	3.47E+10	Dy-165M	3.06E+06
Sr-91	8.56E+12	Sn-128	5.35E+11	Dy-166	1.07E+07
Y-91	8.70E+12	Sb-128	2.57E+10	Ho-166	1.19E+07
Y-91M	4.99E+12	Sb-128M	5.78E+11		
Rb-92	4.99E-09	I-128	1.86E+09		
Sr-92	8.64E+12	Sn-129	2.12E+11		
Y-92	8.84E+12	Sn-129M	1.23E+11		
Rb-93	2.15E-04	Sb-129	1.05E+12		
Sr-93	5.82E+12	Te-129	1.04E+12		
Y-93	9.53E+12	Te-129M	1.56E+11		
Zr-93	7.04E+06	I-129	7.67E+04		
Nb-93M	2.65E+05	Xe-129M	9.70E+04		
Sr-94	4.84E+11	Sn-130	5.35E+11		

Table B.6: Inventory of averaged fuel element in B Ring in 2025

Isotope	Activity[Bq]	Isotope	Activity[Bq]	Isotope	Activity[Bq]
C-14	1.26E+06	Nb-94M	3.91E+05	Sb-130	2.63E+11
N-16	2.38E-09	Sr-95	1.54E+09	Sb-130M	1.25E+12
O-19	3.46E-01	Y-95	6.05E+12	I-130	7.73E+09
Mg-27	7.02E+05	Zr-95	8.38E+12	I1-30M	2.12E+09
Al-28	2.44E+08	Nb-95	8.38E+12	Sn-131	3.98E+10

Continued on next page

Die approbierte gedruckte Originalversion dieser Dissertation ist an der TU Wien Bibliothek verfügbar.
The approved original version of this doctoral thesis is available in print at TU Wien Bibliothek.
TU Bibliothek Your knowledge hub WIEN

Table B.7 – *Continued from previous page*

Isotope	Activity[Bq]	Isotope	Activity[Bq]	Isotope	Activity[Bq]
Al-29	2.40E+07	Nb-95M	5.88E+10	Sb-131	2.91E+12
Si-31	7.37E+08	Y-96	1.62E+12	Te-131	3.34E+12
P-32	1.15E+09	Nb-96	1.79E+09	Te-131M	4.79E+11
P-33	3.97E+04	Zr-97	7.58E+12	I-131	3.77E+12
P-34	4.94E-03	Nb-97	7.64E+12	Xe-131M	4.19E+10
S-35	2.63E+07	Nb-97M	7.18E+12	Sn-132	3.26E+09
S-37	3.25E+04	Zr-98	6.47E+09	Sb-132	6.57E+11
Sc-47	1.06E+03	Nb-98	7.11E+09	Sb-132M	5.83E+11
Sc-48	1.17E+03	Nb-98M	3.38E+10	Te-132	5.58E+12
Sc-49	2.70E+02	Nb-99	2.07E+06	I-132	5.62E+12
Ti-51	2.13E+06	Nb-99M	4.81E+10	Cs-132	8.41E+07
V-52	1.95E+09	Mo-99	7.79E+12	Sb-133	6.39E+11
V-53	3.52E+06	Tc-99	4.09E+07	Te-133	4.27E+12
V-54	6.39E+03	Tc-99M	6.82E+12	Te-133M	3.54E+12
Cr-51	7.52E+11	Zr-100	2.83E-01	I-133	8.76E+12
Cr-55	3.50E+09	Nb-100	2.13E-01	I1-33M	4.59E+00
Mn-54	3.00E+10	Nb-100M	2.14E-01	Xe-133	8.76E+12
Mn-56	1.70E+12	Tc-100	1.08E+05	Xe-133M	2.57E+11
Mn-57	9.88E+06	Nb-101	2.73E-01	Sb-134	8.11E+02
Mn-58	1.10E+04	Mo-101	5.22E+12	Sb-134M	4.40E+02
Fe-55	1.51E+11	Tc-101	6.47E+12	Te-134	7.96E+12
Fe-59	1.26E+10	Zr-102	1.11E+09	I-134	9.81E+12
Co-58	8.18E+10	Nb-102	1.24E+09	I-134M	2.22E+11
Co-60	1.99E+08	Mo-102	4.10E+12	Cs-134	3.64E+10
Co-60M	4.92E+07	Tc-102	4.13E+12	Cs-134M	1.46E+10
Co-61	3.61E+07	Tc-102M	8.05E+08	Te-135	4.77E+07
Co-62	6.01E+05	Rh-102	2.23E+05	I-135	8.08E+12
Ni-59	2.80E+07	Nb-103	2.56E+06	Xe-135	6.28E+12
Ni-63	3.47E+09	Mo-103	1.36E+11	Xe-135M	1.43E+12
Ni-65	8.17E+09	Tc-103	4.74E+11	Cs-135	3.08E+06
Ni-66	7.61E+03	Ru-103	4.18E+12	Cs-135M	1.42E+09

Continued on next page

Die approbierte gedruckte Originalversion dieser Dissertation ist an der TU Wien Bibliothek verfügbar.
The approved original version of this doctoral thesis is available in print at TU Wien Bibliothek.
TU Bibliothek Your knowledge hub WIEN

Table B.7 – *Continued from previous page*

Isotope	Activity[Bq]	Isotope	Activity[Bq]	Isotope	Activity[Bq]
Cu-64	1.30E+06	Rh-103M	3.77E+12	Ba-135M	1.57E+06
Cu-66	1.49E+06	Mo-104	2.55E+11	Te-136	7.20E+07
Actinides		Tc-104	2.27E+12	I-136	3.43E+11
Th-231	2.79E+06	Rh-104	9.84E+09	I-136M	2.15E+10
Th-233	2.81E+03	Rh-104M	7.25E+09	Cs-136	3.52E+10
Th-234	1.90E+06	Mo-105	2.26E+10	Ba-136M	5.81E+09
Pa-232	2.86E+05	Tc-105	1.02E+12	I-137	5.87E+08
Pa-233	1.24E+05	Ru-105	1.45E+12	Xe-137	3.19E+12
Pa-234M	1.90E+06	Rh-105	1.44E+12	Cs-137	2.95E+11
Pa-234	2.63E+03	Rh-105M	4.06E+11	Ba-137M	2.79E+11
U-232	2.28E+03	Mo-106	1.42E+01	I1-38	3.01E-03
U-234	3.45E+04	Tc-106	2.12E+09	Xe-138	6.26E+12
U-235	2.79E+06	Ru-106	4.14E+11	Cs-138	8.57E+12
U-236	1.38E+06	Rh-106	4.14E+11	Cs-138M	9.16E+10
U-237	4.18E+11	Rh-106M	3.98E+09	Xe-139	2.59E+10
U-238	1.90E+06	Mo-107	2.50E-04	Cs-139	5.95E+12
U-239	9.13E+12	Tc-107	1.78E+08	Ba-139	8.32E+12
U-240	2.50E+06	Ru-107	1.51E+11	Xe-140	4.66E+05
Np-236M	2.88E+05	Rh-107	3.05E+11	Cs-140	2.82E+11
Np-237	1.21E+05	Pd-107	5.08E+04	Ba-140	8.05E+12
Np-238	1.20E+10	Pd-107M	1.07E+02	La-140	8.07E+12
Np-239	1.07E+13	Tc-108	7.73E-08	Pr-140	2.24E+06
Np-240M	1.72E+08	Ru-108	7.44E+10	Cs-141	9.14E+08
Np-240	1.04E+09	Rh-108	7.93E+10	Ba-141	6.35E+12
Pu-236	1.79E+04	Rh-108M	2.77E+08	La-141	7.64E+12
Pu-237	1.38E+04	Tc-109	6.74E+08	Ce-141	7.64E+12
Pu-238	5.61E+07	Ru-109	2.02E+09	Ba-142	5.33E+12
Pu-239	4.20E+08	Rh-109	2.62E+10	La-142	7.56E+12
Pu-240	7.50E+07	Rh-109M	4.21E+09	Pr-142	2.16E+10
Pu-241	3.14E+09	Pd-109	9.16E+10	Pr-142M	3.60E+09
Pu-243	3.27E+07	Pd-109M	3.58E+10	Ba-143	7.20E+05

Continued on next page

Die approbierte gedruckte Originalversion dieser Dissertation ist an der TU Wien Bibliothek verfügbar.
The approved original version of this doctoral thesis is available in print at TU Wien Bibliothek.
TU Bibliothek Your knowledge hub WIEN

Table B.7 – *Continued from previous page*

Isotope	Activity[Bq]	Isotope	Activity[Bq]	Isotope	Activity[Bq]
Am-241	2.00E+06	Ag-109M	9.15E+10	La-143	5.95E+12
Am-242M	2.27E+04	Ru-110	6.38E+04	Ce-143	7.64E+12
Am-242	1.41E+08	Rh-110	6.62E+07	Pr-143	7.64E+12
Am-244M	4.38E+05	Ag-110	2.30E+06	Ba-144	1.24E+04
Am-244	2.63E+04	Ag-110M	1.24E+08	La-144	3.77E+10
Cm-242	4.13E+07	Ru-111	2.47E+04	Ce-144	5.44E+12
Cm-244	5.39E+03	Rh-111	1.74E+09	Pr-144	5.45E+12
Fission	Products	Pd-111	4.04E+10	Pr-144M	6.53E+10
H-3	1.27E+09	Pd-111M	4.03E+08	Ba-145	1.18E-03
Cu-72	1.89E-08	Ag-111	4.51E+10	La-145	2.87E+09
Zn-72	1.10E+08	Ag-111M	4.19E+10	Ce-145	1.80E+12
Ga-72	1.11E+08	Cd-111M	5.75E+04	Pr-145	5.05E+12
Zn-73	3.41E+04	Rh-112	1.99E-10	La-146	1.14E+01
Ga-73	3.50E+08	Pd-112	3.21E+10	Ce-146	3.00E+12
Ge-73M	3.50E+08	Ag-112	3.24E+10	Pr-146	3.80E+12
Zn-74	8.44E+07	Pd-113	2.74E+09	Pm-146	1.11E+06
Ga-74	6.68E+08	Ag-113	2.74E+10	La-147	4.43E+02
Zn-75	5.07E-02	Ag-113M	7.16E+08	Ce-147	1.37E+11
Ga-75	3.29E+08	Cd-113M	4.31E+07	Pr-147	2.42E+12
Ge-75	2.04E+09	Ru-114	7.43E-10	Nd-147	2.96E+12
Ge-75M	2.22E+07	Rh-114	1.12E-09	Pm-147	9.51E+11
Zn-76	1.03E-08	Pd-114	6.05E+09	Ba-148	1.64E-06
Ga-76	2.15E+06	Ag-114	6.25E+09	La-148	2.10E-06
As-76	7.44E+06	In-114	1.77E+05	Ce-148	1.23E+10
Ga-77	5.97E+02	In-114M	1.74E+05	Pr-148	6.30E+11
Ge-77	4.61E+09	Rh-115	1.90E-06	Pm-148	2.17E+11
Ge-77M	2.56E+08	Pd-115	8.73E+07	Pm-148M	7.73E+10
As-77	1.33E+10	Ag-115	1.66E+10	Pr-149	2.88E+11
Se-77M	3.31E+07	Ag-115M	4.27E+07	Nd-149	1.40E+12
Ga-78	1.14E-09	Cd-115	2.45E+10	Pm-149	1.47E+12
Ge-78	2.57E+10	Cd-115M	2.40E+09	Pr-150	1.75E+04

Continued on next page

Die approbierte gedruckte Originalversion dieser Dissertation ist an der TU Wien Bibliothek verfügbar.
The approved original version of this doctoral thesis is available in print at TU Wien Bibliothek.
TU Bibliothek Your knowledge hub WIEN

Table B.7 – *Continued from previous page*

Isotope	Activity[Bq]	Isotope	Activity[Bq]	Isotope	Activity[Bq]
As-78	2.70E+10	In-115M	2.45E+10	Pm-150	2.28E+09
Ge-79	3.60E+08	Pd-116	3.81E+03	Nd-151	4.17E+11
As-79	4.94E+10	Ag-116	3.67E+09	Pm-151	5.59E+11
Se-79	1.21E+06	Ag-116M	7.38E+03	Sm-151	4.29E+09
Se-79M	6.26E+10	In-116	6.11E+02	Ce-152	3.17E+03
Ge-80	1.58E+07	In-116M	2.51E+09	Pr-152	7.79E+03
As-80	5.00E+07	Pd-117	2.55E-09	Nd-152	2.60E+11
Br-80	8.50E+05	Ag-117	7.02E+08	Pm-152	3.24E+11
Br-80M	4.26E+05	Ag-117M	2.46E-07	Pm-152M	3.04E+09
Ge-81	7.19E+01	Cd-117	1.67E+10	Eu-152	5.44E+07
As-81	3.74E+08	Cd-117M	9.01E+09	Eu-152M	7.12E+08
Se-81	2.37E+11	In-117	1.56E+10	Pr-153	2.35E-02
Se-81M	8.25E+09	In-117M	1.98E+10	Nd-153	8.04E+09
Ge-82	3.65E-10	Sn-117M	1.35E+06	Pm-153	1.38E+11
As-82	9.72E+06	Cd-118	2.61E+10	Sm-153	2.90E+11
As-82M	5.06E+03	In-118	2.61E+10	Gd-153	1.79E+07
Br-82	1.59E+09	In-118M	2.68E+06	Nd-154	3.25E+08
Br-82M	3.83E+08	Ag-119	3.31E-06	Pm-154	3.17E+10
As-83	5.08E+04	Cd-119	9.16E+09	Pm-154M	1.70E+09
Se-83	2.22E+11	Cd-119M	4.40E+09	Eu-154	1.53E+09
Se-83M	2.26E+10	In-119	5.30E+09	Nd-155	5.64E+06
Br-83	6.88E+11	In-119M	1.92E+10	Pm-155	2.60E+08
Kr-83M	6.95E+11	Sn-119M	3.21E+08	Sm-155	4.57E+10
As-84	1.66E-05	Cd-120	3.73E+08	Eu-155	7.99E+09
Se-84	4.28E+11	In-120	7.85E+08	Nd-156	1.29E+08
Br-84	1.25E+12	In-120M	1.99E+08	Pm-156	1.67E+08
Br-84M	1.35E+10	Cd-121	1.10E+03	Sm-156	2.20E+10
Se-85	2.99E+09	In-121	1.73E+07	Eu-156	4.25E+10
Se-85M	5.82E+06	In-121M	2.14E+09	Pm-157	2.58E+08
Br-85	5.40E+11	Sn-121	2.90E+10	Sm-157	8.04E+09
Kr-85	3.52E+10	Sn-121M	2.63E+05	Eu-157	1.21E+10

Continued on next page

Die approbierte gedruckte Originalversion dieser Dissertation ist an der TU Wien Bibliothek verfügbar.
The approved original version of this doctoral thesis is available in print at TU Wien Bibliothek.
TU Bibliothek Your knowledge hub WIEN

Table B.7 – *Continued from previous page*

Isotope	Activity[Bq]	Isotope	Activity[Bq]	Isotope	Activity[Bq]
Kr-85M	1.63E+12	Cd-122	1.33E-07	Nd-158	1.22E-04
Se-86	3.17E+06	In-122	1.85E+01	Pm-158	2.36E-04
Br-86	2.97E+10	Sb-122	2.51E+08	Sm-158	5.26E+09
Br-86M	2.17E+06	Sb-122M	9.49E+05	Eu-158	6.06E+09
Rb-86	6.93E+08	Cd-123	1.18E-01	Sm-159	4.77E+08
Rb-86M	3.57E+06	In-123	3.14E-01	Eu-159	2.03E+09
Se-87	1.30E-05	In-123M	1.17E+08	Gd-159	2.34E+09
Br-87	5.78E+10	Sn-123	8.01E+09	Sm-160	3.79E+08
Kr-87	3.19E+12	Sn-123M	2.53E+10	Eu-160	4.45E+08
Sr-87M	1.56E+06	Te-123M	9.47E+04	Tb-160	4.01E+07
Br-88	4.75E+06	Cd-124	6.71E+04	Sm-161	4.75E+00
Kr-88	4.58E+12	In-124	8.25E+04	Eu-161	1.84E+06
Rb-88	4.70E+12	Sb-124	1.66E+08	Gd-161	1.55E+08
Br-89	1.77E-09	Sb-124M	9.37E+05	Tb-161	3.41E+08
Kr-89	1.89E+12	In-125M	1.94E+02	Sm-162	3.05E+02
Rb-89	5.58E+12	Sn-125	2.31E+10	Eu-162	4.74E+07
Sr-89	6.15E+12	Sn-125M	2.50E+10	Gd-162	1.43E+08
Y -9M	5.07E-01	Sb-125	1.96E+10	Tb-162	1.66E+08
Kr-90	6.78E+09	Te-125M	3.95E+09	Tb-162M	4.77E+06
Rb-90	1.82E+12	Sn-126	1.15E+06	Eu-163	9.50E+00
Rb-90M	5.88E+11	Sb-126	1.48E+09	Gd-163	6.61E+06
Sr-90	2.82E+11	Sb-126M	5.81E+08	Tb-163	6.22E+07
Y-90	2.84E+11	Sn-127	1.38E+11	Gd-164	2.32E+07
Y-90M	1.80E+07	Sn-127M	2.86E+10	Tb-164	2.72E+07
Kr-91	5.12E+01	Sb-127	2.22E+11	Gd-165	1.17E+06
Rb-91	1.86E+11	Te-127	2.21E+11	Tb-165	1.73E+06
Sr-91	7.49E+12	Te-127M	3.02E+10	Dy-165	2.87E+07
Y-91	7.60E+12	Sn-128	4.66E+11	Dy-165M	2.55E+06
Y-91M	4.36E+12	Sb-128	2.23E+10	Dy-166	9.03E+06
Rb-92	4.37E-09	Sb-128M	5.04E+11	Ho-166	9.86E+06
Sr-92	7.55E+12	I-128	1.41E+09		

Continued on next page

Die approbierte gedruckte Originalversion dieser Dissertation ist an der TU Wien Bibliothek verfügbar.
The approved original version of this doctoral thesis is available in print at TU Wien Bibliothek.
TU Bibliothek Your knowledge hub WIEN

Table B.7 – *Continued from previous page*

Isotope	Activity[Bq]	Isotope	Activity[Bq]	Isotope	Activity[Bq]
Y-92	7.73E+12	Sn-129	1.85E+11		
Rb-93	1.88E-04	Sn-129M	1.07E+11		
Sr-93	5.08E+12	Sb-129	9.12E+11		
Y-93	8.33E+12	Te-129	9.05E+11		
Zr-93	6.19E+06	Te-129M	1.36E+11		
Nb-93M	2.34E+05	I-129	6.74E+04		
Sr-94	4.23E+11	Xe-129M	6.62E+04		
Y-94	7.06E+12	Sn-130	4.67E+11		

Table B.7: Inventory of averaged fuel element in C ring in 2025

Isotope	Activity[Bq]	Isotope	Activity[Bq]	Isotope	Activity[Bq]
C-14	1.10E+06	Zr-95	7.24E+12	Sb-131	2.52E+12
N-16	2.04E-09	Nb-95	7.24E+12	Te-131	2.89E+12
O-19	2.96E-01	Nb-95M	5.08E+10	Te-131M	4.13E+11
Mg-27	6.01E+05	Y-96	1.40E+12	I-131	3.26E+12
Al-28	2.09E+08	Nb-96	1.42E+09	Xe-131M	3.62E+10
Al-29	2.06E+07	Zr-97	6.55E+12	Sn-132	2.82E+09
Si-31	6.31E+08	Nb-97	6.60E+12	Sb-132	5.68E+11
P-32	9.84E+08	Nb-97M	6.21E+12	Sb-132M	5.04E+11
P-33	3.40E+04	Zr-98	5.59E+09	Te-132	4.83E+12
P-34	4.23E-03	Nb-98	6.15E+09	I-132	4.85E+12
S-35	2.25E+07	Nb-98M	2.91E+10	Cs-132	6.29E+07
S-37	2.79E+04	Nb-99	1.79E+06	Sb-133	5.52E+11
Sc-47	7.87E+02	Nb-99M	4.15E+10	Te-133	3.69E+12
Sc-48	8.72E+02	Mo-99	6.73E+12	Te-133M	3.06E+12
Ti-51	1.81E+06	Tc-99	3.57E+07	I-133	7.57E+12
V-52	1.65E+09	Tc-99M	5.90E+12	I-133M	3.96E+00
V-53	3.01E+06	Zr-100	2.44E-01	Xe-133	7.57E+12
V-54	5.46E+03	Nb-100	1.85E-01	Xe-133M	2.22E+11
Cr-51	6.44E+11	Nb-100M	1.85E-01	Sb-134	7.01E+02
Cr-55	3.00E+09	Tc-100	8.03E+04	Sb-134M	3.80E+02

Continued on next page

Die approbierte gedruckte Originalversion dieser Dissertation ist an der TU Wien Bibliothek verfügbar.
The approved original version of this doctoral thesis is available in print at TU Wien Bibliothek.
TU Bibliothek Your knowledge hub WIEN

Table B.8 – *Continued from previous page*

Isotope	Activity[Bq]	Isotope	Activity[Bq]	Isotope	Activity[Bq]
Mn-54	2.59E+10	Nb-101	2.36E-01	Te-134	6.89E+12
Mn-56	1.46E+12	Mo-101	4.51E+12	I-134	8.48E+12
Mn-57	8.44E+06	Tc-101	5.59E+12	I-134M	1.92E+11
Mn-58	9.44E+03	Zr-102	9.60E+08	Cs-134	2.75E+10
Fe-55	1.31E+11	Nb-102	1.07E+09	Cs-134M	1.09E+10
Fe-59	1.08E+10	Mo-102	3.54E+12	Te-135	4.12E+07
Co-58	7.09E+10	Tc-102	3.57E+12	I-135	6.99E+12
Co-60	1.70E+08	Tc-102M	6.86E+08	Xe-135	5.64E+12
Co-60M	3.49E+07	Rh-102	1.68E+05	Xe-135M	1.24E+12
Co-61	3.08E+07	Nb-103	2.21E+06	Cs-135	2.79E+06
Co-62	5.14E+05	Mo-103	1.17E+11	Cs-135M	1.08E+09
Ni-59	2.44E+07	Tc-103	4.09E+11	Ba-135M	1.12E+06
Ni-63	3.01E+09	Ru-103	3.61E+12	Te-136	6.23E+07
Ni-65	7.00E+09	Rh-103M	3.25E+12	I-136	2.97E+11
Ni-66	5.58E+03	Mo-104	2.19E+11	I-136M	1.86E+10
Cu-64	9.80E+05	Tc-104	1.95E+12	Cs-136	2.81E+10
Cu-66	1.11E+06	Rh-104	7.37E+09	Ba-136M	4.64E+09
Actinides	Daughters	Rh-104M	5.44E+09	I-137	5.08E+08
Th-231	2.82E+06	Mo-105	1.95E+10	Xe-137	2.76E+12
Th-233	2.12E+03	Tc-105	8.74E+11	Cs-137	2.57E+11
Th-234	1.90E+06	Ru-105	1.24E+12	Ba-137M	2.43E+11
Pa-232	2.52E+05	Rh-105	1.24E+12	I-138	2.60E-03
Pa-233	9.76E+04	Rh-105M	3.48E+11	Xe-138	5.41E+12
Pa-234M	1.90E+06	Mo-106	1.22E+01	Cs-138	7.41E+12
Pa-234	2.58E+03	Tc-106	1.81E+09	Cs-138M	7.91E+10
U-232	2.01E+03	Ru-106	3.56E+11	Xe-139	2.24E+10
U-234	3.02E+04	Rh-106	3.56E+11	Cs-139	5.14E+12
U-235	2.82E+06	Rh-106M	2.93E+09	Ba-139	7.19E+12
U-236	1.21E+06	Mo-107	2.16E-04	Xe-140	4.03E+05
U-237	3.20E+11	Tc-107	1.52E+08	Cs-140	2.44E+11
U-238	1.90E+06	Ru-107	1.28E+11	Ba-140	6.96E+12

Continued on next page

Die approbierte gedruckte Originalversion dieser Dissertation ist an der TU Wien Bibliothek verfügbar.
The approved original version of this doctoral thesis is available in print at TU Wien Bibliothek.
TU Bibliothek Your knowledge hub WIEN

Table B.8 – *Continued from previous page*

Isotope	Activity[Bq]	Isotope	Activity[Bq]	Isotope	Activity[Bq]
U-239	7.82E+12	Rh-107	2.58E+11	La-140	6.98E+12
U-240	1.84E+06	Pd-107	4.38E+04	Pr-140	1.67E+06
Np-236M	1.94E+05	Pd-107M	7.91E+01	Cs-141	7.91E+08
Np-237	9.52E+04	Tc-108	6.58E-08	Ba-141	5.49E+12
Np-238	8.09E+09	Ru-108	6.26E+10	La-141	6.60E+12
Np-239	9.13E+12	Rh-108	6.67E+10	Ce-141	6.61E+12
Np-240M	1.26E+08	Rh-108M	2.13E+08	Ba-142	4.61E+12
Np-240	7.65E+08	Tc-109	5.69E+08	La-142	6.54E+12
Pu-236	1.24E+04	Ru-109	1.70E+09	Pr-142	1.61E+10
Pu-237	1.02E+04	Rh-109	2.20E+10	Pr-142M	2.69E+09
Pu-238	3.88E+07	Rh-109M	3.54E+09	Ba-143	6.23E+05
Pu-239	3.71E+08	Pd-109	7.63E+10	La-143	5.15E+12
Pu-240	5.78E+07	Pd-109M	2.99E+10	Ce-143	6.61E+12
Pu-241	2.11E+09	Ag-109M	7.63E+10	Pr-143	6.61E+12
Pu-243	1.62E+07	Ru-110	5.41E+04	Ba-144	1.08E+04
Am-241	1.36E+06	Rh-110	5.60E+07	La-144	3.26E+10
Am-242M	1.36E+04	Ag-110	1.70E+06	Ce-144	4.71E+12
Am-242	8.22E+07	Ag-110M	9.21E+07	Pr-144	4.72E+12
Am-244M	1.88E+05	Ru-111	2.11E+04	Pr-144M	5.66E+10
Am-244	1.13E+04	Rh-111	1.49E+09	Ba-145	1.02E-03
Cm-242	2.42E+07	Pd-111	3.45E+10	La-145	2.48E+09
Cm-244	2.34E+03	Pd-111M	3.39E+08	Ce-145	1.56E+12
Fission	Products	Ag-111	3.84E+10	Pr-145	4.37E+12
H-3	1.11E+09	Ag-111M	3.57E+10	La-146	9.88E+00
Cu-72	1.63E-08	Cd-111M	3.67E+04	Ce-146	2.60E+12
Zn-72	9.51E+07	Rh-112	1.70E-10	Pr-146	3.29E+12
Ga-72	9.53E+07	Pd-112	2.75E+10	Pm-146	8.44E+05
Zn-73	2.94E+04	Ag-112	2.78E+10	La-147	3.83E+02
Ga-73	3.03E+08	Pd-113	2.36E+09	Ce-147	1.18E+11
Ge-73M	3.03E+08	Ag-113	2.35E+10	Pr-147	2.09E+12
Zn-74	7.30E+07	Ag-113M	6.15E+08	Nd-147	2.56E+12

Continued on next page

Die approbierte gedruckte Originalversion dieser Dissertation ist an der TU Wien Bibliothek verfügbar.
The approved original version of this doctoral thesis is available in print at TU Wien Bibliothek.
TU Bibliothek Your knowledge hub WIEN

Table B.8 – *Continued from previous page*

Isotope	Activity[Bq]	Isotope	Activity[Bq]	Isotope	Activity[Bq]
Ga-74	5.77E+08	Cd-113M	3.74E+07	Pm-147	8.35E+11
Zn-75	4.38E-02	Ru-114	6.39E-10	Ba-148	1.42E-06
Ga-75	2.84E+08	Rh-114	9.63E-10	La-148	1.82E-06
Ge-75	1.77E+09	Pd-114	5.21E+09	Ce-148	1.06E+10
Ge-75M	1.92E+07	Ag-114	5.38E+09	Pr-148	5.44E+11
Zn-76	8.91E-09	In-114	1.34E+05	Pm-148	1.64E+11
Ga-76	1.86E+06	In-114M	1.31E+05	Pm-148M	6.09E+10
As-76	5.58E+06	Rh-115	1.64E-06	Pr-149	2.49E+11
Ga-77	5.17E+02	Pd-115	7.51E+07	Nd-149	1.21E+12
Ge-77	3.99E+09	Ag-115	1.43E+10	Pm-149	1.26E+12
Ge-77M	2.21E+08	Ag-115M	3.67E+07	Pr-150	1.52E+04
As-77	1.15E+10	Cd-115	2.11E+10	Pm-150	1.76E+09
Se-77M	2.86E+07	Cd-115M	2.07E+09	Nd-151	3.60E+11
Ga-78	9.83E-10	In-115M	2.11E+10	Pm-151	4.83E+11
Ge-78	2.22E+10	Pd-116	3.28E+03	Sm-151	3.96E+09
As-78	2.34E+10	Ag-116	3.16E+09	Ce-152	2.74E+03
Ge-79	3.11E+08	Ag-116M	6.36E+03	Pr-152	6.73E+03
As-79	4.28E+10	In-116	4.63E+02	Nd-152	2.25E+11
Se-79	1.05E+06	In-116M	1.90E+09	Pm-152	2.80E+11
Se-79M	5.41E+10	Pd-117	2.20E-09	Pm-152M	2.61E+09
Ge-80	1.37E+07	Ag-117	6.05E+08	Eu-152	4.53E+07
As-80	4.33E+07	Ag-117M	2.13E-07	Eu-152M	5.95E+08
Br-80	7.25E+05	Cd-117	1.44E+10	Pr-153	2.03E-02
Br-80M	3.62E+05	Cd-117M	7.76E+09	Nd-153	6.94E+09
Ge-81	6.22E+01	In-117	1.35E+10	Pm-153	1.20E+11
As-81	3.25E+08	In-117M	1.71E+10	Sm-153	2.41E+11
Se-81	2.05E+11	Sn-117M	8.79E+05	Gd-153	1.27E+07
Se-81M	7.14E+09	Cd-118	2.25E+10	Nd-154	2.80E+08
Ge-82	3.16E-10	In-118	2.25E+10	Pm-154	2.73E+10
As-82	8.41E+06	In-118M	2.28E+06	Pm-154M	1.46E+09
As-82M	4.38E+03	Ag-119	2.85E-06	Eu-154	1.16E+09

Continued on next page

Die approbierte gedruckte Originalversion dieser Dissertation ist an der TU Wien Bibliothek verfügbar.
The approved original version of this doctoral thesis is available in print at TU Wien Bibliothek.
TU Bibliothek Your knowledge hub WIEN

Table B.8 – *Continued from previous page*

Isotope	Activity[Bq]	Isotope	Activity[Bq]	Isotope	Activity[Bq]
Br-82	1.21E+09	Cd-119	7.90E+09	Nd-155	4.85E+06
Br-82M	2.92E+08	Cd-119M	3.79E+09	Pm-155	2.23E+08
As-83	4.39E+04	In-119	4.57E+09	Sm-155	3.92E+10
Se-83	1.92E+11	In-119M	1.66E+10	Eu-155	7.13E+09
Se-83M	1.96E+10	Sn-119M	2.77E+08	Nd-156	1.11E+08
Br-83	5.95E+11	Cd-120	3.22E+08	Pm-156	1.43E+08
Kr-83M	6.02E+11	In-120	6.77E+08	Sm-156	1.88E+10
As-84	1.43E-05	In-120M	1.71E+08	Eu-156	3.45E+10
Se-84	3.70E+11	Cd-121	9.51E+02	Pm-157	2.21E+08
Br-84	1.08E+12	In-121	1.49E+07	Sm-157	6.86E+09
Br-84M	1.17E+10	In-121M	1.85E+09	Eu-157	1.03E+10
Se-85	2.59E+09	Sn-121	2.50E+10	Nd-158	1.04E-04
Se-85M	5.04E+06	Sn-121M	2.28E+05	Pm-158	2.01E-04
Br-85	4.68E+11	Cd-122	1.14E-07	Sm-158	4.48E+09
Kr-85	3.06E+10	In-122	1.60E+01	Eu-158	5.16E+09
Kr-85M	1.41E+12	Sb-122	1.87E+08	Sm-159	4.03E+08
Se-86	2.74E+06	Sb-122M	7.11E+05	Eu-159	1.72E+09
Br-86	2.57E+10	Cd-123	1.02E-01	Gd-159	1.97E+09
Br-86M	1.88E+06	In-123	2.70E-01	Sm-160	3.21E+08
Rb-86	5.29E+08	In-123M	1.01E+08	Eu-160	3.77E+08
Rb-86M	2.90E+06	Sn-123	6.90E+09	Tb-160	2.98E+07
Se-87	1.13E-05	Sn-123M	2.18E+10	Sm-161	3.96E+00
Br-87	5.00E+10	Te-123M	6.16E+04	Eu-161	1.54E+06
Kr-87	2.76E+12	Cd-124	5.79E+04	Gd-161	1.30E+08
Sr-87M	1.31E+06	In-124	7.12E+04	Tb-161	2.84E+08
Br-88	4.11E+06	Sb-124	1.26E+08	Sm-162	2.59E+02
Kr-88	3.96E+12	Sb-124M	7.97E+05	Eu-162	3.98E+07
Rb-88	4.07E+12	In-125M	1.67E+02	Gd-162	1.19E+08
Br-89	1.53E-09	Sn-125	1.99E+10	Tb-162	1.38E+08
Kr-89	1.64E+12	Sn-125M	2.15E+10	Tb-162M	3.95E+06
Rb-89	4.82E+12	Sb-125	1.70E+10	Eu-163	8.00E+00

Continued on next page

Die approbierte gedruckte Originalversion dieser Dissertation ist an der TU Wien Bibliothek verfügbar.
The approved original version of this doctoral thesis is available in print at TU Wien Bibliothek.
TU Bibliothek Your knowledge hub WIEN

Table B.8 – *Continued from previous page*

Isotope	Activity[Bq]	Isotope	Activity[Bq]	Isotope	Activity[Bq]
Sr-89	5.32E+12	Te-125M	3.91E+09	Gd-163	5.51E+06
Y-89M	4.31E-01	Sn-126	1.00E+06	Tb-163	5.17E+07
Kr-90	5.90E+09	Sb-126	1.27E+09	Gd-164	1.94E+07
Rb-90	1.57E+12	Sb-126M	4.98E+08	Tb-164	2.27E+07
Rb-90M	5.09E+11	Sn-127	1.19E+11	Gd-165	9.81E+05
Sr-90	2.46E+11	Sn-127M	2.46E+10	Tb-165	1.46E+06
Y-90	2.47E+11	Sb-127	1.91E+11	Dy-165	2.28E+07
Y-90M	1.53E+07	Te-127	1.90E+11	Dy-165M	2.11E+06
Kr-91	4.43E+01	Te-127M	2.60E+10	Dy-166	7.53E+06
Rb-91	1.61E+11	Sn-128	4.03E+11	Ho-166	8.12E+06
Sr-91	6.48E+12	Sb-128	1.91E+10		
Y-91	6.51E+12	Sb-128M	4.35E+11		
Y-91M	3.78E+12	I-128	1.06E+09		
Rb-92	3.78E-09	Sn-129	1.60E+11		
Sr-92	6.53E+12	Sn-129M	9.27E+10		
Y-92	6.69E+12	Sb-129	7.87E+11		
Rb-93	1.62E-04	Te-129	7.81E+11		
Sr-93	4.40E+12	Te-129M	1.17E+11		
Y-93	7.20E+12	I-129	5.87E+04		
Zr-93	5.40E+06	Xe-129M	4.45E+04		
Nb-93M	2.07E+05	Sn-130	4.04E+11		
Sr-94	3.66E+11	Sb-130	2.27E+11		
Y-94	6.11E+12	Sb-130M	1.08E+12		
Nb-94M	3.30E+05	I-130	5.80E+09		
Sr-95	1.34E+09	I-130M	1.59E+09		
Y-95	5.23E+12	Sn-131	3.44E+10		

Table B.8: Inventory of averaged fuel element in D ring in 2025

Isotope	Activity[Bq]	Isotope	Activity[Bq]	Isotope	Activity[Bq]
C-14	8.65E+05	Nb-95	5.63E+12	I-131	2.54E+12
N-16	1.57E-09	Nb-95M	3.95E+10	Xe-131M	2.82E+10

Continued on next page

Die approbierte gedruckte Originalversion dieser Dissertation ist an der TU Wien Bibliothek verfügbar.
The approved original version of this doctoral thesis is available in print at TU Wien Bibliothek.
TU Bibliothek Your knowledge hub WIEN

Table B.9 – *Continued from previous page*

Isotope	Activity[Bq]	Isotope	Activity[Bq]	Isotope	Activity[Bq]
O-19	2.28E-01	Y-96	1.09E+12	Sn-132	2.20E+09
Mg-27	4.62E+05	Nb-96	9.66E+08	Sb-132	4.43E+11
Al-28	1.60E+08	Zr-97	5.11E+12	Sb-132M	3.93E+11
Al-29	1.58E+07	Nb-97	5.14E+12	Te-132	3.76E+12
Si-31	4.85E+08	Nb-97M	4.84E+12	I-132	3.78E+12
P-32	7.56E+08	Zr-98	4.35E+09	Cs-132	3.84E+07
P-33	2.61E+04	Nb-98	4.79E+09	Sb-133	4.31E+11
P-34	3.25E-03	Nb-98M	2.25E+10	Te-133	2.87E+12
S-35	1.73E+07	Nb-99	1.39E+06	Te-133M	2.39E+12
S-37	2.14E+04	Nb-99M	3.22E+10	I-133	5.90E+12
Sc-47	4.77E+02	Mo-99	5.24E+12	I-133M	3.07E+00
Sc-48	5.30E+02	Tc-99	2.84E+07	Xe-133	5.90E+12
Ti-51	1.39E+06	Tc-99M	4.60E+12	Xe-133M	1.73E+11
V-52	1.24E+09	Zr100	1.90E-01	Sb-134	5.46E+02
V-53	2.31E+06	Nb-100	1.44E-01	Sb-134M	2.96E+02
V-54	4.19E+03	Nb-100M	1.44E-01	Te-134	5.37E+12
Cr-51	4.95E+11	Tc-100	4.91E+04	I-134	6.61E+12
Cr-55	2.30E+09	Nb-101	1.84E-01	I-134M	1.49E+11
Mn-54	2.02E+10	Mo-101	3.51E+12	Cs-134	1.72E+10
Mn-56	1.12E+12	Tc-101	4.35E+12	Cs-134M	6.67E+09
Mn-57	6.46E+06	Zr-102	7.48E+08	Te-135	3.21E+07
Mn-58	7.25E+03	Nb-102	8.35E+08	I-135	5.45E+12
Fe-55	1.03E+11	Mo-102	2.75E+12	Xe-135	4.64E+12
Fe-59	8.29E+09	Tc-102	2.77E+12	Xe-135M	9.65E+11
Co-58	5.54E+10	Tc-102M	5.24E+08	Cs-135	2.35E+06
Co-60	1.32E+08	Rh-102	1.05E+05	Cs-135M	7.20E+08
Co-60M	1.97E+07	Nb-103	1.72E+06	Ba-135M	6.50E+05
Co-61	2.36E+07	Mo-103	9.10E+10	Te-136	4.86E+07
Co-62	3.96E+05	Tc-103	3.18E+11	I-136	2.31E+11
Ni-59	1.93E+07	Ru-103	2.81E+12	I-136M	1.45E+10
Ni-63	2.38E+09	Rh-103M	2.53E+12	Cs-136	1.92E+10

Continued on next page

Die approbierte gedruckte Originalversion dieser Dissertation ist an der TU Wien Bibliothek verfügbar.
The approved original version of this doctoral thesis is available in print at TU Wien Bibliothek.
TU Bibliothek Your knowledge hub WIEN

Table B.9 – *Continued from previous page*

Isotope	Activity[Bq]	Isotope	Activity[Bq]	Isotope	Activity[Bq]
Ni-65	5.38E+09	Mo-104	1.70E+11	Ba-136M	3.17E+09
Ni-66	3.29E+03	Tc-104	1.51E+12	I-137	3.96E+08
Cu-64	6.10E+05	Rh-104	4.53E+09	Xe-137	2.15E+12
Cu-66	6.72E+05	Rh-104M	3.34E+09	Cs-137	2.04E+11
Actinides	&Daugthers	Mo-105	1.51E+10	Ba-137M	1.93E+11
Th-231	2.86E+06	Tc-105	6.75E+11	I-138	2.03E-03
Th-233	1.33E+03	Ru-105	9.59E+11	Xe-138	4.22E+12
Th-234	1.90E+06	Rh-105	9.60E+11	Cs-138	5.77E+12
Pa-232	2.02E+05	Rh-105M	2.69E+11	Cs-138M	6.16E+10
Pa-233	6.60E+04	Mo-106	9.43E+00	Xe-139	1.75E+10
Pa-234M	1.90E+06	Tc-106	1.39E+09	Cs-139	4.01E+12
Pa-234	2.53E+03	Ru-106	2.76E+11	Ba-139	5.60E+12
U-232	1.64E+03	Rh-106	2.76E+11	Xe-140	3.14E+05
U-234	2.40E+04	Rh-106M	1.74E+09	Cs-140	1.90E+11
U-235	2.86E+06	Mo-107	1.67E-04	Ba-140	5.42E+12
U-236	9.61E+05	Tc-107	1.17E+08	La-140	5.44E+12
U-237	2.05E+11	Ru-107	9.68E+10	Pr-140	1.02E+06
U-238	1.90E+06	Rh-107	1.95E+11	Cs-141	6.16E+08
U-239	6.01E+12	Pd-107	3.43E+04	Ba-141	4.28E+12
U-240	1.08E+06	Pd-107M	4.82E+01	La-141	5.14E+12
Np-236M	1.01E+05	Tc-108	5.02E-08	Ce-141	5.15E+12
Np-237	6.45E+04	Ru-108	4.68E+10	Ba-142	3.59E+12
Np-238	4.21E+09	Rh-108	4.99E+10	La-142	5.10E+12
Np-239	7.02E+12	Rh-108M	1.37E+08	Pr-142	9.86E+09
Np-240M	7.45E+07	Tc-109	4.28E+08	Pr-142M	1.64E+09
Np-240	4.52E+08	Ru-109	1.28E+09	Ba-143	4.86E+05
Pu-236	6.75E+03	Rh-109	1.63E+10	La-143	4.01E+12
Pu-237	6.11E+03	Rh-109M	2.65E+09	Ce-143	5.15E+12
Pu-238	2.12E+07	Pd-109	5.64E+10	Pr-143	5.15E+12
Pu-239	3.00E+08	Pd-109M	2.22E+10	Ba-144	8.39E+03
Pu-240	3.73E+07	Ag-109M	5.64E+10	La-144	2.54E+10

Continued on next page

Die approbierte gedruckte Originalversion dieser Dissertation ist an der TU Wien Bibliothek verfügbar.
The approved original version of this doctoral thesis is available in print at TU Wien Bibliothek.
TU Bibliothek Your knowledge hub WIEN

Table B.9 – *Continued from previous page*

Isotope	Activity[Bq]	Isotope	Activity[Bq]	Isotope	Activity[Bq]
Pu-241	1.07E+09	Ru-110	4.09E+04	Ce-144	3.70E+12
Pu-243	4.98E+06	Rh-110	4.23E+07	Pr-144	3.70E+12
Am-241	7.09E+05	Ag-110	1.03E+06	Pr-144M	4.44E+10
Am-242M	5.71E+03	Ag-110M	5.59E+07	Ba-145	7.94E-04
Am-242	3.30E+07	Ru-111	1.62E+04	La-145	1.93E+09
Am-244M	4.54E+04	Rh-111	1.14E+09	Ce-145	1.21E+12
Am-244	2.73E+03	Pd-111	2.63E+10	Pr-145	3.40E+12
Cm-242	9.84E+06	Pd-111M	2.54E+08	La-146	7.70E+00
Fission	Products	Ag-111	2.94E+10	Ce-146	2.02E+12
H-3	8.79E+08	Ag-111M	2.73E+10	Pr-146	2.56E+12
Cu-72	1.27E-08	Rh-112	1.31E-10	Pm-146	5.30E+05
Zn-72	7.37E+07	Pd-112	2.12E+10	La-147	2.99E+02
Ga-72	7.39E+07	Ag-112	2.14E+10	Ce-147	9.23E+10
Zn-73	2.29E+04	Pd-113	1.82E+09	Pr-147	1.63E+12
Ga-73	2.35E+08	Ag-113	1.82E+10	Nd-147	2.00E+12
Ge-73M	2.35E+08	Ag-113M	4.75E+08	Pm-147	6.68E+11
Zn-74	5.68E+07	Cd-113M	2.95E+07	Ba-148	1.10E-06
Ga-74	4.49E+08	Ru-114	4.95E-10	La-148	1.42E-06
Zn-75	3.41E-02	Rh-114	7.46E-10	Ce-148	8.29E+09
Ga-75	2.21E+08	Pd-114	4.03E+09	Pr-148	4.24E+11
Ge-75	1.37E+09	Ag-114	4.17E+09	Pm-148	1.01E+11
Ge-75M	1.50E+07	In-114	8.33E+04	Pm-148M	4.01E+10
Zn-76	6.95E-09	In-114M	8.15E+04	Pr-149	1.94E+11
Ga-76	1.45E+06	Rh-115	1.27E-06	Nd-149	9.42E+11
As-76	3.44E+06	Pd-115	5.82E+07	Pm-149	9.72E+11
Ga-77	4.03E+02	Ag-115	1.11E+10	Pr-150	1.18E+04
Ge-77	3.11E+09	Ag-115M	2.85E+07	Pm-150	1.15E+09
Ge-77M	1.72E+08	Cd-115	1.63E+10	Nd-151	2.80E+11
As-77	8.99E+09	Cd-115M	1.60E+09	Pm-151	3.75E+11
Se-77M	2.23E+07	In-115M	1.63E+10	Sm-151	3.41E+09
Ga-78	7.67E-10	Pd-116	2.55E+03	Ce-152	2.13E+03

Continued on next page

Die approbierte gedruckte Originalversion dieser Dissertation ist an der TU Wien Bibliothek verfügbar.
The approved original version of this doctoral thesis is available in print at TU Wien Bibliothek.
TU Bibliothek Your knowledge hub WIEN

Table B.9 – *Continued from previous page*

Isotope	Activity[Bq]	Isotope	Activity[Bq]	Isotope	Activity[Bq]
Ge-78	1.73E+10	Ag-116	2.45E+09	Pr-152	5.23E+03
As-78	1.82E+10	Ag-116M	4.93E+03	Nd-152	1.74E+11
Ge-79	2.42E+08	In-116	2.89E+02	Pm-152	2.17E+11
As-79	3.33E+10	In-116M	1.19E+09	Pm-152M	2.02E+09
Se-79	8.37E+05	Pd-117	1.71E-09	Eu-152	3.28E+07
Se-79M	4.22E+10	Ag-117	4.70E+08	Eu-152M	4.30E+08
Ge-80	1.06E+07	Ag-117M	1.65E-07	Pr-153	1.58E-02
As-80	3.37E+07	Cd-117	1.11E+10	Nd-153	5.39E+09
Br-80	5.55E+05	Cd-117M	6.02E+09	Pm-153	9.28E+10
Br-80M	2.74E+05	In-117	1.04E+10	Sm-153	1.77E+11
Ge-81	4.85E+01	In-117M	1.32E+10	Gd-153	7.03E+06
As-81	2.53E+08	Sn-117M	4.28E+05	Nd-154	2.17E+08
Se-81	1.60E+11	Cd-118	1.75E+10	Pm-154	2.11E+10
Se-81M	5.56E+09	In-118	1.75E+10	Pm-154M	1.13E+09
Ge-82	2.47E-10	In-118M	1.74E+06	Eu-154	7.22E+08
As-82	6.56E+06	Ag-119	2.21E-06	Nd-155	3.76E+06
As-82M	3.41E+03	Cd-119	6.12E+09	Pm-155	1.73E+08
Br-82	7.64E+08	Cd-119M	2.94E+09	Sm-155	3.02E+10
Br-82M	1.86E+08	In-119	3.54E+09	Eu-155	5.86E+09
As-83	3.43E+04	In-119M	1.28E+10	Nd-156	8.55E+07
Se-83	1.50E+11	Sn-119M	2.16E+08	Pm-156	1.10E+08
Se-83M	1.53E+10	Cd-120	2.50E+08	Sm-156	1.44E+10
Br-83	4.64E+11	In-120	5.25E+08	Eu-156	2.44E+10
Kr-83M	4.69E+11	In-120M	1.33E+08	Pm-157	1.69E+08
As-84	1.12E-05	Cd-121	7.37E+02	Sm-157	5.24E+09
Se-84	2.89E+11	In-121	1.16E+07	Eu-157	7.81E+09
Br-84	8.41E+11	In-121M	1.43E+09	Nd-158	7.99E-05
Br-84M	9.07E+09	Sn-121	1.94E+10	Pm-158	1.54E-04
Se-85	2.02E+09	Sn-121M	1.80E+05	Sm-158	3.42E+09
Se-85M	3.93E+06	Cd-122	8.88E-08	Eu-158	3.94E+09
Br-85	3.65E+11	In-122	1.24E+01	Sm-159	3.05E+08

Continued on next page

Die approbierte gedruckte Originalversion dieser Dissertation ist an der TU Wien Bibliothek verfügbar.
The approved original version of this doctoral thesis is available in print at TU Wien Bibliothek.
TU Bibliothek Your knowledge hub WIEN

Table B.9 – *Continued from previous page*

Isotope	Activity[Bq]	Isotope	Activity[Bq]	Isotope	Activity[Bq]
Kr-85	2.43E+10	Sb-122	1.14E+08	Eu-159	1.30E+09
Kr-85M	1.10E+12	Sb-122M	4.37E+05	Gd-159	1.48E+09
Se-86	2.14E+06	Cd-123	7.90E-02	Sm-160	2.43E+08
Br-86	2.01E+10	In-123	2.10E-01	Eu-160	2.85E+08
Br-86M	1.47E+06	In-123M	7.81E+07	Tb-160	1.81E+07
Rb-86	3.38E+08	Sn-123	5.37E+09	Sm-161	2.93E+00
Rb-86M	2.06E+06	Sn-123M	1.69E+10	Eu-161	1.13E+06
Se-87	8.79E-06	Te-123M	3.00E+04	Gd-161	9.56E+07
Br-87	3.90E+10	Cd-124	4.50E+04	Tb-161	2.09E+08
Kr-87	2.15E+12	In-124	5.52E+04	Sm-162	1.97E+02
Sr-87M	9.75E+05	Sb-124	7.94E+07	Eu-162	2.98E+07
Br-88	3.21E+06	Sb-124M	6.07E+05	Gd-162	8.84E+07
Kr-88	3.09E+12	In-125M	1.29E+02	Tb-162	1.02E+08
Rb-88	3.17E+12	Sn-125	1.54E+10	Tb-162M	2.88E+06
Br-89	1.19E-09	Sn-125M	1.67E+10	Eu-163	6.01E+00
Kr-89	1.28E+12	Sb-125	1.34E+10	Gd-163	4.07E+06
Rb-89	3.77E+12	Te-125M	3.08E+09	Tb-163	3.80E+07
Sr-89	4.15E+12	Sn-126	7.93E+05	Gd-164	1.43E+07
Y-89M	3.27E-01	Sb-126	9.74E+08	Tb-164	1.68E+07
Kr-90	4.60E+09	Sb-126M	3.83E+08	Gd-165	7.35E+05
Rb-90	1.23E+12	Sn-127	9.24E+10	Tb-165	1.09E+06
Rb-90M	3.97E+11	Sn-127M	1.91E+10	Dy-165	1.56E+07
Sr-90	1.96E+11	Sb-127	1.48E+11	Dy-165M	1.54E+06
Y-90	1.96E+11	Te-127	1.47E+11	Dy-166	5.56E+06
Y-90M	1.16E+07	Te-127M	2.02E+10	Ho-166	5.89E+06
Kr-91	3.46E+01	Sn-128	3.13E+11		
Rb-91	1.25E+11	Sb-128	1.47E+10		
Sr-91	5.05E+12	Sb-128M	3.38E+11		
Y-91	5.08E+12	I-128	6.45E+08		
Y-91M	2.94E+12	Sn-129	1.24E+11		
Rb-92	2.95E-09	Sn-129M	7.22E+10		

Continued on next page

Die approbierte gedruckte Originalversion dieser Dissertation ist an der TU Wien Bibliothek verfügbar.
The approved original version of this doctoral thesis is available in print at TU Wien Bibliothek.
TU Bibliothek Your knowledge hub WIEN

Table B.9 – *Continued from previous page*

Isotope	Activity[Bq]	Isotope	Activity[Bq]	Isotope	Activity[Bq]
Sr-92	5.09E+12	Sb-129	6.12E+11		
Y-92	5.22E+12	Te-129	6.07E+11		
Rb-93	1.27E-04	Te-129M	9.11E+10		
Sr-93	3.43E+12	I-129	4.66E+04		
Y-93	5.62E+12	Sn-130	3.14E+11		
Zr-93	4.29E+06	Sb-130	1.76E+11		
Nb-93M	1.68E+05	Sb-130M	8.42E+11		
Sr-94	2.85E+11	I-130	3.58E+09		
Y-94	4.76E+12	I-130M	9.81E+08		
Nb-94M	2.48E+05	Sn-131	2.68E+10		
Sr-95	1.04E+09	Sb-131	1.96E+12		
Y-95	4.07E+12	Te-131	2.25E+12		
Zr-95	5.63E+12	Te-131M	3.21E+11		

Table B.9: Inventory of averaged fuel element in E ring in 2025

Isotope	Activity[Bq]	Isotope	Activity[Bq]	Isotope	Activity[Bq]
C-14	6.72E+05	Nb-95	4.25E+12	Te-131M	2.43E+11
N-16	1.17E-09	Nb-95M	2.98E+10	I-131	1.92E+12
O-19	1.70E-01	Y-96	8.25E+11	Xe-131M	2.13E+10
Mg-27	3.45E+05	Nb-96	6.44E+08	Sn-132	1.66E+09
Al-28	1.20E+08	Zr-97	3.86E+12	Sb-132	3.35E+11
Al-29	1.18E+07	Nb-97	3.89E+12	Sb-132M	2.97E+11
Si-31	3.63E+08	Nb-97M	3.66E+12	Te-132	2.84E+12
P-32	5.66E+08	Zr-98	3.29E+09	I-132	2.86E+12
P-33	1.95E+04	Nb-98	3.62E+09	Cs-132	2.25E+07
P-34	2.43E-03	Nb-98M	1.70E+10	Sb-133	3.26E+11
S-35	1.30E+07	Nb-99	1.05E+06	Te-133	2.17E+12
S-37	1.60E+04	Nb-99M	2.43E+10	Te-133M	1.80E+12
Sc-47	2.77E+02	Mo-99	3.96E+12	I-133	4.46E+12
Sc-48	3.08E+02	Tc-99	2.22E+07	I-133M	2.32E+00
Ti-51	1.03E+06	Tc-99M	3.47E+12	Xe-133	4.46E+12

Continued on next page

Die approbierte gedruckte Originalversion dieser Dissertation ist an der TU Wien Bibliothek verfügbar.
The approved original version of this doctoral thesis is available in print at TU Wien Bibliothek.
TU Bibliothek Your knowledge hub WIEN

Table B.10 – *Continued from previous page*

Isotope	Activity[Bq]	Isotope	Activity[Bq]	Isotope	Activity[Bq]
V-52	9.16E+08	Zr-100	1.44E-01	Xe-133M	1.30E+11
V-53	1.73E+06	Nb-100	1.09E-01	Sb-134	4.13E+02
V-54	3.13E+03	Nb-100M	1.09E-01	Sb-134M	2.24E+02
Cr-51	3.70E+11	Tc-100	2.87E+04	Te-134	4.06E+12
Cr-55	1.72E+09	Nb-101	1.39E-01	I-134	5.00E+12
Mn-54	1.53E+10	Mo-101	2.66E+12	I-134M	1.12E+11
Mn-56	8.38E+11	Tc-101	3.29E+12	Cs-134	1.04E+10
Mn-57	4.82E+06	Zr-102	5.66E+08	Cs-134M	3.91E+09
Mn-58	5.42E+03	Nb-102	6.32E+08	Te-135	2.43E+07
Fe-55	7.92E+10	Mo-102	2.08E+12	I-135	4.12E+12
Fe-59	6.19E+09	Tc-102	2.10E+12	Xe-135	3.69E+12
Co-58	4.20E+10	Tc-102M	3.90E+08	Xe-135M	7.29E+11
Co-60	1.01E+08	Rh-102	6.38E+04	Cs-135	1.92E+06
Co-60M	1.08E+07	Nb-103	1.30E+06	Cs-135M	4.82E+08
Co-61	1.76E+07	Mo-103	6.86E+10	Ba-135M	3.82E+05
Co-62	2.96E+05	Tc-103	2.40E+11	Te-136	3.68E+07
Ni-59	1.50E+07	Ru-103	2.12E+12	I-136	1.75E+11
Ni-63	1.85E+09	Rh-103M	1.91E+12	I-136M	1.10E+10
Ni-65	4.02E+09	Mo-104	1.28E+11	Cs-136	1.27E+10
Ni-66	1.84E+03	Tc-104	1.14E+12	Ba-136M	2.09E+09
Cu-64	3.67E+05	Rh-104	2.66E+09	I-137	3.00E+08
Cu-66	3.90E+05	Rh-104M	1.96E+09	Xe-137	1.62E+12
Actinides	&Daughters	Mo-105	1.13E+10	Cs-137	1.59E+11
Th-231	2.90E+06	Tc-105	5.07E+11	Ba-137M	1.51E+11
Th-234	1.90E+06	Ru-105	7.20E+11	I-138	1.54E-03
Pa-232	1.59E+05	Rh-105	7.21E+11	Xe-138	3.19E+12
Pa-233	4.40E+04	Rh-105M	2.02E+11	Cs-138	4.37E+12
Pa-234M	1.90E+06	Mo-106	7.08E+00	Cs-138M	4.65E+10
Pa-234	2.50E+03	Tc-106	1.04E+09	Xe-139	1.32E+10
U-232	1.33E+03	Ru-106	2.10E+11	Cs-139	3.03E+12
U-234	1.88E+04	Rh-106	2.10E+11	Ba-139	4.24E+12

Continued on next page

Die approbierte gedruckte Originalversion dieser Dissertation ist an der TU Wien Bibliothek verfügbar.
The approved original version of this doctoral thesis is available in print at TU Wien Bibliothek.
TU Bibliothek Your knowledge hub WIEN

Table B.10 – *Continued from previous page*

Isotope	Activity[Bq]	Isotope	Activity[Bq]	Isotope	Activity[Bq]
U-235	2.90E+06	Rh-106M	9.77E+08	Xe-140	2.38E+05
U-236	7.51E+05	Mo-107	1.26E-04	Cs-140	1.44E+11
U-237	1.27E+11	Tc-107	8.73E+07	Ba-140	4.10E+12
U-238	1.90E+06	Ru-107	7.14E+10	La-140	4.11E+12
U-239	4.50E+12	Rh-107	1.44E+11	Pr-140	5.99E+05
U-240	6.06E+05	Pd-107	2.64E+04	Cs-141	4.66E+08
Np-236M	5.04E+04	Pd-107M	2.83E+01	Ba-141	3.24E+12
Np-237	4.31E+04	Tc-108	3.73E-08	La-141	3.89E+12
Np-238	2.10E+09	Ru-108	3.42E+10	Ce-141	3.90E+12
Np-239	5.25E+12	Rh-108	3.64E+10	Ba-142	2.72E+12
Np-240M	4.17E+07	Rh-108M	8.45E+07	La-142	3.86E+12
Np-240	2.53E+08	Tc-109	3.14E+08	Pr-142	5.77E+09
Pu-236	3.56E+03	Ru-109	9.36E+08	Pr-142M	9.62E+08
Pu-237	3.54E+03	Rh-109	1.19E+10	Ba-143	3.67E+05
Pu-238	1.13E+07	Rh-109M	1.93E+09	La-143	3.04E+12
Pu-239	2.38E+08	Pd-109	4.07E+10	Ce-143	3.90E+12
Pu-240	2.31E+07	Pd-109M	1.61E+10	Pr-143	3.90E+12
Pu-241	5.17E+08	Ag-109M	4.07E+10	Ba-144	6.35E+03
Pu-243	1.39E+06	Ru-110	3.02E+04	La-144	1.93E+10
Am-241	3.55E+05	Rh-110	3.12E+07	Ce-144	2.83E+12
Am-242M	2.25E+03	Ag-110	5.98E+05	Pr-144	2.83E+12
Am-242	1.24E+07	Ag-110M	3.28E+07	Pr-144M	3.40E+10
Am-244M	9.80E+03	Ru-111	1.21E+04	Ba-145	6.01E-04
Cm-242	3.76E+06	Rh-111	8.47E+08	La-145	1.46E+09
Fission	Products	Pd-111	1.96E+10	Ce-145	9.19E+11
H-3	6.85E+08	Pd-111M	1.85E+08	Pr-145	2.57E+12
Cu-72	9.56E-09	Ag-111	2.18E+10	La-146	5.82E+00
Zn-72	5.55E+07	Ag-111M	2.03E+10	Ce-146	1.53E+12
Ga-72	5.56E+07	Rh-112	9.83E-11	Pr-146	1.94E+12
Zn-73	1.73E+04	Pd-112	1.59E+10	Pm-146	3.20E+05
Ga-73	1.78E+08	Ag-112	1.60E+10	La-147	2.26E+02

Continued on next page

Die approbierte gedruckte Originalversion dieser Dissertation ist an der TU Wien Bibliothek verfügbar.
The approved original version of this doctoral thesis is available in print at TU Wien Bibliothek.
TU Bibliothek Your knowledge hub WIEN

Table B.10 – *Continued from previous page*

Isotope	Activity[Bq]	Isotope	Activity[Bq]	Isotope	Activity[Bq]
Ge-73M	1.78E+08	Pd-113	1.37E+09	Ce-147	6.98E+10
Zn-74	4.29E+07	Ag-113	1.36E+10	Pr-147	1.23E+12
Ga-74	3.39E+08	Ag-113M	3.56E+08	Nd-147	1.51E+12
Zn-75	2.58E-02	Cd-113M	2.29E+07	Pm-147	5.24E+11
Ga-75	1.67E+08	Ru-114	3.72E-10	Ba-148	8.35E-07
Ge-75	1.04E+09	Rh-114	5.61E-10	La-148	1.07E-06
Ge-75M	1.13E+07	Pd-114	3.04E+09	Ce-148	6.27E+09
Zn-76	5.26E-09	Ag-114	3.13E+09	Pr-148	3.21E+11
Ga-76	1.10E+06	In-114	5.02E+04	Pm-148	5.97E+10
As-76	2.03E+06	In-114M	4.91E+04	Pm-148M	2.50E+10
Ga-77	3.05E+02	Rh-115	9.56E-07	Pr-149	1.47E+11
Ge-77	2.35E+09	Pd-115	4.38E+07	Nd-149	7.12E+11
Ge-77M	1.30E+08	Ag-115	8.35E+09	Pm-149	7.30E+11
As-77	6.80E+09	Ag-115M	2.14E+07	Pr-150	8.91E+03
Se-77M	1.69E+07	Cd-115	1.23E+10	Pm-150	7.27E+08
Ga-78	5.81E-10	Cd-115M	1.20E+09	Nd-151	2.11E+11
Ge-78	1.31E+10	In-115M	1.23E+10	Pm-151	2.83E+11
As-78	1.37E+10	Pd-116	1.92E+03	Sm-151	2.85E+09
Ge-79	1.83E+08	Ag-116	1.85E+09	Ce-152	1.61E+03
As-79	2.52E+10	Ag-116M	3.72E+03	Pr-152	3.96E+03
Se-79	6.53E+05	In-116	1.71E+02	Nd-152	1.32E+11
Se-79M	3.19E+10	In-116M	7.05E+08	Pm-152	1.64E+11
Ge-80	8.06E+06	Pd-117	1.29E-09	Pm-152M	1.52E+09
As-80	2.55E+07	Ag-117	3.54E+08	Eu-152	2.28E+07
Br-80	4.13E+05	Ag-117M	1.25E-07	Eu-152M	2.93E+08
Br-80M	2.03E+05	Cd-117	8.39E+09	Pr-153	1.19E-02
Ge-81	3.67E+01	Cd-117M	4.53E+09	Nd-153	4.07E+09
As-81	1.92E+08	In-117	7.86E+09	Pm-153	7.00E+10
Se-81	1.21E+11	In-117M	9.96E+09	Sm-153	1.28E+11
Se-81M	4.21E+09	Sn-117M	1.96E+05	Gd-153	3.68E+06
Ge-82	1.87E-10	Cd-118	1.32E+10	Nd-154	1.64E+08

Continued on next page

Die approbierte gedruckte Originalversion dieser Dissertation ist an der TU Wien Bibliothek verfügbar.
The approved original version of this doctoral thesis is available in print at TU Wien Bibliothek.
TU Bibliothek Your knowledge hub WIEN

Table B.10 – *Continued from previous page*

Isotope	Activity[Bq]	Isotope	Activity[Bq]	Isotope	Activity[Bq]
As-82	4.97E+06	In-118	1.32E+10	Pm-154	1.59E+10
As-82M	2.58E+03	In-118M	1.29E+06	Pm-154M	8.45E+08
Br-82	4.66E+08	Ag-119	1.66E-06	Eu-154	4.37E+08
Br-82M	1.15E+08	Cd-119	4.61E+09	Nd-155	2.83E+06
As-83	2.60E+04	Cd-119M	2.21E+09	Pm-155	1.30E+08
Se-83	1.13E+11	In-119	2.67E+09	Sm-155	2.27E+10
Se-83M	1.16E+10	In-119M	9.67E+09	Eu-155	4.70E+09
Br-83	3.51E+11	Sn-119M	1.64E+08	Nd-156	6.40E+07
Kr-83M	3.55E+11	Cd-120	1.88E+08	Pm-156	8.25E+07
As-84	8.47E-06	In-120	3.96E+08	Sm-156	1.08E+10
Se-84	2.19E+11	In-120M	1.00E+08	Eu-156	1.68E+10
Br-84	6.37E+11	Cd-121	5.56E+02	Pm-157	1.26E+08
Br-84M	6.85E+09	In-121	8.71E+06	Sm-157	3.90E+09
Se-85	1.53E+09	In-121M	1.08E+09	Eu-157	5.79E+09
Se-85M	2.97E+06	Sn-121	1.46E+10	Nd-158	5.96E-05
Br-85	2.76E+11	Sn-121M	1.40E+05	Pm-158	1.15E-04
Kr-85	1.90E+10	Cd-122	6.70E-08	Sm-158	2.54E+09
Kr-85M	8.33E+11	In-122	9.33E+00	Eu-158	2.92E+09
Se-86	1.62E+06	Sb-122	6.66E+07	Sm-159	2.24E+08
Br-86	1.52E+10	Sb-122M	2.58E+05	Eu-159	9.54E+08
Br-86M	1.11E+06	Cd-123	5.95E-02	Gd-159	1.09E+09
Rb-86	2.09E+08	In-123	1.58E-01	Sm-160	1.79E+08
Rb-86M	1.43E+06	In-123M	5.89E+07	Eu-160	2.10E+08
Se-87	6.66E-06	Sn-123	4.06E+09	Tb-160	1.06E+07
Br-87	2.95E+10	Sn-123M	1.27E+10	Sm-161	2.11E+00
Kr-87	1.63E+12	Cd-124	3.39E+04	Eu-161	8.16E+05
Sr-87M	7.11E+05	In-124	4.17E+04	Gd-161	6.89E+07
Br-88	2.43E+06	Sb-124	5.53E+07	Tb-161	1.51E+08
Kr-88	2.34E+12	Sb-124M	4.50E+05	Sm-162	1.45E+02
Rb-88	2.40E+12	In-125M	9.71E+01	Eu-162	2.17E+07
Br-89	9.04E-10	Sn-125	1.16E+10	Gd-162	6.39E+07

Continued on next page

Die approbierte gedruckte Originalversion dieser Dissertation ist an der TU Wien Bibliothek verfügbar.
The approved original version of this doctoral thesis is available in print at TU Wien Bibliothek.
TU Bibliothek Your knowledge hub WIEN

Table B.10 – *Continued from previous page*

Isotope	Activity[Bq]	Isotope	Activity[Bq]	Isotope	Activity[Bq]
Kr-89	9.67E+11	Sn-125M	1.25E+10	Tb-162	7.37E+07
Rb-89	2.85E+12	Sb-125	1.04E+10	Tb-162M	2.06E+06
Sr-89	3.14E+12	Te-125M	2.38E+09	Eu-163	4.40E+00
Y-89M	2.42E-01	Sn-126	6.18E+05	Gd-163	2.93E+06
Kr-90	3.47E+09	Sb-126	7.29E+08	Tb-163	2.74E+07
Rb-90	9.30E+11	Sb-126M	2.86E+08	Gd-164	1.04E+07
Rb-90M	3.00E+11	Sn-127	6.96E+10	Tb-164	1.21E+07
Sr-90	1.53E+11	Sn-127M	1.44E+10	Gd-165	5.37E+05
Y-90	1.53E+11	Sb-127	1.12E+11	Tb-165	7.97E+05
Y-90M	8.62E+06	Te-127	1.11E+11	Dy-165	1.05E+07
Kr-91	2.62E+01	Te-127M	1.52E+10	Dy-165M	1.10E+06
Rb-91	9.48E+10	Sn-128	2.36E+11	Dy-166	4.01E+06
Sr-91	3.83E+12	Sb-128	1.11E+10	Ho-166	4.19E+06
Y-91	3.84E+12	Sb-128M	2.55E+11		
Y-91M	2.23E+12	I-128	3.78E+08		
Rb-92	2.23E-09	Sn-129	9.37E+10		
Sr-92	3.86E+12	Sn-129M	5.45E+10		
Y-92	3.95E+12	Sb-129	4.62E+11		
Rb-93	9.59E-05	Te-129	4.58E+11		
Sr-93	2.60E+12	Te-129M	6.87E+10		
Y-93	4.25E+12	I-129	3.64E+04		
Zr-93	3.35E+06	Sn-130	2.38E+11		
Nb-93M	1.36E+05	Sb-130	1.33E+11		
Sr-94	2.16E+11	Sb-130M	6.37E+11		
Y-94	3.60E+12	I-130	2.12E+09		
Nb-94M	1.82E+05	I-130M	5.81E+08		
Sr-95	7.88E+08	Sn-131	2.03E+10		
Y-95	3.08E+12	Sb-131	1.48E+12		
Zr-95	4.25E+12	Te-131	1.70E+12		

Table B.10: Inventory of averaged fuel element in F ring in 2025

Die approbierte gedruckte Originalversion dieser Dissertation ist an der TU Wien Bibliothek verfügbar.
The approved original version of this doctoral thesis is available in print at TU Wien Bibliothek.
TU Bibliothek Your knowledge hub WIEN

Curriculum Vitae

Personal information

First name(s) / Surname	**Eileen Jing Sigrid Langegger (Radde)**
Address	Rudolf Zöllner Str. 31, 2500 Baden, Austria
Mobile	004369910624832
E-mail	eileen.langegger@euronuclear.org
Nationality	Austrian, German
Date of birth	12.06.1986
Gender	female

Occupational field **Radiation Protection, Nuclear science**

Work experience

Dates	October 2017 - ongoing
Occupation or position held	Lecturer (Univ.Lekt)
Main activities and responsibilities	Lecturer at University for "Nuclear Engineering 1" and "Kernkraftwerkstechnik", preparation of lectures and examinations; Consultating for Austrian Armed Forces "CODIBUM"
Name and address of employer	Technische Universität Wien and Technische Universität Graz
Type of business or sector	Education and Training
Dates	February 2013 – ongoing
Occupation or position held	Engineer
Main activities and responsibilities	Manager of Interim Storage – responsible for implementation of Interim Storage structures, development of processes for safe and secure storage of LILW; Project Management of EURAD Management for compilation of Licence Applications and Safety Analyses Radiation Protection duties – officer for NES, implementation and determination of Radiation Protection measures Project management: Characterization of contamination status, Implementation of measurements
Name and address of employer	Nuclear Engineering Seibersdorf GmbH (NES), Campus Seibersdorf, 2444 Seibersdorf
Type of business or sector	Nuclear Waste Management
Dates	Jan.2012 – December 2012
Occupation or position held	Project assistant
Main activities and responsibilities	Development and Implementation of a Master program in Nuclear Security in Cooperation with TU Delft, FH Brandenburg, University of Oslo, University of Manchester
Name and address of employer	Technical University Vienna, Stadionallee 2, 1020 Wien, Austria
Type of business or sector	Education and Training
Dates	Oct. 2011 – Oct.2012
Occupation or position held	Consultant at IAEA, Safeguards Technical Support, Project Engineering Team
Main activities and responsibilities	Pre-test preparations of experiments, evaluation of data (fuel measurements at various facilities) regarding isotopic composition and mass, simulation of spectra, fuel rods and detectors with gamma spectroscopy simulation tool(VGSL), development of software for neutron coincidence counting devices
Name and address of employer	IAEA, Wagramerstrasse 5, 1400 Wien, Austria
Type of business or sector	Research and Development
Dates	Jan.2012 – Jul.2012
Occupation or position held	Consultant, Office of Nuclear Security
Main activities and responsibilities	Development and Peer Review of Teaching Material in the Nuclear Security Education Series NSS12. Topics: "Detection and Response to Criminal and Unauthorized Acts involving Nuclear and other Radioactive Material out of Regulatory Control", "Nuclear Energy, Nuclear Fuel Cycle and Nuclear Applications", "Physical protection Systems, Design and Evaluation"
Name and address of employer	IAEA, Wagramerstrasse 5, 1400 Wien, Austria
Type of business or sector	Education and Training
Dates	Mar 2011 – Jul 2011
Occupation or position held	Group Leader (11 people)
Main activities and responsibilities	Foundation and management of an Information centre concerning the situation in Fukushima Daiichi, Japan at the Atominstitut Vienna. Response to e mail request, telephone calls of public, ministries, interview in all kind of media, and selection of information for all employees of institute

	Consultancy for AVL List, Graz: weekly reports on radiation exposure, contamination and food safety for employees in Japan Consultancy for Austrian Airlines: contact point for employees
Name and address of employer	Self employed
Type of business or sector	Information Management
Dates	May-Jul 2011; Apr-Jun 2010; Apr-May 2009; June 2008
Occupation or position held	Technician of Measurement in German Nuclear Power Plants
Main activities and responsibilities	Monitoring and Calibration of safety control systems and pathway monitoring Technical repairs and Calibration, Record writing (NPP Grohnde, NPP Isar II, NPP Emsland),NPP Brokdorf: Group supervisor (4 people) Monitoring and Calibration of computerized safety control systems and pathway monitoring
Name and address of employer	Ing. Erwin Mühlegger GmbH, Mühlbachtal 7, 4801 Traunkirchen, Austria
Type of business or sector	Control Technology, Nuclear Industry
Dates	Oct.2009 – May 2010
Occupation or position held	Consultant and Staff assistant at Nuclear Security Unit
Main activities and responsibilities	Testing, maintenance and repair of hand held radiation detection equipment Assistant with logistics and assessment management; Preparation of 1st RASE workshop; Analysis of spectrometric equipment performance for RASE equipment
Name and address of employer	IAEA, Wagramerstrasse 5, 1400 Wien, Austria
Type of business or sector	Nuclear Security
Dates	2007 -2009
Occupation or position held	Study Tutor
Main activities and responsibilities	Preparation of experiments, surveillance and mentoring during experiments, grading and tutoring of protocol writing, teaching assistant (Physics for Chemists), giving assignments
Name and address of employer	Institute of Experimental Physics, University of Technology Graz, Prof. Pottlacher Institute of Material Physics, University of Technology Graz, Prof. Sprengel
Type of business or sector	Education and Training

Extra Professional Activities

Dates	Jun 2015 – Jun 2017
Position	Chair of European Nuclear Society –Young Generation Network (ENS YGN)
Main activities and responsibilities	Chairing the ENS YGN, a professional network, connecting all young professionals in the nuclear sector in Europe. Organizing 3 meetings a year Presentation and speeches at various conferences and meetings; www.ensygn.org
Dates	Jun 2013 – Jun 2015
Position	Co-Chair of European Nuclear Society –Young Generation Network (ENS YGN)
Main activities and responsibilities	Assistant to the Chair of the Network

Education and training

Dates	Aug.2013 – to be completed in 2018/2019
Title of qualification awarded	Dr.tech.
Principal subjects/occupational skills covered	Comparing two simulation tools for severe accident scenarios of the TRIGA Mark II reactor Consulting for research reactor PAVIA (August 2018)
Name and type of organisation	Technical University Vienna, Institute of Atomic and Subatomic Physics
Level in national or international classification	PhD
Dates	September 2011 and January 2012
Principal subjects/occupational skills covered	Introduction to Nuclear Security, Professional Development Course
Name and type of organisation providing education and training	Kings College London, Centre for Science and Security Studies and International Nuclear Security Education Network (INSEN)
Dates	Apr.2009 – Mar. 2011
Title of qualification awarded	Dipl. Ing.
Principal subjects/occupational skills covered	Technical Physics, Gamma Spectroscopy, Nuclear Security, Topic of Master Theses: RASE – Replicative Assessment of Spectrometric Equipment, Theoretical Description and Experimental Evaluation
Name and type of organisation providing education and training	University of Technology Graz, Institute of Material Science and Technical University Vienna, Institute of Atomic and Subatomic Physics
Level in national or international classification	Master of Science
Dates	Mar. 2010

Principal subjects/occupational skills covered	ESARDA Course - Nuclear Safeguards and Non - Proliferation
Name and type of organisation	ESARDA (European Safeguards Research and Development Association)
Dates	Oct. 2004 – Apr. 2009
Title of qualification awarded	Bakk.
Principal subjects/occupational skills covered	Technical Physics, Transmutation, Title of Bachelor theses: "Aspects of Nuclear Waste Disposal in Nuclear Power Plants – Transmutation" (in German)
Name and type of organisation	University of Technology Graz, Institute of Material Science
Level in national or international classification	Bachelor of Science

Languages

Mother tongue	German
Other language(s)	English, French, Italian

Professional Memberships	Chair of Austrian Nuclear Society (since 2017) Chairperson of Austrian Nuclear Society – Young Generation Network (2010-2013) Member of INSEN(International Nuclear Security Education Network) Member INENS (International Network of Emerging Nuclear Specialists) Co-Chair of ESARDA Editorial Committee working group (2013 – 2017) Member of Austrian Radiation Protection Association and their Young Scientists and Professionals,
Organisational skills and competences	Organisation of many projects within the Austrian Nuclear Society, such as group travels to Finland Chernobyl or France for 15 people. Organisation of Student Days at the Institute of Atomic and Subatomic Physics
Other qualifications	Radiation Protection "Strahlenschutzabzeichen Bronze and Silber"
Computer skills and competences	Programming Languages: Matlab, Labview, C++ (basics) Origin, Microsoft Office
Artistic skills and competences	Violin and Viola since 1991
Driving licence	Category B, ADR driving licence
References	Prof. Günter Hillebrand hillebrand@aon.at Helmuth Böck helmuth.boeck@tuwien.ac.at

Publications, Presentation and Lectures

Nov.2014-2018 Lectures "Einführung in die Kernenergie", Montanuniversität Leoben

Sep.2013: Lecture "Detection of criminal or unauthorized acts involving nuclear and other radioactive material out of regulatory control" Institute for Atomic and Subatomic Physics, Vienna University of Technology

2020, A novel comparison of RODOS and LASAIR for simulation of dispersion scenarios after severe accidents in TRIGA MARK II reactors, RRFM Conference proceedings 2020 (planned)

2019, The Nuclear for Climate Initiative, International Conference on Climate Change and the Role of Nuclear Power, IAEA

2018, Radioactive Waste Management in Austria, NENE Conference proceedings 2018

2018, Simulation of Consequences of Severe Accidents of TRIGA Mark II reactor in Vienna with Rodos, RRFM Conference proceedings 2018

2017, Simulation of Consequences of Severe Accidents of TRIGA Mark II reactor in Vienna with Rodos, NENE Conference proceedings 2017

Jul.2014: "Reduction of Radioactive Waste by Improvement of Conditioning Facilities", Nuclear España – Journal of Spanish Nuclear Professionals, 2014, best track paper at IYNC 2014

Jun.2014: "Finding Hot Spots with the help of ISOCS for easier decommissioning of former research facilities and its surroundings", Stockholm

Apr.2012: „Information Management of the Fukushima reactor accident in Austria", G.Steinhauser, E.Radde et.al., Disaster Advances, Vol.5(2)

Oc.2011: „Kernfrage Atomkraft Was passiert wenn etwas passiert", H.Böck, M.Gerstmayr, E.Radde, Goldegg Verlag, Wien 2011

Full publications list can be found at: https://www.linkedin.com/in/eileen-langegger-19812442/

Key note speeches at ENYGF 2013, Nestet2013, ENYGF 2015, WIN GLOBAL 2015, AMNT 2016, ENC 2016, ENYGF 2017, HTR conference October 2018

Workshops at EAFES, PIME2013, PIME2014, PIME2015, ENC2014, ENC 2016, IYNC 2016, ENYGF 2017

Acknowledgements

Firstly, I would like to express my sincere gratitude to my advisor Prof. Helmuth Böck for his continuous support of my work, his patience and motivation. Besides my advisor I would like to thank Dr. Mario Villa for his insightful comments and encouragement. My sincere thanks also go to Dr. Peter Hofer, who gave me access to the research facilities. I would also like to thank the team at the KIT for their technical support. Thanks to my company, who provided me with adequate time for this work.

Last but not the least I would like to thank my family, my beloved husband, my daughter and my parents. They did not only support me spiritually but made this work possible.

Die approbierte gedruckte Originalversion dieser Dissertation ist an der TU Wien Bibliothek verfügbar.
The approved original version of this doctoral thesis is available in print at TU Wien Bibliothek.
TU Bibliothek Your knowledge hub WIEN